

Electronic Thesis and Dissertation Repository

---

7-22-2011 12:00 AM

## Double Helical Hydrogen-Bonded AAA-DDD Complexes and Supramolecular Polymers


Hong-Bo Wang, *The University of Western Ontario*

Supervisor: James A. Wisner, *The University of Western Ontario*

A thesis submitted in partial fulfillment of the requirements for the Doctor of Philosophy degree in Chemistry

© Hong-Bo Wang 2011

Follow this and additional works at: <https://ir.lib.uwo.ca/etd>

 Part of the [Materials Chemistry Commons](#), [Organic Chemistry Commons](#), and the [Polymer Chemistry Commons](#)

---

### Recommended Citation

Wang, Hong-Bo, "Double Helical Hydrogen-Bonded AAA-DDD Complexes and Supramolecular Polymers" (2011). *Electronic Thesis and Dissertation Repository*. 211.  
<https://ir.lib.uwo.ca/etd/211>

This Dissertation/Thesis is brought to you for free and open access by Scholarship@Western. It has been accepted for inclusion in Electronic Thesis and Dissertation Repository by an authorized administrator of Scholarship@Western. For more information, please contact [wlsadmin@uwo.ca](mailto:wlsadmin@uwo.ca).

**DOUBLE HELICAL HYDROGEN-BONDED AAA-DDD COMPLEXES AND  
SUPRAMOLECULAR POLYMERS**

(Spine title: Hydrogen-Bonded Double Helices and Supramolecular Polymers)

(Thesis format: Integrated Article)

by

Hong-Bo Wang

Graduate Program in Chemistry

A thesis submitted in partial fulfillment  
of the requirements for the degree of  
Doctor of Philosophy

The School of Graduate and Postdoctoral Studies  
The University of Western Ontario  
London, Ontario, Canada

© Hong-Bo Wang 2011

THE UNIVERSITY OF WESTERN ONTARIO  
School of Graduate and Postdoctoral Studies

**CERTIFICATE OF EXAMINATION**

Supervisor

Examiners

\_\_\_\_\_  
Dr. James A. Wisner

\_\_\_\_\_  
Dr. Stephen J. Loeb

\_\_\_\_\_  
Dr. Robert H. E. Hudson

\_\_\_\_\_  
Dr. Mel C. Usselman

\_\_\_\_\_  
Dr. Jin Zhang

The thesis by

**Hong-Bo Wang**

entitled:

**Double Helical Hydrogen-Bonded AAA-DDD Complexes and  
Supramolecular Polymers**

is accepted in partial fulfillment of the  
requirements for the degree of  
Doctor of Philosophy

\_\_\_\_\_  
Date

\_\_\_\_\_  
Chair of the Thesis Examination Board

## Abstract

The design and characterization of linear oligomers that self-assemble into double helical structures has been a subject of interest to chemists since the elucidation of the double helix structure of DNA in 1953. Transition metal templates have been widely used in the construction of artificial double helical complexes from linear multidentate ligands. The use of other non-covalent interactions as the driving force in the self-assembly of these types of complexes is less common. Aromatic stacking interactions, anion templates, and salt-bridges have all been applied in this context. The great majority of these investigations have been concerned with the dimerization of identical linear oligomers to form homoduplex products. There are very few examples of artificial double helices that form from complementary strands to give heteroduplexes. Notably, Yashima, Furusho and coworkers have demonstrated that two complementary molecules may interact via amidinium-carboxylate salt bridges in a sequence dependent manner resembling the hybridization of ss-DNA. Our group has reported the formation of a double helical complex based on self-complementary molecular strands containing alternating hydrogen bond donors and acceptors but its association constant was very low. In this thesis, we attempt to design and synthesize complementary hydrogen bonded AAAA-DDD double helices with high association constants and further develop supramolecular polymers based on them.

The first non-coplanar DDD molecule including three thiazine dioxide subunits and AAA component including two pyridine and one 3,5-lutidine subunits can form the double helical structure. The DDD component is insoluble in chloroform. However, DDD analogue based on indole and thiazine dioxide subunits can be dissolved in chloroform and the AAA-DDD binding property in solution was investigated.

Electron- withdrawing groups on DDD component increase the stabilities of AAA-DDD complexes and electron-donating groups on AAA component also improve the stabilities of AAA-DDD complexes. Substituent groups on DDD or AAA molecules not only change their electronic distributions but also their conformations. Therefore, the substituent effect is not simply equal to electronic effect.

Two DDD and AAA components were linked with an aliphatic chain respectively. The main-chain supramolecular polymer is formed from the 1:1 mixture of bisAAA and bisDDD. BisAAA and bisDDD follow the ring-chain supramolecular polymerization mechanism. Relative to the same length linkers in bisAAA and bisDDD, the different length of linkers led to the lower critical polymerization concentration.

## Keywords

Complementary, Hydrogen Bond, Double Helix, Substituent Effect, Supramolecular Polymer, NMR Titrations, Isothermal Titration Calorimetry

## Co-Authorship Statement

Bhanu Mudrboyina synthesized compounds **16**, **40**, **55** and **56**, and solved the crystal structures of complex **7·11** and compound **16**. Doug Hairsine (manager, mass spectrometry) run the mass spectrometry. All of the remaining work in this thesis has been done by the author himself.

## Acknowledgments

It is difficult to overstate my gratitude to my Ph. D. supervisor, Dr. James A. Wisner. Throughout my Ph.D. study and research in the past five years, he has provided wise advice, encouragement, good teaching, good conversations and lots of good ideas with his enthusiasm and inspiration. Personally, I am so proud of keeping a friendship with Dr. Wisner in my lifetime.

I would like to thank my thesis examination committee, Dr. Stephen J. Loeb, Dr. Robert H. E. Hudson, Dr. Mel C. Usselman and Dr. Jin Zhang. In particular, I wish to thank Dr. Robert H. E. Hudson for his kind assistance with writing letters and helping various applications.

I offer my regards to all of those (Secretaries in chemistry department, Staff in ChemBioStore, mass spectrometry, NMR, X-ray analysis) who supported me in any respect during my Ph. D. study and research. I am grateful to all the current and past labmates in Wisner group for providing fun and friendly environment in which to learn and grow.

I thank my entire family for providing a loving environment for me. My parents, parents in-law and grandparents in-law deserve special mention. My parents provide the best conditions as they can to raise and support me. My parents in-law and grandparents in-law raised a wonderful daughter and granddaughter and are willing to let her take an adventure in Canada with me.

Last and most importantly, I wish to thank my wife, Jin Xu, who always encouraged me and support me through difficult time.

# Table of Contents

CERTIFICATE OF EXAMINATION .....	ii
Abstract .....	iii
Co-Authorship Statement.....	v
Acknowledgments.....	vi
Table of Contents .....	vii
List of Tables .....	x
List of Figures .....	xi
List of Schemes.....	xiv
List of Abbreviations and Symbols.....	xviii
Chapter 1 Introduction .....	1
1.1 Factors Affecting Hydrogen-Bonded Association .....	3
1.1.1 Numbers of Hydrogen Bonds .....	6
1.1.2 Secondary Interactions .....	8
1.1.3 Intramolecular Hydrogen Bonds .....	10
1.1.4 Preorganization .....	14
1.1.5 Solvent.....	14
1.2 Hydrogen Bonded Supramolecular Polymers .....	17
1.3 Scope of the Thesis .....	19
1.4 References .....	24
Chapter 2 Design and Optimization of Hydrogen-Bonded AAA-DDD Double Helices .....	30
2.1 Artificial Double Helical Structures .....	30
2.1.1 Double Helices through Template Synthesis.....	30
2.1.2 Double Helices through Aromatic Interactions .....	34



2.1.3 Double Helices through Salt Bridges .....	39
2.2 Results and Discussions .....	41
2.3 Summary .....	56
2.4 Experimental Section .....	57
2.5 References .....	69
Chapter 3 Substituent Effects in Double Helical Hydrogen-Bonded AAA-DDD Complexes.....	74
3.1 Substituent Effects for Hydrogen-Bonded Complexation .....	112
3.2 Results and Discussions .....	80
3.2.1 Electron-Withdrawing Groups on DDD.....	80
3.2.2 Substituent Groups on AAA .....	86
3.3 Summary .....	112
3.4 Experimental Section .....	112
3.5 References .....	110
Chapter 4 Supramolecular Copolymer Formed from Ditopic Monomers Containing AAA-DDD Hydrogen Bonds.....	112
4.1 Supramolecular Polymers .....	112
4.1.1 Supramolecular Polymerization Based on Three-Point Complementary Hydrogen Bonds .....	113
4.1.2 Supramolecular Polymerization Based on Four-Point Complementary Hydrogen Bonds.....	117
4.1.3 Supramolecular Polymerization Based on Six-Point Complementary Hydrogen Bonds.....	120
4.2 Supramolecular Copolymer Based on Double Helical AAA-DDD Hydrogen Bonds .....	125
4.2.1 Synthesis of Monomers Ready for BisDDD and BisAAA .....	127
4.2.2 Synthesis of BisDDD and BisAAA .....	130
4.3 Results and Discussion .....	132
4.4 Summary .....	139

4.5 Experimental Section .....	140
4.6 References .....	149
Chapter 5 Conclusion and Outlook.....	155
5.1 Conclusion.....	155
5.2 Outlook.....	157
Appendices.....	159
Curriculum Vitae .....	165

## List of Tables

<b>Table 1-1</b> Calculated electrostatic interactions between each pair of complexes <b>I</b> and <b>II</b> .....	22
<b>Table 2-1</b> Association constant and indole N-H chemical shifts for the complexations of <b>28</b> with <b>30</b> and <b>31</b> in CDCl <sub>3</sub> at 298 K.....	55
<b>Table 3-1</b> Changes in the chemical shifts of N-H ( $\Delta\delta$ ), substituent constants ( $\sigma_p$ ), association constants ( $K_a$ ), and free energy of the complexations of <b>28</b> , <b>38a-38g</b> and <b>11</b> in chloroform at 298K (experimental errors in brackets are twice the standard deviations).....	82
<b>Table 3-2</b> The binding data of different AAAs and DDDs in chloroform at 25°C.....	88

## List of Figures

- Figure 1-1** Molecular electrostatic potential surfaces of (a) methanol, (b) methanethiol, (c) pyridine and (d) DMSO by using AM1. Positive point charge regions are shown in blue and negative charge regions are shown in red.....5
- Figure 1-2** Possible sequences of triply hydrogen bonded dimers including different numbers of secondary interactions.....8
- Figure 1-3** Dimerization constants in various DMSO-*d*<sub>6</sub>/CDCl<sub>3</sub> mixtures at 298K.....16
- Figure 1-4** Main-chain and cross-linked supramolecular polymers.....17
- Figure 2-1** Crystal structures of the single helical conformer and the double helical complex of nonaresorcinol.....35
- Figure 2-2** Structures of oligopyridinecarboxamides and crystal structures of the single helix and double helix dimer of **1**.....36
- Figure 2-3** Structure of *N*-oxidized oligomers and crystal structures of **4**<sub>2</sub> and **4**•**7**.....37
- Figure 2-4** <sup>1</sup>H NMR spectrum of **7**•**11** (1:1 mixture) in CDCl<sub>3</sub> at 298 K.....44
- Figure 2-5** The solid state structure of **7**•**11**. All C-H hydrogen atoms have been removed for clarity. NH···N hydrogen bonds are indicated by dashed orange lines. Carbon is grey, Nitrogen is blue, oxygen is red and sulfur is orange.....45
- Figure 2-6** Stick representations of the solid state structure of **16**. View along b direction (top). View perpendicular to b direction (bottom). All C-H hydrogen atoms have been removed for clarity. NH···N hydrogen bonds are indicated by dashed orange lines. Carbon is grey, Nitrogen is blue, oxygen is red and sulfur is orange.....47

<b>Figure 2-7</b>	$^1\text{H}$ NMR titration curve of <b>22</b> and <b>11</b> in $\text{CDCl}_3$ at 298K ( $K_a = 300 \text{ M}^{-1}$ ).....	50
<b>Figure 2-8</b>	$^1\text{H}$ NMR titration curve of <b>28</b> and <b>11</b> in $\text{CDCl}_3$ at 298K ( $K_a = 3700 \text{ M}^{-1}$ ).....	52
<b>Figure 2-9</b>	$^1\text{H}$ NMR titration curves for <b>28</b> and <b>30</b> in $\text{CDCl}_3$ at 298K.....	53
<b>Figure 2-10</b>	$^1\text{H}$ NMR titration curves for <b>28</b> and <b>31</b> in $\text{CDCl}_3$ at 298K.....	54
<b>Figure 2-11</b>	Crystal structures of known AAAs terpyridine, 2,6-bis(1-methyl benzimidazol-2-yl)pyridine, and 2,6-bis(3,5-dimethyl-1H-imidazol-1-yl)pyridine.....	56
<b>Figure 3-1</b>	(a) Structures of phenol and its derivatives; (b) the change in hydrogen bonded strength ( $\Delta$ ) relative to the original phenol-formaldehyde system plotted against the Hammett constant ( $\sigma_p$ ).....	75
<b>Figure 3-2</b>	Relationship between the substitution interaction energy ( $\Delta\Delta E$ , kJ/mol) calculated by GAUSSIAN03 and the Hammett constant ( $\sigma_m$ ) .....	78
<b>Figure 3-3</b>	Hammett plot of $\log(K_{X,Y}/K_{H,H})$ vs $\Sigma\sigma_p$ .....	85
<b>Figure 3-4</b>	Hammett plots of <b>11</b> , <b>40</b> , <b>43</b> , <b>44</b> , <b>28</b> , <b>38b</b> , <b>38f</b> and <b>38g</b> .....	92
<b>Figure 4-1</b>	(a) Chemical junction of perylene tetra-carboxylic di-imide and melamine; (b) STM image of the honeycomb network; (c) monotopic imide/melamine complex; (d) binding model of ditopic imide and melamine.....	114
<b>Figure 4-2</b>	Co-aggregations of OPVs and cyanurates.....	117
<b>Figure 4-3</b>	Solution viscosities of 2,7-diamino-1,8-naphthyridine / 2-ureido-4[1H]-pyrimidinone monomers in chloroform at 25°C.....	119
<b>Figure 4-4</b>	Double dynamic supramolecular polymers generated by reversible covalent and noncovalent bonds.....	124

<b>Figure 4-5</b>	The relationship between Degree of polymerization and $K_a$ .....	126
<b>Figure 4-6</b>	ITC data for the binding of <b>55</b> and <b>58</b> in chloroform at 25°C. The top plot shows the power as a function of time and the bottom plot shows integrated enthalpy values as a function of the molar ratio of <b>55</b> titrated into <b>58</b> ( $\Delta H$ is $-25.08 \pm 0.14$ kJ/mol and $\Delta S$ is 13.8 J/mol).....	132
<b>Figure 4-7</b>	Specific viscosity vs concentration for the 1:1 mixture of <b>59a</b> and <b>60</b> at different temperatures (the top plot) and their double-logarithmic plot (the bottom plot). $\Delta$ displays -15°C, o displays 5°C and $\square$ displays 25°C.....	135
<b>Figure 4-8</b>	Dynamic light scattering of an equimolar solution of <b>60</b> and <b>59a</b> (0.08 M) in chloroform at 25°C.....	136
<b>Figure 4-9</b>	Specific viscosity vs molar ratio of bisAAA <b>60</b> and bisDDD <b>59a</b> .....	137
<b>Figure 4-10</b>	Specific viscosity vs molar fraction of <b>55</b> in the 1:1 mixture of <b>60</b> and <b>59a</b> ...	138
<b>Figure 4-11</b>	Specific viscosity vs concentration for the 1:1 mixture of <b>60</b> and <b>59b</b> at room temperature.....	139
<b>Figure A-1</b>	$^1\text{H}$ NMR titration curve of <b>38a</b> and <b>11</b> in $\text{CDCl}_3$ at 298K.....	159
<b>Figure A-2</b>	$^1\text{H}$ NMR titration curve of <b>38b</b> and <b>11</b> in $\text{CDCl}_3$ at 298K.....	160
<b>Figure A-3</b>	$^1\text{H}$ NMR titration curve of <b>38c</b> and <b>11</b> in $\text{CDCl}_3$ at 298K.....	161
<b>Figure A-4</b>	$^1\text{H}$ NMR titration curve of <b>38d</b> and <b>11</b> in $\text{CDCl}_3$ at 298K.....	162
<b>Figure A-5</b>	$^1\text{H}$ NMR titration curve of <b>38e</b> and <b>11</b> in $\text{CDCl}_3$ at 298K.....	163

**Figure A-6**  $^1\text{H}$  NMR titration curve of **38f** and **11** in  $\text{CDCl}_3$  at 298K.....164

## List of Schemes

**Scheme 1-1** Natural hydrogen bonded base pairs and typical association constant values at 298 K in  $\text{CDCl}_3$ .....2

**Scheme 1-2** Oligoamide duplexes including DADA and DDAA sequences of four hydrogen bonds.....6

**Scheme 1-3** Oligoamide duplex including six hydrogen bonds.....7

**Scheme 1-4** Triply hydrogen bonded complexes containing different sequences and their measured  $K_a$  values in  $\text{CDCl}_3$  at 298 K.....10

**Scheme 1-5** Dimerization constants for some DADA arrays in  $\text{CDCl}_3$  at 298K.....11

**Scheme 1-6** Competitive hydrogen bonding of DDA-ADD arrays in  $\text{CDCl}_3$  at 298K.....12

**Scheme 1-7** Meijer and coworkers' 2-ureido-4[1H]-pyrimidinone tautomeric forms and dimers.....13

**Scheme 1-8** Zimmerman group's AADD tautomeric structures and dimers.....14

**Scheme 1-9** Liquid crystalline supramolecular polymers formed from bifunctional 2,6-diaminopyridines and uracils.....18

**Scheme 1-10** Example structures of a 2-ureido-4[1H]-pyrimidinone dimer and monomer for supramolecular polymer formation.....18

<b>Scheme 1-11</b> Some reported AAA-DDD complexes with high association constants and their mother structure.....	20
<b>Scheme 1-12</b> Hydrogen bonded double helical structure.....	21
<b>Scheme 1-13</b> Primary hydrogen bonds and secondary interactions in DD/AA and AD/DA complexes.....	22
<b>Scheme 1-14</b> Schematic summary of the thesis scope.....	23
<b>Scheme 2-1</b> Length-dependent copper (I) double helicates.....	31
<b>Scheme 2-2</b> Anion-templated double helical structure.....	32
<b>Scheme 2-3</b> Formation of a boron templated double helicate.....	33
<b>Scheme 2-4</b> Removal and insertion of sodium ion in the H <sub>4</sub> L based double helicate.....	34
<b>Scheme 2-5</b> Structures of oligoamides <b>8</b> and <b>9</b> .....	38
<b>Scheme 2-6</b> Structures of oligoamides <b>10</b> , <b>11</b> and <b>12</b> .....	38
<b>Scheme 2-7</b> Furusho and Yashima's complementary salt-bridged double helix.....	39
<b>Scheme 2-8</b> All chiral or edge-chiral amidine strands and carboxylic acid strands.....	40
<b>Scheme 2-9</b> Synthesis of <b>7</b> and <b>11</b> .....	43
<b>Scheme 2-10</b> Structures of compounds <b>7</b> and <b>16</b> .....	46
<b>Scheme 2-11</b> Synthesis of DDD <b>16</b> including indole and thiazine dioxide donors.....	46
<b>Scheme 2-12</b> Possible modified structures for soluble DDD.....	48



<b>Scheme 2-13</b> Synthesis of DDD <b>22</b> .....	49
<b>Scheme 2-14</b> Synthesis of DDD <b>28</b> .....	51
<b>Scheme 2-15</b> Three known AAA examples.....	54
<b>Scheme 3-1</b> The hydrogen-bonded complexation between tetralactam macrocycle and adipamide guest (when X = Y = NMe <sub>2</sub> , ΔG = -2.5 kcal/mol; when X = Y = H, ΔG = -3.9 kcal/mol; when X = Y = NO <sub>2</sub> , ΔG = -5.9 kcal/mol) at 23±1°C in CDCl <sub>3</sub> .....	77
<b>Scheme 3-2</b> Structures of triply hydrogen-bonded heterodimers with different functional groups.....	79
<b>Scheme 3-3</b> The model AAA-DDD system where the R and R' substituents are varied and binding energies (kcal/mol).....	79
<b>Scheme 3-4</b> Synthesis of DDD compounds <b>38</b> with different electron-withdrawing groups.....	81
<b>Scheme 3-5</b> Synthesis of AAA components <b>40</b> , <b>43</b> and <b>44</b> .....	87
<b>Scheme 4-1</b> Gels based on bismelamine/cyanurate or barbiturate hydrogen bonds.....	115
<b>Scheme 4-2</b> Pseudo-block copolymers consisting of poly(isobutylene) and poly(ether ketone) held together by three hydrogen bonds.....	116
<b>Scheme 4-3</b> Competitive associations between self-complementary AADD and complementary ADDA-DAAD.....	118
<b>Scheme 4-4</b> Zimmerman's ADDA-DAAD and bifunctional polymers.....	120

<b>Scheme 4-5</b>	(a) An ordered supramolecular strand by the molecular recognition of barbituric acid and 2,4,6-triaminopyrimidine derivatives; (b) Complementary hydrogen bonded networks from CA and M monomers.....	121
<b>Scheme 4-6</b>	(a) A rosette formation in the elamine/cyanuric acid lattice; (b) Bismelamine, biscyanic acid and some linkers.....	122
<b>Scheme 4-7</b>	Hamilton wedge type Building blocks for linear or cross-linked supramolecular polymers.....	123
<b>Scheme 4-8</b>	AB diblock copolymers linked by six hydrogen bonds.....	125
<b>Scheme 4-9</b>	Retrosynthetic analysis for bisDDD.....	127
<b>Scheme 4-10</b>	Synthesis of the intermediate thioether <b>49</b> .....	128
<b>Scheme 4-11</b>	Synthesis of the possible monomer for bisAAA.....	128
<b>Scheme 4-12</b>	Synthesis of the possible bisAAA monomer <b>57</b> .....	129
<b>Scheme 4-13</b>	Synthesis of bisDDD monomers linked with different length chains.....	130
<b>Scheme 4-14</b>	Synthesis of bisAAA <b>60</b> .....	131
<b>Scheme 5-1</b>	Pre-organized DDD molecules.....	155
<b>Scheme 5-2</b>	AAA molecules including spacers.....	156

## List of Abbreviations and Symbols

DNA	deoxyribonucleic acid
RNA	ribonucleic acid
PNA	peptide nucleic acid
$\text{CDCl}_3$	deuterated chloroform
DMSO	dimethylsulfoxide
NMR	nuclear magnetic resonance
$\text{M}^{-1}$	$(\text{mol/liter})^{-1}$
$K_a$	association constant
K	kelvin
$^{\circ}\text{C}$	Celsius degree
$\delta$	chemical shift
kJ	kilojoule
kcal	kilocalorie
$\Delta G$	Gibbs free energy
$\Delta H$	enthalpic change
$\Delta S$	entropic change
ROESY	rotating frame nuclear overhauser effect spectroscopy
AcOH	acetic acid
DMF	dimethylformamide

EtI	iodoethane
n-BuLi	n-butyl lithium
KSAc	potassium thioacetate
m-CPBA	meta-chloroperoxybenzoic acid
Pd(PPh <sub>3</sub> ) <sub>4</sub>	tetrakis(triphenylphosphine) palladium (0)
Ph	phenyl
ppm	part per million
s	singlet
d	doublet
t	triplet
m	multiplet
g	gram
min	minute
h	hour
Hz	hertz
mL	milliliter
HRMS	high resolution mass sepectrometry
ESI	electrospray ionization
EI	electron impact ionization
mmol	millimole

T	temperature
$\sigma$	Hammett substituent constant
THF	tetrahydrofuran
Et <sub>3</sub> N	Triethylamine
DMAP	4-dimethylaminopyridine
PhNMe <sub>3</sub> Br <sub>3</sub>	trimethylphenylammonium tribromide
UHP	urea-hydrogen peroxide
TFAA	trifluoroacetic anhydride
ITC	isothermal titration calorimetry

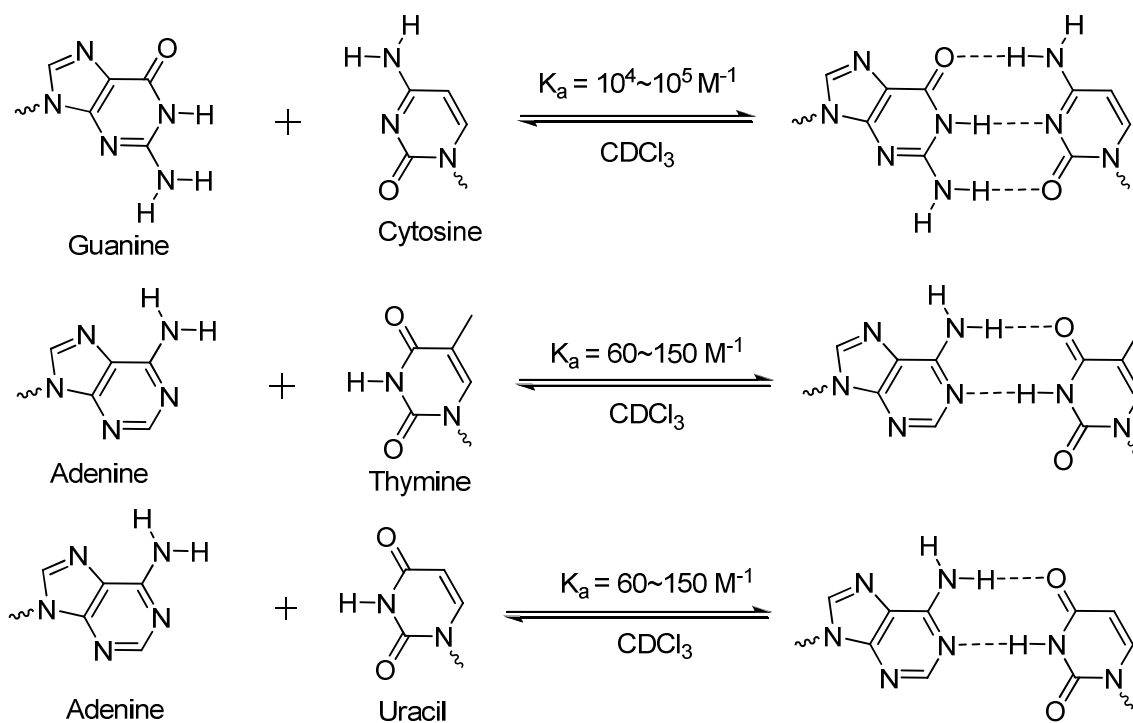
## CHAPTER 1

### Introduction

When a cell uses the information in a gene, the DNA sequence is copied to the complementary RNA sequence through the hydrogen bonding interactions between the DNA and RNA nucleobases.<sup>1</sup> DNA and RNA biomacromolecular structures contain several nucleobases, such as adenine (A), thymine (T), guanine (G), cytosine (C) and uracil (U). Therefore, genetic information transmission is achieved via complementary base pairing.<sup>2</sup> In fact, complementary hydrogen bonds are the cornerstone for information storage and processing.<sup>3</sup> The self-assembly of two strands in DNA structure is mediated by intermolecular hydrogen bonds between the two complementary base pairs A-T and C-G and in the corresponding RNA structure where U is substituted for T. The association constants among the natural complementary nucleobases, A-T, A-U, and G-C have been determined in chloroform. The G-C complex including three hydrogen bonds has a stronger association constant ( $K_a \approx 10^4 \sim 10^5 \text{ M}^{-1}$ ) while both A-T and A-U systems have a weaker association constant ( $K_a \approx 60 \sim 150 \text{ M}^{-1}$ ), in part because there exist only two hydrogen bonds in A-T or A-U (Scheme 1-1).<sup>4</sup>

Inspired by complementary hydrogen bonds in biopolymers, biochemists and chemists have been exploring natural and unnatural hydrogen-bonded complexes and further studying the possibility for the construction of smart materials based on complementary hydrogen bonds. Two-stranded DNA biopolymers including thousands of hydrogen bonds have been directly considered as building blocks to form controlled nanostructures.<sup>5</sup> Peptide nucleic acid (PNA), an artificially synthesized polymer similar

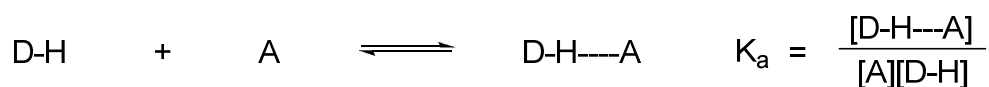
to DNA or RNA, has also been investigated for probes of biosensor, antigene and antisense drugs.<sup>6</sup> In order that natural biomacromolecules form hydrogen bonds in water, hydrophobic interactions always occur because oily molecular parts pack together to avoid their exposure to water. Thus, when chemists look to follow biology lead, they will simplify the self-assembled biomacromolecules in water, mimic the molecular self-assembly in organic solvents and further study the details on weak intermolecular interactions.



**Scheme 1-1** Natural hydrogen bonded base pairs and typical association constant values at 298 K in CDCl<sub>3</sub>.

## 1.1 Factors Affecting Hydrogen-Bonded Association

Hydrogen bonds are formed between functional groups containing an electronegative atom that possesses lone electron pairs, called hydrogen bond acceptors (A), and functional groups containing covalent bonds between hydrogen and a more electronegative atom, called hydrogen bond donors (D). The polarized nature of the X-H bond (e.g. X = O, N) results in a highly electropositive hydrogen atom that is amenable to weak bond formation with the electron-rich electronegative acceptor atoms. The measure of the binding strength is the association constant ( $K_a$ ), defined in terms of the equilibrium between associated and dissociated units:



There appears to be a relationship between acid-base ( $\text{p}K_a$ ) and hydrogen bonded donor-acceptor ( $K_a$ ) but it is not a simple relationship. For example, pyridine is much more basic than DMSO because it can stabilize the charged cationic state formed on protonation, but DMSO is a much better hydrogen bond acceptor because it is more polar. Similarly, a thiol is much more acidic than an alcohol, but an alcohol is a much better hydrogen bond donor.

Generally, the basic theory of intermolecular interactions in the gas phase separates the enthalpy of two molecular interactions into four components: repulsion, induction, dispersion and electrostatics.<sup>7</sup> Because other contributions can be negligible in intermolecular interactions, it is believed that to a first approximation electrostatics may explain all the intermolecular interactions including hydrogen bonds.<sup>7</sup> There is a good



experimental evidence for the role of electrostatics in intermolecular interactions. The association constants for a large number of simple systems (only one intermolecular hydrogen bond) have been measured in solution and the gas phase.<sup>8</sup> According to data analysis from the experimental work, there is a quantitative relationship between two simple hydrogen-bonded pairs:<sup>9</sup>

$$\log K_a = m \alpha_2^H \beta_2^H - n$$

Where  $m$  and  $n$  are constants related with the chosen medium (e.g.  $m = 7.354$  and  $n = 1.094$  in tetrachloromethane,  $m = 6.856$  and  $n = 1.144$  in 1,1,1-trichloroethane,  $m = 9.13$  and  $n = 0.87$  in the gas phase).<sup>9</sup> Although, as expected for electrostatic interactions, the constant  $m$  increases with the decrease of the medium polarity, the constant  $n$  is relatively insensitive to the medium, which indicates that it is a fundamental property of complex formation.  $\alpha_2^H$  and  $\beta_2^H$  are functional group constants that depend on the hydrogen bonded donor and acceptor properties respectively. The above equation is equivalent to an expression of the electrostatics of the hydrogen bonds, where the positive charge on the hydrogen bond donor ( $\alpha_2^H$ ) and the negative charge on the hydrogen bond acceptor ( $\beta_2^H$ ) create the interaction enthalpy.<sup>4</sup> The values of  $\alpha_2^H$  and  $\beta_2^H$  have been correlated with a number of computed molecular properties, such as electrostatic potential and atomic charge.<sup>10</sup>

Therefore, the interaction between hydrogen bond donor and acceptor is an electrostatically attractive interaction (Figure 1-1). For hydrogen bond donors, the maximum in the electrostatic potential on the van der Waals surface of a molecule is generally located on a hydrogen atom. For hydrogen bond acceptors, the electrostatic

potential minimum is generally located over a lone pair or an area of  $\pi$ -electron density.<sup>7</sup> The dominant electrostatic interactions between two molecules are pairwise interactions between these maxima and minima in the electrostatic potential that may be considered hydrogen bonds. The maxima ( $E_{\max}$ ) and minima ( $E_{\min}$ ) in the AM1 molecular electrostatic potential surfaces of a variety of simple molecules including only one functional group correlate well with the experimentally measured values of  $\alpha_2^{\text{H}}$  and  $\beta_2^{\text{H}}$ , giving  $E_{\max} = 211(\alpha_2^{\text{H}} + 0.33\text{kJ/mol})$  and  $E_{\min} = -535(\beta_2^{\text{H}} + 0.06\text{kJ/mol})$ .<sup>7</sup>

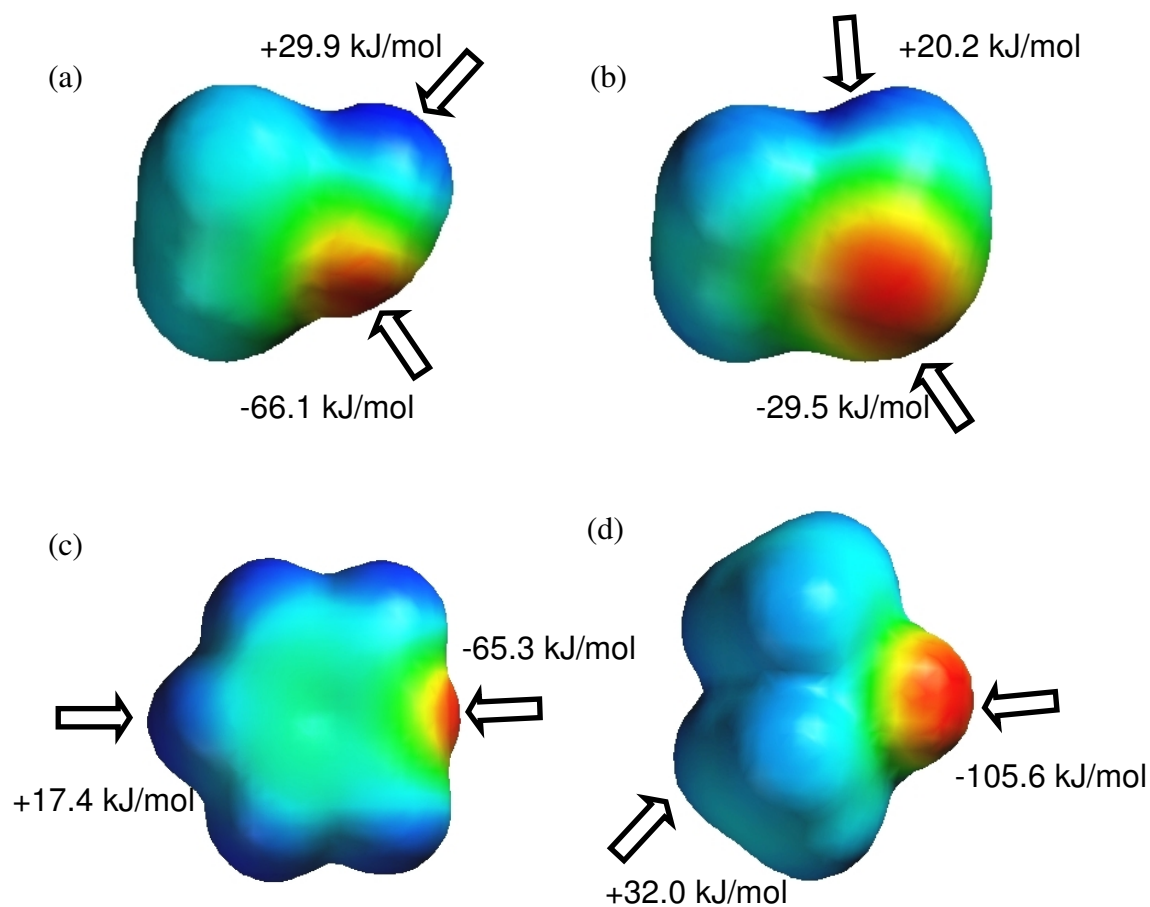
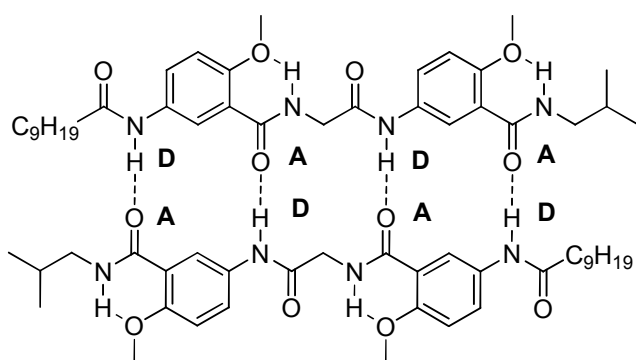


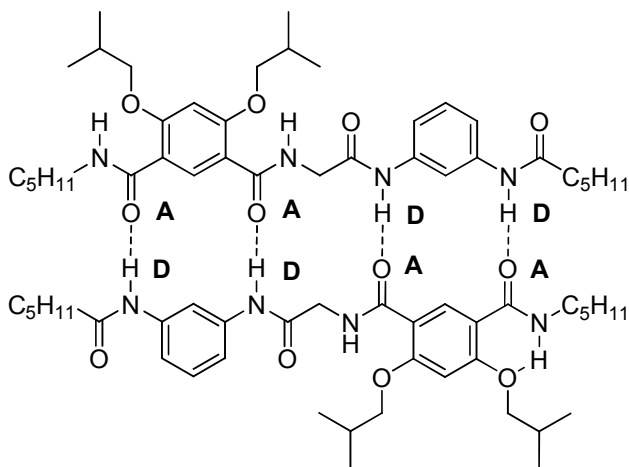
**Figure 1-1** Molecular electrostatic potential surfaces of (a) methanol, (b) methanethiol, (c) pyridine and (d) DMSO by using AM1. Positive point charge regions are shown in blue and negative charge regions are shown in red.

It is well known that a complex formed by only one or two hydrogen bonds is usually weak but multiple hydrogen bonds may provide extremely strong binding for complexation. However, compared with predictable and simple singly hydrogen bonded systems, multiple hydrogen bonded systems can be very complicated. Herein, several factors which affect association constants in such complexes will be summarized.

### 1.1.1 Numbers of Hydrogen Bonds



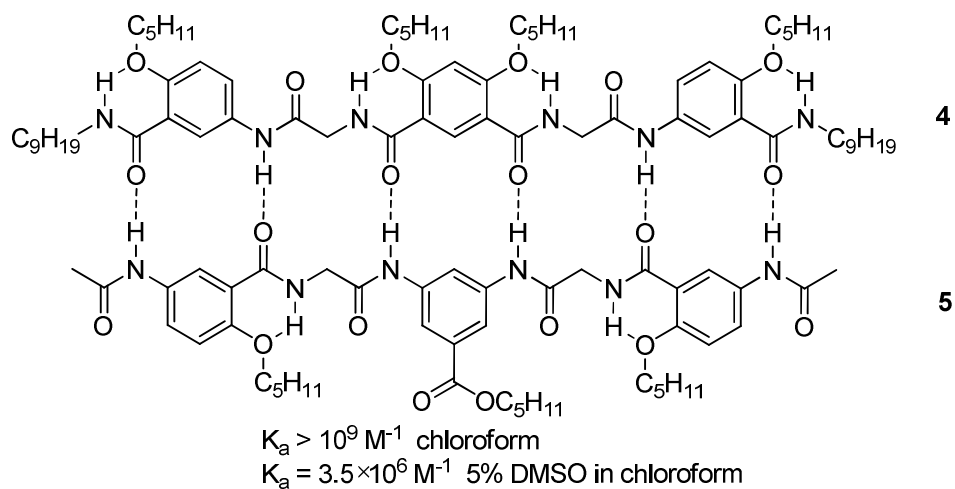
1•1  $K_{\text{dimer}} = 4.4 \times 10^4 \text{ M}^{-1}$  in chloroform



2•2  $K_{\text{dimer}} = 6 \times 10^4 \text{ M}^{-1}$  in chloroform

**Scheme 1-2** Oligoamide duplexes including DADA and DDAA sequences of four hydrogen bonds.

With the increase of numbers of hydrogen bonds, cooperativity contributes to the improved stabilities of systems. That is to say, hydrogen bonded systems may show predictable and adjustable stabilities based on the numbers of hydrogen bonds. Gong and coworkers have shown a combination of subunits from substituted isophthalic acid and m-phenylenediamine results in oligoamides including various hydrogen bonded arrays, which are expected to form hydrogen bonded duplexes. The number of hydrogen bonded sites can be adjusted to afford duplexes with different stabilities. Oligoamides **1** and **2** form homoduplexes (Scheme 1-2).<sup>11</sup> Although oligoamides **1** and **2** have two different self-complementary sequences DADA and AADD respectively, if the experimental error of <sup>1</sup>H NMR titration experiments ( $\pm 10\%$ ) is considered, these two duplexes have similar association constant, which lies in the range of  $10^4 \text{ M}^{-1}$  in chloroform. These results suggest that the dimerization of these oligoamides only depend on the number of hydrogen bonds in each duplex but not the sequence that they are arranged in.



**Scheme 1-3** Oligoamide duplex including six hydrogen bonds.

Since the stability of oligoamide duplexes in this case depends only on the number of intermolecular hydrogen bonds, increasing the number of inter-strand hydrogen bonds in a duplex should lead to an increase in duplex stability. The association constant of hetero-duplex **4/5** including six hydrogen bonds is  $10^9 \text{ M}^{-1}$  in chloroform and still  $3.5 \times 10^6 \text{ M}^{-1}$  even in the mixture of 5% DMSO and 95% chloroform (Scheme 1-3).<sup>12</sup>

### 1.1.2 Secondary Interactions

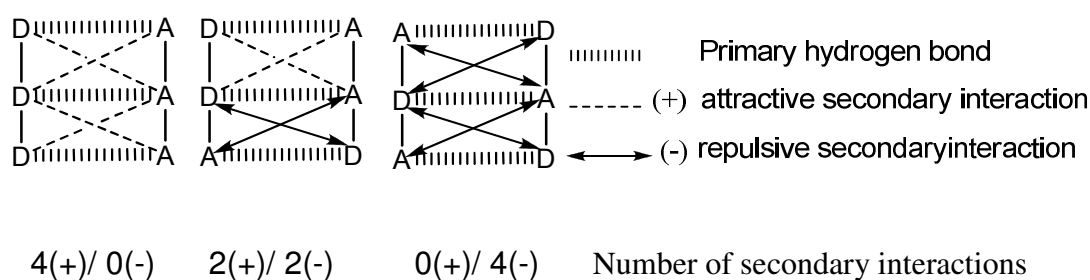


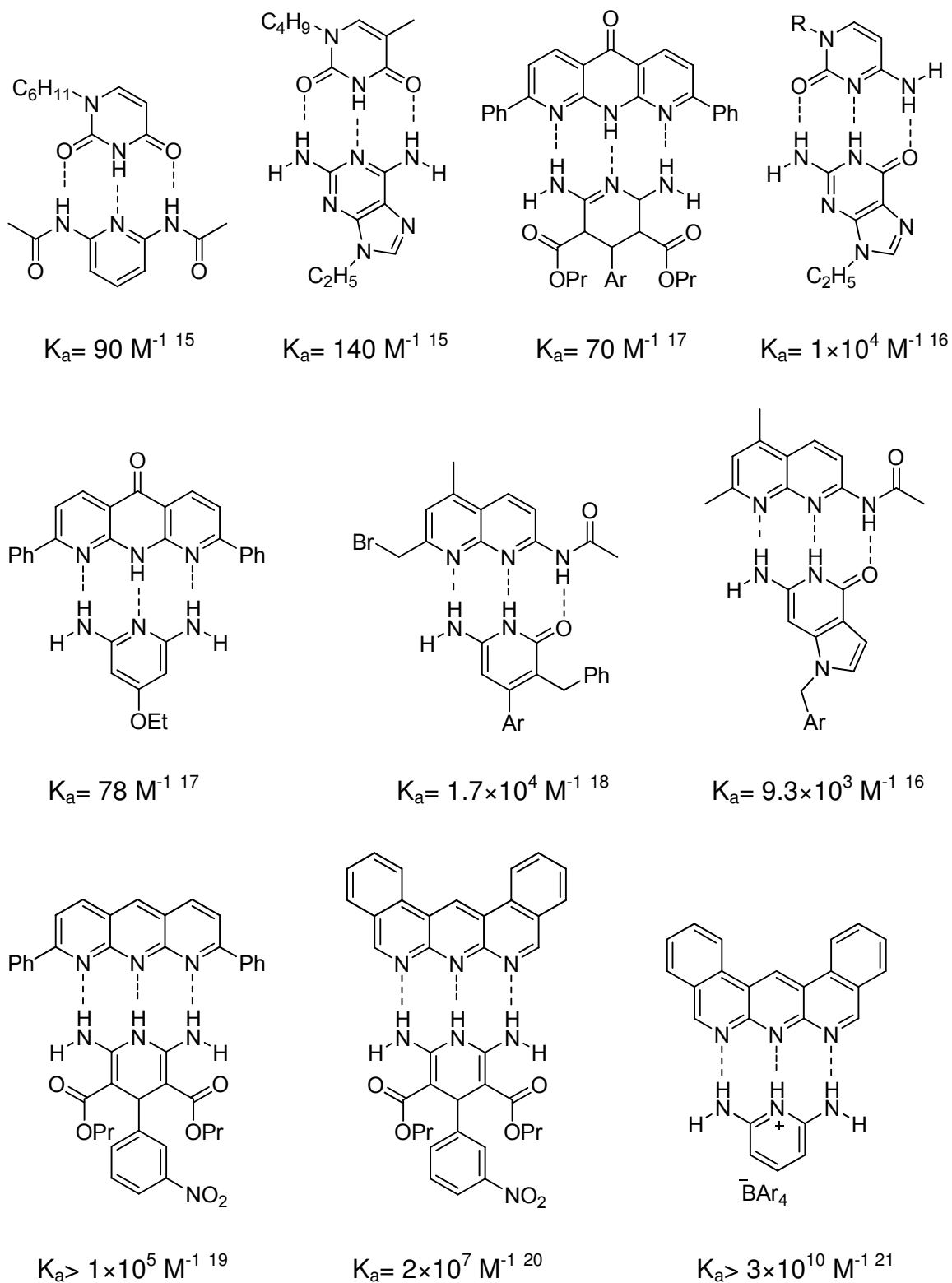
**Figure 1-2** Possible sequences of triply hydrogen bonded dimers including different numbers of secondary interactions.

In multiple hydrogen-bond systems, the arrangement of hydrogen-bond donors and acceptors can play an important role in the stability of the complexes. Jorgensen and coworkers proposed the existence of secondary interactions in multiple hydrogen-bond complexes when the D/A pairs are in close proximity to one another (e. g. DNA nucleobases).<sup>13</sup> The secondary interactions are defined as follows: hydrogen bond donor (D) or acceptor (A) can form the attractive or repulsive interaction with a neighboring hydrogen bond donor and acceptor. For example, there are three possible complementary sequences for triply hydrogen-bonded complexes including different numbers of secondary interactions (Figure 1-2). The AAA-DDD sequence contains the maximum

number of attractive secondary interactions and is anticipated to be the most stable sequence for triply hydrogen-bonded complexes.

Several research groups have determined the association constants of different ADA-DAD, DDA-AAD and DDD-AAA complexes (Scheme 1-4). Generally, the association constant of an ADA-DAD sequence is weaker than that of a DDA-AAD, but the DDD-AAA sequence's association constant is the highest measured one of the three sequences. On the basis of the theory of secondary interactions and available experimental data, Schneider and Sartorius demonstrated that the standard free energy of complex formation consists of -7.9 kJ/mol for each primary hydrogen bond and  $\pm 2.9$  kJ/mol for each secondary interaction (attractive or repulsive). It was found that complexation energies of 58 different complexes were predicted with an average difference between measured and calculated values within 1.8 kJ/mol.<sup>14</sup> From the theoretical studies, association constants for AAA-DDD, AAD-DDA and ADA-DAD are predicted to be  $1.5 \times 10^6$ ,  $1.4 \times 10^4$ , and  $1.3 \times 10^2 \text{ M}^{-1}$  in chloroform respectively. Although the association constant data are from different groups and there may be some experimental error, the practical and calculated results are reasonably well matched.

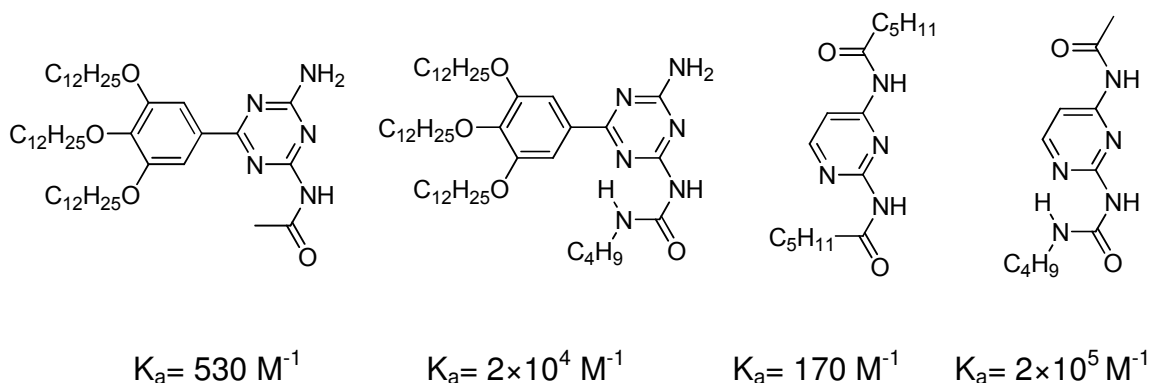
Of course, when neighbouring functional groups are far enough apart, the secondary interactions will be eliminated. The above mentioned examples from Gong and coworkers demonstrate there are no secondary interactions in their hydrogen-bonded systems.



**Scheme 1-4** Triply hydrogen bonded complexes containing different sequences and their measured  $K_a$  values in  $\text{CDCl}_3$  at 298 K.

### 1.1.3 Intramolecular Hydrogen Bonds

According to Etter's hydrogen bond rules,<sup>22</sup> six-member ring intramolecular hydrogen bonds form in preference to intermolecular hydrogen bonds; hydrogen bond donors and acceptors are firstly considered to intramolecular hydrogen bonds and then intermolecular hydrogen bonds. Of course, intramolecular hydrogen bonds may also provide a pre-organized structure for further hydrogen bonding. For example, an intramolecular hydrogen bond evidently increases the association constants in the DADA arrays, as shown in Scheme 1-5.<sup>23</sup> X-ray crystal structures also show that the intramolecular N-H····N hydrogen bonds are longer than the potential intermolecular N-H····O hydrogen bonds and intramolecular hydrogen bonds evidently rigidify the molecular structure.

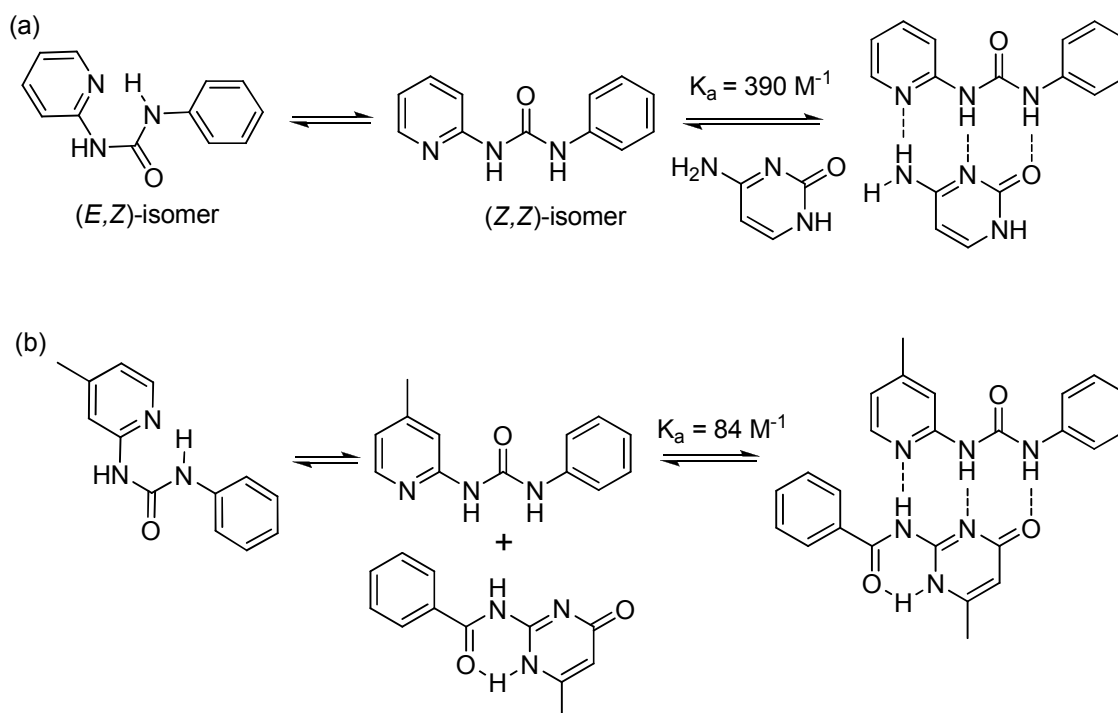


**Scheme 1-5** Dimerization constants for some DADA arrays in  $\text{CDCl}_3$  at 298K.

However, intramolecular hydrogen bonds are not always helpful for intermolecular binding. Pyrid-2-yl ureas are known to have significant biological activity, such as anticancer properties. Pyrid-2-yl ureas have two isomers, *E,Z* and *Z,Z*. Although the *Z,Z* isomer contains an ADD hydrogen bonding array that is complementary to the array of



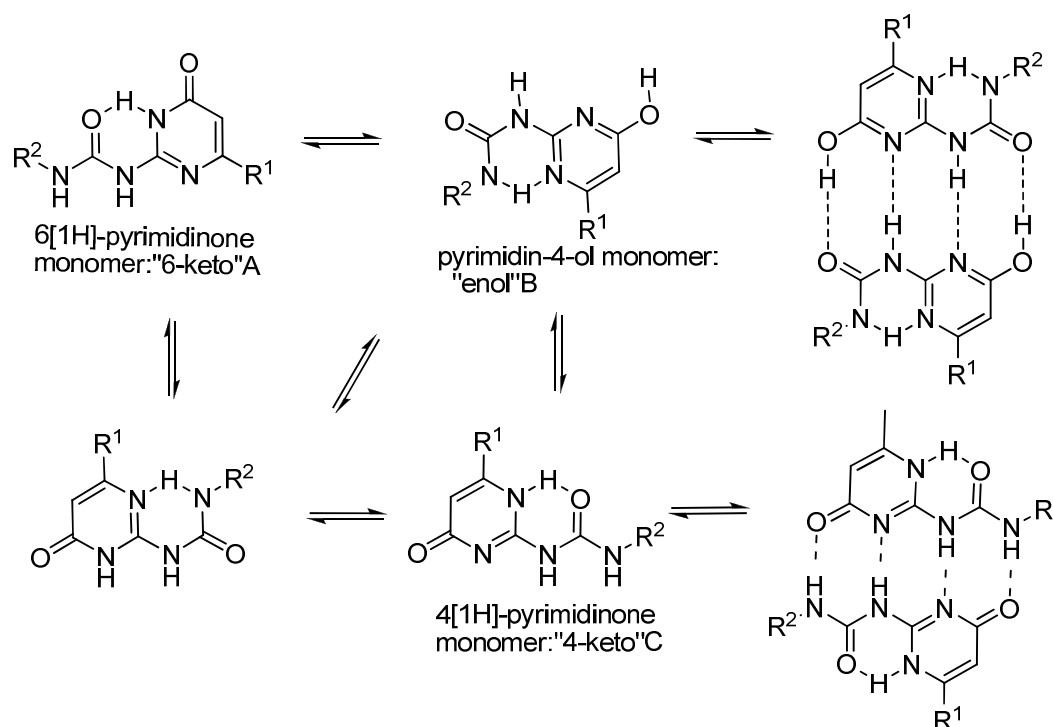
cytosine (a) or phenyl isocytosine (b), their binding is hindered by a competitive intramolecular hydrogen bond between the pyridyl nitrogen and a ureido hydrogen that stabilizes the pyrid-2-yl urea in the *E,Z* isomeric form (Scheme 1-6).<sup>24, 25</sup> In order to form the complementary ADD-DAA complex, the intramolecular hydrogen bond in pyrid-2-yl urea must first be broken.



**Scheme 1-6** Competitive hydrogen bonding of DDA-ADD arrays in  $\text{CDCl}_3$  at 298K.

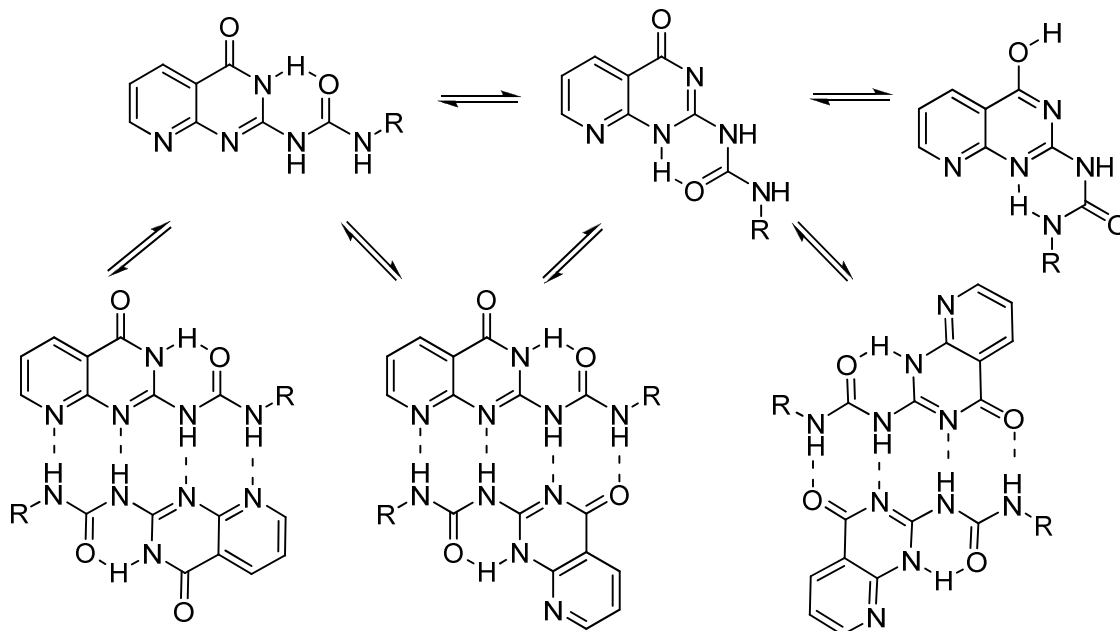
In addition, if there are at least two forms of intramolecular hydrogen bonds, it can create problems with tautomerization. Meijer and coworkers showed that tautomeric forms of ureidopyrimidinones including different intramolecular hydrogen bonds are highly dependent on solvent and framework substitution ( $\text{R}^1$  and  $\text{R}^2$ ) (Scheme 1-7).<sup>26</sup> In the polar solvent DMSO the ureidopyrimidinones existed in the 6[1H]-pyrimidinone monomeric form A (6-keto), whereas in less polar solvents, such as chloroform or

toluene, the pyrimidin-4-ol B (enol) and 4[1H]-pyrimidinone form C (4-keto) can both dimerize via a DDAA and DADA array, respectively. Electron-withdrawing groups ( $R^1 =$  trifluoro- or *p*-nitrophenyl-) favored the pyrimidin-4-ol form B in chloroform or toluene, but when the substituent was the electron donating group (e. g.  $R^1 =$  aryl), the 4[1H]-pyrimidinone C predominated in chloroform.



**Scheme 1-7** Meijer and coworkers' 2-ureido-4[1H]-pyrimidinone tautomeric forms and dimers.

Zimmerman and coworkers developed a similar AADD with several different tautomeric structures (Scheme 1-8).<sup>27</sup>  $^1\text{H}$  NMR spectra in toluene- $d_8$  were consistent with the formation of different 'dimers'. When the solution was diluted from 20 mM to 48  $\mu\text{M}$ , the N-H chemical shifts did not move at room temperature. This indicates there are extremely strong hydrogen bond interactions in the dimers.



**Scheme 1-8** Zimmerman group's AADD tautomeric structures and dimers

### 1.1.4 Preorganization

During the complexation process, the conformations of the two species will adapt to match each other and further form hydrogen bonds. That is to say, the hydrogen bonded complexation process has an entropic cost and this entropic cost will detract from the stability of the complex. There are two major methods to minimize this entropic cost: covalent rigidification and intramolecular hydrogen bond internal preorganization. Both rigid frameworks and intramolecular hydrogen bonds can restrict internal rotations and decrease the entropic cost of the hydrogen bonding process.

### 1.1.5 Solvent

Hydrogen bonding is greatly affected by the solvent polarity, that is, the formation and stability of hydrogen bonded complexes are dependent on the extent of solvation of

donors and acceptors. Generally, the lower the solvent polarity is, the stronger hydrogen bond association is. Thus the contribution of hydrogen bonds in complex formation is generally very weak or nonexistent in protic or highly polar solvents such as DMSO. Purely hydrogen-bonded supramolecular assembly usually only works well in low polarity environments.<sup>28</sup> Therefore chloroform and toluene are often chosen as common solvents in hydrogen bond studies, but unfortunately the solubilities of some donors or acceptors are poor in these solvents and this can cause complications.

In solution there is competition between molecule-solvent, molecule-molecule and solvent-solvent interactions. Hunter has provided a universal equation for the free energy of hydrogen bonding in any solvent:<sup>7</sup>

$$\Delta G = - (\alpha - \alpha_s) (\beta - \beta_s)$$

$\alpha$  and  $\beta$  are hydrogen bond donor and acceptor constants for molecules, and  $\alpha_s$  and  $\beta_s$  are the corresponding hydrogen bond donor and acceptor constants for solvent. The new parameters,  $\alpha$  and  $\beta$  correspond to normalized versions of  $E_{\max}$  and  $E_{\min}$  [ $\alpha = E_{\max}/52 = 4.1(\alpha_2^H + 0.33)$ ,  $\beta = -E_{\min}/52 = 10.3(\beta_2^H + 0.06)$ ] determined from AM1 electrostatic potential surfaces.

Increasing the polarity of the solvent should decrease the complex binding stability. Due to the strong dimerization of ureidopyrimidone, Meijer and coworkers determined the values of  $K_{\text{dim}}$  in several different ratio  $\text{CDCl}_3/\text{DMSO-}d_6$  mixtures with the objective of extrapolating the values to a value in pure  $\text{CDCl}_3$ .<sup>29</sup> The ratio between the dimeric form and the 6[1H]-pyrimidinone tautomer varies in a different ratio mixture of

$\text{CDCl}_3/\text{DMSO-}d_6$ . An increasing ratio of  $\text{DMSO-}d_6$  from 0.3% to 15% in  $\text{CDCl}_3$  resulted in a drastic decrease of dimerization constant from  $1.2 \times 10^6 \text{ M}^{-1}$  to  $100 \text{ M}^{-1}$ .

Chen and coworkers studied the dimerization of an amidourea oligomer in a series of  $\text{DMSO-}d_6/\text{CDCl}_3$  mixtures.<sup>30</sup> As shown in Figure 1-3, the  $K_{\text{dim}}$  values were determined in the range from 1% to 20%  $\text{DMSO-}d_6/\text{CDCl}_3$  mixtures. An increasing amount of  $\text{DMSO-}d_6$  drastically decreases the dimerization constant. With more than 20%  $\text{DMSO-}d_6$  in  $\text{CDCl}_3$ , the dimerization becomes too weak to be quantified by NMR titration.

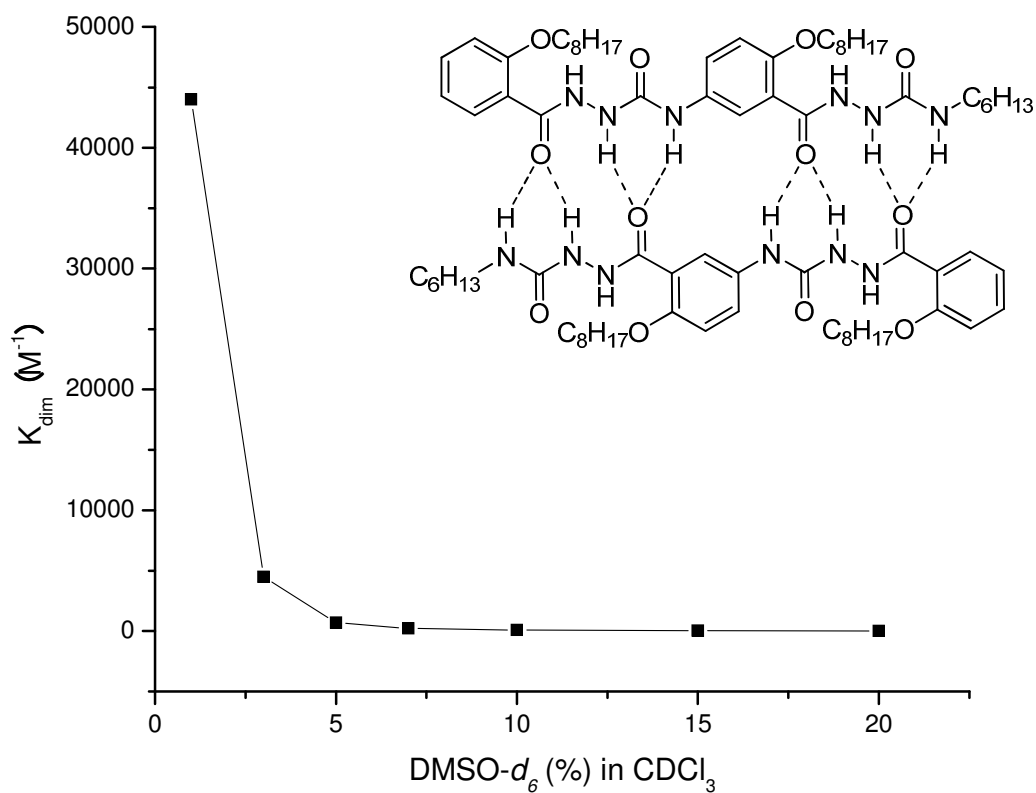


**Figure 1-3** Dimerization constants in various  $\text{DMSO-}d_6/\text{CDCl}_3$  mixtures at 298K.

## 1.2 Hydrogen-Bonded Supramolecular Polymers

Supramolecular polymers are built up via noncovalent interactions (such as hydrogen bonds,<sup>31</sup> metal-ligand coordination,<sup>32</sup> hydrophobic or  $\pi$ -stacking interactions<sup>33</sup>) between monomers while traditional polymers are composed of covalently linked monomers (Figure 1-4). Supramolecular polymerizations, main-chain and side-chain supramolecular polymers have been extensively reviewed.<sup>34</sup> A brief overview is provided here and a more detailed description is provided in Chapter 4.

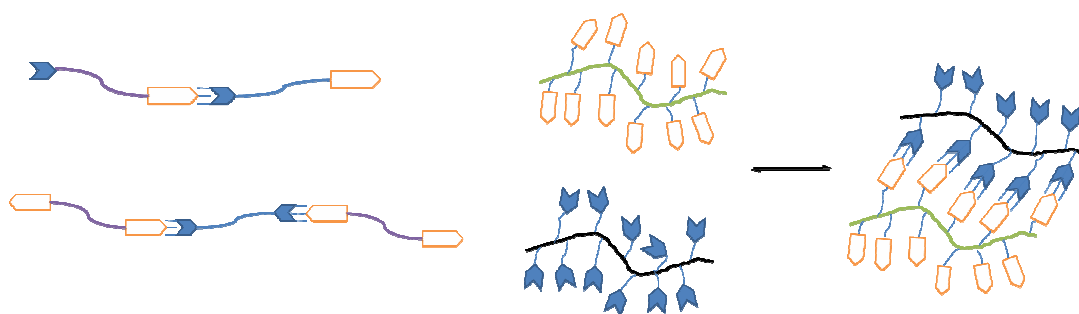
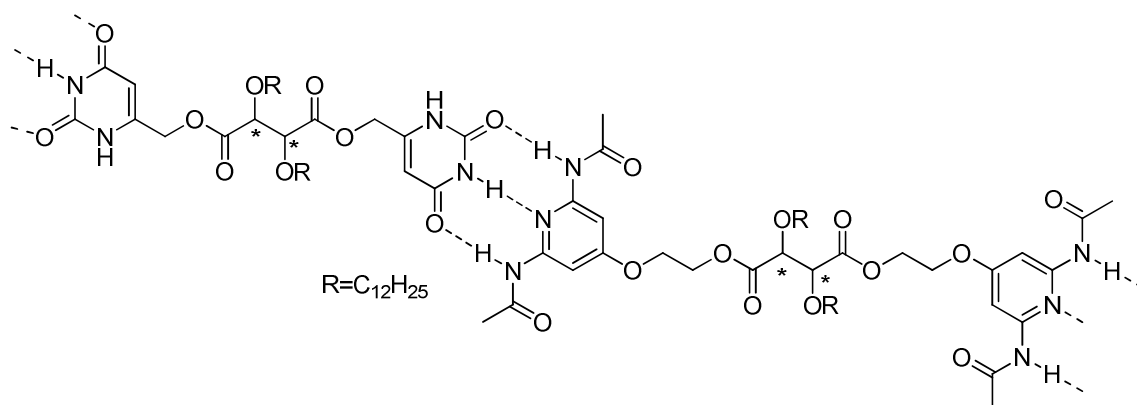


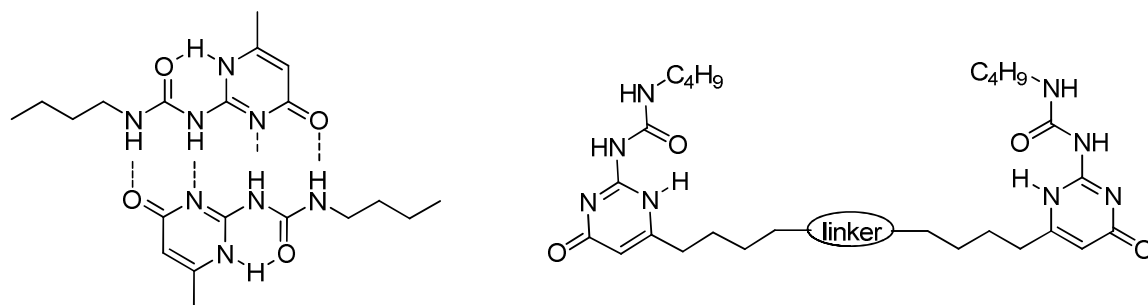
**Figure 1-4** Main-chain and cross-linked supramolecular polymers.

Lehn and coworkers developed the first liquid crystalline supramolecular polymers (Scheme 1-9).<sup>35</sup> The association of a bis-uracil terminated monomer including an ADA sequence and a bis-2,6-diaminopyridine terminated monomer including a DAD sequence was investigated. Although there is a weak association ( $K_a = 500 \text{ M}^{-1}$ ) between 2,6-diaminopyridine and uracil, the thermodynamics of the molecular recognition still favors the complexation. Both bis-uracil and bis-2,6-diaminopyridine functionalized monomers were shown not to be mesogenic by themselves; however, their equimolar mixture gave rise to thermotropic hexagonal columnar mesophases with a wide temperature domain of liquid crystallinity. The columns had a triple-helical superstructure. For a given pair of

chiral bifunctional 2,6-diaminopyridine and uracil, the triple-helical structures would further organize into higher-order hierarchical assemblies displaying the same handedness as the chiral monomers. This pioneering work demonstrated that the self-assembly of small molecular building blocks into macromolecular chains was feasible.



**Scheme 1-9** Liquid crystalline supramolecular polymers formed from bifunctional 2,6-diaminopyridines and uracils



**Scheme 1-10** Example structures of a 2-ureido-4[1H]-pyrimidinone dimer and monomer for supramolecular polymer formation.

Perhaps the milestone work in the development of supramolecular polymers was the elaboration of self-complementary 2-ureido-4[1H]-pyrimidinone (UPy) derivatives by Meijer and coworkers. The extremely strong dimerization of UPy units (association

constant  $K_{\text{dim}} > 10^6 \text{ M}^{-1}$  in  $\text{CHCl}_3$ ) was used to provide the associating end groups in self-assembled polymer systems (Scheme 1-10).<sup>36</sup> These types of polymers form highly viscous dilute solutions and display self-healing properties.

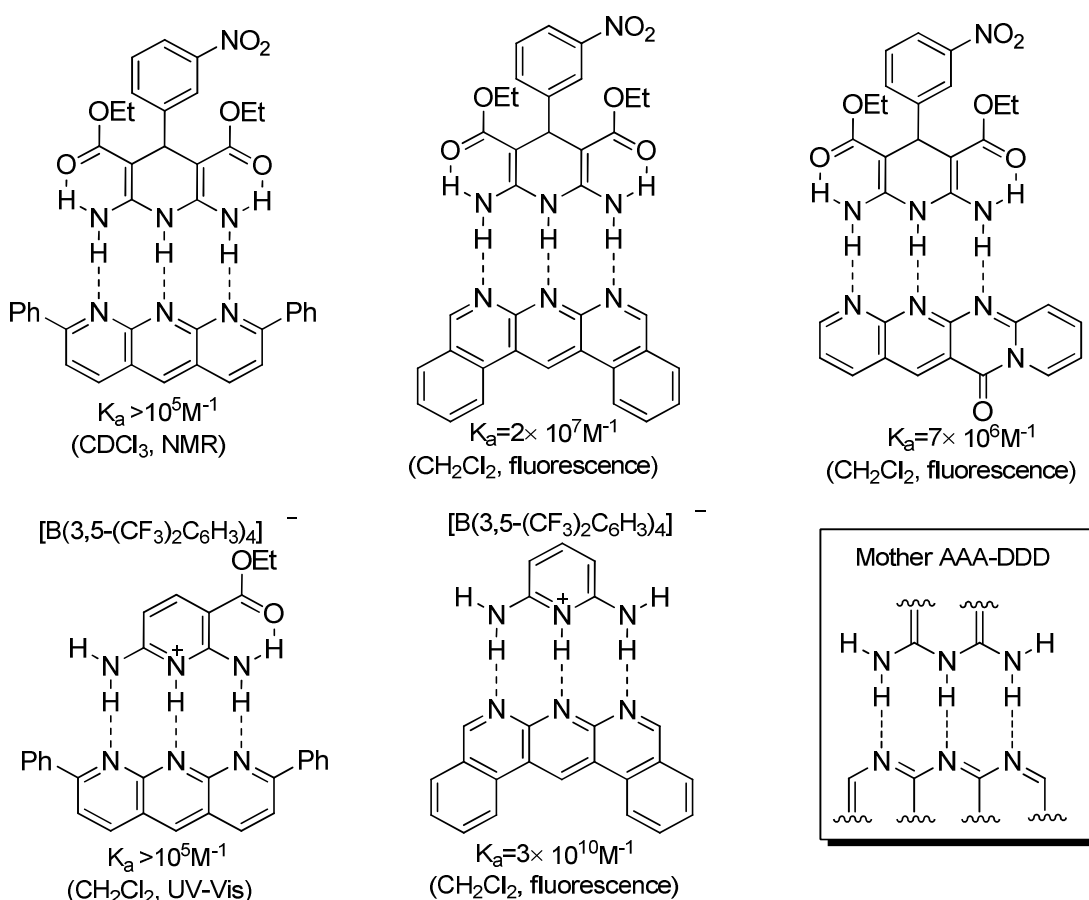
Although the development of UPy functionality with a high association constant opened the way for the exploration of supramolecular polymers, self-complementary systems can be undesirable for controlled polymer synthesis and functionalization since once the functional groups are formed, they participate in uncontrolled functional group dimerization and further lead to uncontrolled polymerization or cross-linking. Supramolecular polymerizations based on complementary hydrogen bonds are significantly important in life science and have also attracted scientific interest. Supramolecular copolymers self-assembled by complementary quadruple or more hydrogen bonds have been extensively investigated.<sup>37</sup>

### 1.3 Scope of the Thesis

Although three hydrogen bonds provide several complementary binding arrays (i. e. ADA-DAD, AAD-DDA and AAA-DDD), the DDD-AAA pattern has been demonstrated to produce the strongest triple hydrogen bond arrangement because of the favorable secondary interactions. There are few examples of DDD-AAA triple hydrogen bond complexes. Zimmerman *et al* reported the first DDD-AAA complex but could not obtain the association constant as a result of the instability of the complex.<sup>38</sup> In addition, there is another tautomerized structure for the DDD molecule in chloroform. Leigh and coworkers demonstrated that a similar AAA molecule could be used to improve the complex's stability and obtained an extremely high association constant.<sup>39</sup> Cationic

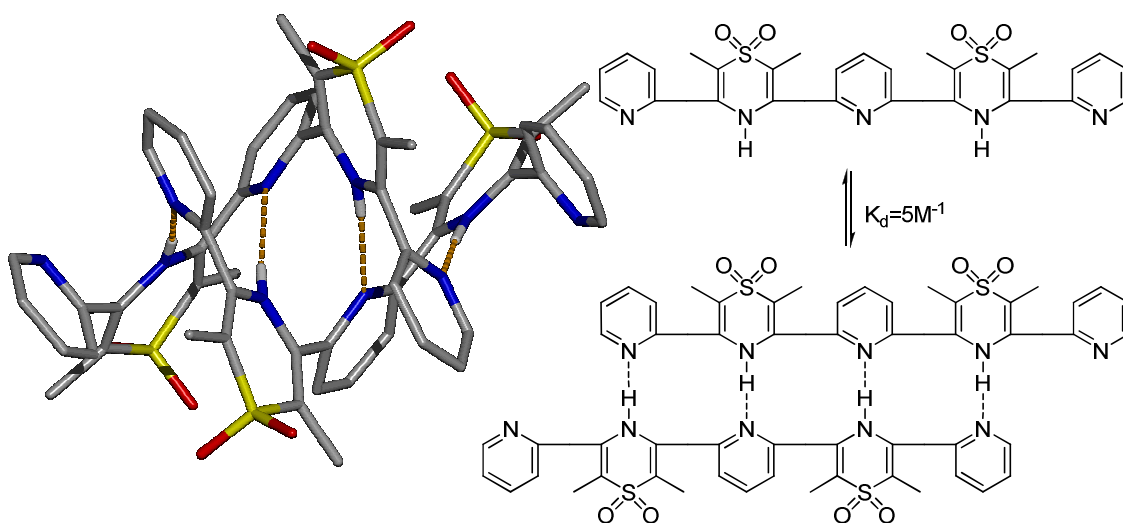


DDD's also can form complexes with AAAs that display even higher association constants.<sup>40</sup> Unfortunately, the proton in this kind of cationic DDDs is highly sensitive to solvent  $pK_a$ . In addition, the corresponding anion for cationic DDD must be conjugated base of extremely strong acid. Although all the reported AAA-DDD examples show very high association constants, they have been developed from the same coplanar mother structures (Scheme 1-11) that limit the options for modification.



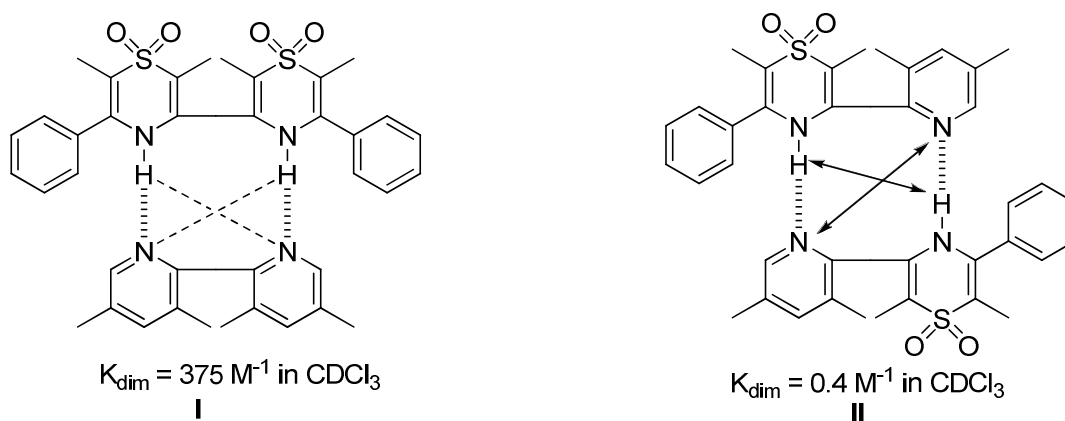
**Scheme 1-11** Some reported AAA-DDD complexes with high association constants and their mother structure (there are titration method and solvent for the investigation of association constants in parentheses)

All the above known AAA and DDD structures contain some advantages for hydrogen bonding, such as favorable secondary interactions, pre-organized and rigid structures. Although hydrogen bonds are exploitable and versatile for supramolecular assemblies, it remains difficult and challenging to design double helices of which the formation is predictable because there are no pre-organized and rigid structures and the effect of secondary interactions has not been explored in non-coplanar structures. Wisner and coworkers have recently described the formation of a double-helical complex from a pentacyclic oligomer of pyridine and thiazine-1,1-dioxide heterocycles that self-associates through an ADADA hydrogen bond array (Scheme 1-12).<sup>41</sup> In contrast to planar arrays, the adjacent hydrogen bond donor-acceptor pairs in this double helical example are oriented at an approximately 90° angle to one another when viewed down the axis of the double helix. Surprisingly, even though the complex forms through four primary hydrogen bonds, the overall dimer stability in solution is remarkably low ( $K_{\text{dim}} = 5 \text{ M}^{-1}$ ).



**Scheme 1-12** Hydrogen bonded double helical structure.

In an attempt to rationalize why the association constant of our hydrogen bonded double helical complex is very low, former Ph.D. student Jiaxin Li synthesized a variety of homo- and hetero- complexes and determined whether the arrangement of the donor/acceptor pairs in this type of complex has a significant effect on stability.<sup>42</sup> Here, we highlight the binding properties of two complexes in Scheme 1-13.

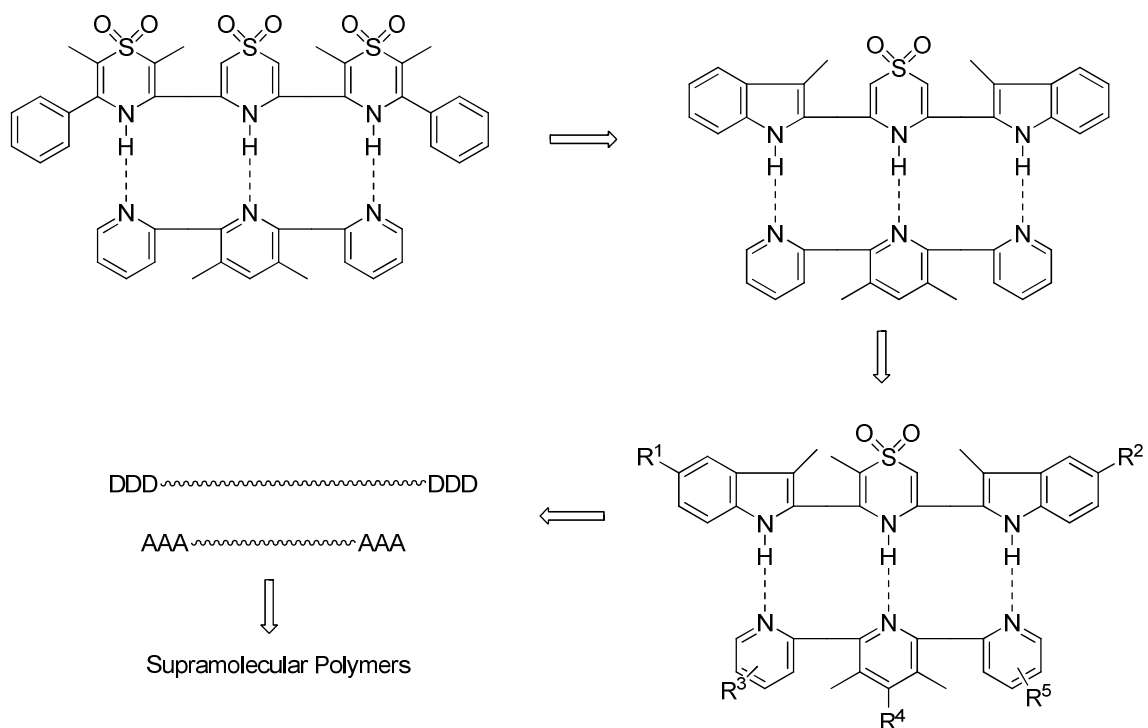


**Scheme 1-13** Primary hydrogen bonds and secondary interactions in DD/AA and AD/DA complexes

**Table 1-1** Calculated electrostatic interactions between each pair of complexes **I** and **II**.

Complex	<b>I</b>	<b>II</b>
Primary hydrogen bonds (kcal/mol)	-8.3	-8.0
Secondary hydrogen bonds (kcal/mol)	6.0	16.2
Total hydrogen bonds (kcal/mol)	-2.3	8.2
Total electrostatic interactions (kcal/mol)	-15.8	-11.0

The experimental investigation showed that the binding energy for complexes **I** and **II** are 3.5 kcal/mol and 0.5 kcal/mol respectively. Theoretical calculations demonstrate that secondary interactions lead to the stability difference of two complexes (Table 1-1). Although complexes **I** and **II** have the same number of primary hydrogen bonds, their secondary hydrogen bonds are definitely different (10.2 kcal/mol). Therefore, secondary hydrogen bonds play an important role in the formation of a stable hydrogen bonded double helix.



**Scheme 1-14** Schematic summary of the thesis scope

In order to achieve a highly stable hydrogen-bonded double helix, we must make sure that the secondary interactions are favorable in the sequence and hence a non-coplanar AAA-DDD array will be the best choice. In this thesis, we firstly designed and synthesized a DDD oligomer based on thiazine dioxides. Moreover, we have developed a

new kind of DDD based on indole and thiazine dioxide subunits. Secondly, how electron-withdrawing groups on indole subunits and electron-donating groups on pyridine subunits affect the complex stability was investigated. Finally, supramolecular copolymers were formed from bisAAA and bisDDD and their supramolecular polymerization was studied.

## 1.4 References

1. Alberts, B.; Johnson, A.; Lewis, J.; Raff, M.; Roberts, K.; Walter, P. *Molecular Biology of the Cell (Fourth Edition)*, New York: Garland Science, **2002**.
2. Alba, M. M. *Genome Bio.* 2001, 2, reviews3002.1-3002.4.
3. Albercht, M. *Angew. Chem. Int. Ed.* **2005**, 44, 6448.
4. (a) Kyogoku, Y.; Lord, R. C.; Rich, A. *J. Am. Chem. Soc.* **1967**, 89, 496. (b) Sartorius, J.; Schneider, H.-J. *Chem. Eur. J.* **1996**, 2, 1446.
5. For example: (a) Nangreave, J.; Yan, H.; Liu, Y. *J. Am. Chem. Soc.* **2011**, 133, 4490. (b) Nangreave, J.; Yan, H.; Liu, Y. *Biophys. J.* **2009**, 97, 563. (c) Endo, M.; Katsuda, Y.; Hidaka, K.; Sugiyama, H. *J. Am. Chem. Soc.* **2010**, 132, 1592. (d) Aldaye, F. A.; Sleiman, H. *J. Am. Chem. Soc.* **2007**, 129, 10070. (e) Aldaye, F. A.; Sleiman, H. *J. Am. Chem. Soc.* **2007**, 129, 13376. (f) Gao, P.; Cai, Y. *ACS Nano* **2009**, 3, 3475. (g) Seeman, N. C. *Chem. Bio.* **2003**, 10, 1151. (h) Krishnan, Y.; Simmel, F. C. *Angew. Chem. Int. Ed.* **2011**, 50, 3124.
6. Uhlmann, E.; Peyman, A.; Breipohl, G.; Will, D. W. *Angew. Chem. Int. Ed.* **1998**, 37, 2796.
7. Hunter, C. A. *Angew. Chem. Int. Ed.* **2004**, 43, 5310.

8. (a) Abraham, M. H.; Greller, P. L.; Prior, D. V.; Taft, R. W.; Morris, J. J.; Taylor, P. J.; Laurence, C.; Berthelot, M.; Doherty, R. M.; Kamlet, M. J.; Abboud, J. L. M.; Sraidi, K.; Guiheneuf, G. *J. Am. Chem. Soc.* **1988**, *110*, 8534. (b) Marco, J.; Orza, J. M.; Notario, R.; Abboud, J. L. M. *J. Am. Chem. Soc.* **1994**, *116*, 8841. (c) Abraham, M. H.; Berthelot, M.; Laurence, C.; Taylor, P. J. *J. Chem. Soc., Perkin Trans.2* **1998**, 187.
9. Abraham, M. H.; Platts, J. A. *J. Org. Chem.* **2001**, *66*, 3484.
10. (a) Zissimos, A. M.; Abraham, M. H.; Klamt, A.; Eckert, F.; Wood, J. *J. Chem. Inf. Comput. Sci.* **2002**, *42*, 1320. (b) Platts, J. A. *Phys. Chem. Chem. Phys.* **2000**, *2*, 973.
11. (a) Gong, B.; Yan, Y.; Zeng, H. Q.; Skrzypczak-Jankunn, E.; Kim, Y. W.; Zhu, J.; Ickes, H. *J. Am. Chem. Soc.* **1999**, *121*, 5607. (b) Zeng, H. Q.; Miller, R. S.; Flowers, R. A.; Gong, B. *J. Am. Chem. Soc.* **2000**, *122*, 2635.
12. Yuan, L. H.; Zeng, H. Q.; Yamato, K.; Sanford, A. R.; Feng, W.; Atreya, H.; Sukumaran, D. K.; Szyperski, T.; Gong, B. *J. Am. Chem. Soc.* **2004**, *126*, 16528.
13. (a) Jorgensen, W. L.; Pranata, J. *J. Am. Chem. Soc.* **1990**, *112*, 2008. (b) Pranata, J.; Wierschke, S. G.; Jorgensen, W. L. *J. Am. Chem. Soc.* **1991**, *113*, 2810.
14. Sartorius, J.; Schneider, H.-J. *Chem. Eur. J.* **1996**, *2*, 1446.
15. Kyogoku, Y.; Lord, R. C.; Rich, A. *Proc. Natl. Acad. Sci. USA*, **1967**, *57*, 250.
16. Hamilton, A. D.; Van Engen, D. *J. Am. Chem. Soc.* **1987**, *109*, 6549.
17. Murray, T. J.; Zimmerman, S. C. *J. Am. Chem. Soc.* **1992**, *114*, 4010.
18. Kelly, T. R.; Bridger, G. J.; Zhao, C. *J. Am. Chem. Soc.* **1990**, *112*, 8024.

19. Murray, T. J.; Zimmerman, S. C.; Kolotuchin, S. V. *Tetrahedron*, **1994**, *50*, 635.
20. Djurdjevic, S.; Leigh, D. A.; McNab, H.; Parsons, S.; Teobaldi, G.; Zerbetto, F. J. *Am. Chem. Soc.* **2007**, *129*, 476.
21. Blight, B. A.; Camara-Campos, A.; Djurdjevic, S.; Kaller, M.; Leigh, D. A.; McMillan, F. M.; McNab, H.; Slawin, A. M. Z. *J. Am. Chem. Soc.* **2009**, *131*, 14116.
22. Etter, M. C. *Acc. Chem. Res.* **1990**, *23*, 120.
23. Beijer, F. H.; Kooijman, H.; Spek, A. L.; Sijbesma, R. P.; Meijer, E. W. *Angew. Chem. Int. Ed.* **1998**, *37*, 75.
24. (a) Corbin, P. S.; Zimmerman, S. C.; Thiessen, P. A.; Hawryluk, N. A.; Murray, T. J. *J. Am. Chem. Soc.* **2001**, *123*, 10475. (b) Chien, C. H.; Leung, M. K.; Su, J. K.; Li, G. H.; Liu, Y. H.; Wang, Y. *J. Org. Chem.* **2004**, *69*, 1866.
25. McGhee, A. M.; Kilner, C.; Wilson, A. J. *Chem. Commun.* **2008**, 344.
26. (a) Beijer, F. H.; Kooijman, H.; Spek, A. L.; Sijbesma, R. P.; Meijer, E. W. *J. Am. Chem. Soc.* **1998**, *120*, 6761. (b) Sijbesma, R. P.; Meijer, E. W. *Chem. Commun.* **2003**, 5. (c) Sontjens, S. H. M.; Sijbesma, R. P.; van Genderen, M. H. P.; Meijer, E. W. *J. Am. Chem. Soc.* **2000**, *122*, 7487.
27. Corbin, P. S.; Zimmerman, S. C. *J. Am. Chem. Soc.* **1998**, *120*, 9710.
28. (a) Kelly, T. R.; Kim, M. H. *J. Am. Chem. Soc.* **1994**, *116*, 7072. (b) Jeffrey, G. A. *An introduction to Hydrogen Bonding*, Oxford University Press, New York, 1997. (c) Cook, J. L.; Hunter, C. A.; Low, C. M. R.; Perez-Velasco, A.; Winter, J. G. *Angew. Chem. Int. Ed.* **2007**, *46*, 3706.

29. Beijer, F. H.; Sijbesma, R. P.; Kooijman, H.; Spek, A. L.; Meijer, E. W. *J. Am. Chem. Soc.* **1998**, *120*, 6761.
30. Chu, W. -J.; Yang, Y.; Chen, C. -F. *Org. Lett.* **2010**, *12*, 3156.
31. Some examples for hydrogen-bonded supramolecular polymers, see: (a) Beijer, F. H.; Sijbesma, R. P.; Kooijman, H.; Spek, A. L.; Meijer, E. W. *J. Am. Chem. Soc.* **1998**, *120*, 6761. (b) Beijer, F. H.; Kooijman, H.; Spek, A. L.; Sijbesma, R. P.; Meijer, E. W. *Angew. Chem. Int. Ed.* **1998**, *37*, 75. (c) Boileau, S.; Bouteiller, L.; Laupretre, F.; Lortie, F. *New. J. Chem.* **2000**, *24*, 845. (d) Corbin, P. S.; Zimmerman, S. C. *J. Am. Chem. Soc.* **1998**, *120*, 9710. (e) Scherman, O.A.; Lighthart, G. B. W. L.; Sijbesma, R. P.; Meijer, E. W. *Angew. Chem. Int. Ed.* **2006**, *45*, 2072.
32. Some examples for supramolecular polymers based on metal-ligand coordination interaction, see: (a) Fraser, C. S. A.; Jennings, M. C.; Puddephatt, R. J. *Chem. Commun.* **2001**, 1310. (b) Hofmeier, H.; Hoogenboom, R.; Wouters, M. E. L.; Schubert, U.S. *J. Am. Chem. Soc.* **2005**, *127*, 2913. (c) Beck, J. B.; Ineman, J. M.; Rowan, S. J. *Macromolecules* **2005**, *38*, 5060. (d) Yount, W. C.; Loveless, D. M.; Craig, S. L. *J. Am. Chem. Soc.* **2005**, *127*, 14488. (e) Carlise, J. R.; Weck, M. J. *Polym. Sci. Polym. Chem.* **2004**, *42*, 2973. (f) Kurth, D. G.; Higuchi, M. *Soft Matter* **2006**, *2*, 915. (g) Paulusse, J. M. J.; Sijbesma, R.P. *Chem. Commun.* **2003**, 1494.
33. Some examples for  $\pi$ - $\pi$  stacking in supramolecular polymers, see: (a) Adam, D.; Schuhmacher, P.; Simmerer, J.; Haussling, L.; Siemensmeyer, K.; Etzbach, K. H.; Ringsdorf, H.; Haarer, D. *Nature* **1994**, *371*, 141. (b) Tracz, A.; Jeszka, J. K.; Watson, M. D.; Pisula, W.; Mullen, K.; Pakula, T. *J. Am. Chem. Soc.* **2003**, *125*, 1682. (c) Wu, J.; Watson, M. D.; Zhang, L.; Wang, Z.; Mullen, K. *J. Am. Chem. Soc.* **2004**, *126*,



177. (d) Rohr, U.; Schiliching, P.; Bohm, A.; Gross, M.; Meerholz, K.; Brauchle, C.; Mullen, K. *Angew. Chem. Int. Ed.* **1998**, *37*, 1434.
34. (a) Fox, J. D.; Rowan, S. J. *Macromolecules*. **2009**, *42*, 6823. (b) De Greef, T. F. A.; Smulders, M. M. J.; Wolffs, M.; Schenning, A. P. H. J.; Sijbesma, R. P.; Meijer, E. W. *Chem. Rev.* **2009**, *109*, 5687. (c) Ciferri, A. *Macromol. Rap. Commun.* **2002**, *23*, 511. (d) Shimizu, L. S. *Polym. Int.* **2007**, *56*, 444. (e) Weck, M. *Polym. Int.* **2007**, *56*, 453. (f) Brunsveld, L.; Folmer, B. J. B.; Meijer, E. W.; Sijbesma, R. P. *Chem. Rev.* **2001**, *101*, 4071.
35. (a) Fouquey, C.; Lehn, J. -M.; Levelut, A. -M. *Adv. Mater.* **1990**, *2*, 254. (b) Gulik-Krzywicki, T.; Fouquey, C.; Lehn, J. -M. *Proc. Natl. Acad. Sci. U. S. A.* **1993**, *90*, 163.
36. (a) Sijbesma, R. P.; Beijer, F. H.; Brunsveld, L.; Folmer, B. J. B.; Ky Hirschberg, J. H. K.; Lange, R. F. M.; Lowe, J. K. L.; Meijer, E. W. *Science* **1997**, *278*, 1601. (b) Beijer, F. H.; Sijbesma, R. P.; Kooijman, H.; Spek, A. L.; Meijer, E. W. *J. Am. Chem. Soc.* **1998**, *120*, 6761. (c) Beijer, F. H.; Kooijman, H.; Spek, A. L.; Sijbesma, R. P.; Meijer, E. W. *Angew. Chem. Int. Ed.* **1998**, *37*, 75.
37. (a) Park, T.; Zimmerman, S.C. *J. Am. Chem. Soc.* **2006**, *128*, 13986. (b) Yang, X.; Hua, F.; Yamato, K.; Ruckenstein, E.; Gong, B.; Kim, W.; Ryu, C. Y. *Angew. Chem. Int. Ed.* **2004**, *43*, 6471.
38. (a) Murray, T. J.; Zimmerman, S. C. *J. Am. Chem. Soc.* **1992**, *114*, 4010. (b) Murray, T. J.; Zimmerman, S.C.; Kolotuchin, S. V. *Tetrahedron* **1995**, *51*, 635.

39. Djurdjevic, S.; Leigh, D. A.; McNab, H.; Parsons, S.; Teobaldi, G.; Zerbetto, F. J. *Am. Chem. Soc.* **2007**, *129*, 476.
40. (a) Bell, D. A.; Anslyn, E. A. *Tetrahedron* **1995**, *51*, 7161. (b) Blight, B. A.; Camara-Campos, A.; Djurdjevic, S.; Kaller, M.; Leigh, D. A.; McMillan, F. M.; McNab, H.; Slawin, A. M. Z. *J. Am. Chem. Soc.* **2009**, *131*, 14116.
41. Li, J.; Wisner, J. A.; Jennings, M. C. *Org. Lett.* **2007**, *9*, 3267.
42. Li, J. Ph. D. thesis. University of Western Ontario, London, Ontario, **2009**.

## CHAPTER 2

### Design and Optimization of Hydrogen-Bonded AAA-DDD Double Helices

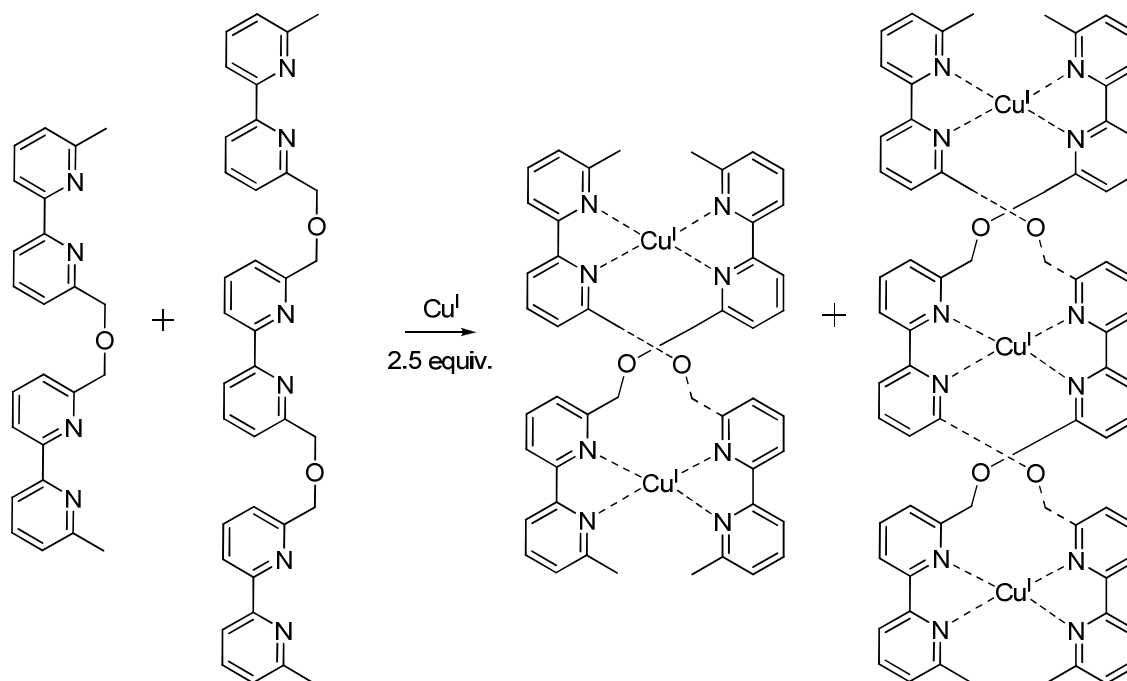
#### 2.1 Artificial Double Helical Structures

Since the discovery of DNA's double helix in 1953, chemists have made extensive efforts to explore how linear molecules can mimic natural DNA to self-assemble into artificial double-helical polymers and oligomers.<sup>1</sup> While a number of synthetic polymers and oligomers fold into single helical conformations, only a few types of backbones have been available for constructing double helical structures. We will focus here on examples employing discrete (i.e., non-polymeric) oligomers that self-assemble into double helices in solution.

##### 2.1.1 Double Helices through Template Synthesis

Template synthesis is the use of a template to play the role of a skeleton in order to organize different building blocks around it and form well-defined architectures. The term "template" has been popularly used in biology, chemistry and materials science. Bush gave the following definition of "chemical template":<sup>2</sup> "*A chemical template organizes an assembly of atoms, with respect to one or more geometric loci, in order to achieve a particular linking of atoms.*" Chemical templates have been successfully applied to control covalent molecular reactions. Template-based synthesis is also a well-established method in the construction of supramolecular architectures. In order to form a

complex supramolecular structure, the template must induce an assembly of several building blocks via non-covalent interactions. The template effect has been diversely achieved by cationic, neutral and anionic species.

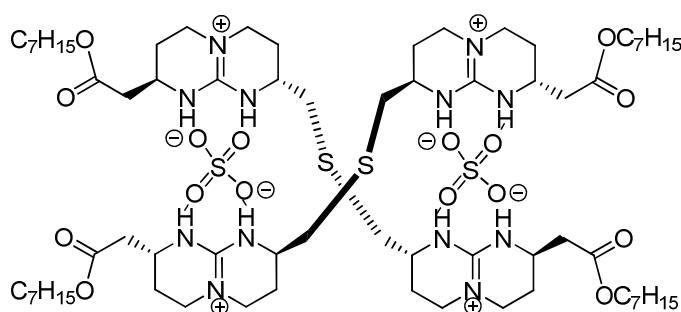


**Scheme 2-1** Length-dependent copper (I) double helicates.

The most common artificial double helical structures are the so-called helicates that consists of ligand-containing molecular strands and transitional metal ion templates, of which geometrical preference determines the three-dimensional structures. Lehn and coworkers systematically studied the helically oriented self-assembling oligomers in the presence of a metal template.<sup>3</sup> Such two 2,2'-bipyridine units interweaved into a double helix around the metal Cu(I). Only a metal ion with the appropriate feature allows the formation of the double helix. Oligomers with various two 2,2'-bipyridine unit numbers showed the unit-number-dependent self-recognition selectivity: A mixture of oligomers

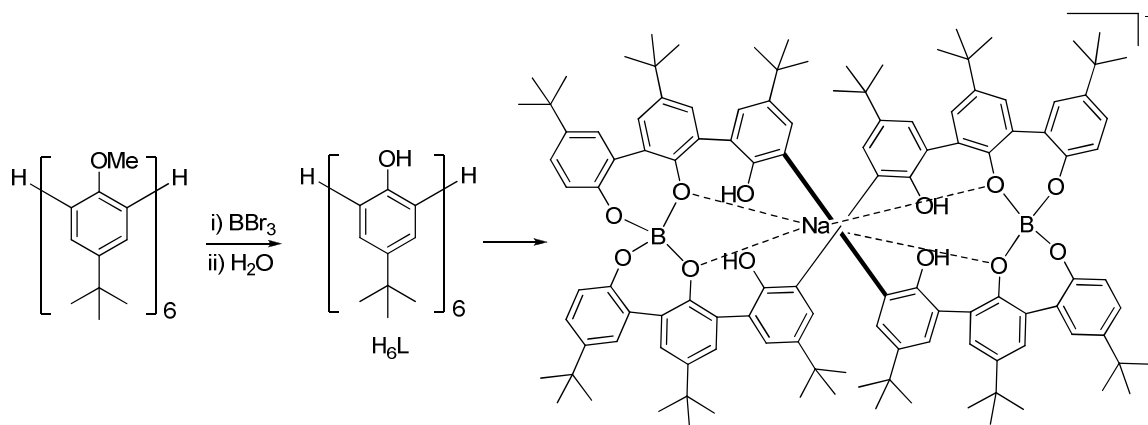
including different 2,2'-bipyridine units gave only homostrand double helices (Scheme 2-1).<sup>4</sup>

Anion templates have also been used in the assembly of double helical complexes (Scheme 2-2). Enantiomerically pure chiral bicyclic guanidinium salts self-assembled into a double stranded helical structure via sulfate templates are a good example of anion-template double helix.<sup>5</sup> ROESY NMR and circular dichroism spectra demonstrated the formation of the helical structure.



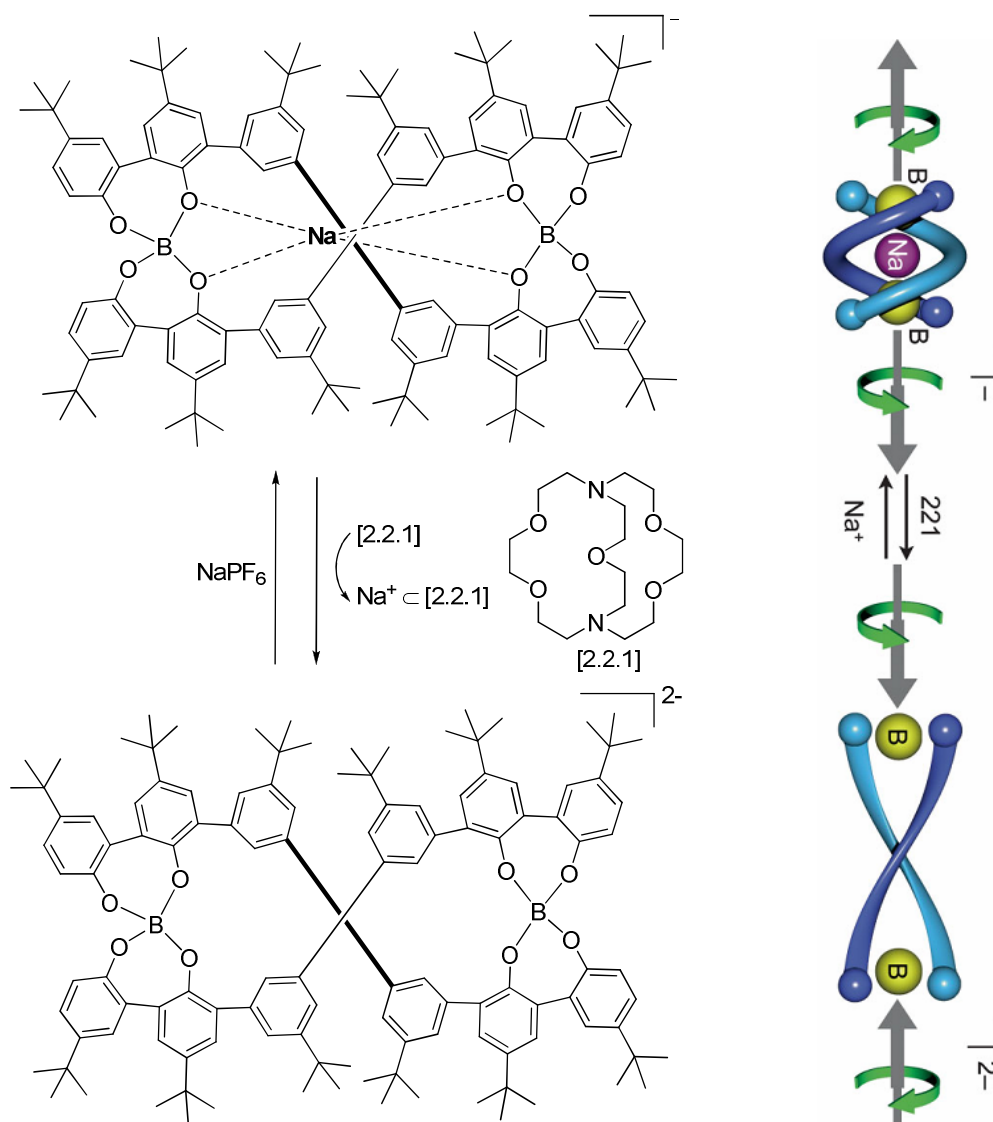
**Scheme 2-2** Anion-templated double helical structure.

Furusho, Yashima and coworkers found that when *ortho*-linked hexaphenol ( $H_6L$ ) was prepared, a double helicate boron complex unexpectedly crystallized from a  $CDCl_3$  solution containing a small amount of boric acid in toluene (Scheme 2-3).<sup>6</sup> The single crystal X-ray structure revealed that the two strands were bridged by spiroborates formed from the terminal biphenol units and the boron atoms. The boron helicate could also be synthesized by heating a mixture of sodium borohydride and  $H_6L$  in ethanol /1,2-dichloro ethane at  $80^\circ C$ .<sup>7</sup> Interestingly, because the helicate embraces a sodium ion at the center that was coordinated by eight oxygen atoms, the sodium ion can not be removed by crown ethers or cryptands.



**Scheme 2-3** Formation of a boron templated double helicate.

The crystal structure of the hexaphenol helicate also demonstrated that the four central hydroxyl groups did not participate in the boron coordination for the formation of double helicate. With this mind,  $H_6L$ , which contains a tetraphenol lacking two central hydroxyl groups on the hexa(*m*-phenylene)backbone, still can form the double helicate; however, the central sodium ion was completely removed by cryptand [2.2.1] to afford the dianionic helicate (Scheme 2-4).<sup>8</sup> The removal of sodium ion unmasked the negative charges between the borates and caused them to repel each other, triggering a large extension of the helicate. The crystal structure and  $^1\text{H}$  NMR spectra demonstrated that the double helicate was extended in length by a factor of two and unwound by  $100^\circ$ . Upon the addition of  $\text{NaPF}_6$ , the trinuclear helicate was quantitatively regenerated through contraction and rewinding. The extension-contraction motion could be repeated many times by simply adding the sodium ion or cryptand.



**Scheme 2-4** Removal and insertion of sodium ion in the H<sub>4</sub>L based double helicate.

### 2.1.2 Double Helices through Aromatic Interactions

Oligo-*m*-phenylene was also used as an important structure for artificial helices. Poly- and oligo-*m*-phenylenes are known to take a helical conformation in the solid state, but adopt a random conformation in solution.<sup>9</sup> With the aim of inducing dynamic helical structures on the oligo-*m*-phenylene backbones through a supramolecular approach,

oligo-*m*-phenylene derivatives with hydroxyl groups on the outer rims of the oligo-*m*-phenylene backbones were synthesized. Oligoresorcinols such as these form double helices in water, whereas they are found to crystallize in a single helix from the mixed solvents of chloroform and acetonitrile (Figure 2-1).<sup>10</sup> This is consistent with the observation that the double helix formation of oligoresorcinols is primarily driven by aromatic-aromatic interactions in water.

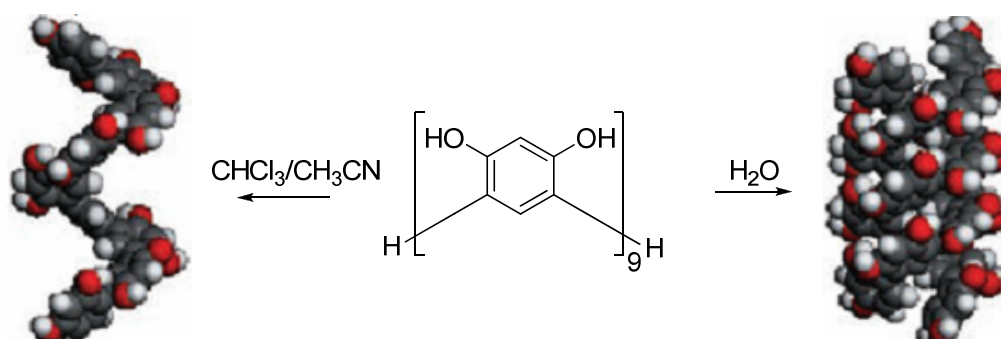


**Figure 2-1** Crystal structures of the single helical conformer and the double helical complex of nonaresorcinol.

In the past decade, it has been disclosed that some readily available oligoamides fold into double helical structures with the aid of interstrand hydrogen bonds and aromatic-aromatic interactions.<sup>11</sup>

Huc, Lehn and coworkers demonstrated that both single and double helices of **S1** can be formed and crystallized from different media (Figure 2-2).<sup>12</sup> The single helix crystallized from a polar solvent mixture (DMSO/CH<sub>3</sub>CN), but the double helix crystallized from a less polar solvent mixture (nitrobenzene/heptane). The dimerization constant of **S2** was only approximately 30 M<sup>-1</sup> in CDCl<sub>3</sub> at 298K and increasing the concentration led to broadened signals in <sup>1</sup>H NMR spectra and precipitation. Compared



with **S2**, **S3** including four extra-decyloxy chains was more soluble in non-polar solvents. The dimerization constant of **S3** was measured to be  $6.5 \times 10^4 \text{ M}^{-1}$  in  $\text{CDCl}_3$  at 298K, which was three orders of magnitude larger than that of **S2** in the same solvent. This value was similar in other non-polar solvents, being  $5.5 \times 10^4 \text{ M}^{-1}$ ,  $1.0 \times 10^5 \text{ M}^{-1}$ , and  $1.6 \times 10^5 \text{ M}^{-1}$  in toluene- $\text{D}_8$ ,  $\text{CD}_2\text{Cl}_2$ , and  $\text{C}_2\text{D}_2\text{Cl}_4$  respectively.

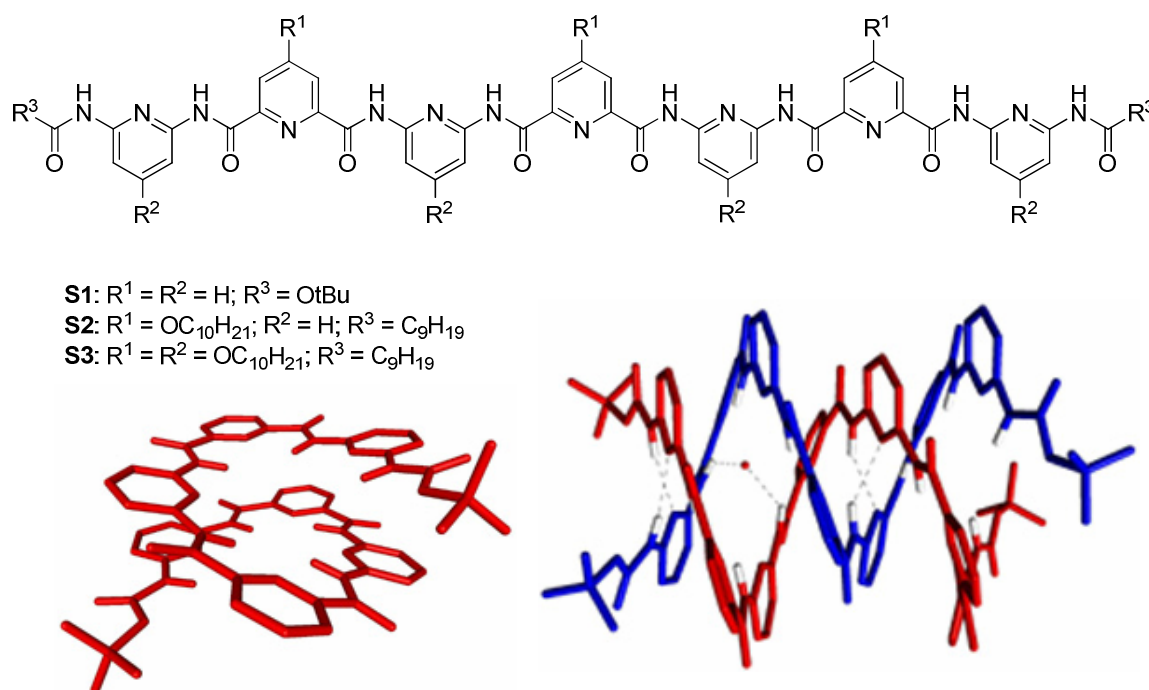


**Figure 2-2** Structures of oligopyridinecarboxamides and crystal structures of the single helix and double helix dimer of **S1**.

Huc and co-workers showed that an *N*-oxidized strand can still dimerize into a double helix (Figure 2-3). The dimerization constant of **S5** was  $125 \text{ M}^{-1}$ , which was 4-fold larger than that for **S2** in the same solvent.<sup>13</sup> **S4** (grown from  $\text{CDCl}_3/\text{hexane}$ ) provided the double helical structure information. The same groups also reported the cross-hybridization of pyridinecarboxamide helical strands and their *N*-oxides.<sup>14</sup> The cross-hybridized complex is more stable than their homodimers:  $K_a(\text{S5} \cdot \text{S6}) = 1140 \text{ M}^{-1}$ ,

but  $K_{\text{dim}}(\mathbf{S6}) = 30 \text{ M}^{-1}$ . The hybridization was confirmed in the solid state by crystal structure.

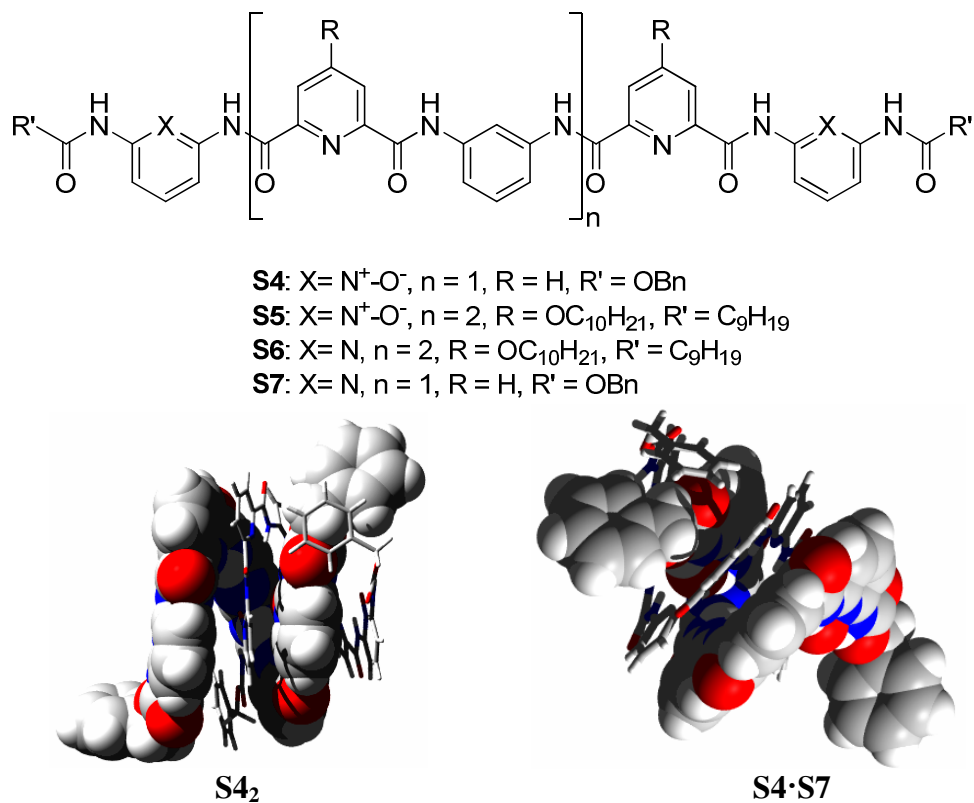
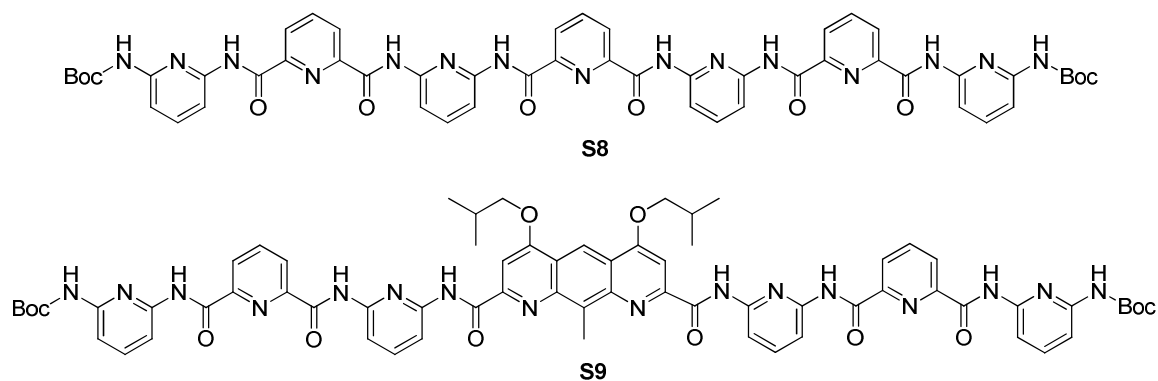
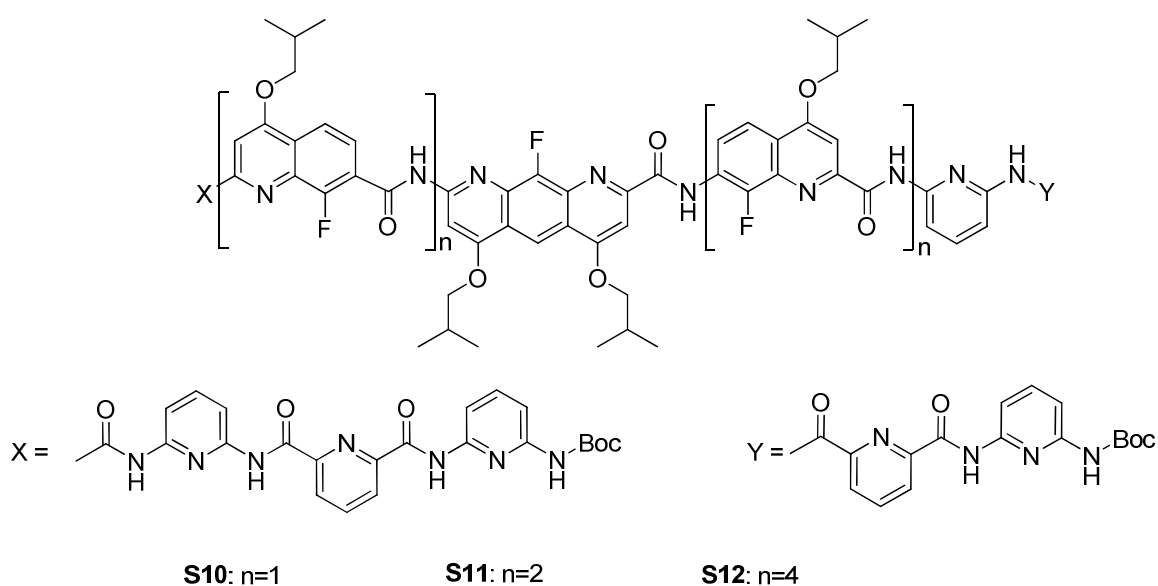


**Figure 2-3** Structure of *N*-oxidized oligomers and crystal structures of **S4<sub>2</sub>** and **S4·S7**.

When a pyridine unit in the oligoamide was replaced by a 1,8-diazaanthracene, the stability of the double helix was remarkably improved ( $K_{\text{dim}}$  for **S9** =  $6.5 \times 10^5 \text{ M}^{-1}$  in pyridine but  $K_{\text{dim}}$  for **S8** =  $100 \text{ M}^{-1}$  in  $\text{CDCl}_3$ ).<sup>15</sup> For the hybridization of **S8** in  $\text{CDCl}_3$ ,  $\Delta H = -4.4 \text{ kJ/mol}$  and  $\Delta S = 37 \text{ J/K}$ , but for the hybridization of **S9** in pyridine,  $\Delta H = -40.2 \text{ kJ/mol}$  and  $\Delta S = 27.6 \text{ J/K}$ . Even though those data were collected in different solvents, the small change of entropy suggested that the hybridization of **S9** is driven by enthalpy. Crystal structures demonstrated that aromatic  $\pi$ -stacking is one of the main factors to contribute to the stability of **S9<sub>2</sub>**.



**Scheme 2-5** Structures of oligoamides **S8** and **S9**.

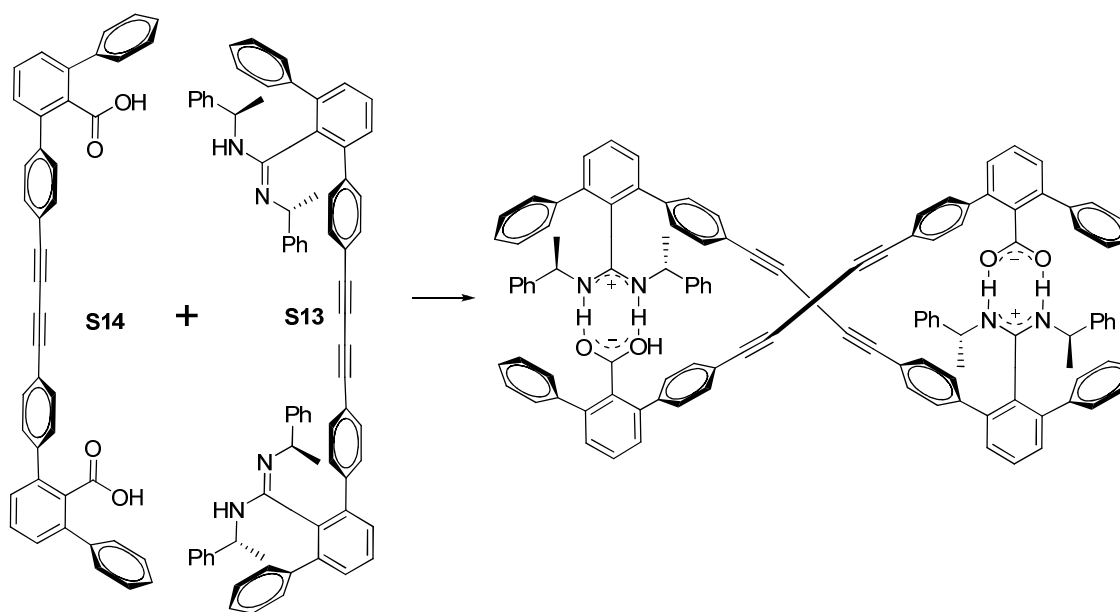


**Scheme 2-6** Structures of oligoamides **S10**, **S11** and **S12**.

Similar aromatic oligoamides **S10**, **S11** and **S12** were folded into both single and double helical structures stabilized by local preferential conformations at arylamide linkers and intermolecular  $\pi$ -stacking interactions between aromatic groups (Scheme 2-6).<sup>16</sup> Interestingly, the fluoroaromatic units in the sequence center can form enough internal space in the folded structure to accommodate an alkyl chain but nothing much

larger, with each terminal 2,6-pyridinedicarboxamide unit acting as a hydrogen bond motif to anchor the guest at a defined position in the helix cavity. Increasing strand length adjusted the distance between the anchor points along the helix axis and their relative orientation in a plane perpendicular to the helix axis.

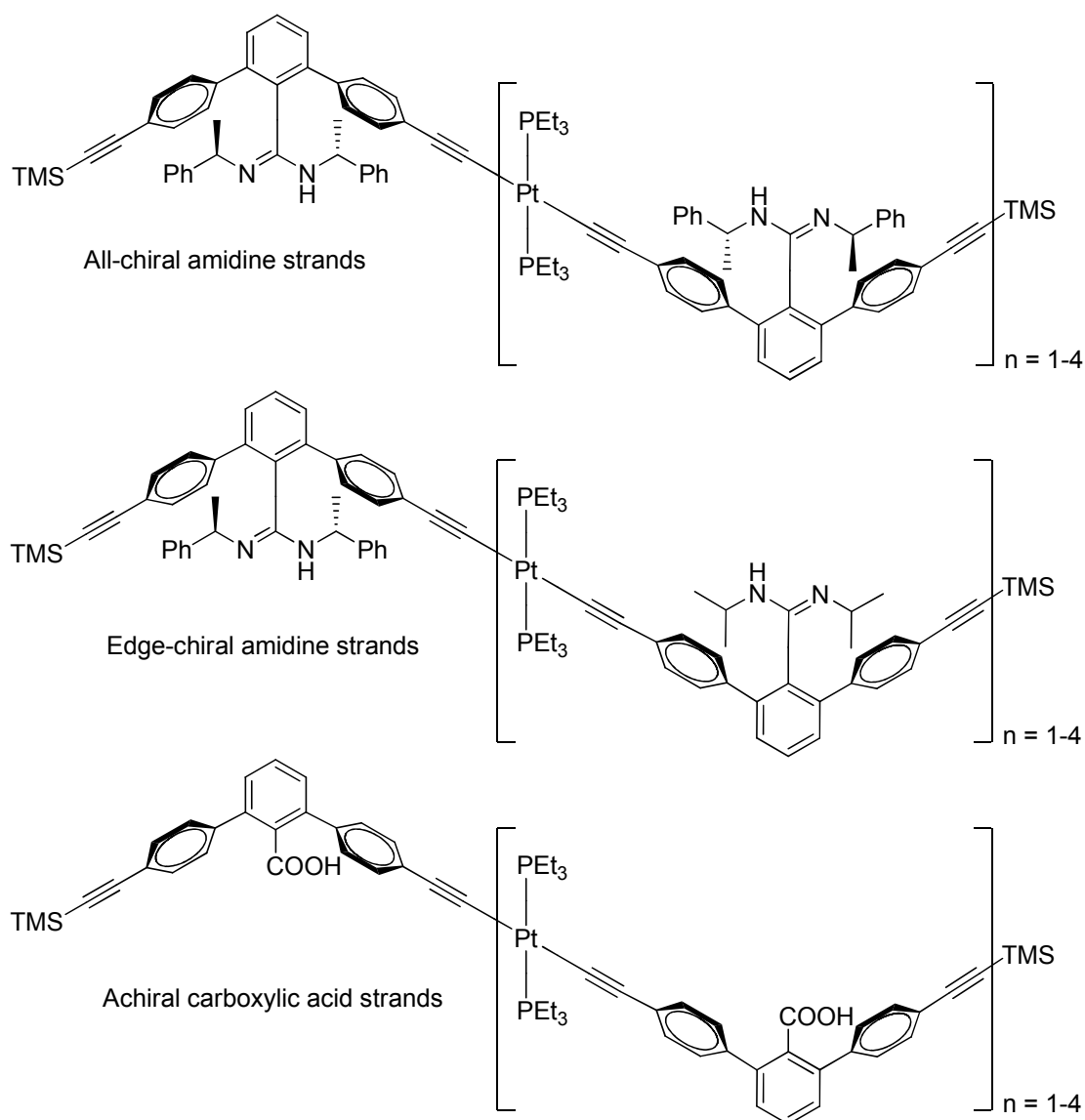
### 2.1.3 Double Helices through Salt Bridges



**Scheme 2-7** Furusho and Yashima's complementary salt-bridged double helix.

Amidinium-carboxylate salt bridges have a well-defined geometry and have been employed as useful modules for constructing supramolecular architectures.<sup>17</sup> A feature of amidinium-carboxylate salt bridges is the potential to generate complementary pairs of supramolecular double helical complexes in a controlled fashion with high association constants.<sup>18</sup> Yashima, Furusho and coworkers demonstrated that two complementary sequences form double-helical structures via amidinium-carboxylate salt bridges (Scheme 2-7).<sup>19</sup> When **S13** was mixed with **S14** in chloroform, the duplex **S13·S14** was formed

containing two salt bridges. The X-ray crystal structure demonstrated that the complex of *R*-**S13**•**S14** with the *R*-phenylethyl substituent on the amidine groups adopted a right-hand double-helical structure in the solid state. Circular dichroism spectra revealed that the formation of the double helical complex resulted in an enhancement of the weak Cotton effects exhibited by *R*- or *S*-**S13** in the region of 260 nm to 370 nm in chloroform.



**Scheme 2-8** All chiral or edge-chiral amidine strands and carboxylic acid strands.

The same group also investigated the chiroptical properties upon double helix formation through a series of complementary strands composed of *m*-terphenyl units bearing chiral/achiral amidine or achiral carboxylic acid groups linked by Pt(II) acetylide complexes (Scheme 2-8).<sup>20</sup> In chloroform, the formation of preferred-handed double helices from the all-chiral amidine strands and corresponding achiral carboxylic acid strands resulted in characteristic induced circular dichroism (CD) spectra in the Pt(II) acetylide complex regions (300-380 nm), which indicated that the chiral substituents on the amidine units biased a helical sense preference. The cotton effect patterns and intensities were highly reliant on the oligomer lengths. The effect of the sequences of the chiral and achiral amidine units on the amplification of chirality in the double-helix formation was studied via comparing the CD intensities with those of the corresponding all-chiral amidine double helices with the same molecular lengths. The chiral/achiral hybrid amidine oligomers also formed similar double helices in the presence of the complementary carboxylic acid oligomers, displaying induced CD spectra and patterns similar to each other when the molecular lengths are the same.

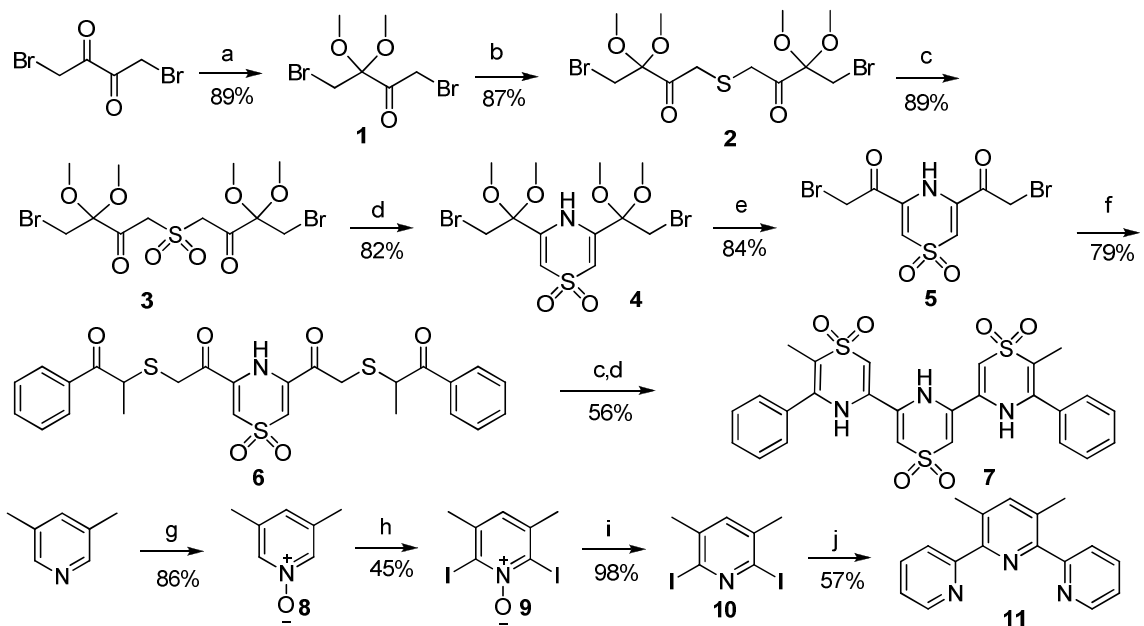
## 2.2 Results and Discussions

Most of the above mentioned examples are self-complementary double-helical structures based on metal coordination, anion templation, or aromatic stacking interactions. However, there are two complementary sequences of base pairs in the natural DNA and hence artificial double helices should also have complementary two strands for DNA-like information storage and processing.<sup>21</sup> There are few examples about artificial double helices including complementary binding sites. With the exception

of salt bridges, hydrogen bonds are definitely another choice for complementary strands. In the last years, complementary hydrogen bond strands have been employed for a large number of ladder- or zipper-like supramolecular duplexes.<sup>22</sup> To date, the rational design and synthesis of artificial double helices based on complementary hydrogen bond strands has been considered as being quite difficult.

According to previous work in our group, oligomers containing three thiazine dioxide subunits may be an excellent hydrogen bond DDD subunit. The beginning method for the synthesis of compound **7** including three thiazine dioxides was developed by former Ph.D. student Jiabin Li but most of steps required chromatography to purify the intermediates.<sup>23</sup> In addition, there was no X-ray structural information for the putative complex formation with an AAA complement.

We designed a new method for heterocyclic **7** (Scheme 2-9). Intermediate **5** was synthesized from easy and accessible starting materials. It should be noted that the first five steps of the synthesis can be carried out without the need of chromatography in good overall yield (45%) to produce **5**. The further conversion of this intermediate to **7** was achieved by repeating the previous steps of substitution, oxidation and cyclization. The new method is definitely an improvement on the initial route. The suitable complement to **7** is **11**, which was obtained via Stille coupling. Although the synthesis of the dibromo analogue of intermediate **10** (2,6-diiodo-3,5-dimethyl pyridine) may be carried out via the use of oleum and bromine at 433 K,<sup>24</sup> our method is much safer and more reasonable. Compared with the known ladder-like AAA- DDD complexes, there are no intramolecular hydrogen bonds, preorganized structures or tautomerization in our AAA- DDD system.



**Scheme 2-9** Synthesis of **7** and **11**. Reaction conditions and reagents: a)  $\text{HC}(\text{OMe})_3$ , conc.  $\text{H}_2\text{SO}_4$ ; b)  $\text{Na}_2\text{S}$ , acetone/water,  $0^\circ\text{C}$  to rt; c) UHP/TFAA,  $\text{CH}_3\text{CN}$ ; d)  $\text{NH}_4\text{OAc}/\text{AcOH}$ , reflux; e)  $\text{HCOOH}$ , reflux; f) 2,6-lutidine,  $\text{CH}_3\text{CN}$ ; g) 30%  $\text{H}_2\text{O}_2$ ,  $\text{AcOH}$ ,  $100^\circ\text{C}$ ; h) (i)  $n\text{-BuLi}$ , THF, hexane,  $-78^\circ\text{C}$ , (ii)  $\text{I}_2$ , THF,  $-78^\circ\text{C}$  to rt; i)  $\text{PCl}_3$ ,  $\text{CHCl}_3$ , reflux; j) 2-tributyltinpyridine,  $\text{Pd}(\text{PPh}_3)_4$ , toluene, reflux.

Unfortunately, this model molecule **7** is insoluble in chloroform, acetonitrile and even acetone. It is well-known that the polarity of solvent significantly affects the stability of hydrogen bonded systems and apolar solvents are chosen to investigate hydrogen bond interactions between donors and acceptors.<sup>25</sup>

It is interesting that when one equivalent molar **11** was added to the cloudy chloroform solution of **7**, the mixed solution turned transparent. The  $^1\text{H}$  NMR spectrum of the complex in  $\text{CDCl}_3$  displays extreme downfield shifts for the thiazine dioxide NH protons of **7** at 12.88 ppm and 12.00 ppm as would be expected from a strong hydrogen



bond interaction with **11** (Figure 2-4). The association constant of **7** and **11** was attempted using  $^1\text{H}$  NMR dilution. When the 1:1 mixture of **7** and **11** was diluted to 0.1 mM, the N-H chemical shifts remained constant. This result indicated a very high association constant between **7** and **11** ( $> 10^5 \text{ M}^{-1}$ ).

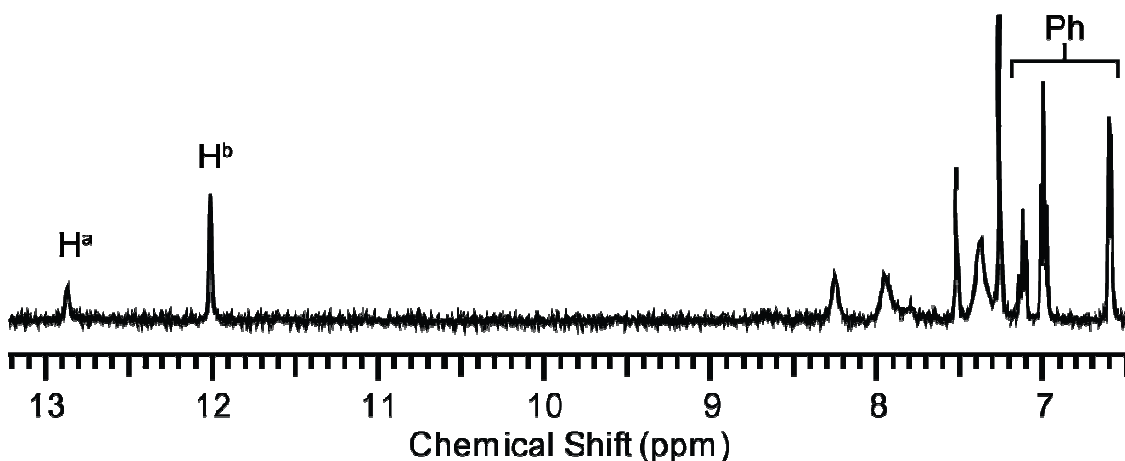


**Figure 2-4**  $^1\text{H}$  NMR spectrum of **7•11** (1:1 mixture) in  $\text{CDCl}_3$  at 298 K.

The solid state structure of complex **7•11** further supports the hydrogen bonded nature of the complex in solution. Single crystals were grown by slow diffusion of isopropyl ether into a chloroform solution of **7•11** and analyzed by X-ray diffraction analysis.<sup>26</sup> The complex crystallizes with the two molecular strands intertwined in a double helical conformation (Figure 2-5). The three NH groups of the thiazine-1,1-dioxide heterocycles form short primary hydrogen bonds with the three nitrogen atoms of the pyridyl rings ( $\text{N6H}\cdots\text{N1} = 2.85$ ,  $\text{N5H}\cdots\text{N2} = 2.88$ ,  $\text{N4H}\cdots\text{N3} = 3.06$  Å and (respectively)  $\text{N6H}\cdots\text{N1} = 162$ ,  $\text{N5H}\cdots\text{N2} = 177$ ,  $\text{N4H}\cdots\text{N3} = 169^\circ$ ). Three carbon atoms (*ipso*, *ortho*, and *meta*) of a terminal phenyl ring of **7** are positioned over and engaged in  $\pi$ -stacking with the central pyridyl ring of **11** ( $\text{C}\cdots\pi(\text{pyridyl least squares plane}) = 3.59$ ,

3.37, and 3.42 Å) providing further rationalization of the upfield shifts observed for the attached phenyl proton resonances in the  $^1\text{H}$  NMR spectrum.

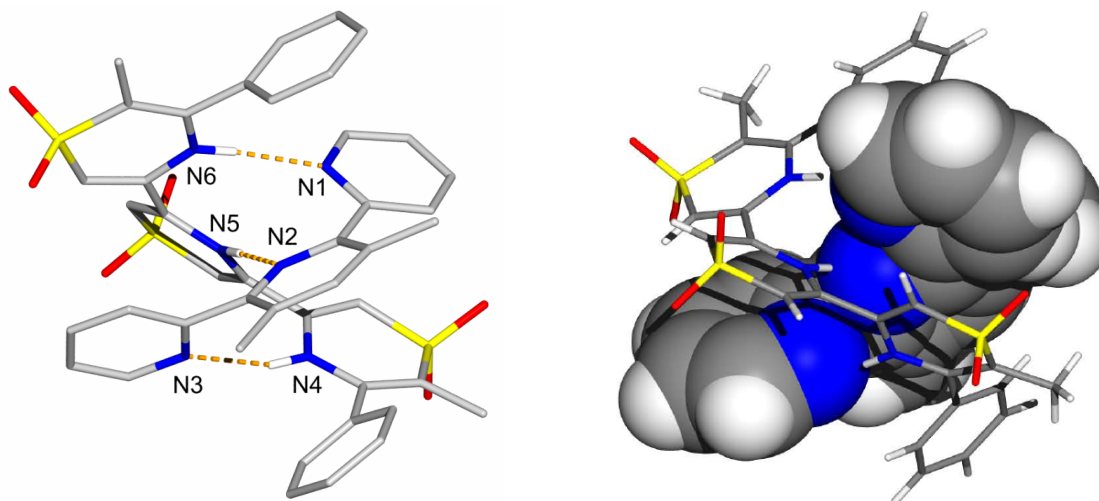
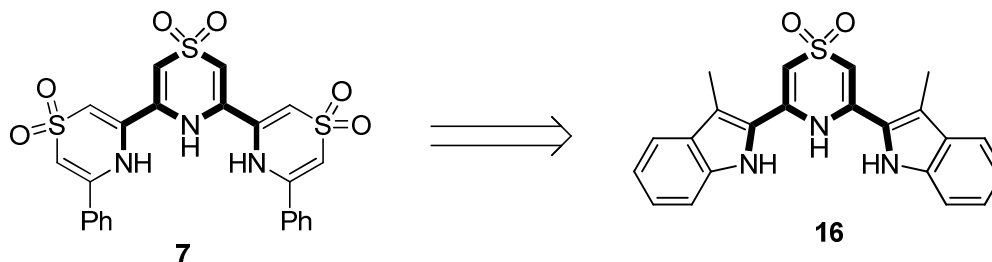


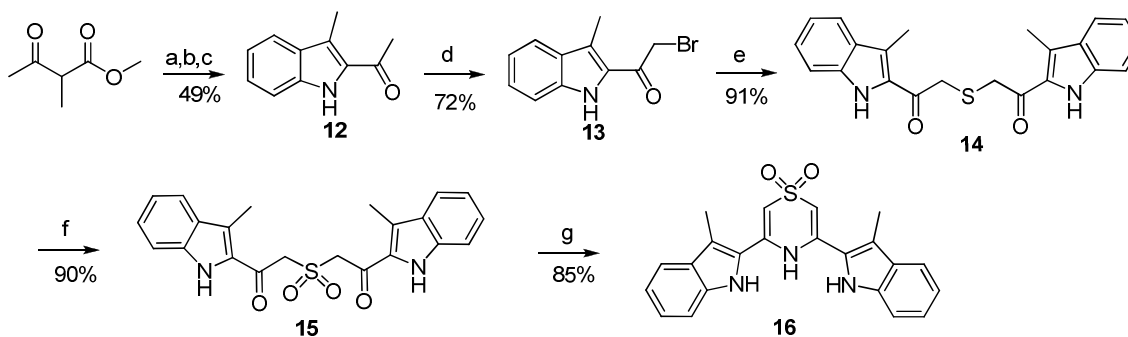
**Figure 2-5** The solid state structure of **7•11**. All C-H hydrogen atoms have been removed for clarity. NH...N hydrogen bonds are indicated by dashed orange lines. Carbon is grey, Nitrogen is blue, oxygen is red and sulfur is orange.

In order to obtain a comparable association constant, both the AAA and DDD components must be dissolved in a non-polar solvent. Unfortunately DDD **7** is completely insoluble in any non-polar solvents. Although the method for the synthesis of oligo(thiazine dioxide)s was improved, solubility was still an obstacle. Therefore, we wished to develop a new soluble DDD analogue. Indole has been used as a hydrogen bond donor in anion recognition.<sup>27</sup> There are also a large number of methods to synthesize and modify indole derivatives. With this in mind, we designed another DDD compound **16** that has a similar configuration of hydrogen bond sites as compound **11** (Scheme 2-10). The Fischer indole synthesis among a number of methods for preparing

indoles satisfies the requirements of modern organic synthesis in its convenience and simplicity.<sup>28</sup>



**Scheme 2-10** Structures of compounds **7** and **16**.



**Scheme 2-11** Synthesis of DDD **16** including indole and thiazine dioxide donors.

Reaction conditions and reagents: a) NaOH, CH<sub>3</sub>OH/H<sub>2</sub>O; b) aniline, NaNO<sub>2</sub>/HCl; c) HCOOH, reflux; d) PhNMe<sub>3</sub>Br<sub>3</sub>, THF, reflux; e) Na<sub>2</sub>S, acetone/water, 0°C to rt; f) UHP/TFAA, CH<sub>3</sub>CN; g) NH<sub>4</sub>OAc/AcOH, reflux.

Compound **16** including two indole and one thiazine dioxide heterocycles was prepared via the Japp-Klingemann /Fischer indole synthesis (Scheme 2-11). We have tried to improve the yield for intermediate **12**, though the by-product smelly 3-methylindole (skatole) could not be avoided.<sup>29</sup> Although we tried different acids (e. g.

acetic acid, conc. HCl, sulfuric acid, H<sub>3</sub>PO<sub>4</sub>, HCl in acetic acid), formic acid was the best choice for Fischer indole reaction. Trimethylphenylammonium tribromide was effective bromination reagent because the bromination by-product is a salt, which precipitates from THF. Sodium sulfide was a good choice for the synthesis of sulfide from the bromo intermediate. UHP/TFAA oxidized the sulfide into the sulfone in high yield and directly gave pure product and thus avoided chromatography.

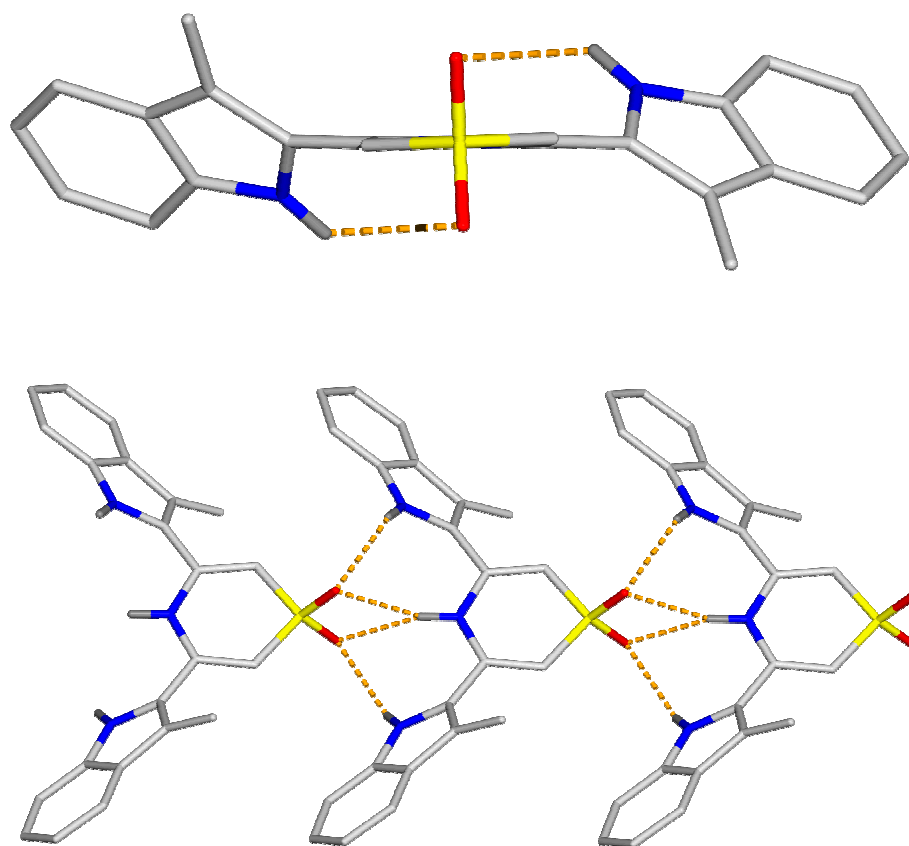
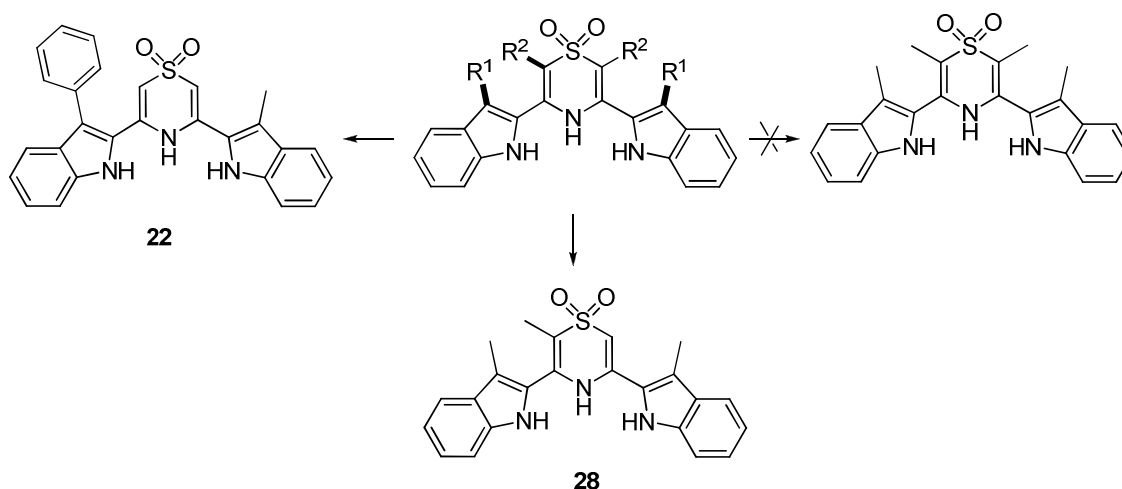


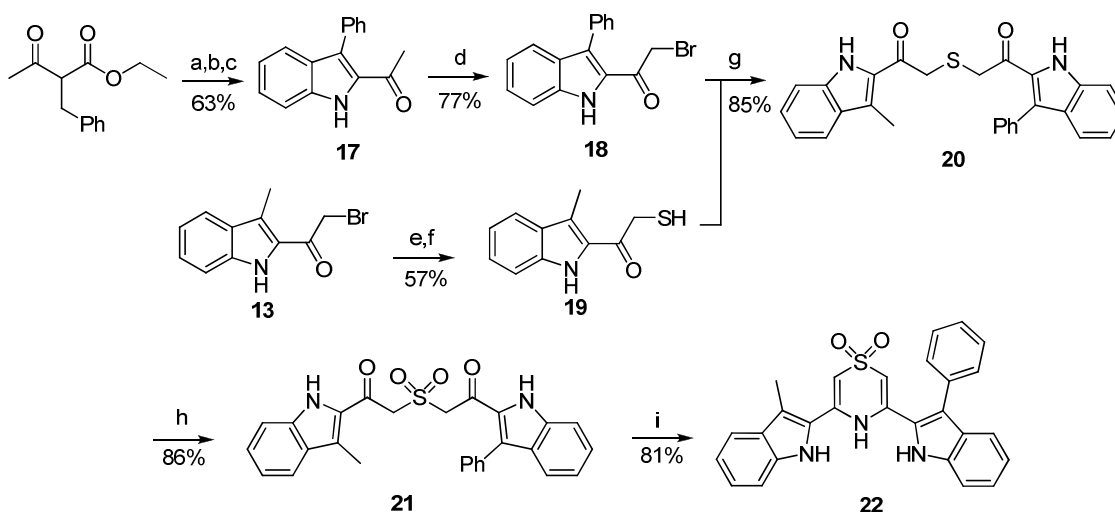
**Figure 2-6** Stick representations of the solid state structure of **16**. View along b direction (top). View perpendicular to b direction (bottom). All C-H hydrogen atoms have been removed for clarity. NH...N hydrogen bonds are indicated by dashed orange lines. Carbon is grey, Nitrogen is blue, oxygen is red and sulfur is orange.

Compound **16** has similarly poor solubility in non-polar solvents as the model DDD **7** in solubility. An X-ray crystal structure confirmed that intermolecular hydrogen bonds result in **16** being insoluble in chloroform. The single crystal X-ray analysis revealed a structure composed of anti-parallel C<sub>2</sub> symmetric 1-D chains (Figure 2-6) that lie along the b direction of the lattice.<sup>30</sup> The chains are held together by three intermolecular hydrogen bonds between the donor NH groups of one molecule of **16** and the sulfone oxygen atoms of the next in the chain. The individual molecules reside in a helical conformation such that each indole NH donor forms a hydrogen bond with one or the other of the two sulfone oxygen atoms in the adjacent molecule ( $\text{NH}\cdots\text{O} = 3.04 \text{ \AA}$  and  $\text{NH}\cdots\text{O} = 139^\circ$ ). The thiazine NH donor participates in a bifurcated hydrogen bonding arrangement with both oxygen atoms of the same sulfone ( $\text{NH}\cdots\text{O} = 3.10 \text{ \AA}$  and  $\text{NH}\cdots\text{O} = 149^\circ$ ). In non-polar solvents this intermolecular attraction is likely strong enough to generate the observed insolubility of **16** (and by analogy **7**).



**Scheme 2-12** Possible modified structures for soluble DDD.

If these intermolecular hydrogen bonds could be prevented, compound **16** may be soluble in chloroform. Addition of one more group to the molecular skeleton could block the sulfone and break up the intermolecular hydrogen bonds. Following this idea, there are two possible positions ( $R^1$  and  $R^2$ ) to modify the DDD structure (Scheme 2-12).



**Scheme 2-13** Synthesis of DDD **22**. Reaction conditions and reagents: a) NaOH, CH<sub>3</sub>OH/ H<sub>2</sub>O; b) aniline, NaNO<sub>2</sub>/HCl; c) HCOOH, reflux; d) PhNMe<sub>3</sub>Br<sub>3</sub>, THF, reflux; e) KSAc, DMF; f) cysteamine hydrochloride, NaHCO<sub>3</sub>, CH<sub>3</sub>OH; g) Et<sub>3</sub>N, CH<sub>3</sub>CN; h) UHP/ TFAA, CH<sub>3</sub>CN; i) NH<sub>4</sub>OAc/AcOH, reflux.

We firstly tried to add a phenyl group on the indole component. In the structure of compound **22**, one 3-methyl group on an indole ring system was replaced with a large phenyl ring (Scheme 2-13). Intermediate indole **17** was synthesized from ethyl 2-benzylacetoacetate via the Fischer indole synthesis. Intermediate thiol **19** was prepared through a two-step reaction: the bromo compound was changed into thioacetate; thioacetate was hydrolyzed by cysteamine hydrochloride. As expected, compound **22** is now soluble in chloroform. This phenyl ring led to the multiple signs from 7.68 to 7.12

ppm in  $^1\text{H}$  NMR spectrum and therefore we chose the easily identified indole N-H proton at 8.75 ppm to determine the association constant of **22** and **11**, as shown in Figure 2-6.

Although one phenyl ring renders **22** soluble in chloroform, the binding constant is low ( $K_a = 300 \text{ M}^{-1}$ ).

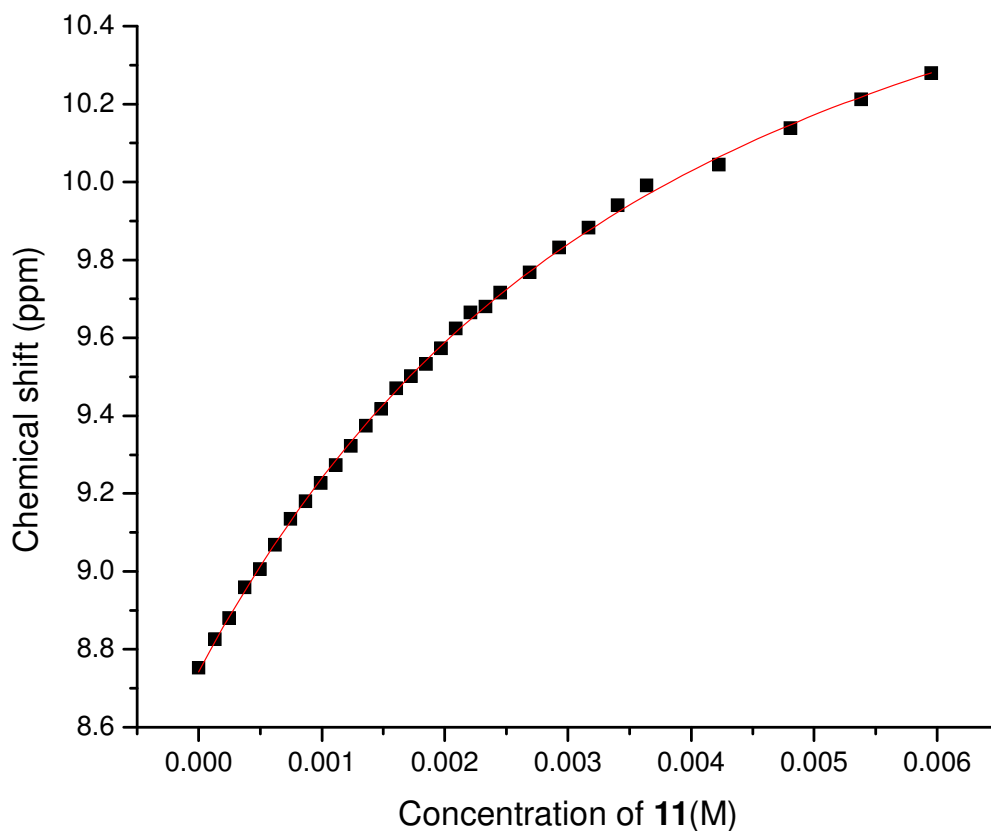
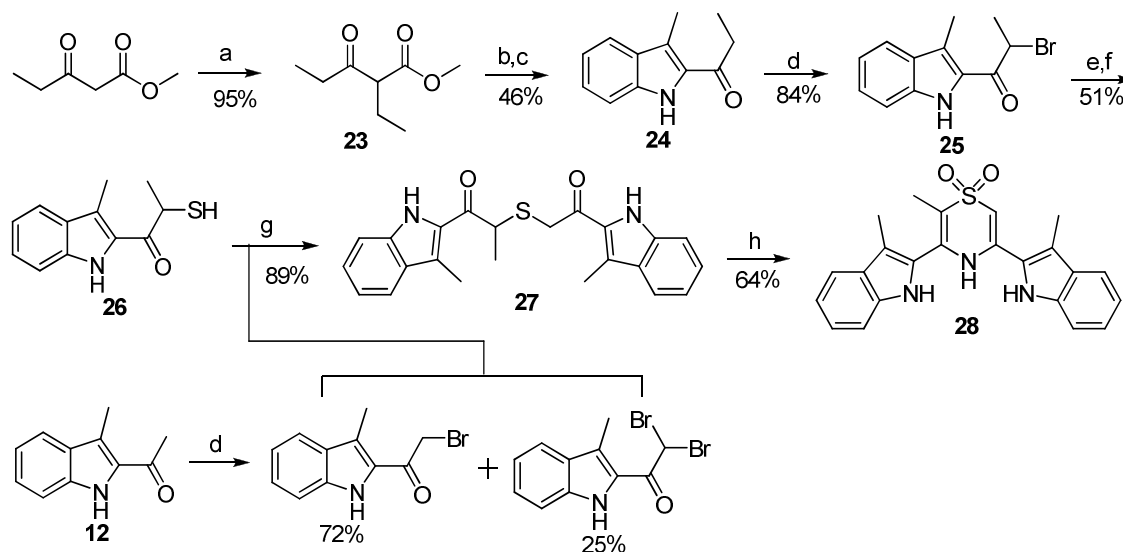


**Figure 2-7**  $^1\text{H}$  NMR titration curve of **22** and **11** in  $\text{CDCl}_3$  at 298K ( $K_a = 300 \text{ M}^{-1}$ ).

Alternatively to the modification of indole ring, the thiazine dioxide ring system could be further modified to block the intermolecular hydrogen bonds as well. Hence, we tried to modify the thiazine dioxide ring via the addition of two extra-methyl groups ( $\text{R}^2 = \text{CH}_3$ ). Unfortunately, during the preparation of this compound, the last cyclization step was unsuccessful and thus we could not synthesize the methyl-substituted derivative.

However, the addition of only one methyl group on the 2-position of the thiazine dioxide

ring in **28** (Scheme 2-14) appeared to be enough steric bulk to render the DDD framework soluble in chloroform. The extramethyl group was easily incorporated by using a propioacetate starting material.



**Scheme 2-14** Synthesis of DDD **28**. Reaction conditions and reagents: a) EtI,  $K_2CO_3$ , THF, reflux; b) i, NaOH,  $CH_3OH/H_2O$ , ii, aniline,  $NaNO_2/HCl$ ; c)  $HCOOH$ , reflux; d)  $PhNMe_3Br_3$ , THF, reflux; e)  $KSac$ , DMF; f) cysteamine hydrochloride,  $NaHCO_3$ ,  $CH_3OH$ ; g)  $Et_3N$ ,  $CH_3CN$ ; h) *m*-CPBA,  $CH_2Cl_2$ ; i)  $NH_4OAc/AcOH$ , reflux.

During the synthesis of intermediate **27**, an inseparable mixture of monobromo and dibromo indoles was treated with **26**, yielding only the thioether **27**. The successful dissolution of **28** in chloroform allowed a determination of the association constant using  $^1H$  NMR titration. **28** was titrated with a solution of **11** in  $CDCl_3$  at 298K and changes in the chemical shifts of the NH resonances were monitored during the addition (Figure 2-8). Although the three N-H protons showed different magnitude shifts ( $\Delta\delta_{max}$  for N-H on indole and thiazine dioxide subunits were 2.8, 3.5 and 3.0 ppm respectively), each group



of data was fitted to a 1:1 host/guest binding model<sup>31</sup> using non-linear regression analysis to produce very close  $K_a$  values (3616, 3705 and 3810  $M^{-1}$ ). That indicated that regardless of the chemical shift changes of N-H, the NMR titration result for association constant is the same within error. The mean association constant for **11**•**28** is 3700  $M^{-1}$  ( $\Delta G = -20.4$  kJ mol<sup>-1</sup>). The lower magnitude of the stability constant for **11**•**28** in comparison to **7**•**11** is likely a result of the markedly weaker donor ability of skatole versus thiazine dioxide (which approximates a sulfonamide).

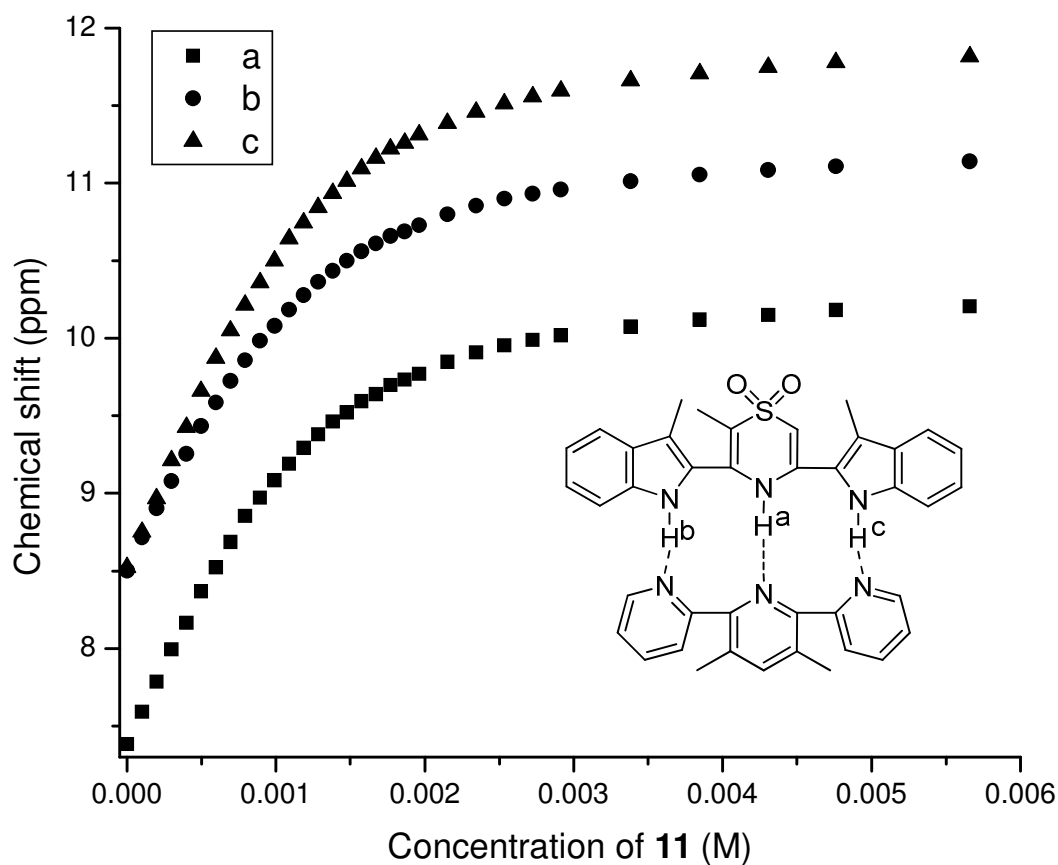


**Figure 2-8** <sup>1</sup>H NMR titration curve of **28** and **11** in CDCl<sub>3</sub> at 298K ( $K_a = 3700M^{-1}$ ).

Compared with the leading AAA **11**, both terpyridine and 2,6-bis(3,5-dimethyl-1H-prazol-1-yl)pyridine contain three-point hydrogen bonded acceptors as well. According

to the literature<sup>32</sup>, 1-methylbenzimidazole group is one of the best nitrogen-based hydrogen bond acceptors and thus 2,6-bis(1-methylbenzimidazol-2-yl)pyridine might be predicted as a better AAA complement than **11**. In addition, from the view of synthesis, terpyridine is commercially available and there are well-developed methods for the preparation of 2,6-bis(3,5-dimethyl-N-pyrazolyl) pyridine and 2,6-bis(1-methylbenzimidazol-2-yl)pyridine. So, we studied the binding properties between these three known AAAs and DDD **28**. <sup>1</sup>H NMR titrations demonstrate that all the three known AAA compounds showed weak association with **28** in CDCl<sub>3</sub> at 298 K (Scheme 2-15).

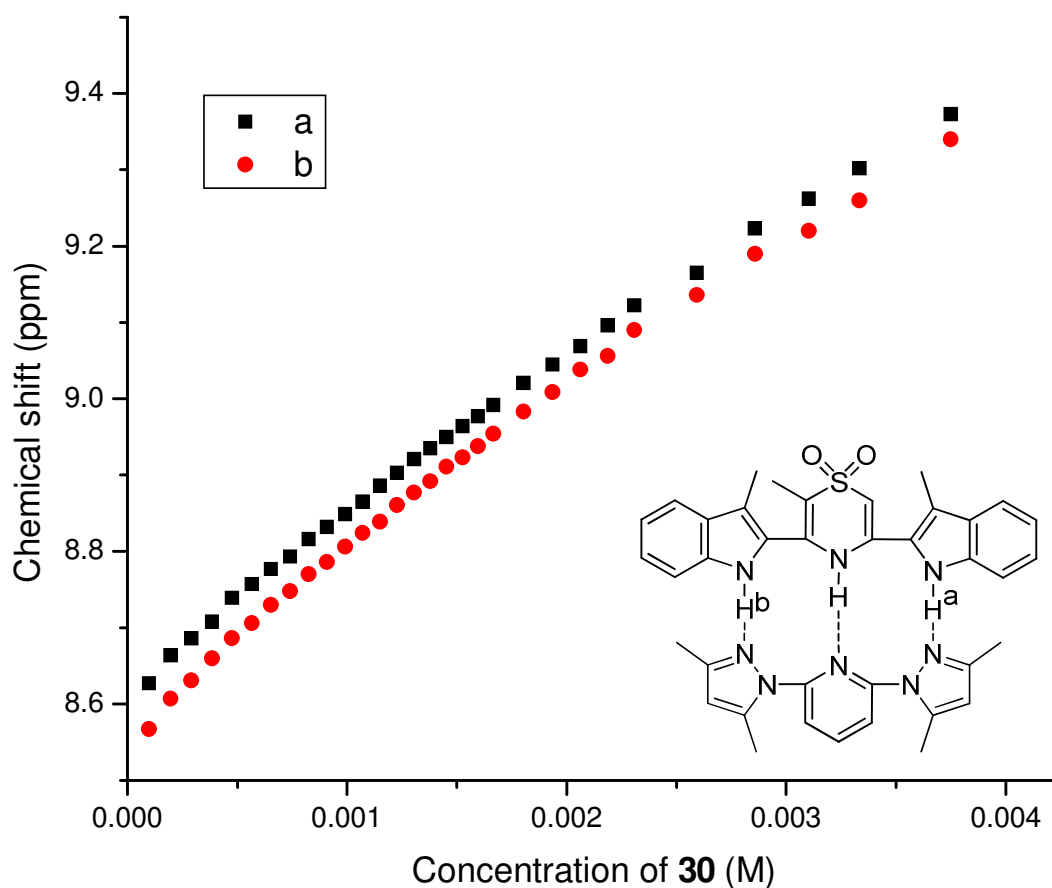


**Figure 2-9** <sup>1</sup>H NMR titration curves for **28** and **30** in CDCl<sub>3</sub> at 298K.

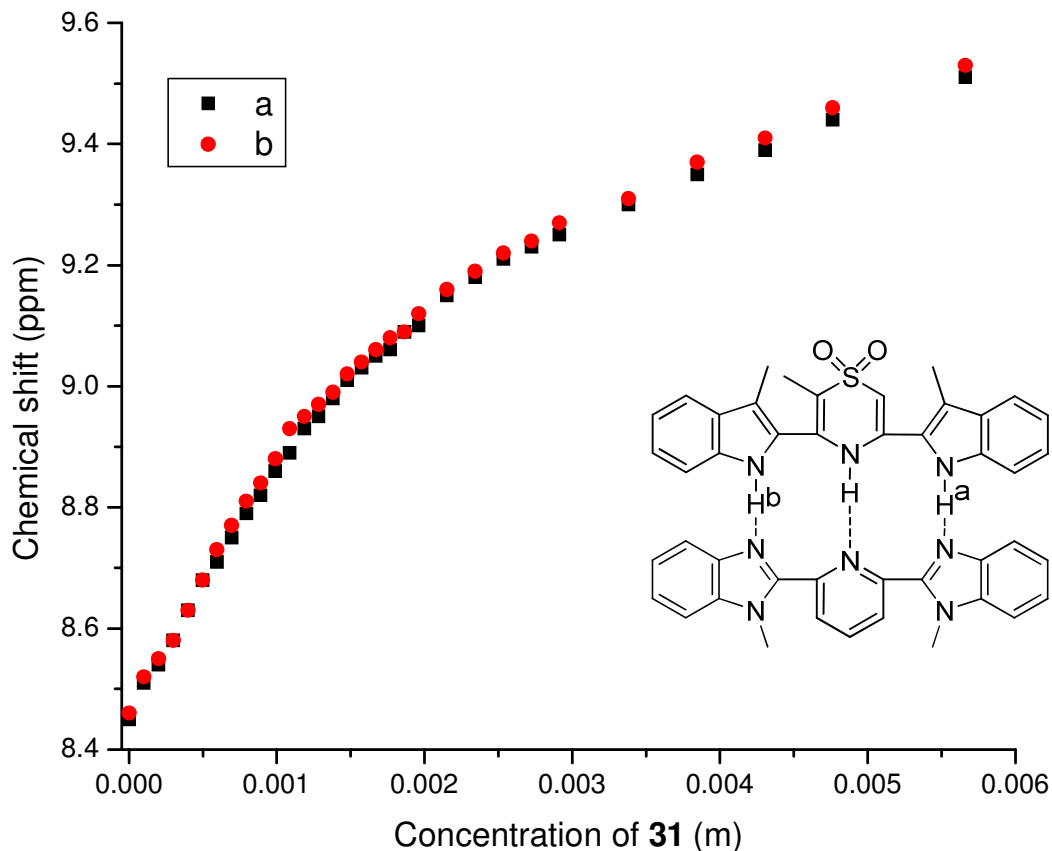
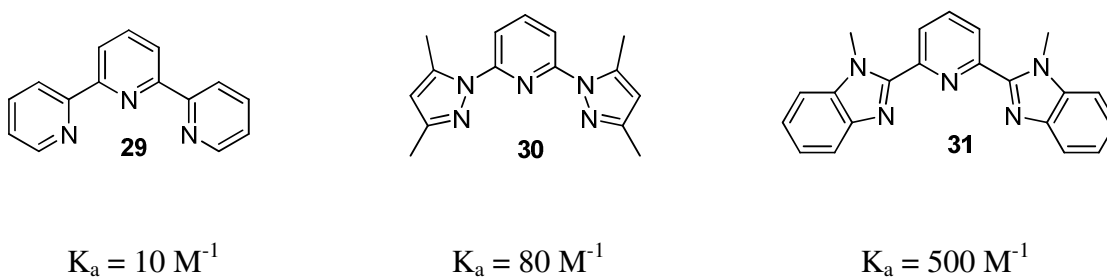


**Figure 2-10**  $^1\text{H}$  NMR titration curves for **28** and **31** in  $\text{CDCl}_3$  at 298K.



**Scheme 2-15** Three known AAA examples.

From the NMR titration curves in Figure 2-9 and Figure 2-10, the indole N-H proton chemical shifts moved down field upon the addition of 2,6-bis(3,5-dimethyl-1H-pyrazol-1-yl)pyridine or 2,6-bis(1-methyl benzimidazol-2-yl)pyridine. The proton signals

of 2,6-bis(3,5-dimethyl-1H-prazol-1-yl)pyridine and 2,6-bis(1-methyl benzimidazol-2-yl)pyridine overlap with the N-H signals of thiazine dioxide. Hence, the movement of that N-H proton could not be tracked and we summarize only the two indole N-H movements.

Table 2-1 lists all the data regarding association constants and changes of N-H proton chemical shifts. Obviously, for each complexation, different N-H protons provided different movements but produced almost the same association constants. Although there are many examples demonstrating a linear relationship between  $\Delta\delta_{\max}$  and  $K_a$  within a series of related complexes, in our case this relationship does not appear to follow such a relationship.

**Table 2-1** Association constant and indole N-H chemical shifts for the complexations of **28** with **30** and **31** in  $\text{CDCl}_3$  at 298 K.

	$K_a$ ( $\text{M}^{-1}$ )	$\delta_{\text{free}}$ (ppm) <sup>[a]</sup>	$\delta_{\text{max}}$ (ppm) <sup>[b]</sup>	$\Delta\delta_{\text{max}}$ (ppm)
<b>28</b> and <b>30</b>	90	8.55	11.59	3.04
	80	8.61	12.05	3.44
<b>28</b> and <b>31</b>	460	8.45	9.94	1.49
	550	8.44	9.87	1.43

[a] indole N-H chemical shift of **28**; [b] the extrapolated complex chemical shift upon the addition of a theoretical maximum of AAA **30** or **31**.

When the AAA component binds to the DDD component, the subunits in AAA and DDD change their conformations to accommodate binding. Compared with the structure of **11**, terpyridine has no methyl groups on the central pyridine ring and three pyridine rings prefer a coplanar anti-anti conformation (Figure 2-11). This led to a large enthalpic cost in the binding process. Likewise, the three heterocycles are nearly coplanar (interplanar angles are 6-7°) in 2,6-bis(3,5-dimethyl-*N*-pyrazolyl)pyridine as well<sup>33</sup>, but there is a large torsion (37°) between pyridine and the second benzimidazole in 2,6-bis(1-methylbenzimidazol-2-yl)pyridine<sup>34</sup>. In other words, the formation of a stable AAA-DDD complex in these cases relies on both the strength of the hydrogen bonding interaction and the energy required to take up the binding conformation. A lack of steric bias to enforce a non-coplanar conformation in these three AAA's results in low binding constants.

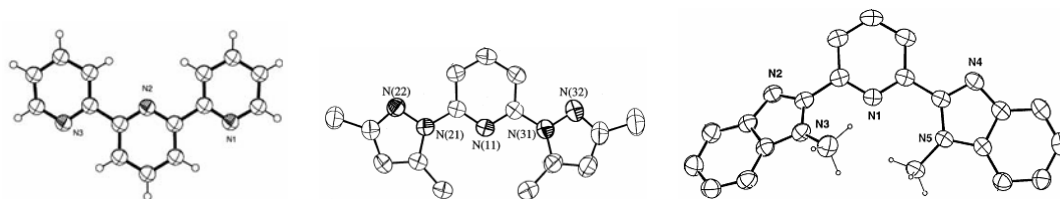


**Figure 2-11** Crystal structures of known AAAs terpyridine, 2,6-bis(1-methyl benzimidazol-2-yl)pyridine, and 2,6-bis(3,5-dimethyl-*N*-pyrazolyl)pyridine.

## 2.3 Summary

We have designed and synthesized several DDD triple hydrogen bonding molecules that form stable to very stable double helical complexes with terpyridyl derivative **11**. Oligomers based solely on thiazine dioxides can form a double helical complex with **11** but poor solubility in non-polar solvents resulted in difficulty

investigating their binding behavior in solution. We demonstrated that strong intermolecular hydrogen bonds between molecules of **7** or **16** greatly reduce solubility in non-polar solvents. Modified DDD **28** was proved to be soluble in chloroform and provided a reasonably high association constant with **11**. It should be noted that accessing **28** analogues with significantly greater hydrogen bond donor character (e.g. similar to thiazine dioxide) and, likely much higher  $K_a$  values, can be accomplished by the addition of withdrawing groups to the 5-positions of the indole rings.

On the other hand, the backbone of the AAA subunit is difficult to improve and steric effect is very important for the stable formation of the AAA-DDD complexes. Following the same principles on the electronic effect of hydrogen bond donor/acceptor, we may add electron donating groups to the pyridine or lutidine rings to improve their abilities as hydrogen bond acceptors and further produce higher association constants with the DDD components.

In summary, we have designed and synthesized a new kind of hydrogen bond double helices. The synthesis of double helical AAA-DDD is reasonably simple and effective. Although the basic AAA-DDD **11-28** complex gave the relatively low association constant ( $3700 \text{ M}^{-1}$ ), the modifications of electron withdrawing groups on DDD and electron donating groups on AAA could significantly increase the complex binding ability. These modifications will be the subject of the following chapter.

## 2.4 Experimental Section

Chemicals were purchased from Aldrich and used as received. All non-deuterated solvents were dried using an Innovative Technology solvent purification system SPS-

400-5. Chromatography was performed on Merck 240-400 mesh silica gel-60.  $\text{CDCl}_3$  and acetone- $\text{d}_6$  were purchased from Cambridge Isotope Laboratories and dried over  $3\text{\AA}$  (acetone) or  $4\text{\AA}$  (chloroform) molecular sieves before use.  $^1\text{H}$  and  $^{13}\text{C}$  NMR spectra were collected on a Varian Mercury 400 MHz spectrometer. Spectra are reported with residual solvent peak as reference from TMS. Mass spectra were obtained on a Finnigan MAT 8200 mass spectrometer.  $^1\text{H}$  NMR titration experiments were performed on a Varian Inova 600 MHz spectrometer. Crystal structure data were collected at low temperature (150 K) on a Nonius Kappa-CCD area detector diffractometer with COLLECT (Nonius B.V., 1997-2002). The unit cell parameters were calculated and refined from the full data set. Crystal cell refinement and data reduction were carried out using HKL2000 DENZO-SMN (Otwinowski & Minor, 1997). The absorption correction was applied using HKL2000 DENZO-SMN (SCALEPACK). The SHELXTL/PC V6.14 for Windows NT (Sheldrick, G.M., 2001) suite of programs was used to solve the structure by direct methods. Subsequent difference Fourier syntheses allowed the remaining atoms to be located.

**1:** Concentrated sulfuric acid (1mL) was added into the mixture of 1,4-dibromo-2,3-butanedione (82.6 mmol, 20 g) and trimethylorthoformate (182 mmol, 19.5 g) in 100 mL flask at a nitrogen atmosphere. The reaction solution was stirred for 16 hours. Then water (100 mL) and  $\text{CH}_2\text{Cl}_2$  (100 mL) were added. The organic layer was washed with 10% HCl and saturated NaCl solution. The solvent was evaporated under reduced pressure and crude product was dissolved in hexane and filtered to remove some insoluble precipitates. The filtrate was cooled down to  $-78^\circ\text{C}$  and the resulting white solid was collected, 89% yield.  $^1\text{H}$  NMR (400 MHz,  $\text{CDCl}_3$ )  $\delta$  ppm 4.44(s, 2 H), 3.50(s, 2 H), 3.30(s, 6 H);  $^{13}\text{C}$

NMR (100 MHz, CDCl<sub>3</sub>)  $\delta$  ppm 216.2, 102.4, 50.3, 35.8, 29.6; ESI-HRMS (m/z) calculated for C<sub>6</sub>H<sub>10</sub>Br<sub>2</sub>O<sub>3</sub> 287.8997, found 288.9483.

**2:** A solution of compound **1** (40 mmol, 11.56 g) in 120 mL acetone was cooled down in an ice bath. Sodium sulfide enneahydrate (20 mmol, 4.8 g) was dissolved in 60 mL water and dropwise added at a nitrogen atmosphere. Then the reaction mixture was warmed to room temperature and stirred for 3 hours. The solution was diluted with water (200 mL) and extracted with CH<sub>2</sub>Cl<sub>2</sub> (2  $\times$  50 mL). The organic layer was dried over anhydrous MgSO<sub>4</sub>, filtered and concentrated under reduced pressure. Yellow oil, 87% yield. <sup>1</sup>H NMR (400 MHz, CDCl<sub>3</sub>)  $\delta$  ppm 3.76(s, 4H), 3.50(s, 4H), 3.30(s, 12H); <sup>13</sup>C NMR (100 MHz, CDCl<sub>3</sub>)  $\delta$  ppm 202.5, 102.0, 50.3, 38.9, 29.8; HRMS (m/z) calculated for C<sub>12</sub>H<sub>20</sub>SBr<sub>2</sub>O<sub>6</sub>Na [m + Na<sup>+</sup>] 472.9245, found 472.9243.

**3:** Urea hydrogen peroxide (UHP) (50 mmol, 4.85 g) was introduced to the solution of trifluoroacetic anhydride (TFAA) (37.56 mmol, 7.89 g) in acetonitrile (40 mL) and the resulting solution was stirred for 3 minutes. The starting material thioether **2** (12.52 mmol, 5.66 g) in acetonitrile (20 mL) was slowly added. The reaction mixture was stirred for 2 hours at room temperature. The solution was diluted with water (150 mL) and extracted with CH<sub>2</sub>Cl<sub>2</sub> (3  $\times$  50 mL). The organic layer was dried over anhydrous MgSO<sub>4</sub>, filtered and concentrated under reduced pressure to give the pure product, yield 89%. <sup>1</sup>H NMR (400 MHz, CDCl<sub>3</sub>)  $\delta$  ppm 4.83(s, 4H), 3.47(s, 4H), 3.33(s, 12H); <sup>13</sup>C NMR (100 MHz, CDCl<sub>3</sub>)  $\delta$  ppm 199.3, 101.6, 61.6, 50.4, 28.9; HRMS (m/z) calculated for C<sub>12</sub>H<sub>20</sub>SBr<sub>2</sub>O<sub>8</sub>Na [m + Na<sup>+</sup>] 504.9143, found 504.9167.



**4:** Sulfone **3** (9.15 mmol, 4.43 g) and ammonium acetate (100 mmol, 7.7 g) were refluxed in 40 mL glacial acetic acid for 40 hours. When cooled down to room temperature, the mixture was diluted by 200 mL water and extracted with CH<sub>2</sub>Cl<sub>2</sub> (4 ×50 mL). The organic layer was collected and dried over anhydrous MgSO<sub>4</sub>, filtered and concentrated under reduced pressure to get pure product, yield 82%. <sup>1</sup>H NMR (400 MHz, CDCl<sub>3</sub>) δ ppm 8.39(s, 1H), 6.11(d, 2H), 3.53(s, 4H), 3.32(s, 12H); <sup>13</sup>C NMR (100 MHz, CDCl<sub>3</sub>) δ ppm 141.0, 102.2, 99.0, 50.2, 32.9; HRMS (m/z) calculated for C<sub>12</sub>H<sub>19</sub>SBr<sub>2</sub>O<sub>6</sub>N 462.9290, found 462.9285.

**5:** Compound **4** (7.47 mmol, 3.45 g) in 40 mL 96% formic acid was refluxed for 2 hours. The mixture was concentrated under reduced pressure and the residue was washed with water, yield 84%. <sup>1</sup>H NMR (400 MHz, CDCl<sub>3</sub>) δ ppm 8.39(s, 1H), 6.11(d, 2H), 3.53(s, 4H); <sup>13</sup>C NMR (100 MHz, DMSO-*d*<sub>6</sub>) δ ppm 194.4, 134.5, 106.7, 64.6; HRMS (m/z) calculated for C<sub>8</sub>H<sub>7</sub>SBr<sub>2</sub>O<sub>4</sub>N 370.8463, found 370.8472.

**6:** 2-Mercaptopropiophenone<sup>35</sup> (6.3 mmol, 1.05 g) and compound **5** (3 mmol, 1.11g) were dissolved separately in anhydrous acetonitrile (20 mL) respectively, bubbling nitrogen over 3 minutes. The acetonitrile solution of 2-mercapto- propiophenone was added via syringe. Then 2,6-lutidine (0.3 mL) was added and the reaction mixture was stirred over 16 hours. The reaction solution was acidified with 10% HCl at 0°C and diluted with 100 mL water. The precipitate was collected, dried and purified with the flash chromatography, yield 79%. <sup>1</sup>H NMR (400 MHz, CDCl<sub>3</sub>) δ ppm 8.53(s, 1H), 7.95(m, 4H), 7.58(m, 2H), 7.47(m, 4H), 6.65(s, 2H), 4.48(q, *J*=6.6Hz, 2H), 3.76(s, 4H), 1.54(d, *J*=6.6Hz, 6H); <sup>13</sup>C NMR (400 MHz, CDCl<sub>3</sub>) δ ppm 196.0, 188.3, 134.9, 134.4, 133.7,

128.8, 128.7, 128.6, 107.8, 42.2, 33.5, 16.8; HRMS (m/z) calculated for C<sub>26</sub>H<sub>25</sub>S<sub>3</sub>O<sub>6</sub>N 543.0844, found 543.0891.

**7:** UHP (5 mmol, 0.51 g) was introduced to the solution of TFAA (4 mmol, 0.83 g) in acetonitrile (10 mL) and the resulting solution was stirred for 3 minutes. Compound **6** (1.3 mmol, 0.73 g) in acetonitrile (10 mL) was slowly added. The reaction mixture was stirred for 2 hours. The solution was diluted with water (100 mL) and the resulting precipitate was collected. The solid sulfone and ammonium acetate (0.2 g) in glacial acetic acid (20 mL) were refluxed for 40 hours. Then the reaction solution was cooled down and diluted with water (20 mL). The resulting precipitate was collected and purified with the flash column chromatography (10% CH<sub>3</sub>OH in CH<sub>2</sub>Cl<sub>2</sub>, 56% yield). <sup>1</sup>H NMR (400 MHz, DMSO-*d*<sub>6</sub>) δ ppm 11.33(s, 1H), 10.52(s, 2H), 7.54(m, 10H), 6.59(s, 2H), 6.53(s, 2H), 1.89(s, 6H); <sup>13</sup>C NMR (100 MHz, DMSO-*d*<sub>6</sub>) δ ppm 158.5, 152.3, 148.2, 142.9, 136.9, 131.7, 129.4, 128.8, 124.2, 123.0, 19.6; HRMS (m/z) calculated for C<sub>26</sub>H<sub>23</sub>S<sub>3</sub>O<sub>6</sub>N<sub>3</sub>Na 592.0647, found 592.0633.

**9:** 3,5-Dimethylpyridine-1-oxide (5.6 g, 45.5 mmol) in 30 mL THF was added into a solution of *n*-butyl lithium (2.5 M in hexanes, 45.79 mL) and cooled to -78°C. The reaction solution was stirred for 2 hours at -78°C. Iodine (11.56 g, 90.1 mmol) in 25 mL THF was added dropwise and the temperature of reaction mixture was kept at -78°C. After an hour at -78 °C, the reaction solution was allowed to warm up to room temperature and stirred overnight. The mixture was basified with 80 mL aqueous Na<sub>2</sub>S<sub>3</sub>O<sub>3</sub> and the light yellow solid was pure product (45%, 7.22 g). <sup>1</sup>H NMR (400 MHz,

$\text{CDCl}_3$ )  $\delta$  ppm 6.87 (s, 1H), 2.45 (s, 6H) ;  $^{13}\text{C}$  NMR (100 MHz,  $\text{CDCl}_3$ )  $\delta$  ppm 148.3, 137.7, 132.1, 16.7; HRMS (m/z) calculated for  $\text{C}_{11}\text{H}_{10}\text{N}_2$  374.8617, found 374.8626.

**10:** To a 25 mL chloroform solution of **17** (1.72 g, 4.59 mmol) was added dropwise 10 mL chloroform solution of phosphorous trichloride (1.18 mL, 13.77 mmol) and refluxed overnight. The reaction mixture was basified to pH = 9 and extracted with 2 x30 mL chloroform. The combined organic layers were dried over  $\text{MgSO}_4$ . Chloroform was removed under reduced pressure to afford light yellow solid. The crude product was further purified by flash column chromatography (chloroform) to give colorless crystalline solid (98%, 1.62 g).  $^1\text{H}$  NMR and  $^{13}\text{C}$  NMR spectra match the literature.<sup>36</sup>

**11:** 2,6-Diiodo-3,5-dimethylpyridine (1.0 g, 2.8 mmol), 2-tributylstannylpyridine (1.4 g, 5.6 mmol) and  $\text{Pd}(\text{PPh}_3)_4$  (0.2 g, 0.17 mmol) were dissolved in dry toluene and refluxed for 24h. The reaction solution was cooled down, filtered through Celite and washed with  $\text{CH}_2\text{Cl}_2$  (3 x20 mL). The filtrate was wash with water and the organics was dried over anhydrous  $\text{MgSO}_4$ . The crude product was concentrated under reduced pressure and purified with flash chromatography to give a white solid (57% yield).  $^1\text{H}$  NMR (400 MHz,  $\text{CDCl}_3$ )  $\delta$  ppm 8.67(d,  $J=4.7\text{Hz}$ , 2H), 7.92(d,  $J=8.0\text{Hz}$ , 2H), 7.79(dd,  $J=7.2$ , 8.0Hz, 2H), 7.53 (s, 1H), 7.28 (m, 2H), 2.64(s, 6H);  $^{13}\text{C}$  NMR (100 MHz,  $\text{CDCl}_3$ )  $\delta$  ppm 158.7, 152.7, 148.0, 142.5, 136.4, 131.7, 124.2, 122.3, 19.5; HRMS (m/z) calculated for  $\text{C}_{17}\text{H}_{15}\text{N}_3$  261.1266, found 261.1258.

**12:** Methyl 2-ethylacetoacetate (20 mmol, 2.88 g) and 1.08 g NaOH were dissolved and stirred for 10 hours in a water/ethanol solution. The diazonium salt was prepared from aniline (20 mmol, 1.86 g), concentrated HCl (10 mL) and aqueous solution of sodium

nitrate (20 mmol, 1.38 g) in an ice bath according to the standard procedure. The diazonium salt was added to the pre-prepared sodium carboxylate solution at 0°C. The resulting solution was modified at pH 7-8 with sodium acetate and stirred at room temperature for 2 hours. The precipitate was collected, dried and refluxed overnight in formic acid (20 mL). Then the reaction solution was cooled down and diluted with water (100 mL). The precipitate was crude product and purified with the flash chromatography (CH<sub>2</sub>Cl<sub>2</sub>), yield 49%. <sup>1</sup>H NMR (400 MHz, CDCl<sub>3</sub>) δ ppm 9.25(s, 1H), 7.69(m, 1H), 7.40-7.33(m, 2H), 7.12 (m, 1H), 2.98(q, *J*=7.2Hz, 2H), 2.64(s, 3H), 1.30(t, *J*=7.2Hz, 3H); <sup>13</sup>C NMR (100 MHz, CDCl<sub>3</sub>) δ ppm 194.0, 136.1, 132.5, 129.1, 126.3, 121.2, 120.1, 118.0, 112.0, 34.4, 11.3, 8.2; HRMS (m/z) calculated for C<sub>12</sub>H<sub>13</sub>NO 187.0997, found 187.0994.

**13:** Trimethylphenylammonium tribromide (3.76 g, 100 mmol) was added into the THF (50 mL) solution of 2-acetyl-3-methylindole (1.73 g, 10 mmol). The reaction mixture was refluxed over an hour and filtered through celite. The filtrate was concentrated under reduced pressure and further purified with the flash chromatography, 72% yield. <sup>1</sup>H NMR (400 MHz, CDCl<sub>3</sub>) δ ppm 9.03(s, 1H), 7.71(m, 1H), 7.38(m, 2H), 7.16 (m, 1H), 5.17(q, *J*=6.6Hz, 1H), 2.72(s, 3H), 1.95(d, *J*=6.6Hz, 3H); <sup>13</sup>C NMR (100 MHz, CDCl<sub>3</sub>) δ ppm 186.7, 137.0, 129.8, 129.0, 127.3, 121.6, 120.6, 112.1, 43.7, 20.2, 11.2; HRMS (m/z) calculated for C<sub>12</sub>H<sub>12</sub>NOBr 265.0098, found 265.0094.

**14:** To a solution of compound **13** (1.0 g, 3.97 mmol) in acetone (15 mL), sodium sulfide nonahydrate (0.48 g, 1.98 mmol) in water (10 mL) was added dropwise at 0°C under nitrogen atmosphere. The reaction mixture was stirred for about 16 h. and the crude product was washed with water (3x 50 mL) to get rid of impurities and aqueous wastes,

yielding a pure yellowish brown solid, 91% yield.  $^1\text{H}$  NMR (400 MHz,  $\text{DMSO-}d_6$ )  $\delta$  ppm 11.52 (s, 2H), 7.68 (d,  $J=8.2$  Hz, 2H), 7.40 (d,  $J=8.2$  Hz, 2H), 7.28 (dt,  $J=7.0$  Hz,  $J=1.2$  Hz, 2H), 7.05 (dt,  $J=7.0$  Hz,  $J=1.2$  Hz, 2H), 4.06 (s, 4H) 2.56 (s, 6H);  $^{13}\text{C}$  NMR (100MHz,  $\text{DMSO-}d_6$ )  $\delta$  ppm 187.4, 136.5, 130.7, 127.9, 125.8, 120.8, 119.6, 118.8, 112.5, 40.0, 10.6; HRMS (m/z) calcd. for  $\text{C}_{22}\text{H}_{20}\text{N}_2\text{O}_2\text{S}$   $[\text{M}]^+$ : 376.1245, found : 376.1229.

**15:** To a solution of **14** (0.36 g, 0.96 mmol) in acetonitrile (10 mL), UHP (0.36 g, 3.83 mmol) dissolved in acetonitrile solution (5 mL) of TFAA (0.6 g, 2.86 mmol), was added dropwise at room temperature and stirred for 2 h. and the crude product was washed with 3x25 ml of water, filtered and air dried yielding pure yellowish brown solid which was further purified with flash column chromatography (1/1 hexane/ethyl acetate) (0.35 g, 90% yield).  $^1\text{H}$  NMR (400 MHz,  $\text{DMSO-}d_6$ )  $\delta$  ppm 11.75(s, 2H), 7.75(d,  $J=8.2$ Hz, 2H), 7.46(d,  $J=8.2$ Hz, 2H), 7.35(dt,  $J=8.2$ Hz,  $J=1.2$ Hz, 2H), 7.11(dt,  $J=7.42$ Hz,  $J=0.8$ Hz, 2H), 5.18 (s, 4H), 2.63 (s, 6H);  $^{13}\text{C}$  NMR (100MHz,  $\text{DMSO-}d_6$ )  $\delta$  ppm 181.5, 137.0, 131.3, 127.8, 126.7, 121.2, 121.1, 120.0, 112.6, 61.8, 54.9, 10.6. ESI HRMS calcd. for  $\text{C}_{22}\text{H}_{20}\text{N}_2\text{O}_4\text{S}$   $[\text{M}]^+$ : 408.1144, found : 408.1152.

**16:** To a solution of **15** (1.12 g, 2.74 mmol) in acetic acid (20 mL), ammonium acetate (2.53 g, 33 mmol) was added in two portions with an interval of 5 h. and the reaction mixture was refluxed for 26 h. The crude product was washed with 3x 25 ml of water, filtered and air dried giving yellowish brown solid (85% yield).  $^1\text{H}$  NMR (400 MHz,  $\text{DMSO-}d_6$ )  $\delta$  ppm 11.29 (s, 2H), 10.63 (s, 1H), 7.62 (d,  $J=7.8$ Hz, 2H), 7.44 (d,  $J=8.2$ Hz, 2H), 7.23 (t,  $J=7.8$ Hz, 2H), 7.09 (t, 7.8Hz, 2H), 6.32 (s, 2H), 2.47 (s, 6H);  $^{13}\text{C}$  NMR

(100MHz, DMSO-*d*<sub>6</sub>) δ ppm 136.6, 135.8, 128.2, 126.6, 123.3, 119.4, 119.2, 112.0, 111.5, 102.9, 9.5; HRMS calcd. for C<sub>22</sub>H<sub>19</sub>N<sub>3</sub>O<sub>2</sub>S [M]<sup>+</sup>: 389.1198, found : 389.1192.

**17:** The procedure is the same as that of compound **12**, starting from aniline and ethyl 2-benzylacetoacetate, yield 63%. <sup>1</sup>H NMR (400 MHz, CDCl<sub>3</sub>) δ ppm 9.29(s, 1H), 7.52-7.44(m, 7H), 7.38(m, 1H), 7.12(m, 1H), 2.19(s, 3H); <sup>13</sup>C NMR (100 MHz, CDCl<sub>3</sub>) δ ppm 191.6, 135.8, 134.3, 132.1, 130.8, 129.8, 128.9, 128.1, 126.8, 122.3, 121.0, 115.4, 112.0, 28.5; HRMS (m/z) calculated for C<sub>16</sub>H<sub>13</sub>ON 235.0997, found 235.0990.

**18:** The procedure is the same as that of compound **13**, starting from compound **17**, yield 77%. <sup>1</sup>H NMR (400 MHz, CDCl<sub>3</sub>) δ ppm 9.42(s, 1H), 7.47-7.32(m, 16H), 7.07(m, 2H), 3.38(s, 4H); <sup>13</sup>C NMR (100 MHz, CDCl<sub>3</sub>) δ ppm 185.1, 136.8, 133.6, 130.5, 129.0, 128.7, 127.6, 122.5, 121.4, 112.3, 32.7; HRMS (m/z) calculated for C<sub>16</sub>H<sub>12</sub>ONBr 313.0102, found 313.0102.

**19:** Bromoacetylkatole **13** (6.60 g, 24.9 mmol) and potassium thioacetate (3.13 g, 27.4 mmol) were dissolved in dry DMF (200 mL) under a nitrogen atmosphere. The reaction solution was stirred for 12 hours and diluted with water (600 mL). The precipitate was collected, dried (MgSO<sub>4</sub>) and dissolved in methanol (200 mL). Cysteamine hydrochloride (2.84 g, 25.0 mmol) and NaHCO<sub>3</sub> (2.1 g, 25 mmol) were added into the reaction solution. The reaction mixture was degassed for 5 minutes and stirred overnight. The reaction solution was quenched with 10% aqueous HCl, diluted with water (100 mL) and extracted with CH<sub>2</sub>Cl<sub>2</sub> (3×200 mL). The organic layer was dried over anhydrous MgSO<sub>4</sub> and concentrated under reduced pressure. The crude product was purified using flash column chromatography to give light yellow oil (2.8 g, 51% yield). <sup>1</sup>H NMR (400 MHz,

$\text{CDCl}_3$ )  $\delta$  ppm 9.09 (s, 1H), 7.70 (m, 1H), 7.38(m, 2H), 7.16(m, 1H);  $^{13}\text{C}$  NMR (100 MHz,  $\text{CDCl}_3$ )  $\delta$  ppm 187.7, 136.7, 130.9, 128.9, 127.1, 121.5, 120.5, 119.4, 112.1, 32.9, 11.4; HRMS calcd. for  $\text{C}_{11}\text{H}_{11}\text{NOS}$   $[\text{M}]^+$  : 205.0561, found : 205.0565.

**20:** Compounds **19** (0.39 g, 1.9 mmol) and **18** (0.56 g, 1.8 mmol) was dissolved in 20 mL dry acetonitrile under a  $\text{N}_2$  atmosphere. Triethylamine (0.3 mL) was added. The reaction mixture was stirred for 6 hours at room temperature. The reaction solution was quenched by 10% aqueous HCl, diluted with water (100 mL). The precipitate is pure product without any further purification (0.7 g, 85% yield).  $^1\text{H}$  NMR (400 MHz,  $\text{CDCl}_3$ )  $\delta$  ppm 9.63(s, 1H), 9.58(s, 1H), 7.57(m, 1H), 7.50-7.42(m, 6H), 7.38-7.28(m, 4H), 7.06(m, 2H), 3.91(s, 2H), 3.48(s, 2H), 2.58(s, 3H);  $^{13}\text{C}$  NMR (100 MHz,  $\text{CDCl}_3$ )  $\delta$  ppm 188.4, 187.3, 136.7, 136.4, 133.9, 131.3, 130.7, 130.4, 128.8, 128.4, 127.1, 126.7, 125.5, 122.3, 121.3, 121.1, 120.2, 120.1, 115.4, 112.1, 39.9, 37.8, 11.4; HRMS calcd. for  $\text{C}_{27}\text{H}_{22}\text{N}_2\text{O}_2\text{S}$   $[\text{M}]^+$  438.1402, found 438.1475.

**21:** To a solution of **20** (0.43g, 0.96mmol) in acetonitrile (10mL), UHP (0.36g, 3.83mmol) dissolved in acetonitrile solution (5mL) of TFAA (0.6g, 2.86mmol), was added dropwise at room temperature and stirred for 2 h. and the crude product was washed with water (3x25ml), filtered and further purified with the flash column chromatography to give a light yellow solid (0.36 g, 86%yield).  $^1\text{H}$  NMR (400 MHz,  $\text{CDCl}_3$ )  $\delta$  ppm 9.21(s, 1H), 9.03(s, 1H), 7.69(m, 1H), 7.55-7.44(m, 6H), 7.36-7.28(m, 4H), 7.15(m, 2H), 4.93(s, 2H), 4.51(s, 2H), 2.68(s, 3H); HRMS calcd. for  $\text{C}_{27}\text{H}_{22}\text{N}_2\text{O}_4\text{S}$   $[\text{M}]^+$  470.1302, found 470.1363.

**22:** The mixture of compound **21** (0.45g) and ammonium acetate (1.3g) in glacial acetic acid (15 mL) was reflux overnight. The reaction solution was cooled down and poured into ice-water (100mL). The precipitate was crude product and purified with the flash chromatography, yield 81%. <sup>1</sup>H NMR (400 MHz, CDCl<sub>3</sub>) δ ppm 11.98(s, 1H), 11.11(s, 1H), 10.65(s, 1H), 7.67(m, 1H), 7.59-7.52(m, 6H), 7.44-7.36(m, 2H), 7.32-7.28(m, 1H), 7.234-7.14(m, 2H), 7.06(m, 1H), 6.32(d, *J*=3.5Hz, 2H), 6.18(s, *J*=3.5Hz, 2H), 2.08(s, 3H); <sup>13</sup>C NMR (100 MHz, CDCl<sub>3</sub>) δ ppm 137.0, 136.8, 136.0, 135.9, 133.8, 129.5, 128.9, 128.3, 126.9, 126.7, 126.6, 126.2, 123.4, 120.5, 119.5, 119.4, 117.0, 112.3, 111.6, 104.1, 102.4, 21.8, 21.1, 8.8; HRMS calcd. for C<sub>27</sub>H<sub>22</sub>N<sub>3</sub>O<sub>2</sub>S [M]<sup>+</sup> 451.1534, found 451.1549.

**24:** This compound was prepared as described in the case of compound **12**, starting from compound **23**<sup>35</sup> and aniline, giving a 46% yield. <sup>1</sup>H and <sup>13</sup>C NMR data are in agreement with those reported in the literature.<sup>36</sup>

**25:** This compound was prepared as described in the case of compound **13**, by reacting compound **24** with trimethylphenylammonium tribromide, yield 84%. <sup>1</sup>H NMR (400 MHz, DMSO-*d*<sub>6</sub>) δ ppm 11.59(s, 1H), 7.72(m, 1H), 7.43(m, 1H), 7.31(m, 1H), 7.08(m, 1H), 4.77(s, 2H), 2.59(s, 3H); <sup>13</sup>C NMR (100 MHz, DMSO-*d*<sub>6</sub>) δ ppm 184.2, 136.8, 129.5, 127.8, 126.1, 120.1, 119.7, 119.5, 112.5, 34.9, 10.5; HRMS (m/z) calculated for C<sub>11</sub>H<sub>10</sub>BrON 250.9946, found 250.9906.

**26:** compound **25** (6.6 g, 24.9 mmol) and potassium thioacetate (3.13 g, 27.4 mmol) were dissolved in dry DMF (200 mL) under a nitrogen atmosphere. The reaction solution was stirred for 12 hours and diluted with water (600 mL). The precipitate was collected, dried and dissolved in methanol (200 mL). Cysteamine hydrochloride (2.84 g, 25 mmol) and



NaHCO<sub>3</sub> (2.1 g, 25 mmol) were added into the reaction solution. The reaction mixture was degassed for 5 minutes and stirred overnight. The reaction solution was quenched by 10% aqueous HCl, diluted with water (100 mL) and extracted with CH<sub>2</sub>Cl<sub>2</sub> (3×200 mL). The organic layer was dried over anhydrous MgSO<sub>4</sub> and concentrated under reduced pressure. The crude product was purified with the flash column chromatography. Light yellow oil, 51% yield. <sup>1</sup>H NMR (400 MHz, CDCl<sub>3</sub>) δ ppm 9.09 (s, 1H), 7.70 (m, 1H), 7.38(m, 2H), 7.16(m, 1H); <sup>13</sup>C NMR (100 MHz, CDCl<sub>3</sub>) δ ppm 187.7, 136.7, 130.9, 128.9, 127.1, 121.5, 120.5, 119.4, 112.1, 32.9, 11.4; HRMS calcd. for C<sub>11</sub>H<sub>11</sub>NOS [M]<sup>+</sup> : 219.0561, found : 219.0565.

**27**: Compounds **26** (0.38 g, 1.9 mmol) and **13** (0.5 g, 1.8 mmol) was dissolved in 20 mL dry acetonitrile under a N<sub>2</sub> atmosphere. Triethylamine (0.3 mL) was added. The reaction mixture was stirred for 6 hours at room temperature. The reaction solution was quenched by 10% aqueous HCl, diluted with water (100 mL). The precipitate is pure product without further purification. <sup>1</sup>H NMR (400 MHz, DMSO-*d*<sub>6</sub>) δ ppm 11.54(s, 1H), 11.52(s, 1H), 7.71(m, 2H), 7.42(m, 2H), 7.28(m, 2H), 7.07 (m, 2H), 4.59(q, *J*=6.8Hz, 1H), 4.10(d, *J*=15.5Hz, 1H), 4.02(d, *J*=15.5Hz, 1H), 2.58(s, 3H), 2.54(s, 3H), 1.53(d, *J*=6.8Hz, 3H); <sup>13</sup>C NMR (100 MHz, DMSO-*d*<sub>6</sub>) δ ppm 189.5, 187.8, 136.6, 130.1, 127.9, 125.7, 120.8, 119.6, 118.7, 112.4, 42.9, 37.5, 16.6, 10.5; HRMS (*m/z*) calculated for C<sub>22</sub>H<sub>20</sub>SN<sub>3</sub>O<sub>2</sub> 390.1402, found 390.1413.

**28**: This compound was prepared as described in the case of **14a**, starting from compound **27**, giving a 64% yield. <sup>1</sup>H NMR (400 MHz, DMSO-*d*<sub>6</sub>) δ ppm 11.32(s, 2H), 11.23(s, 1H), 10.52(s, 1H), 7.61(t, *J*=7.4Hz, 2H), 7.43(dd, *J*=8.2, 5.5Hz, 2H), 7.22 (t, *J*=7.8Hz,

2H), 7.08 (t, 7.8Hz, 2H), 6.19(s, 1H), 2.45(s, 3H), 2.29(s, 3H), 1.98(s, 3H); <sup>13</sup>C NMR (100MHz, DMSO-*d*<sub>6</sub>) δ ppm 137.1, 136.1, 135.9, 133.0, 128.3, 127.7, 126.5, 123.3, 122.8, 119.4, 119.2, 119.0, 112.0, 111.5, 111.4, 99.1, 9.5, 9.3, 8.7; HRMS calcd. for C<sub>22</sub>H<sub>19</sub>N<sub>3</sub>O<sub>2</sub>S [M]<sup>+</sup>: 389.1198, found : 389.1192.

## 2.5 References

1. (a) Haldar, D.; Schmuck, C. *Chem. Soc. Rev.* **2009**, *38*, 363. (b) Green, M. M.; Park, J. -W.; Sato, T.; Teramoto, A.; Lifson, S.; Selinger, R. L. B.; Selinger, J. V. *Angew. Chem. Int. Ed.* **1999**, *38*, 3138. (c) Hill, D. J.; Mio, M. J.; Prince, R. B.; Hughes, T. S.; Moore, J. S. *Chem. Rev.* **2001**, *101*, 3893. (d) Nakano, T.; Okamoto, Y. *Chem. Rev.* **2001**, *101*, 4013. (e) Yashima, E.; Maeda, K.; Nishimura, T. *Chem. Eur. J.* **2004**, *10*, 42. (f) Yashima, E.; Meada, K.; Lida, H.; Furusho, Y.; Nagai, K. *Chem. Rev.* **2009**, *109*, 6102.
2. Busch, D. H. *J. Inclusion Phenom. Mol. Recognit. Chem.* **1992**, *12*, 389.
3. (a) Lehn, J. -M.; Rigault, A.; Siegel, J.; Harrowfield, J.; Chevrier, B.; Moras, D. *Proc. Natl. Acad. Sci. USA* **1987**, *84*, 2565. (b) Koert, U.; Harding, M. M.; Lehn, J. -M. *Nature* **1990**, *346*, 339. (c) Bell, T. W.; Jouselin, H. *Nature* **1994**, *367*, 441. (d) Albrecht, M. *Chem. Rev.* **2001**, *101*, 3457.
4. Kramer, R.; Lehn, J. M.; Rigault, A. *Proc. Natl. Acad. Sci. USA* **1993**, *90*, 5394.
5. Sanchez-Quesada, J.; Seel, C.; Prados, P.; de Mendoza, J. *J. Am. Chem. Soc.* **1996**, *118*, 277.
6. Furusho, Y.; Yashima, E. *Chem. Rec.* **2007**, *7*, 1.

7. Katagiri, H.; Miyagawa, T.; Furusho, Y.; Yashima, E. *Angew. Chem. Int. Ed.* **2006**, *45*, 1741.
8. Miwa, K.; Furusho, Y.; Yashima, E. *Nat. Chem.* **2010**, *2*, 444.
9. (a) Colquhoun, H. M.; Williams, D. J. *Acc. Chem. Res.* **2000**, *331*, 189. (b) Kobayashi, N.; Sasaki, S.; Abe, M.; Watanabe, S.; Fukumoto, H.; Yamamoto, T. *Macromolecules* **2004**, *37*, 7986.
10. Goto, H.; Katagiri, H.; Furusho, Y.; Yashima, E. *J. Am. Chem. Soc.* **2006**, *128*, 7176.
11. Huc, I. *Eur. J. Org. Chem.* **2004**, 17.
12. (a) Berl, V.; Huc, I.; Khoury, R. G.; Krische, M. J.; Lehn, J. -M. *Nature* **2000**, 407, 720. (b) Berl, V.; Huc, I.; Khoury, R. G.; Lehn, J. -M. *Chem. Eur. J* **2001**, *7*, 2810.
13. Dolain, C.; Zhan, C.; Leger, J. -M.; Daniels, L.; Huc, I. *J. Am. Chem. Soc.* **2005**, *127*, 2400.
14. Zhan, C.; Leger, J. -M.; Huc, I. *Angew. Chem. Int. Ed.* **2006**, *45*, 4625.
15. Berni, E.; Kauffmann, B; Bao, C.; Lefeuvre, J.; Bassani, D. M.; Huc, I. *Chem. Eur. J.* **2007**, *13*, 8463.
16. Gan, Q.; Ferrand, Y.; Bao, C.; Kauffmann, B.; Grelard, A.; Jiang, H.; Huc, I. *Science* **2011**, *331*, 1172.
17. (a) Kraft, A.; Peters, L.; Powell, H. R. *Tetrahedron* **2002**, *58*, 3499. (b) Otsuki, J.; Iwasaki, K.; Nakano, Y.; Itou, M.; Araki, Y.; Ito, O. *Chem. Eur. J.* **2004**, *10*, 3461. (c) Corbellini, F.; di Constanzo, L.; Creges-Calama, M.; Geremia, S.; Reinhoudt, D. N. *J. Am. Chem. Soc.* **2003**, *125*, 9946.

18. (a) Goto, H.; Katagiri, H.; Furusho, Y.; Yashima, E. *J. Am. Chem. Soc.* **2006**, *128*, 7176. (b) Goto, H.; Furusho, Y.; Yashima, E. *J. Am. Chem. Soc.* **2007**, *129*, 109. (c) Goto, H.; Furusho, Y.; Yashima, E. *J. Am. Chem. Soc.* **2007**, *129*, 9168. (d) Goto, H.; Furusho, Y.; Miwa, K.; Yashima, E. *J. Am. Chem. Soc.* **2009**, *131*, 4710.
19. Tanaka, Y.; Katagiri, H.; Furusho, Y.; Yashima, E. *Angew. Chem. Int. Ed.* **2005**, *44*, 3867.
20. Ito, H.; Ikeda, M.; Hasegawa, T.; Furusho, Y.; Yashima, E. *J. Am. Chem. Soc.* **2011**, *133*, 3419.
21. Albrecht, M. *Angew. Chem. Int. Ed.* **2005**, *44*, 6448.
22. (a) Gong, B.; Yan, Y.; Zeng, H.; Skrzypczak-Jankunn, E.; Kim, Y. W.; Zhu, J.; Ickes, H. *J. Am. Chem. Soc.* **1999**, *121*, 5607. (b) Folmer, B. J. B.; Sijbesma, R. P.; Kooijman, H.; Spek, A. L.; Meijer, E. W. *J. Am. Chem. Soc.* **1999**, *121*, 9001. (c) Corbin, P. S.; Zimmerman, S. C. *J. Am. Chem. Soc.* **2000**, *122*, 3779. (d) Bisson, A. P.; Carver, F. J.; Eggleston, D. S.; Haltiwanger, R. C.; Hunter, C. A.; Livingstone, D. L.; McCabe, J. F.; Rotger, C.; Rowan, A. E. *J. Am. Chem. Soc.* **2000**, *122*, 8856. (e) Archer, E. A.; Goldberg, N. T.; Lynch, V.; Krische, M. J. *J. Am. Chem. Soc.* **2000**, *122*, 5006. (f) Moriuchi, T.; Tamura, T.; Hirao, T. *J. Am. Chem. Soc.* **2002**, *124*, 9356.
23. Li, J. Ph. D. Thesis, University of Western Ontario, London, Ontario, **2009**.
24. Pugh, D. *Acta Cryst.* 2006, **C62**, o590.

25. (a) Kelly, T. R.; Kim, M. H. *J. Am. Chem. Soc.* **1994**, *116*, 7072. (b) Cook, J. L.; Hunter, C. A.; Low, C. M. R.; Perez-Velasco, A.; Winter, J. G. *Angew. Chem. Int. Ed.* **2007**, *46*, 3706.
26. Crystal data for :  $C_{43}H_{38}N_6O_6S_3 \cdot CHCl_3$ , MW = 950.34 g/mol, triclinic,  $a = 12.1851(4)$  Å,  $b = 12.7756(4)$  Å,  $c = 15.7666(5)$  Å,  $\alpha = 82.465(1)^\circ$ ,  $\beta = 77.978(1)^\circ$ ,  $\gamma = 70.320(1)^\circ$ ,  $U = 2255.40(12)$  Å<sup>3</sup>,  $T = 150$  K, space group P1,  $Z = 2$ , 143783 reflections measured, 14429 unique reflections ( $R_{int} = 0.0804$ ),  $R(F^2 > 2\sigma) = 0.0456$ ,  $R_w(F^2, all\ data) = 0.1181$ . CCDC Number: 783459.
27. Recent review: Gale, P. A. *Chem. Commun.* **2008**, 4525.
28. (a) Robinson, B. *The Fisher Indole Synthesis*. J. Wiley & Sons, New York, **1982**. (b) Humphrey, G. R.; Kuethe, J. T. *Chem. Rev.* **2006**, *106*, 2875.
29. Celebi-Olcum, N.; Boal, B. W.; Hutters, A. D.; Garg, N. K.; Houk, K. N. *J. Am. Chem. Soc.* **2011**, *133*, 5752.
30. Crystal data for :  $C_{22}H_{19}N_3O_2S_3$ , MW = 389.46 g/mol, monoclinic,  $a = 27.9372(56)$  Å,  $b = 6.7394(13)$  Å,  $c = 9.871(2)$  Å,  $\beta = 92.107(30)^\circ$ ,  $U = 1857.24(60)$  Å<sup>3</sup>,  $T = 150$  K, space group C2/c,  $Z = 2$ , 6382 reflections measured, 1657 unique reflections ( $R_{int} = 0.0637$ ),  $R(F^2 > 2\sigma) = 0.0482$ ,  $R_w(F^2, all\ data) = 0.1289$ . CCDC Number: 783460.
31. Bisson, A. P.; Hunter, C. A.; Morales, J. C.; Young, K. *Chem. Eur. J.* **1998**, *4*, 845.
32. Gancia, E.; Montana, J. G.; Manallack, D. T. *J. Mol. Graphics. Modell.* **2001**, *19*, 349.

33. (a) Constable, E. C. *Chem. Soc. Rev.* **2007**, 36, 246. (b) Calderazzo, F.; Englert, U.; Hu, C.; Marchetti, F.; Pampaloni, G.; Passarelli, V.; Romano, A.; Santi, R. *Inorg. Chim. Acta.* **2003**, 344, 197.
34. Benech, J. -M.; Piguet, C.; Bernardinelli, G.; Bunzli, J. -C. G.; Hopfgartner, G. *J. Chem. Soc. Dalton Trans.* **2001**, 684.
35. Jones, S. M.; Urch, J. E.; Kaiser, M.; Brun, R.; Harwood, J. L.; Berry, C.; Gilbert, I. *H. J. Med. Chem.* **2005**, 48, 5932.
36. Pal, M.; Dakarapu, R.; Padakanti, S. *J. Org. Chem.* **2004**, 69, 2913.

## CHAPTER 3

### Substituent Effects in Double Helical Hydrogen-Bonded AAA-DDD Complexes

#### 3.1 Substituent Effects for Hydrogen-Bonded Complexation

Hydrogen bonds are attractive electrostatic interactions. The association constant is a key measurement of the binding strength and determines the dynamics of systems incorporating the hydrogen-bond groups. For weaker hydrogen bonds, the lifetimes of associated species are shorter than for systems with higher association constants. Thus, it is important to tune the binding strength for hydrogen bonded system.

The binding process is enthalpically dominated, but binding entropy often shows an unfavorable contribution. In general, there are two equations about the relationships among all the thermodynamic parameters ( $K_a$ , association constant,  $\Delta G$ , change in free energy,  $\Delta H$  and  $\Delta S$ , changes in enthalpy and entropy, respectively):

$$K_a = e^{-\Delta G/RT} \quad (1)$$

$$\Delta G = \Delta H - T\Delta S \quad (2)$$

It is clear that strong binding can be reached either by a more negative  $\Delta H$ , a more positive  $\Delta S$ , or a combination of both. The binding enthalpy itself depends on hydrogen-bond donor and acceptor properties, while the association entropy is made up of conformational changes. The binding complexation is related with not only structures

(enthalpy) but also the dynamics (entropy) of the interacting sites. Therefore, an aim is to alter the chemical properties of the hydrogen-bond donor and acceptor by adding functional groups or modifying existing groups in order to achieve higher association constants.

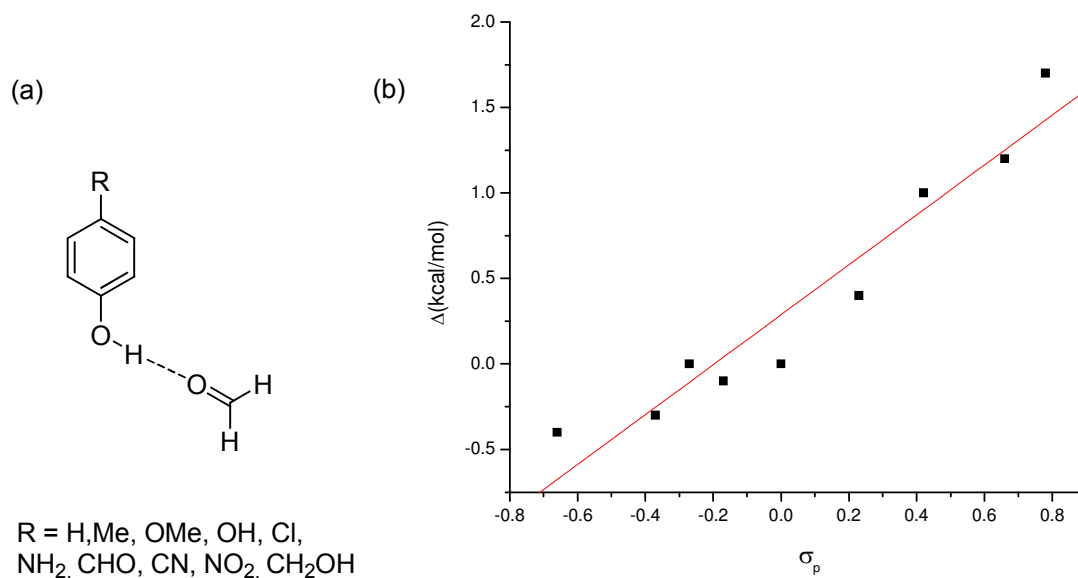


**Figure 3-1** (a) Structures of phenol and its derivatives; (b) the change in hydrogen bonded strength ( $\Delta$ ) relative to the original phenol-formaldehyde system plotted against the Hammett constant ( $\sigma_p$ ). (Data from Reynisson, J.; McDonald, E. *J. Comput. Aided Mol. Des.* **2004**, *18*, 421.)

Reynisson et al. investigated the computed change in free energy between *p*-substituted phenols and anilines as hydrogen bond donors and the influence of different substituent groups on the hydrogen bond strength with a formaldehyde acceptor.<sup>1</sup> The binding energies for the phenol-formaldehyde system lie between 3.5 to 5.5 kcal/mol and those for the aniline-formaldehyde system are from 1.1 to 3.4 kcal/mol. Theoretical calculations indicated that aniline is a poorer hydrogen-bond donor than phenol, which is

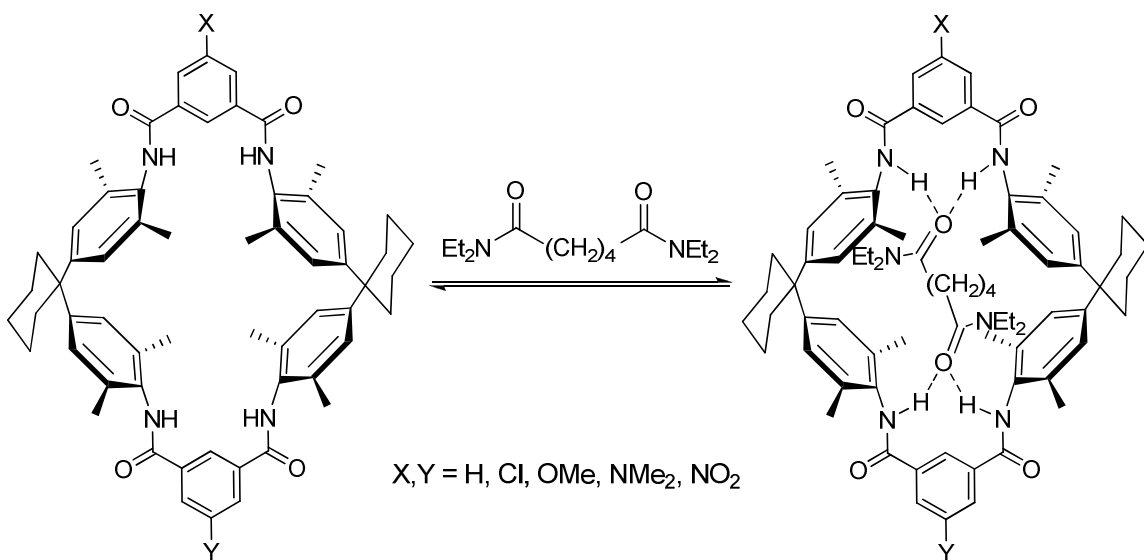


consistent with nitrogen having a lower electron affinity than oxygen. The Hammett substituent constants, which quantify the electron withdrawing or electron donating ability of one group at given position, have enjoyed success as structural factors in structure-activity/property relationships. As shown in Figure 3-1, the plot for the difference binding strength relative to the original phenol vs the Hammett constant is linear.

Pu and coworkers also investigated substituent effects on the hydrogen bonded complex of *para*-substituted anilines with one water molecule.<sup>2</sup> The result suggested that the substitution induced changes in the electron density transfer from the water molecule to the aniline while this change in the electron density transfer would give rise to the variation on the electron densities in the proton donating N-H bond and the N-H $\cdots$ O hydrogen bond and ultimately influence the length and frequency of the N-H bond, the H $\cdots$ O distance, and the binding energy.

Tetralactam macrocycles have been widely used in the synthesis of interlocked rotaxanes and pseudorotaxanes. The binding properties of tetralactam with different substituents on the isophthalamide rings and an adipamide guest were investigated in chloroform with <sup>1</sup>H NMR titrations (Scheme 3-1).<sup>3</sup> The binding stability depends greatly on the substituent groups, and the complexation for macrocycle and guest could be modulated by the remote substituent groups varying up to 3.4 kcal/mol. The hydrogen-bond donor ability of the amide hydrogen atoms in the macrocycle are likely responsible for the substituent effects. The electron withdrawing groups increase the donor ability and the electron donating groups decrease it. The association constants also increase in parallel with the donor abilities of the amides in substituted macrocycles. So, electron-

withdrawing groups such as  $\text{NO}_2$ ,  $\text{Cl}$  increase the bind stability, while electron-donating groups such as  $\text{OMe}$ ,  $\text{NMe}_2$  decrease it.



**Scheme 3-1** The hydrogen-bonded complexation between tetralactam macrocycle and adipamide guest (when  $\text{X} = \text{Y} = \text{NMe}_2$ ,  $\Delta G = -2.5$  kcal/mol; when  $\text{X} = \text{Y} = \text{H}$ ,  $\Delta G = -3.9$  kcal/mol; when  $\text{X} = \text{Y} = \text{NO}_2$ ,  $\Delta G = -5.9$  kcal/mol) at  $23 \pm 1^\circ\text{C}$  in  $\text{CDCl}_3$ .

Popelier and coworkers used ab initio descriptors to investigate the substituent effects on interaction energies of the Watson-Crick hydrogen-bonded base pair guanine and cytosine in the gas phase. The complexations of unsubstituted guanine and cytosine with 42 substituted groups both at the C6 and C5 positions ( $\text{X}_5$  and  $\text{X}_6$ ) were firstly studied.<sup>4</sup> The calculated results demonstrated that a more strongly electron withdrawing group at  $\text{X}_5$  and  $\text{X}_6$  positions form less stable base pair.

On other hand, the interaction energies between guanine substituted with different functional groups at  $\text{Y}_8$  position and unsubstituted cytosine ( $\text{X}_5 = \text{H}$ ,  $\text{X}_6 = \text{H}$ ) were calculated.<sup>5</sup> There was a linear relationship between substitution interaction energy and

the Hammett constant (Figure 3-2). The negative slope means that the substitution interaction energy decreases with the increase of  $\sigma_m$ , corresponding to more stable base pair; that is to say, electron withdrawing groups at  $Y_8$  position will help to form the stable base pair complexes.

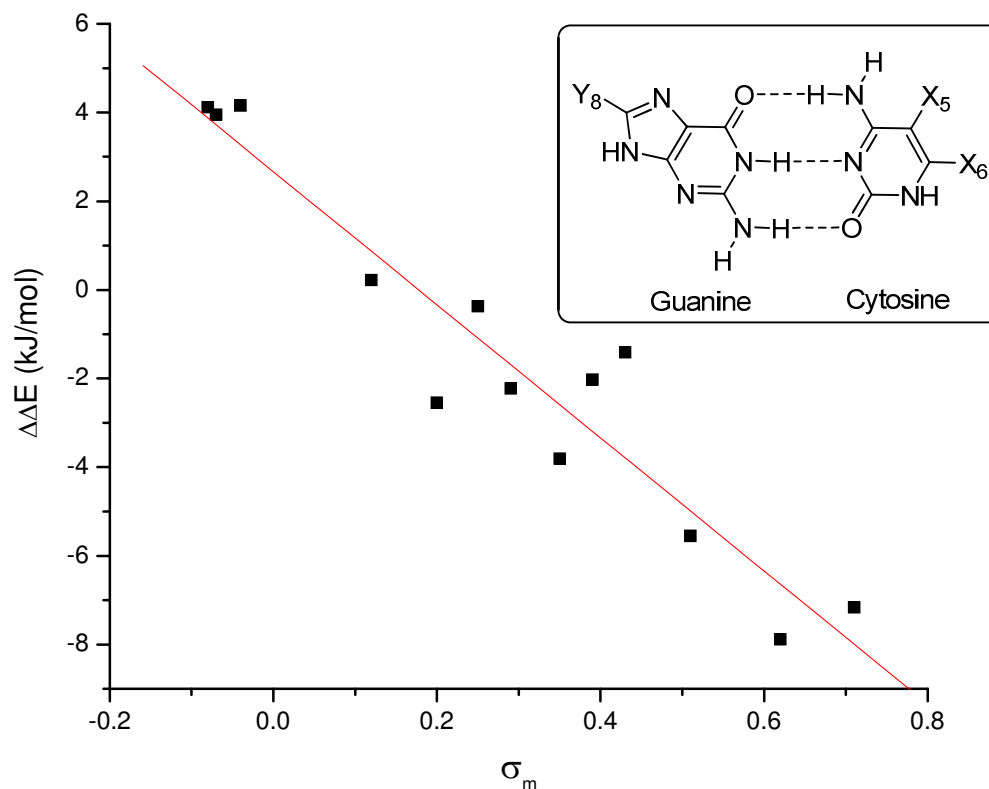
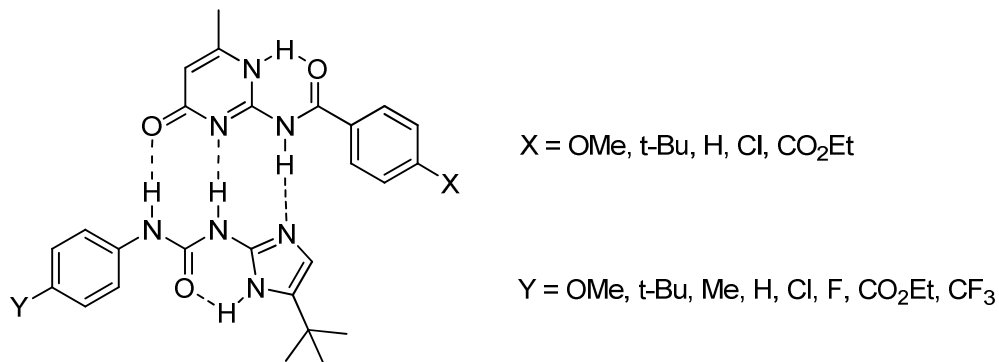


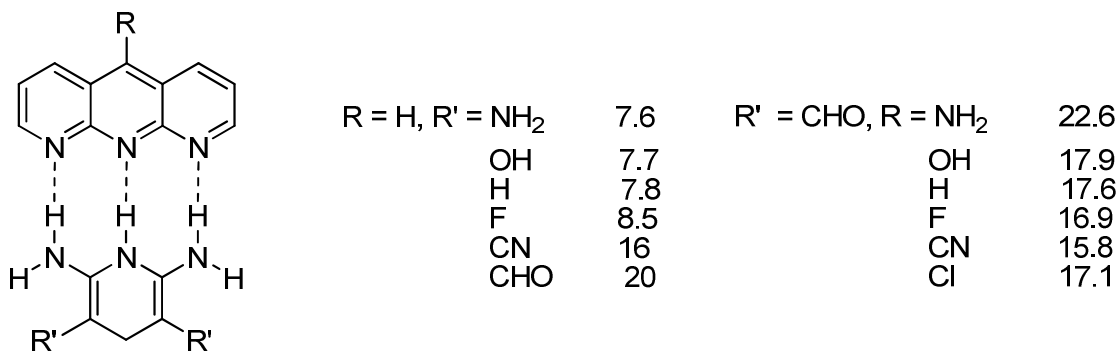
**Figure 3-2** Relationship between the substitution interaction energy ( $\Delta\Delta E$ , kJ/mol) calculated by GAUSSIAN03 and the Hammett constant ( $\sigma_m$ ) ( $X_5 = H$ ,  $X_6 = H$ ) (Data from Xue, C.; Popelier, P. L. A. *J. Phys. Chem. B* **2009**, *113*, 3245.)

Wilson and coworkers did some experimental work on remote substituent effects (Scheme 3-2).<sup>6</sup> They found that electron donating groups on the phenyl ring of amidocytosine (AAD) and electron withdrawing group on the phenyl ring of

ureidoimidazole (DDA) lead to a higher stability complex. This result was the same as what Popelier calculated.



**Scheme 3-2** Structures of triply hydrogen-bonded heterodimers with different functional groups.



**Scheme 3-3** The model AAA-DDD system where the R and R' substituents are varied and binding energies (kcal/mol).

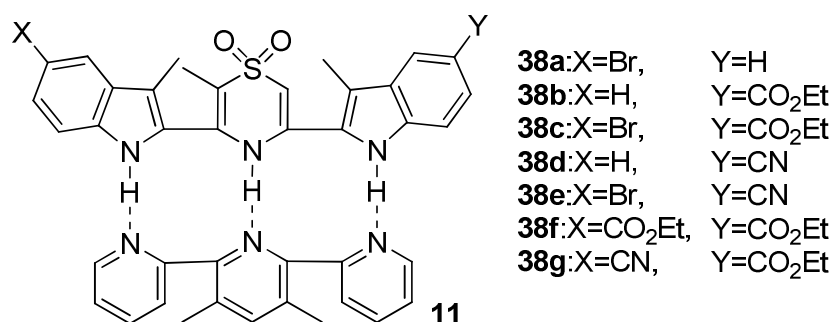
The aforementioned coplanar AAA-DDD complexes exhibit extremely high association constants over other arrays based on three hydrogen bonds. Boyd and coworkers performed theoretical studies on how the hydrogen-bond strength of coplanar AAA-DDD complexes changes by varying the substituents in specific positions (Scheme 3-3).<sup>7</sup> The results suggested that electron-withdrawing groups on the DDD component or

electron donating groups on the AAA component increase the binding constants of hydrogen-bonded AAA-DDD complexes. In addition, the electron withdrawing groups on DDD have a larger effect on the binding energy than the electron donating groups on AAA.

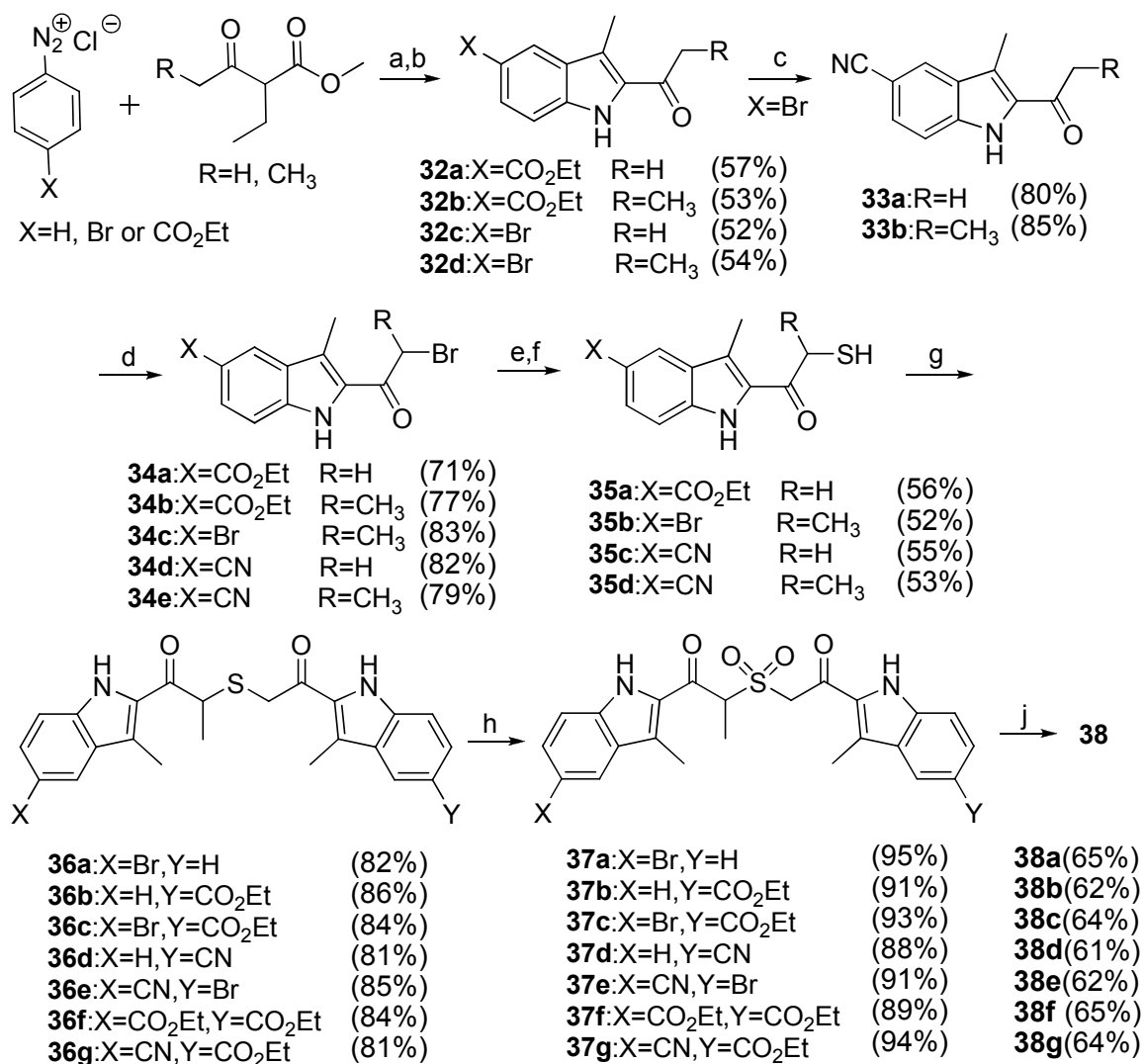
As the above examples demonstrate, electron withdrawing groups on the DDD component or electron donating groups on the AAA component may improve the binding stability and increase the association constants. In Chapter 2, we developed the easily accessible DDD-AAA system based on pyridine-lutidine-pyridine and indole-thiazine dioxide-indole. In this chapter, DDD including electron-withdrawing groups and electron-donating groups on AAA are designed to achieve more stable DDD-AAA complexes.

## 3.2 Results and Discussions

### 3.2.1 Electron-Withdrawing Groups on DDDs



The installation of electron-withdrawing groups (Br, CO<sub>2</sub>Et and CN) on the indole rings was firstly designed and synthesized. The association constants of these DDDs and AAA **11** were investigated with <sup>1</sup>H NMR titrations.



**Scheme 3-4** Synthesis of DDD compounds **38** with different electron-withdrawing

groups. Reagents and conditions: a) NaOH, C<sub>2</sub>H<sub>5</sub>OH /H<sub>2</sub>O, methyl 2-ethylacetoacetate for **32a** and **32c** (or ethyl (2-ethyl)propionylacetate for **32b** and **32d**), 8h; b) HCOOH, reflux, 24h; c) Zn(CN)<sub>2</sub>, DMF, Pd(PPh<sub>3</sub>)<sub>4</sub>, 170°C, microwave, 6h; d) PhNMe<sub>3</sub>Br<sub>3</sub>, THF, reflux, 1h; e) KSAc, DMF, 12h; f) NaHCO<sub>3</sub>, cysteamine hydrochloride, CH<sub>3</sub>CN, 18h; g) Et<sub>3</sub>N, CH<sub>3</sub>CN, 18h; h) *m*-CPBA, DMF, -25°C to r.t., 12h; j) NH<sub>4</sub>OAc, glacial acetic acid, microwave, 180°C, 3h.

**Table 3-1** Changes in the chemical shifts of N-H ( $\Delta\delta$ ), substituent constants ( $\sigma_p$ ), association constants ( $K_a$ ), and free energy of the complexations of **28**, **38a-38g** and **11** in chloroform at 298K (experimental errors in brackets are twice the standard deviations).

	<b>28</b>	<b>38a</b>	<b>38b</b>	<b>38c</b>	<b>38d</b>	<b>38e</b>	<b>38f</b>	<b>38g</b>
Groups (X, Y)	H, H	Br, H	H, CO <sub>2</sub> Et	Br, CO <sub>2</sub> Et	H, CN	Br, CN	CO <sub>2</sub> Et, CO <sub>2</sub> Et	CN, CO <sub>2</sub> Et
$\Delta\delta_{\max}$ (ppm)	3.00 <sup>[a]</sup>	2.60 <sup>[a]</sup>	3.09 <sup>[a]</sup>	2.86 <sup>[a]</sup>	2.72 <sup>[a]</sup>	2.80 <sup>[a]</sup>	2.78 <sup>[a]</sup>	/
	2.79 <sup>[b]</sup>	3.88 <sup>[b]</sup>	2.71 <sup>[b]</sup>	2.46 <sup>[b]</sup>	2.36 <sup>[b]</sup>	2.36 <sup>[b]</sup>	3.94 <sup>[b]</sup>	/
	3.51 <sup>[c]</sup>	3.22 <sup>[c]</sup>	3.56 <sup>[c]</sup>	3.21 <sup>[c]</sup>	3.02 <sup>[c]</sup>	3.93 <sup>[c]</sup>	4.02 <sup>[c]</sup>	3.29
$\Sigma\sigma_p$	0.00	0.23	0.45	0.68	0.66	0.89	0.90	1.11
$K_a$ (M <sup>-1</sup> ) <sup>[d]</sup>	3.7×10 <sup>3</sup>	7×10 <sup>3</sup>	1.1×10 <sup>4</sup>	2.6×10 <sup>4</sup>	2.9×10 <sup>4</sup>	4.9×10 <sup>4</sup>	5.4×10 <sup>4</sup>	1.1×10 <sup>5</sup>
	(±180)	(±280)	(±340)	(±1.1×10 <sup>3</sup> )	(±1.6×10 <sup>3</sup> )	(±1.3×10 <sup>3</sup> )	(±1.7×10 <sup>3</sup> )	(±5.0×10 <sup>3</sup> )
$\Delta G$ (kJ·mol <sup>-1</sup> )	- 20.4	- 21.9	- 23.1	- 25.2	- 25.5	- 26.8	- 27.0	- 28.8
$\Delta\Delta G$ (kJ·mol <sup>-1</sup> )	0	1.5	2.7	4.8	5.1	6.4	6.6	8.4

[a] change in the chemical shift of N-H on thiazine dioxide; [b] change in the chemical shift of N-H on X-substituted indole; [c] change in the chemical shift of N-H on Y-substituted indole; [d] Values are averages calculated from triplicate measurements.

As shown in Scheme 3-4, Fischer indole synthesis was used to prepare the starting 2-acetyl-3-methyl indoles in formic acid. The intermediate hydrazones for the synthesis of indoles were produced from  $\beta$ -ketoesters and aryl diazonium salts via the Japp-Klingemann reaction. After the bromination of the indoles, thiols were synthesized via hydrolysis of the corresponding thioacetates. Once the thiols were ready, the other remaining steps (substitution, oxidation and cyclization) were easily accomplished according to our previous methods. For the cyano substituted indoles, the Pd-catalyzed cyanation of aryl halides allows for the conversion of indolyl halides into the corresponding nitrile.<sup>15</sup> Cyano is a strong electron-withdrawing group and the esters are a medium strength electron-withdrawing group.

The interaction between each of the eight DDD molecules that were soluble in  $\text{CDCl}_3$  (**38a-g**) and **11** was observed using  $^1\text{H}$  NMR spectroscopy. A  $\text{CDCl}_3$  solution of each of **38a-g** was titrated with **11** and the resulting change in chemical shift of the three N-H protons was used to determine the binding constant ( $K_{X,Y}$ ) by non-linear curve fitting of the data to a simple 1:1 binding model. In all cases, the three N-H protons of **38** undergo large downfield shifts upon addition of excess **11** ( $4.02 \geq \Delta\delta_{\text{max}} \geq 2.36$  ppm) indicating a strong hydrogen bond interaction with all three sites. In the case of **38g/11**, when less than 0.5 equivalents **11** were added into the solution of **38g**, the N-H peaks disappeared. However, when more than 0.5 equivalents **11** were added, all the N-H peaks reappeared. Non-linear regression analysis demonstrated that the association constant of **38g** and **11** may be over  $10^5 \text{ M}^{-1}$ . That means the association constant of **38g** and **11** is over the limit ( $K_a < 10^5 \text{ M}^{-1}$ ) of the  $^1\text{H}$  NMR titration. For the strong binding system ( $K_a \geq 10^5 \text{ M}^{-1}$ ), isothermal titration calorimetry (ITC) is a better way to measure the



association constant.<sup>16</sup> Although there is a good concordance for  $K_a$  values from the different measurements NMR and ITC in this case, a high  $K_a$  value from the NMR titration is in question and not reliable.

The results are summarized in Table 3-1. It is evident about the tendency in the magnitudes of association constants, that is, electron-withdrawing groups increase the association constants from  $3.7 \times 10^3 \text{ M}^{-1}$  to  $1.13 \times 10^5 \text{ M}^{-1}$ . Electron withdrawing groups on the X or/and Y positions of the indole rings improve the hydrogen bond interactions by decreasing the electron density on the DDD N-H hydrogen atoms and further producing a higher partial positive charge on the indole-NH. We could find no obvious correlations to draw between either the electronic character of the substituents X and Y (expressed as Hammett  $\sigma_p$  values) or the stabilities of the resulting complexes ( $K_{X,Y}$ ) with the  $\delta_{\text{free}}$ ,  $\delta_{\text{max}}$  and  $\Delta\delta_{\text{max}}$  values obtained from the titration curves (see supplementary information). The effects are therefore the result of a more complex relationship with the chemical shifts of the NMR resonances than the simple linear variance that one might expect. The results imply that the effect of X and Y on **38a-g** is not only electronic and perturbing the NH hydrogen bond acidities but also conformational. We interpret the apparently random variation of the  $\delta$  values in the series of eight donor molecules to mean that the free donor molecules have very different average conformations with respect to their interplanar dihedral angles.

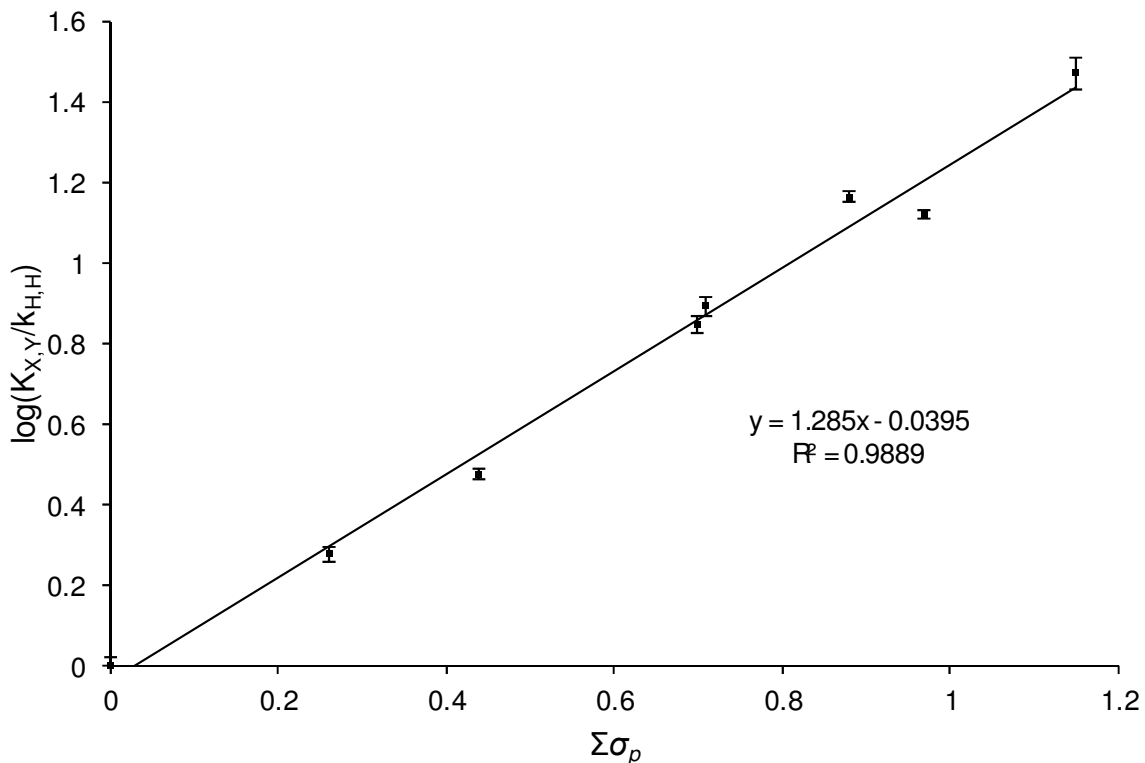


**Figure 3-3** Hammett plot of  $\log(K_{X,Y}/K_{H,H})$  vs  $\Sigma\sigma_p$ .

However, there is a clear linear free energy relationship between the magnitude of the complex stability and the electronic character of the substituents on the indole rings. It is apparent that, as one might expect, the installation of electron withdrawing substituents at the 5-positions of either skatole ring system in **38** results in a predictable increase in the stability of the complex with **11**. According to the Hammett substituent constants  $\sigma_p$ , the electron withdrawing or donating ability of different groups can be predicted. In our cases, the  $\sigma_p$  values of electron withdrawing groups are:  $\text{CO}_2\text{Et} = 0.44$ ,  $\text{CN} = 0.71$ .<sup>17</sup> Apparently, DDD including cyano group should exhibit a higher binding ability than that of DDD including ester group. The results demonstrated that an ester group increases the binding energy of the AAA-DDD complex by 2.9 kJ/mol and a cyano group increases it by 5.2 kJ/mol. There is a linear relationship between  $\sigma_p$  and  $\Delta G$  in

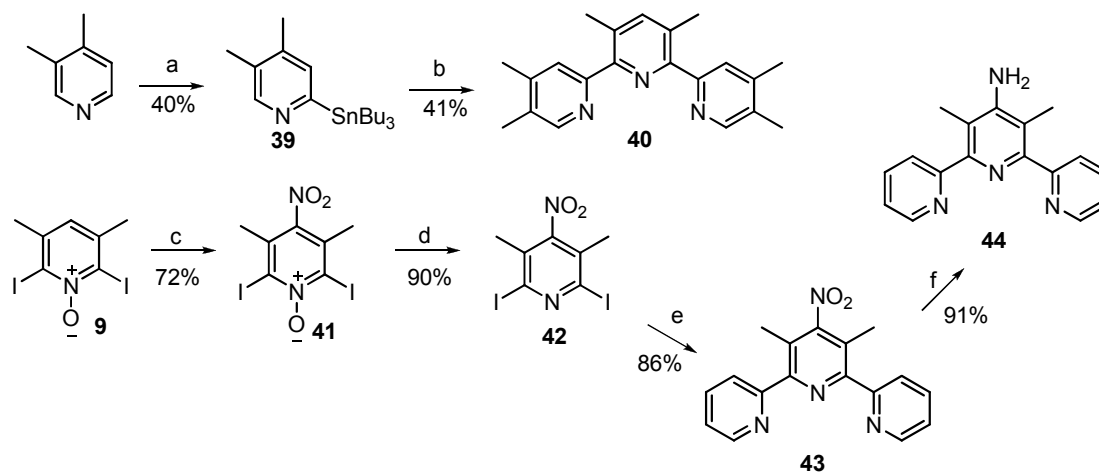
Figure 3-3. A plot of the sum of the Hammett substituent constants for X and Y ( $\Sigma\sigma_p$ ) against  $\log(K_{X,Y}/K_{H,H})$  displays a linear correlation with  $\rho = 1.29$  and  $R^2 = 0.9889$ . The positive value of  $\rho$  indicates that electron withdrawing groups stabilize the developing partial negative charge on the nitrogen atom of the skatole rings, as a result of the hydrogen bonding interaction. The magnitude of  $\rho$  recorded here is similar to that observed by Wilson and coworkers in their examination of AAD/DDA hydrogen bond complexes. Though electron donating groups have not been specifically explored in this context it is reasonable to assume that the linear relationship observed extends to these cases as well.

### 3.2.2 Substituent Groups on AAA

The DDD molecules synthesized with electron withdrawing groups display a large increase (more than 8 kJ/mol) in the binding energy of AAA-DDD complexes. On the other hand, we wondered whether electron donating groups attached to the AAA component would strengthen the complexation in the same but opposite manner.

From the view of synthetic ease and Hammett constant  $\sigma$  values of electron donating groups, compounds **40**, **43** and **44** were prepared (Scheme 3-5). Generally, the AAA components were synthesized via the Stille coupling reaction. 4,5-Dimethyl-2-tributyltinpyridine which was achieved through the ring-selective lithiation of 3,4-lutidine<sup>17</sup>, was an important intermediate for **39**. 2,6-diiodo-3,5-lutidine coupled with **39** to afford the AAA component **40**. 4-Nitrile pyridine can be easily reduced into strong electron donating group containing 4-aminopyridine. When pyridine is substituted with electron withdrawing group, the Stille coupling is relatively easier than that substituted

with electron donating group. Hence, we prepared the intermediate **42**, which was coupled with 2-tributyltinpyridine to produce **43** and followed by the reduction reaction to provide **44**.



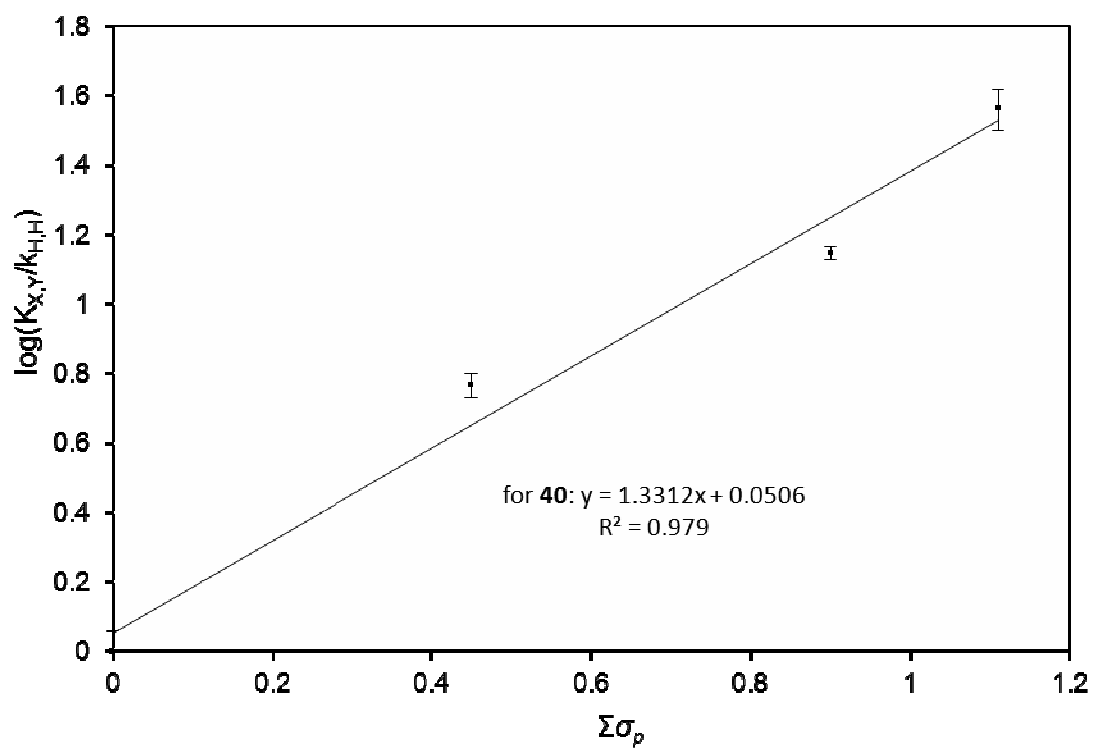
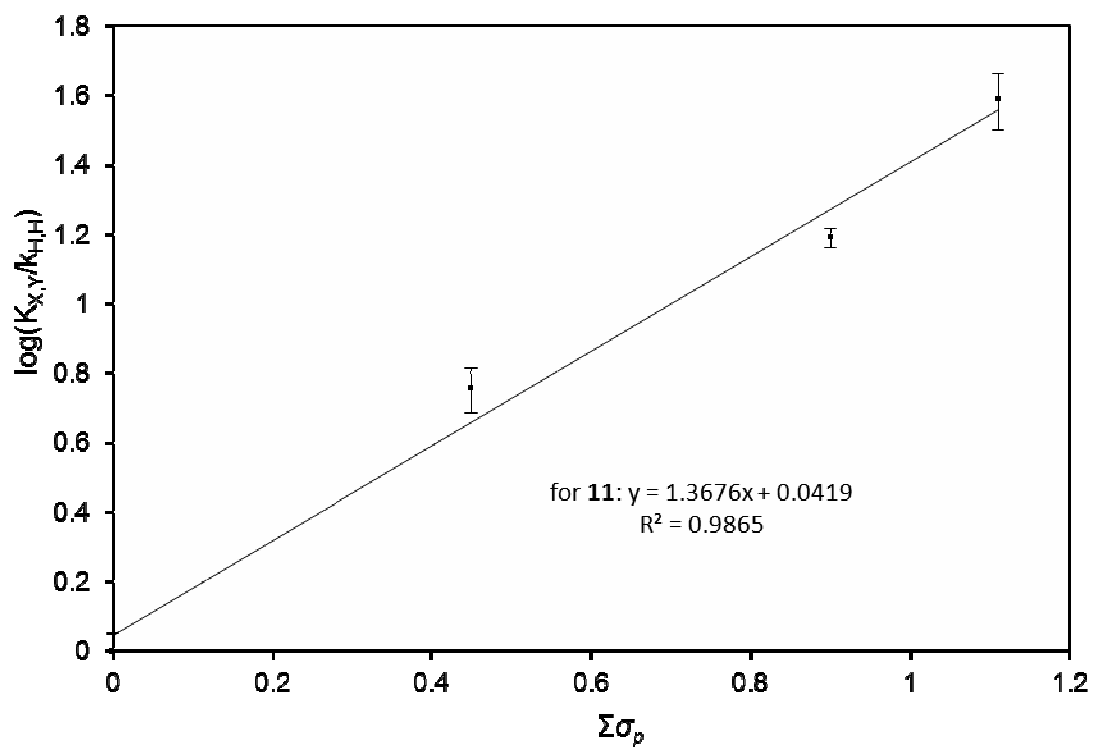
**Scheme 3-5** Synthesis of AAA components **40**, **43** and **44**. Reagents and conditions: a) (i) *n*-BuLi, hexane, 2-dimethylaminoethanol, 0°C, 1h, (ii) Bu<sub>3</sub>SnCl, THF, -78°C to r.t., 1h; b) 2,6-diiodo-3,5-dimethyllutidine, Pd(PPh<sub>3</sub>)<sub>4</sub>, toluene, reflux, 7 days; c) HNO<sub>3</sub>, H<sub>2</sub>SO<sub>4</sub>, 70°C, 12h; d) PCl<sub>3</sub>, CHCl<sub>3</sub>, reflux, 12h; e) 2-tributyltinpyridine, Pd(PPh<sub>3</sub>)<sub>4</sub>, toluene, reflux, 16h; f) 10%Pd/C, hydrazine hydrate, EtOH, reflux, 1.5h.

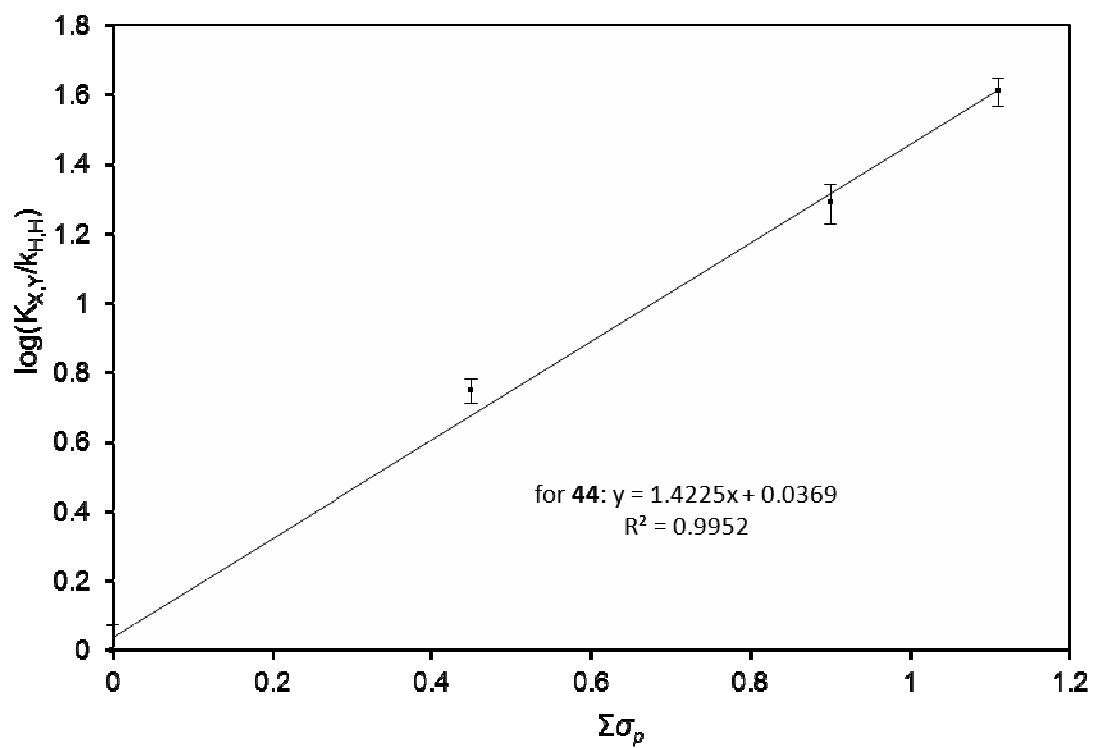
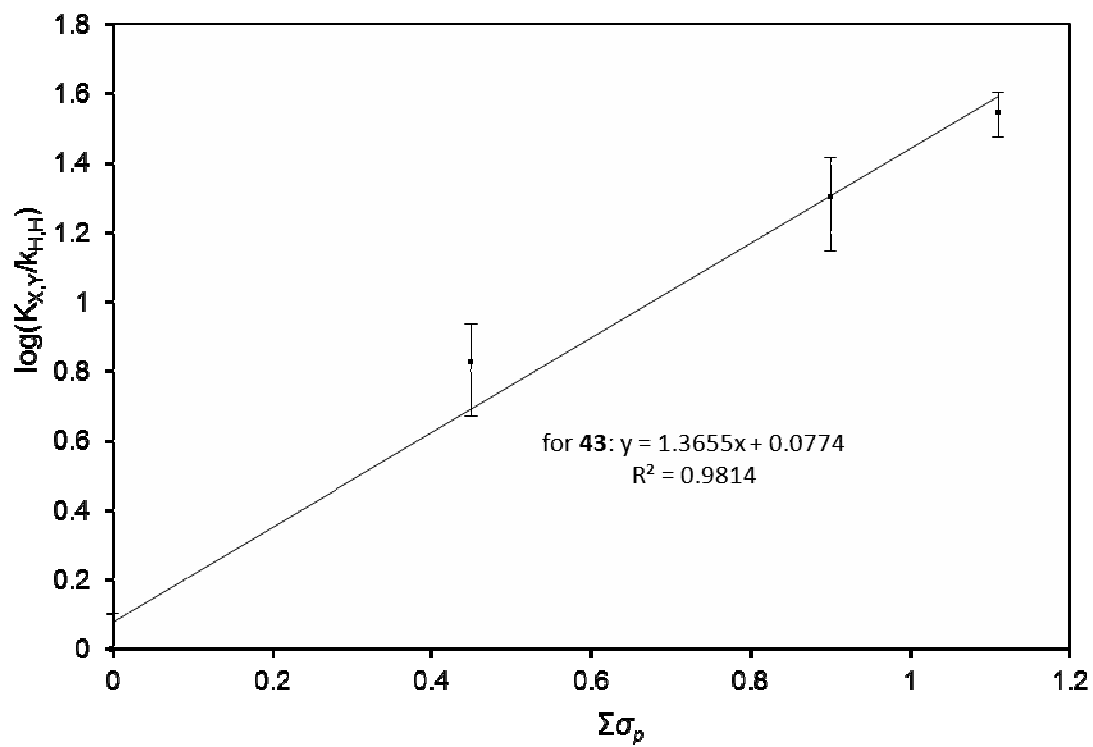
The AAA components containing electron donating groups are predicted to show very high complexation with the DDD components. In order to obtain the accurate association constant values, ITC was chosen to determine association constants, and moreover we can analyze enthalpic and entropic contributions to the complexations of AAA and DDD through ITC technique. In the Table 3-2, all the complexation processes are both negative  $\Delta H$  (favorable) and negative  $T\Delta S$  (unfavorable) values.

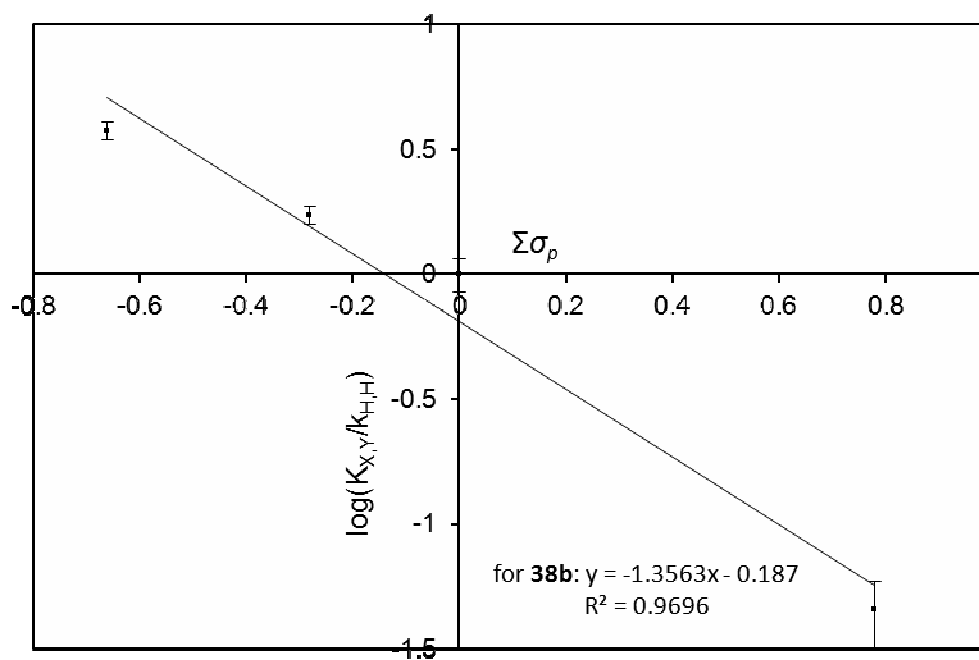
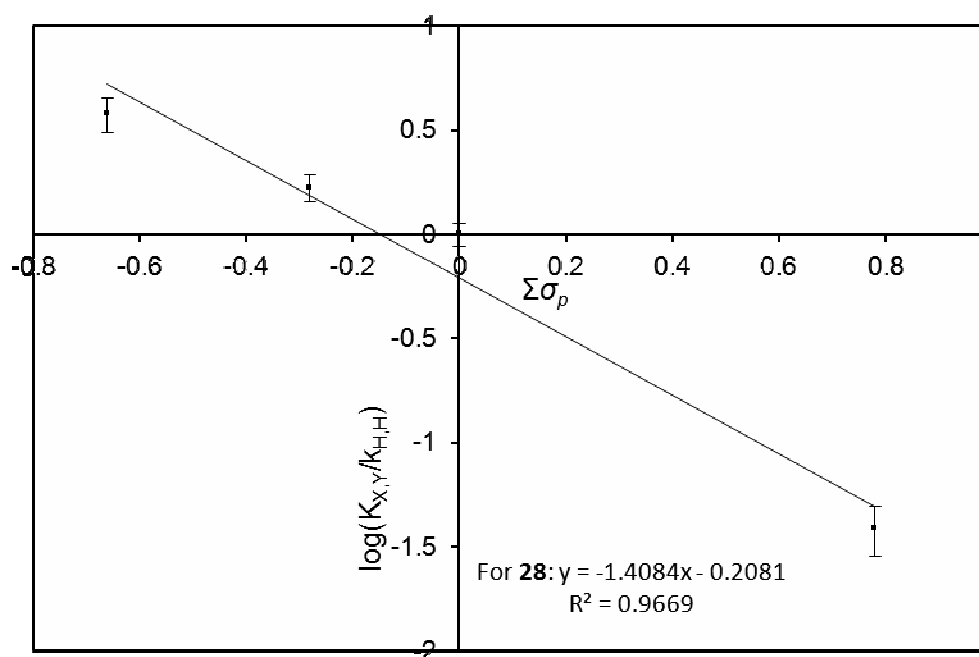
**Table 3-2** The binding data of different AAAs and DDDs in chloroform at 25°C.

	$K_a$ ( $M^{-1}$ )	$\Delta G$ ( $kJ\cdot mol^{-1}$ )	$\Delta H$ ( $kJ\cdot mol^{-1}$ )	$T\Delta S$ ( $kJ\cdot mol^{-1}$ )
<b>28-11</b>	3100 ( $\pm 380$ )	- 19.9 ( $\pm 0.3$ )	- 35.1( $\pm 0.6$ )	- 15.2 ( $\pm 0.7$ )
<b>28-40</b>	5200( $\pm 760$ )	- 21.2 ( $\pm 0.4$ )	- 31.4( $\pm 1.8$ )	- 10.2( $\pm 1.8$ )
<b>28-43</b>	120( $\pm 32$ ) <sup>[a]</sup>	- 11.9 ( $\pm 0.7$ ) <sup>[a]</sup>	/	/
<b>28-44</b>	1.18( $\pm 0.22$ ) $\times 10^4$	- 23.2 ( $\pm 0.5$ )	- 32.1( $\pm 2.4$ )	- 8.9( $\pm 2.5$ )
<b>38b-11</b>	1.76( $\pm 0.26$ ) $\times 10^4$	- 24.2 ( $\pm 0.4$ )	- 40.4( $\pm 3.0$ )	- 16.2( $\pm 3.0$ )
<b>38b-40</b>	3.04( $\pm 0.24$ ) $\times 10^4$	- 25.6 ( $\pm 0.2$ )	- 36.2( $\pm 2.6$ )	- 10.6( $\pm 2.6$ )
<b>38b-43</b>	800( $\pm 240$ ) <sup>[a]</sup>	- 16.6 ( $\pm 0.7$ ) <sup>[a]</sup>	/	/
<b>38b-44</b>	6.6( $\pm 0.54$ ) $\times 10^4$	- 27.5 ( $\pm 0.2$ )	- 41.3( $\pm 2.8$ )	- 13.8( $\pm 2.8$ )
<b>38f-11</b>	4.8( $\pm 0.30$ ) $\times 10^4$	- 26.7 ( $\pm 0.2$ )	- 33.8( $\pm 1.6$ )	- 7.1( $\pm 1.6$ )
<b>38f-40</b>	7.3( $\pm 0.32$ ) $\times 10^4$	- 27.7 ( $\pm 0.1$ )	- 29.5( $\pm 1.8$ )	- 1.8( $\pm 1.8$ )
<b>38f-43</b>	2400( $\pm 720$ ) <sup>[a]</sup>	- 19.3 ( $\pm 0.7$ ) <sup>[a]</sup>	/	/
<b>38f-44</b>	2.3( $\pm 0.30$ ) $\times 10^5$	- 30.6 ( $\pm 0.3$ )	- 42.7( $\pm 3.2$ )	- 12.1( $\pm 3.2$ )
<b>38g-11</b>	1.2( $\pm 0.22$ ) $\times 10^5$	- 29.0 ( $\pm 0.4$ )	-45.2( $\pm 2.8$ )	-16.2( $\pm 2.8$ )
<b>38g-40</b>	1.9( $\pm 0.26$ ) $\times 10^5$	- 30.1 ( $\pm 0.3$ )	-42.4( $\pm 2.6$ )	-12.3( $\pm 2.6$ )
<b>38g-43</b>	4200( $\pm 620$ ) <sup>[a]</sup>	- 20.7 ( $\pm 0.4$ ) <sup>[a]</sup>	/	/
<b>38g-44</b>	4.8( $\pm 0.23$ ) $\times 10^5$	- 32.4 ( $\pm 0.2$ )	-47.7( $\pm 2.2$ )	-15.3( $\pm 2.2$ )

[a] Association constants were measured with  $^1H$  NMR titrations in chloroform at 25°C.









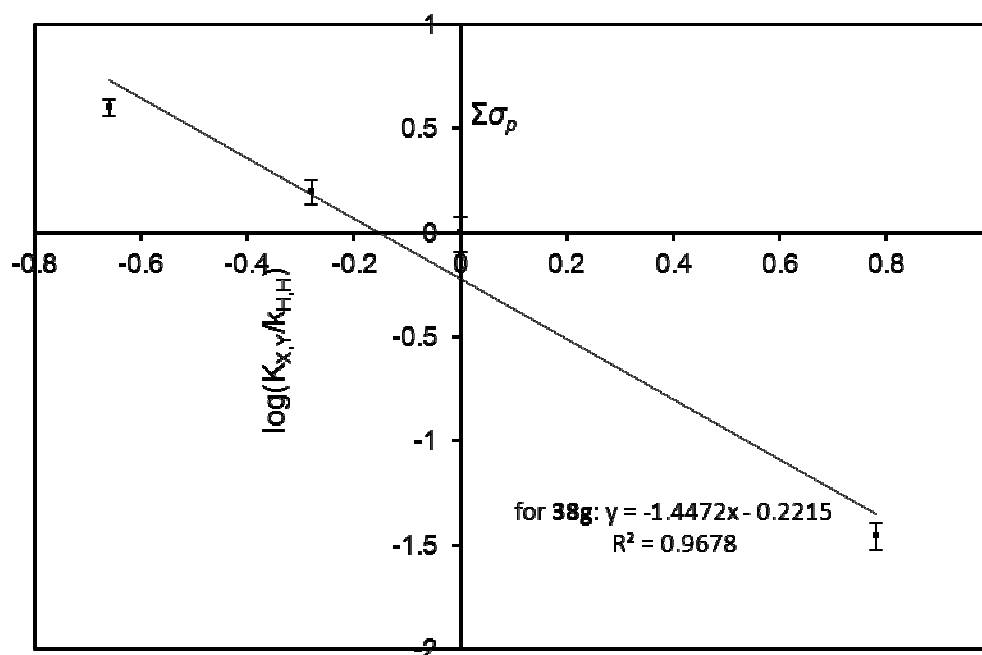
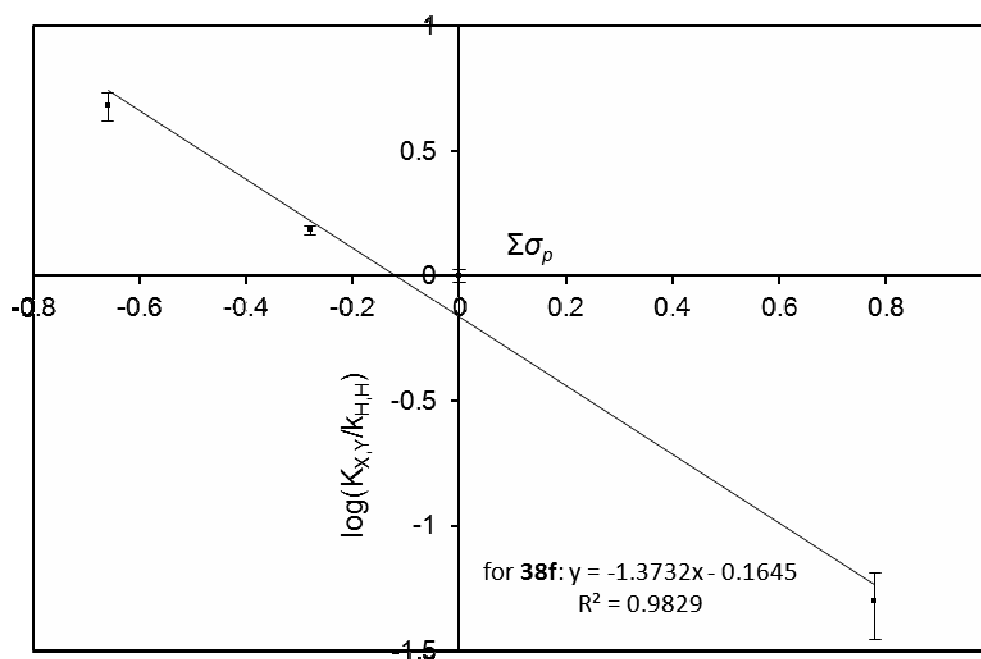


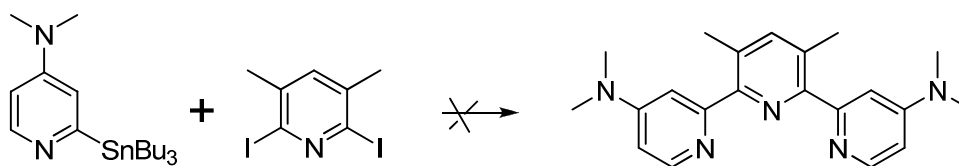
Figure 3-4 Hammett plots of 11, 40, 43, 44, 28, 38b, 38f and 38g.

As might be expected, plots of the Hammett substituent constants for X and Y ( $\Sigma\sigma_p$ ) against  $\log(K_{X,Y}/K_{H,H})$  display a linear correlation for each of **11**, **40**, **43** and **44** yielding  $\rho \approx 1.37$  for all four and  $R^2 \geq 0.97$ . Thus, regardless of the AAA component examined, the complex stability varies in the same way with the character of X and Y in **38**. Plots of the Hammett substituent constants ( $\Sigma\sigma_p$ ) of **40**, **43** and **44** (using **11** as the unsubstituted AAA reference) with each of **28**, **38b**, **38f**, and **38g** also yielded a linear relationship with a similar correlation in Figure 3-4. In all four cases,  $\rho \approx -1.4$  and  $R^2 > 0.96$  indicating the magnitude of the influence of substitution on the AAA components towards complex stability is nearly identical to that observed upon substitution of the DDD partner **28**. This observation is somewhat surprising considering the closer proximity (i.e. four bonds distant versus six) of the substituents to the reactive sites in **40**, **43** and **44** versus **28**. The negative value of  $\rho$  indicates that electron donating groups stabilize the developing partial positive charge on the nitrogen atom of the pyridyl rings in **11**, **40**, **43** and **44** as a result of the hydrogen bonding interaction with **28**.

The ITC experiments also allowed an examination of the relationship between the free energies of complexation between **28** and **11**, **40**, and **43** and the enthalpic and entropic contributions to binding. In all the cases tested, the driving force for complexation is enthalpic, as one might expect from complementary hydrogen bond association between two molecules in a non-polar solvent such as chloroform. Neither of the plots of  $\Delta G$  vs.  $\Delta H$  or  $\Delta G$  vs.  $\Delta S$  give recognizably linear relationships in any of the series examined. The data underline the difficulty in rationalizing incremental free energy relationships using enthalpic and entropic data. The linearity of the free energy data when examined with respect to the sums of the Hammett substituent parameters in

the present cases appear to result from a complex compensation between the entropic and enthalpic contributions to binding. Compared with other so-called “enthalpy-entropy compensation” systems, our systems are relatively complicated because different substituent groups change not only the chemical property but also their original conformations. So, substituent effect in double helical AAA-DDD complexes is not just the electronic effect.

In addition, electron donating groups on AAA enhance the stability of AAA-DDD complex and this result encouraged us to synthesize the extremely strong binding AAA-DDD complex via the dimethylamino ( $\sigma_p = -0.83$ ) -substituted AAA. Unfortunately, the Stille coupling did not run well.



### 3.3 Summary

We have synthesized two series of derivatives containing either DDD or AAA hydrogen bond sequences that, when combined, form triply hydrogen bonded double helical complexes in  $\text{CDCl}_3$  solution. In our cases, during the complexation process, both AAA and DDD change their original conformations and form the stable double helix via the induced-fit. Therefore, the entropy cost is no way to avoid. However, chemical property will be easy to change via the substituent group and further affect the enthalpy. The addition of electron withdrawing groups to the 5-positions of the skatole rings in the DDD components increases the complex association constants by a factor of

30. These increases, expressed in terms of their free energy, are a linear function of the sum of the Hammett constants of the substituents on both skatole rings. Similarly, introduction of electron donating or withdrawing groups into the AAA components produces a nearly identical but opposite response with respect to complex stability. This kind of substituent effect is not simply equal to the electronic effect because substituent groups also affect the conformations. Overall, the various combinations of these modifications demonstrate a variance in complex affinities of more than three orders of magnitude from  $10^2$  to  $>10^5 \text{ M}^{-1}$  within the same underlying recognition motif. The high association constant (over  $10^5 \text{ M}^{-1}$ ) has been achieved and could be considered as basic units for supramolecular polymers.

### 3.4 Experimental Section

Chemicals were purchased from Aldrich and used as received. All non-deuterated solvents were dried using an Innovative Technology solvent purification system SPS-400-5. Chromatography was performed on Merck 240-400 mesh silica gel-60.  $\text{CDCl}_3$  was purchased from Cambridge Isotope Laboratories and dried over  $4\text{\AA}$  molecular sieves before use.  $^1\text{H}$  and  $^{13}\text{C}$  NMR spectra were collected on a Varian Mercury 400 MHz spectrometer. Spectra are reported with residual solvent peak as reference from TMS. EI and CI ( $\text{CH}_4$ ) mass spectra were obtained on a Finnigan MAT 8200 mass spectrometer and ESI mass spectra were obtained using Micromass LCT instrumentation.  $^1\text{H}$  NMR titration experiments were performed on a Varian Inova 600 MHz spectrometer. Isothermal titration calorimetry experiments were carried out with a Microcal VP-ITC microcalorimeter.

**32a:** Methyl 2-ethylacetoacetate (50 mmol, 7.2 g) and 3.0 g NaOH were dissolved and stirred for 10 hours in a water/ethanol solution. The diazonium salt was prepared from ethyl 4-aminobenzoate (50 mmol, 4.13 g), concentrated HCl (50 mL) and aqueous solution of sodium nitrate (50 mmol, 3.5 g) in an ice bath (4-aminobenzoate and water were first mixed at 0°C and concentrated HCl was added. After 15 min, sodium nitrate solution was added dropwise). The diazonium salt was added to the pre-prepared sodium carboxylate solution at 0°C. The resulting solution was modified at pH 7-8 with sodium acetate and stirred at room temperature for 4 hours. The precipitate was collected, dried and refluxed overnight in formic acid (100 mL). Then the reaction solution was cooled down and diluted with water (500 mL). The precipitated crude product was purified by the flash column chromatography (CH<sub>2</sub>Cl<sub>2</sub>) to give pale yellow solid (5.33g, 57% yield). <sup>1</sup>H NMR (400 MHz, DMSO-d<sub>6</sub>) δ ppm 11.81(s, 1H), 8.35(m, 1H), 7.86(m, 1H), 7.45 (m, 1H), 4.31(q, *J*= 7.0Hz, 2H), 2.59(s, 3H), 2.58(s, 3H), 1.34(t, *J*=7.0Hz, 3H); <sup>13</sup>C NMR (100 MHz, DMSO-d<sub>6</sub>) δ ppm 190.7, 166.3, 138.5, 133.6, 127.5, 125.7, 123.6, 121.2, 119.0, 112.4, 60.3, 29.1, 14.3, 10.4; ESI-HRMS (*m/z*) calculated for C<sub>12</sub>H<sub>13</sub>NO 187.0997, found 187.0994.

**32b:** This compound was synthesized according to the method in the case of **32a**, starting from ethyl (2-ethyl) propionylacetate and ethyl 4-aminobenzoate, yield 53%. <sup>1</sup>H NMR (400 MHz, CDCl<sub>3</sub>) δ ppm 9.26 (s, 1H), 8.43 (s, 1H), 8.02 (m, 1H), 7.38 (m, 1H), 4.41 (q, *J*= 7.0Hz, 2H), 2.99 (q, *J*= 7.4Hz, 2H), 2.68 (s, 3H), 1.43 (t, *J*= 7.4Hz, 3H), 1.29 (t, *J*= 7.0Hz, 3H); <sup>13</sup>C NMR (100 MHz, CDCl<sub>3</sub>) δ ppm 193.7, 135.9, 132.3, 128.9, 126.2, 121.1, 120.0, 117.8, 111.8, 34.3, 11.2, 8.0; ESI-HRMS (*m/z*) calculated for C<sub>15</sub>H<sub>17</sub>NO<sub>3</sub> 259.1208, found 259.1202.

**32c:** This compound was synthesized according to the method in the case of **32a**, starting from methyl 2-ethylacetoacetate and 4-bromoaniline, giving a 52% yield.  $^1\text{H}$  NMR (400 MHz,  $\text{DMSO-}d_6$ )  $\delta$  ppm 11.61 (s, 1H), 7.89(s, 1H), 7.37 (m, 2H), 2.58 (s, 3H), 2.52 (s, 3H);  $^{13}\text{C}$  NMR (100 MHz,  $\text{DMSO-}d_6$ )  $\delta$  ppm 190.7, 134.7, 133.2, 129.7, 127.9, 123.1, 117.0, 114.5, 111.9, 36.7, 29.0, 10.4; ESI-HRMS (m/z) calculated for  $\text{C}_{11}\text{H}_{10}\text{BrNO}$  250.9946, found 250.9904.

**32d:** This compound was synthesized according to the method in the case of **32a**, starting from ethyl (2-ethyl) propionylacetate and 4-bromoaniline, giving a 54% yield.  $^1\text{H}$  NMR (400 MHz,  $\text{DMSO-}d_6$ )  $\delta$  ppm 11.61 (s, 1H), 7.89 (s, 1H), 7.36 (m, 2H), 2.96 (q,  $J=7.42$  Hz, 2H), 2.52 (s, 3H), 1.11 (t,  $J=7.42$  Hz, 1H);  $^{13}\text{C}$  NMR (100 MHz,  $\text{DMSO-}d_6$ )  $\delta$  ppm 193.7, 134.7, 132.9, 129.7, 127.7, 123.0, 116.5, 114.5, 111.8, 33.5, 10.5, 7.8; ESI-HRMS (m/z) calculated for  $\text{C}_{12}\text{H}_{12}\text{BrNO}$  265.0102, found 265.0173.

**33a:** The mixture of **32c** (2.65 g, 10 mmol),  $\text{Zn}(\text{CN})_2$  (20 mmol, 2.35 g) and  $\text{Pd}(\text{PPh}_3)_4$  (0.58 g, 0.5 mmol) in 20 mL dry DMF was refluxed under a nitrogen atmosphere for 3 days. The reaction solution was filtered through the celite and filtrate was diluted with 200 mL water. The precipitate was crude product and purified with the flash chromatography (chloroform) to give a pure product (2.11 g, 80% yield).  $^1\text{H}$  NMR (400 MHz,  $\text{DMSO-}d_6$ )  $\delta$  ppm 11.97 (s, 1H), 8.35 (s, 1H), 7.55 (m, 2H), 2.60 (s, 3H), 2.59 (s, 3H);  $^{13}\text{C}$  NMR (100 MHz,  $\text{DMSO-}d_6$ )  $\delta$  ppm 190.9, 137.5, 134.0, 127.8, 127.5, 127.3, 120.3, 118.5, 113.7, 101.6, 29.2, 10.4; ESI-HRMS (m/z) calculated for  $\text{C}_{12}\text{H}_{10}\text{N}_2\text{O}$  198.0793, found 198.0797.

**33b:** The procedure was the same as that of **33a**, 85% yield.  $^1\text{H}$  NMR (400 MHz, DMSO- $d_6$ )  $\delta$  ppm 11.93 (s, 1H), 8.30 (s, 1H), 7.53 (m, 2H), 2.97 (q,  $J=7.03$  Hz, 2H), 2.56 (s, 3H), 1.11 (t,  $J=7.03$  Hz, 3H);  $^{13}\text{C}$  NMR (100 MHz, DMSO- $d_6$ )  $\delta$  ppm 193.7, 137.4, 133.7, 129.3, 127.3, 127.1, 120.3, 117.9, 113.7, 110.5, 33.7, 10.4, 7.7; ESI-HRMS (m/z) calculated for  $\text{C}_{13}\text{H}_{12}\text{N}_2\text{O}$  212.0590, found 212.0591.

**34a:** Trimethylphenylammonium tribromide (3.76 g, 10 mmol) was added to a THF (50 mL) solution of **32a** (2.5 g, 10 mmol). The reaction mixture was refluxed over an hour and filtered through celite. The filtrate was concentrated under reduced pressure and further purified with the flash chromatography (chloroform/ethyl acetate: 99/1) (1.32 g, 71% yield).  $^1\text{H}$  NMR (400 MHz, DMSO- $d_6$ )  $\delta$  ppm 11.81(s, 1H), 8.35(m, 1H), 7.86(m, 1H), 7.45 (m, 1H), 4.31(q,  $J=7.0$  Hz, 2H), 2.59(s, 3H), 2.58(s, 3H), 1.34(t,  $J=7.0$  Hz, 3H);  $^{13}\text{C}$  NMR (100 MHz, DMSO- $d_6$ )  $\delta$  ppm 190.7, 166.3, 138.5, 133.6, 127.5, 125.7, 123.6, 121.2, 119.0, 112.4, 60.3, 29.1, 14.3, 10.4; ESI-HRMS (m/z) calculated for  $\text{C}_{12}\text{H}_{13}\text{NO}$  187.0997, found 187.0994.

**34b:** The procedure was the same as that of compound **34a**, 77% yield.  $^1\text{H}$  NMR (400 MHz, DMSO- $d_6$ )  $\delta$  ppm 11.98(s, 1H), 8.38(m, 1H), 7.88(m, 1H), 7.51 (m, 1H), 5.50(q,  $J=6.3$  Hz, 1H), 4.31(q,  $J=7.0$  Hz, 2H), 2.65(s, 3H), 1.82(d,  $J=6.3$  Hz, 2H), 1.34(t,  $J=7.0$  Hz, 3H);  $^{13}\text{C}$  NMR (100 MHz, DMSO- $d_6$ )  $\delta$  ppm 186.6, 166.2, 138.9, 130.4, 127.4, 126.3, 123.7, 121.6, 121.1, 112.6, 60.4, 45.0, 19.8, 14.3, 10.4; ESI-HRMS (m/z) calculated for  $\text{C}_{15}\text{H}_{16}\text{NBrO}_3$  337.0314, found 337.0311.

**34c:** The procedure was the same as that of compound **34a**, 83% yield.  $^1\text{H}$  NMR (400 MHz, DMSO- $d_6$ )  $\delta$  ppm 11.81 (s, 1H), 7.95 (m, 1H), 7.41 (m, 2H), 5.49 (q,  $J=6.6$  Hz,

1H), 2.58 (s, 3H), 1.81(d,  $J=6.6$  Hz, 3H);  $^{13}\text{C}$  NMR (100 MHz, DMSO- $d_6$ )  $\delta$  ppm 190.9, 134.9, 130.6, 129.6, 128.1, 123.0, 118.1, 114.4, 112.0, 38.4, 20.4, 10.6; ESI-HRMS (m/z) calculated for  $\text{C}_{12}\text{H}_{11}\text{NOBr}_2$  342.9207, found 342.9204.

**34d:** The procedure was the same as that of **34a**, 82% yield.  $^1\text{H}$  NMR (400 MHz, DMSO- $d_6$ )  $\delta$  ppm 12.12 (s, 1H), 8.37 (s, 1H), 7.61 ((dd,  $J=8.6$  Hz, 1.6 Hz, 1H), 7.55 (dd,  $J=8.6$  Hz, 1.6 Hz, 1H), 4.81 (s, 2H), 2.61 (s, 3H);  $^{13}\text{C}$  NMR (100 MHz, DMSO- $d_6$ )  $\delta$  ppm 192.7, 184.5, 138.0, 131.4, 127.8, 127.3, 120.2, 118.6, 113.8, 101.9, 66.8, 35.3; ESI-HRMS (m/z) calculated for  $\text{C}_{12}\text{H}_9\text{BrN}_2\text{O}$  275.9898, found 275.9891.

**34e:** The procedure was the same as that of **34a**, 79% yield.  $^1\text{H}$  NMR (400 MHz, acetone- $d_6$ )  $\delta$  ppm 11.22 (s, 1H), 8.29 (s, 1H), 7.67 (d,  $J=8.6$  Hz, 1H), 7.60 (dd,  $J=8.6$  Hz, 1.6 Hz, 1H), 5.49 (q,  $J=6.6$  Hz, 1H), 2.76 (s, 3H), 1.89 (d,  $J=6.6$  Hz, 3H);  $^{13}\text{C}$  NMR (100 MHz, DMSO- $d_6$ )  $\delta$  ppm 195.1, 186.7, 137.9, 130.8, 127.7, 127.6, 120.4, 119.5, 113.8, 101.9, 45.0, 19.7, 10.3; ESI-HRMS (m/z) calculated for  $\text{C}_{13}\text{H}_{11}\text{BrN}_2\text{O}$  290.0055, found 290.0061.

**35a:** Bromoacetylkatole **34a** (7.25 g, 25 mmol) and potassium thioacetate (3.13 g, 27.4 mmol) were dissolved in dry DMF (200 mL) under a nitrogen atmosphere. The reaction solution was stirred for 12 hours and diluted with water (800 mL). The precipitate was collected, dried ( $\text{MgSO}_4$ ) and dissolved in acetonitrile (300 mL). Cysteamine hydrochloride (2.84 g, 25 mmol) and  $\text{NaHCO}_3$  (2.1 g, 25 mmol) were added into the reaction solution. The reaction mixture was degassed for 5 minutes and stirred overnight. The reaction solution was quenched with 10% aqueous HCl, diluted with water (100 mL) and extracted with  $\text{CH}_2\text{Cl}_2$  (3 $\times$ 200 mL). The organic layer was dried over anhydrous



MgSO<sub>4</sub> and concentrated under reduced pressure. The crude product was purified using flash column chromatography to give a light yellow solid (3.42 g, 56% yield). <sup>1</sup>H NMR (400 MHz, DMSO-*d*<sub>6</sub>) δ ppm 11.89 (s, 1H), 8.39 (s, 1H), 7.89 (m, 1H), 7.50 (m, 1H), 4.33 (q, *J*=7.0 Hz, 2H), 4.02 (brs, 2H), 2.93 (brs, 1H), 2.63 (s, 3H), 1.35(d, *J*=7.0 Hz, 3H); <sup>13</sup>C NMR (100 MHz, DMSO-*d*<sub>6</sub>) δ ppm 190.7, 166.3, 138.5, 133.6, 127.5, 125.7, 123.6, 121.2, 119.0, 112.4, 60.3, 26.7, 14.3, 10.4; ESI-HRMS (m/z) calculated for C<sub>14</sub>H<sub>15</sub>NO<sub>3</sub>S 277.0773, found 277.0777.

**35b:** The procedure was the same as that of **35a**, 52% yield. <sup>1</sup>H NMR (400 MHz, CDCl<sub>3</sub>) δ ppm 9.03 (s, 1H), 7.83 (m, 1H), 7.42 (m, 1H), 7.27 (m, 1H), 4.20 (m, 1H), 2.62 (s, 3H), 2.04 (t, *J*=10.6 Hz, 1H), 1.67(d, *J*=7.0 Hz, 3H); <sup>13</sup>C NMR (100 MHz, DMSO-*d*<sub>6</sub>) δ ppm 190.9, 134.9, 130.6, 129.7, 128.1, 123.0, 118.1, 114.5, 112.0, 37.6, 20.3, 10.4; ESI-HRMS (m/z) calculated for C<sub>12</sub>H<sub>12</sub>NOSBr 296.9823, found 296.9829.

**35c:** The procedure was the same as that of **35a**, 55% yield. <sup>1</sup>H NMR (400 MHz, DMSO-*d*<sub>6</sub>) δ ppm 11.72 (s, 1H), 7.92 (s, 1H), 7.39 (m, 2H), 3.99 (d, *J*=7.4Hz, 2H), 2.90 (t, *J*=7.4 Hz, 1H), 2.54 (s, 3H); <sup>13</sup>C NMR (100 MHz, DMSO-*d*<sub>6</sub>) δ ppm 188.4, 135.0, 131.4, 129.6, 128.3, 123.1, 118.0, 114.6, 112.1, 109.5, 32.3, 10.4; ESI-HRMS (m/z) calculated for C<sub>12</sub>H<sub>10</sub>ON<sub>2</sub>S 230.0514, found 230.0517.

**35d:** The procedure was the same as that of **35a**, 53% yield. <sup>1</sup>H NMR (400 MHz, DMSO-*d*<sub>6</sub>) δ ppm 12.03 (s, 1H), 8.34 (s, 1H), 7.58 (m, 2H), 4.39 (q, *J*=6.6 Hz, 1H), 2.61 (s, 3H), 1.52(d, *J*=6.6 Hz, 3H); <sup>13</sup>C NMR (100 MHz, DMSO-*d*<sub>6</sub>) δ ppm 190.9, 137.7, 131.5, 127.7, 127.4, 120.2, 119.4, 113.7, 101.7, 37.6, 20.2, 10.4; ESI-HRMS (m/z) calculated for C<sub>13</sub>H<sub>12</sub>N<sub>2</sub>OS 244.0670, found 244.0672.

**36a:** 2-Mercapto-1-(3-methyl-1H-indol-2-yl)propan-1-one (0.42 g, 1.9 mmol) and **35b** (0.34 g, 1.8 mmol) was dissolved in 20 mL dry acetonitrile under a N<sub>2</sub> atmosphere. Triethylamine (0.3mL) was added. The reaction mixture was stirred for 6 hours at room temperature. The reaction solution was quenched by 10% aqueous HCl, diluted with water (100 mL). The precipitate is pure product without any further purification (0.68 g, 82% yield). <sup>1</sup>H NMR (400 MHz, DMSO-*d*<sub>6</sub>) δ ppm 11.78 (s, 1H), 11.53 (s, 1H), 7.90 (s, 1H), 7.66 (m, 1H), 7.40 (m, 4H), 7.29 (m, 1H), 7.06 (m, 1H), 4.58 (q, *J*=6.6 Hz, 1H), 4.07 (q, *J*=15.6 Hz, 2H), 2.56 (s, 3H), 2.54 (s, 3H), 1.55 (d, *J*=6.6 Hz, 3H); <sup>13</sup>C NMR (100 MHz, DMSO-*d*<sub>6</sub>) δ ppm 189.5, 187.8, 136.6, 134.9, 131.2, 130.8, 129.7, 128.2, 127.9, 127.4, 125.9, 123.0, 120.9, 119.6, 118.8, 118.4, 114.5, 112.5, 112.1, 43.0, 37.5, 16.5, 10.6, 10.5; ESI-HRMS (m/z) calculated for C<sub>23</sub>H<sub>21</sub>N<sub>2</sub>O<sub>2</sub>SBr 468.0507, found 468.0501.

**36b:** The procedure is the same as that of **36a**, starting from 2-mercapto-1-(3-methyl-1H-indol-2-yl)propan-1-one and **35a**, 86% yield. <sup>1</sup>H NMR (400 MHz, DMSO-*d*<sub>6</sub>) δ ppm 11.90 (s, 1H), 11.53 (s, 1H), 8.36 (s, 1H), 7.87 (m, 1H), 7.68 (d, *J*=8.2 Hz, 1H), 7.47 (d, *J*=8.8 Hz, 1H), 7.41 (d, *J*=8.2 Hz, 1H), 7.28 (m, 1H), 7.06 (m, 1H), 4.58 (q, *J*=6.8 Hz, 1H), 4.32 (q, *J*=7.1 Hz, 2H), 4.08 (q, *J*=15.6 Hz, 2H), 2.58 (s, 3H), 2.57 (s, 3H), 1.52 (d, *J*=6.8 Hz, 3H), 1.34 (t, *J*=7.1 Hz, 3H); <sup>13</sup>C NMR (100 MHz, DMSO-*d*<sub>6</sub>) δ ppm 189.5, 188.0, 166.3, 138.7, 136.5, 132.3, 130.1, 127.9, 127.4, 126.0, 125.7, 123.7, 121.4, 120.7, 120.0, 119.5, 119.1, 112.5, 112.4, 60.4, 42.9, 37.7, 16.6, 14.3, 10.5; ESI-HRMS (m/z) calculated for C<sub>26</sub>H<sub>26</sub>N<sub>2</sub>O<sub>4</sub>S 462.1613, found 462.1619.

**36c:** The procedure is the same as that of **36a**, starting from **35b** and **34a**, 84% yield.  $^1\text{H}$  NMR (400 MHz,  $\text{DMSO-}d_6$ )  $\delta$  ppm 11.88 (s, 1H), 11.73 (s, 1H), 8.35 (s, 1H), 7.87 (m, 2H), 7.46 (d,  $J=8.6$  Hz, 1H), 7.37 (s, 1H), 4.56 (q,  $J=6.6$  Hz, 1H), 4.32 (q,  $J=7.0$  Hz, 2H), 4.07 (q,  $J=16.0$  Hz, 2H), 2.56 (s, 3H), 2.53 (s, 3H), 1.51 (d,  $J=6.6$  Hz, 3H), 1.42 (t,  $J=7.0$  Hz, 3H);  $^{13}\text{C}$  NMR (100 MHz,  $\text{DMSO-}d_6$ )  $\delta$  ppm 199.9, 187.9, 166.3, 138.7, 134.9, 132.2, 131.1, 129.6, 128.2, 127.4, 126.1, 123.7, 123.0, 121.4, 120.0, 118.4, 114.5, 114.1, 112.5, 112.0, 109.6, 60.4, 42.9, 37.7, 16.5, 14.3, 10.4; ESI-HRMS (m/z) calculated for  $\text{C}_{26}\text{H}_{25}\text{BrN}_2\text{O}_4\text{S}$  540.0718, found 540.0713.

**36d:** The procedure is the same as that of **36a**, starting from 2-mercapto-1-(3-methyl-1H-indol-2-yl)propan-1-one and **35c**, 81% yield.  $^1\text{H}$  NMR (400 MHz,  $\text{DMSO-}d_6$ )  $\delta$  ppm 12.04 (s, 1H), 11.53 (s, 1H), 8.31 (s, 1H), 7.65 (d,  $J=7.8$  Hz, 1H), 7.59 -7.52 (m, 2H), 7.42 (d,  $J=8.2$  Hz, 1H), 7.28 (m, 1H), 7.05 (m, 1H), 4.59 (q,  $J=6.6$  Hz, 1H), 4.32 (q,  $J=7.1$  Hz, 2H), 4.08 (q,  $J=15.6$  Hz, 2H), 2.57 (s, 3H), 2.55 (s, 3H), 1.53 (d,  $J=6.6$  Hz, 3H);  $^{13}\text{C}$  NMR (100 MHz,  $\text{DMSO-}d_6$ )  $\delta$  ppm 189.5, 188.1, 137.7, 136.5, 132.6, 130.1, 127.9, 127.6, 127.5, 125.7, 120.7, 120.2, 119.5, 119.5, 119.4, 119.1, 113.7, 112.4, 101.8, 42.9, 37.7, 16.7, 10.5, 10.4; ESI-HRMS (m/z) calculated for  $\text{C}_{24}\text{H}_{21}\text{N}_3\text{O}_2\text{S}$  415.1354, found 415.1366.

**36e:** The procedure is the same as that of **36a**, starting from **35d** and **34c**, 85% yield.  $^1\text{H}$  NMR (400 MHz,  $\text{DMSO-}d_6$ )  $\delta$  ppm 11.65 (s, 1H), 11.62 (s, 1H), 7.82 (d,  $J=3.9$  Hz, 2H), 7.39 (m, 4H), 4.45 (q,  $J=6.6$  Hz, 1H), 3.97 (q,  $J=15.6$  Hz, 2H), 2.45 (s, 3H), 2.41 (s, 3H), 1.42 (d,  $J=6.6$  Hz, 1H);  $^{13}\text{C}$  NMR (100 MHz,  $\text{DMSO-}d_6$ )  $\delta$  ppm 189.5, 187.9, 135.0,

134.9, 131.8, 129.6, 129.5, 128.3, 123.2, 123.0, 118.4, 118.0, 114.5, 112.1, 42.9, 37.6, 16.5, 10.4; ESI-HRMS (m/z) calculated for C<sub>24</sub>H<sub>20</sub>BrN<sub>3</sub>O<sub>2</sub>S 493.0461, found 493.0466.

**36f**: The procedure is the same as that of **36a**, starting from **35a** and **34b**, 84% yield. <sup>1</sup>H NMR (400 MHz, DMSO-*d*<sub>6</sub>) δ ppm 11.89 (s, 1H), 11.86 (s, 1H), 8.31 (d, *J*=4.3 Hz, 2H), 7.85 (m, 2H), 7.46 (d, *J*=9.0 Hz, 2H), 4.58 (q, *J*=6.6 Hz, 1H), 4.31 (m, 4H), 4.07 (q, *J*=16.0 Hz, 2H), 2.60 (s, 3H), 2.55 (s, 3H), 1.53 (d, *J*=7.0 Hz, 3H), 1.42 (t, *J*=7.0 Hz, 6H); <sup>13</sup>C NMR (100 MHz, DMSO-*d*<sub>6</sub>) δ ppm 189.6, 187.8, 166.3, 146.2, 144.0, 138.7, 138.6, 132.2, 131.6, 127.4, 125.9, 123.4, 121.4, 120.4, 120.0, 112.5, 112.4, 60.3, 42.9, 37.6, 16.4, 14.3, 10.5; ESI-HRMS (m/z) calculated for C<sub>29</sub>H<sub>30</sub>N<sub>2</sub>O<sub>6</sub>S 534.1825, found 534.1829.

**36g**: The procedure is the same as that of **36a**, starting from **35d** and **34a**, 81% yield. <sup>1</sup>H NMR (400 MHz, DMSO-*d*<sub>6</sub>) δ ppm 12.23 (s, 1H), 11.73 (s, 1H), 8.39 (s, 1H), 7.71 (d, *J*=8.2 Hz, 1H), 7.63 (dd, *J*=8.6 Hz, 1.6 Hz, 1H), 7.56 (d, *J*=8.6 Hz, 1H), 7.44 (d, *J*=8.2 Hz, 1H), 7.33 (t, *J*=7.4 Hz, 1H), 7.08 (t, *J*=7.4 Hz, 1H), 5.44 (q, *J*=6.6 Hz, 1H), 5.09 (q, *J*=7.0 Hz, 2H), 2.62 (s, 3H), 2.61 (s, 3H), 1.73 (t, *J*=7.0 Hz, 3H); <sup>13</sup>C NMR (100 MHz, DMSO-*d*<sub>6</sub>) δ ppm 189.5, 187.9, 166.3, 138.7, 134.9, 132.2, 131.1, 129.6, 128.2, 127.4, 126.0, 123.6, 123.0, 121.4, 120.0, 118.4, 114.5, 112.5, 112.1, 60.3, 42.9, 37.7, 16.5, 14.3, 10.5, 10.4; ESI-HRMS (m/z) calculated for C<sub>27</sub>H<sub>25</sub>N<sub>3</sub>O<sub>4</sub>S 487.1566, found 487.1567.

**37a**: To the 10 mL dry DMF solution of **36a** (0.95 g, 2 mmol) was dropwise added the 15 mL dry DMF of *m*-CPBA (77%, 8 mmol, 1.84 g) at -25°C. The reaction solution was allowed to warm up to room temperature and stirred overnight. The reaction mixture was pulled into ice-water (150 mL) and basified with aqueous Na<sub>2</sub>SO<sub>3</sub>. The precipitate was

pure product (1.76 g, 95% yield).  $^1\text{H}$  NMR (400 MHz,  $\text{CDCl}_3$ )  $\delta$  ppm 9.32 (s, 1H), 9.04 (s, 1H), 7.70 (s, 1H), 7.38 (m, 4H), 7.15 (m, 2H), 5.29 (m, 1H), 4.79 (q,  $J=7.3$  Hz, 2H), 2.72 (s, 3H), 2.70 (s, 3H), 1.86 (d,  $J=6.6$  Hz, 3H); ESI-HRMS (m/z) calculated for  $\text{C}_{23}\text{H}_{21}\text{BrN}_2\text{O}_4\text{S}$  500.0405, found 500.0408.

**37b:** The procedure is the same as that of **37a**, 91% yield.  $^1\text{H}$  NMR (400 MHz,  $\text{DMSO-}d_6$ )  $\delta$  ppm 12.07 (s, 1H), 11.73 (s, 1H), 8.39 (s, 1H), 7.91 (d,  $J=8.6$  Hz, 1H), 7.72 (d,  $J=8.2$  Hz, 1H), 7.51 (d,  $J=8.6$  Hz, 1H), 7.45 (d,  $J=8.6$  Hz, 1H), 7.34 (d,  $J=7.4$  Hz, 1H), 7.09 (d,  $J=7.4$  Hz, 1H), 5.54 (q,  $J=6.6$  Hz, 1H), 5.09 (q,  $J=7.0$  Hz, 2H), 4.33 (q,  $J=7.0$  Hz, 2H), 2.64 (s, 3H), 2.63 (s, 3H), 1.73 (d,  $J=6.6$  Hz, 3H), 1.34 (t,  $J=7.0$  Hz, 3H);  $^{13}\text{C}$  NMR (100 MHz,  $\text{DMSO-}d_6$ )  $\delta$  ppm 185.0, 181.1, 166.2, 139.0, 137.0, 132.9, 131.0, 127.9, 127.3, 126.7, 124.0, 122.4, 121.8, 121.3, 121.2, 112.0, 112.7, 112.6, 65.0, 60.5, 59.4, 14.3, 12.5, 10.6, 10.4; ESI-HRMS (m/z) calculated for  $\text{C}_{26}\text{H}_{26}\text{N}_2\text{O}_6\text{SNa}$  517.1409, found 517.1415.

**37c:** The procedure is the same as that of **37a**, 93% yield.  $^1\text{H}$  NMR (400 MHz,  $\text{DMSO-}d_6$ )  $\delta$  ppm 12.03 (s, 1H), 11.90 (s, 1H), 8.38 (s, 1H), 7.93 (m, 1H), 7.90 (m, 1H), 7.50 (m, 1H), 7.40 (m, 2H), 5.43 (q,  $J=7.0$  Hz, 1H), 5.06 (q,  $J=15.2$  Hz, 2H), 4.33 (q,  $J=7.0$  Hz, 2H), 2.62 (s, 3H), 2.58 (s, 3H), 1.71 (d,  $J=7.0$  Hz, 3H), 1.35 (t,  $J=7.0$  Hz, 3H); ESI-HRMS (m/z) calculated for  $\text{C}_{26}\text{H}_{25}\text{BrN}_2\text{O}_6\text{S}$  572.0617, found 572.0611.

**37d:** The procedure is the same as that of **37a**, 88% yield.  $^1\text{H}$  NMR (400 MHz,  $\text{DMSO-}d_6$ )  $\delta$  ppm 11.87 (s, 1H), 11.72 (s, 1H), 8.39 (s, 1H), 7.71 (d,  $J=8.2$  Hz, 1H), 7.63 (dd,  $J=8.6$  Hz, 1.6 Hz, 1H), 7.56 (d,  $J=8.6$  Hz, 1H), 7.44 (d,  $J=8.2$  Hz, 1H), 7.33 (t,  $J=7.4$  Hz, 1H), 7.08 (t,  $J=7.4$  Hz, 1H), 5.44 (q,  $J=6.6$  Hz, 1H), 5.09 (q,  $J=7.0$  Hz, 2H), 2.62 (s, 3H),

2.61 (s, 3H), 1.73 (d,  $J=7.0$  Hz, 3H);  $^{13}\text{C}$  NMR (100 MHz, DMSO- $d_6$ )  $\delta$  ppm 184.9, 181.3, 162.3, 138.0, 137.0, 133.2, 130.9, 128.8, 128.1, 127.8, 127.5, 126.7, 121.6, 121.4, 121.2, 120.0, 114.0, 112.6, 102.2, 65.1, 59.5, 35.8, 30.8, 12.5, 10.3; ESI-HRMS (m/z) calculated for  $\text{C}_{24}\text{H}_{21}\text{N}_3\text{O}_4\text{S}$  447.1253, found 447.1235.

**37e:** The procedure is the same as that of **37a**, 91% yield.  $^1\text{H}$  NMR (400 MHz, DMSO- $d_6$ )  $\delta$  ppm 11.90 (s, 1H), 11.86 (s, 1H), 7.95 (s, 2H), 7.40 (m, 4H), 5.43 (q,  $J=7.0$  Hz, 1H), 5.04 (q,  $J=14.7$  Hz, 2H), 2.58 (s, 3H), 2.54 (s, 3H), 1.71 (d,  $J=7.0$  Hz, 3H); ESI-HRMS (m/z) calculated for  $\text{C}_{24}\text{H}_{20}\text{BrN}_3\text{O}_4\text{S}$  525.0358, found 525.0354.

**37f:** The procedure is the same as that of **37a**, 89% yield.  $^1\text{H}$  NMR (400 MHz, DMSO- $d_6$ )  $\delta$  ppm 12.07 (s, 1H), 12.02 (s, 1H), 8.35 (m, 2H), 7.88 (m, 2H), 7.49 (m, 2H), 7.40 (m, 2H), 5.46 (m, 1H), 5.07 (q,  $J=11.7$  Hz, 2H), 4.33 (q,  $J=7.0$  Hz, 4H), 2.65 (s, 3H), 2.60 (s, 3H), 1.71 (m, 3H), 1.34 (t,  $J=7.0$  Hz, 6H); ESI-HRMS (m/z) calculated for  $\text{C}_{29}\text{H}_{30}\text{N}_2\text{O}_8\text{S}$  566.1723, found 566.1727.

**37g:** The procedure is the same as that of **37a**, 94% yield.  $^1\text{H}$  NMR (400 MHz, DMSO- $d_6$ )  $\delta$  ppm 12.06 (s, 1H), 11.93 (s, 1H), 8.37 (s, 1H), 7.93 (m, 2H), 7.49 (m, 3H), 5.44 (q,  $J=6.6$  Hz, 1H), 5.08 (q,  $J=14.5$  Hz, 2H), 4.33 (q,  $J=7.2$  Hz, 2H), 2.62 (s, 3H), 2.59 (s, 3H), 1.72 (d,  $J=6.6$  Hz, 3H), 1.34 (t,  $J=7.2$  Hz, 3H); ESI-HRMS (m/z) calculated for  $\text{C}_{24}\text{H}_{21}\text{N}_3\text{O}_4\text{S}$  519.1464, found 519.1477.

**38a:** The procedure is the same as our previous method, 65% yield.  $^1\text{H}$  NMR (400 MHz, DMSO- $d_6$ )  $\delta$  ppm 11.41 (s, 2H), 11.25 (s, 1H), 10.55 (s, 1H), 7.63 (m, 2H), 7.42 (m, 1H), 7.24 (m, 2H), 7.06 (m, 2H), 6.18 (s, 1H), 2.46 (s, 3H), 2.27 (s, 3H), 1.96 (s, 3H);  $^{13}\text{C}$

NMR (100MHz, DMSO- $d_6$ )  $\delta$  ppm 137.4, 136.2, 135.7, 133.1, 128.2, 127.8, 126.6, 123.4, 122.8, 119.6, 119.1, 118.8, 112.1, 111.5, 111.4, 99.1, 9.7, 9.2, 8.6; EI HRMS (m/z) calculated for  $C_{23}H_{20}N_3O_2SBr$  481.0460, found 481.0463.

**38b:** 62% yield.  $^1H$  NMR (400 MHz, DMSO- $d_6$ )  $\delta$  ppm 11.83 (s, 1H), 11.46 (s, 1H), 10.62 (s, 1H), 8.26 (s, 1H), 7.82 (m, 1H), 7.60 (m, 1H), 7.45(m, 2H), 7.20 (m, 1H), 7.07 (m, 1H), 6.24 (s, 1H), 4.33 (q,  $J=7.0$  Hz, 2H), 2.47 (s, 3H), 2.27 (s, 3H), 1.97 (s, 3H), 1.34 (t,  $J=7.0$  Hz, 3H);  $^{13}C$  NMR (100 MHz, DMSO- $d_6$ )  $\delta$  ppm 184.9, 181.3, 162.3, 138.0, 137.0, 133.2, 130.9, 128.8, 128.1, 127.8, 127.5, 126.7, 121.6, 121.4, 121.2, 120.0, 114.0, 112.6, 102.2, 65.1, 59.5, 35.8, 30.8, 12.5, 10.3; ESI-HRMS (m/z) calculated for  $C_{25}H_{23}N_3O_4S$  461.1409, found 461.1422.

**38c:** 64% yield.  $^1H$  NMR (400 MHz, DMSO- $d_6$ )  $\delta$  ppm 12.08 (s, 1H), 11.90 (s, 1H), 10.76 (s, 1H), 8.26 (s, 1H), 7.78 (m, 2H), 7.47 (m, 1H), 7.37 (m, 1H), 7.28 (m, 1H), 6.24 (s, 1H), 4.32 (q,  $J=7.0$  Hz, 2H), 2.46 (s, 3H), 2.24 (s, 3H), 1.95 (s, 3H), 1.34 (t,  $J=7.0$  Hz, 3H);  $^{13}C$  NMR (100 MHz, DMSO- $d_6$ )  $\delta$  ppm 184.7, 181.5, 162.1, 138.0, 137.2, 133.1, 130.7, 128.8, 128.1, 127.8, 127.5, 126.7, 121.6, 121.4, 121.2, 120.0, 114.0, 112.6, 102.2, 65.1, 59.5, 35.8, 30.8, 12.6, 10.4; ESI-HRMS (m/z) calculated for  $C_{26}H_{24}N_3O_4SBr$  553.0671, found 553.0672.

**38d:** 61% yield.  $^1H$  NMR (400 MHz, DMSO- $d_6$ )  $\delta$  ppm 11.62 (s, 1H), 11.31 (s, 1H), 10.60 (s, 1H), 8.28 (s, 1H), 7.82 (m, 1H), 7.60 (m, 1H), 7.45(m, 2H), 7.21 (m, 1H), 7.08 (m, 1H), 6.25 (s, 1H), 2.48 (s, 3H), 2.28 (s, 3H), 1.98 (s, 3H);  $^{13}C$  NMR (100 MHz, DMSO- $d_6$ )  $\delta$  ppm 168.2, 138.2, 136.6, 133.1, 128.1, 127.8, 126.4, 122.8, 122.1, 121.8,

119.0, 113.3, 111.7, 111.4, 99.6, 9.4, 9.3, 8.7; ESI-HRMS (m/z) calculated for  $C_{23}H_{18}N_4O_2S$  414.1151, found 414.1172.

**38e**: 62% yield.  $^1H$  NMR (400 MHz, DMSO- $d_6$ )  $\delta$  ppm 11.80 (s, 1H), 11.73 (s, 1H), 10.64 (s, 1H), 8.28 (s, 1H), 7.79 (m, 2H), 7.36 (m, 4H), 6.22 (s, 1H), 2.40 (s, 3H), 2.24 (s, 3H), 1.95 (s, 3H);  $^{13}C$  NMR (100 MHz, DMSO- $d_6$ )  $\delta$  ppm 168.1, 138.0, 136.5, 133.0, 128.2, 127.6, 126.3, 122.9, 122.4, 121.8, 119.1, 113.3, 111.6, 111.4, 99.7, 9.6, 9.3, 8.6; ESI-HRMS (m/z) calculated for  $C_{24}H_{19}N_4O_2SBr$  506.0412, found 506.0417.

**38f**: 65% yield.  $^1H$  NMR (400 MHz, DMSO- $d_6$ )  $\delta$  ppm 11.75 (s, 1H), 11.67 (s, 1H), 10.68 (s, 1H), 8.29 (m, 2H), 7.83 (m, 2H), 7.48(m, 2H), 6.28 (s, 1H), 4.32 (m, 4H), 2.47 (s, 3H), 2.33 (s, 3H), 1.96 (s, 3H), 1.34 (m, 6H);  $^{13}C$  NMR (100 MHz, DMSO- $d_6$ )  $\delta$  ppm 166.6, 151.4, 150.5, 138.6, 138.3, 132.4, 131.7, 128.0, 127.8, 127.3, 123.6, 121.2, 121.8, 121.0, 113.4, 112.8, 112.2, 111.6, 60.3, 14.4, 9.4, 9.1, 8.6; ESI-HRMS (m/z) calculated for  $C_{29}H_{29}N_3O_6S$  547.1777, found 547.1773.

**38g**: 64% yield.  $^1H$  NMR (400 MHz, DMSO- $d_6$ )  $\delta$  ppm 11.66 (s, 1H), 11.54 (s, 1H), 10.64 (s, 1H), 8.27 (s, 1H), 7.82 (m, 2H), 7.48(m, 1H), 7.37 (m, 1H), 7.30 (m, 1H), 6.29 (s, 1H), 4.32 (q,  $J=6.7$  Hz, 2H), 2.46 (s, 3H), 2.25 (s, 3H), 1.94 (s, 3H), 1.34 (t,  $J=6.7$  Hz, 3H);  $^{13}C$  NMR (100 MHz, DMSO- $d_6$ )  $\delta$  ppm 169.4, 140.2, 137.6, 134.1, 129.1, 127.8, 126.4, 122.8, 122.1, 121.8, 119.0, 114.3, 113.7, 111.4, 99.6, 9.6, 9.4, 8.6; ESI-HRMS (m/z) calculated for  $C_{26}H_{22}N_4O_4S$  486.1362, found 486.1379.

**39**: A solution of 2-(dimethylamino)ethanol (1.06 ml, 10.5 mmol) in dry hexane (25 mL) was mixed with *n*-BuLi (8.5 mL, 22.1 mmol) at 0 °C. After the mixture was stirred for 15



min at 0 °C, a hexane (5 mL) solution of 3,4-lutidine (0.6 mL, 5.3 mmol) was added dropwise. After 1 h at 0 °C, the orange solution was cooled to -78 °C and tributyltin chloride (3.7 mL, 13.64 mmol) in THF (12.5 mL) was added. After 1 h at -78 °C, the reaction mixture was warmed to room temperature. The reaction was quenched with water (20 mL) at 0 °C. The organic layer was then extracted with diethylether (2x15 mL), dried over MgSO<sub>4</sub>, and the solvent was removed under reduced pressure. The crude product was purified by column chromatography (hexane/EtOAc: 4/1) to afford yellow liquid pure product (0.85 g, 40% yield). <sup>1</sup>H NMR (400 MHz, CDCl<sub>3</sub>) δ ppm 8.46 (s, 1H), 7.14 (s, 1H), 2.22 (s, 3H), 2.20 (s, 3H), 1.60-1.44 (m, 6H), 1.38-1.25 (m, 8H) 1.11-1.07 (m, 4H) 0.88 (t, 9H); <sup>13</sup>C NMR (100MHz, CDCl<sub>3</sub>) δ ppm 169.7, 151.0, 142.8, 133.4, 130.5, 29.3, 29.1, 27.8, 27.3, 26.8, 18.9, 17.5, 16.3, 13.7, 9.7, 8.7; ESI-HRMS (m/z) calculated for C<sub>19</sub>H<sub>35</sub>NSn 397.1791, found 396.1701.

**40:** A mixture of 4,5-Dimethyl-2-(tributylstannyl)pyridine (2.15 g, 5.43 mmol), 2,6-diiodo-3,5-lutidine (0.97 g, 2.71 mmol) and Pd(PPh<sub>3</sub>)<sub>4</sub> (0.31 g, 10 mol %, 0.27 mmol) in 100 mL of dry toluene was refluxed under nitrogen for 36 h. When cooled down, the reaction solution was filtered and filtrate was concentrated under reduced pressure. The crude product was purified by chromatography (ethyl acetate/ hexane: 1/1) to give pure white product (0.35 g 41% yield). <sup>1</sup>H NMR (400 MHz, CDCl<sub>3</sub>) δ ppm 8.37 (s, 2H), 7.62 (s, 2H), 7.48 (s, 1H), 2.50 (s, 6H), 2.31 (s, 6H), 2.28 (s, 6H); <sup>13</sup>C NMR (100MHz, CHLOROFORM-d) δ ppm 156.9, 153.3, 148.5, 146.0, 142.2, 131.3, 131.0, 125.1, 19.5, 19.3, 16.2; ESI-HRMS (m/z) calculated for C<sub>15</sub>H<sub>15</sub>N<sub>3</sub> 317.1892, found 317.1885.

**41:** To a mixture of concentrated nitric acid (30 mL) and concentrated sulfuric acid (50 mL) were cautiously added 2,6-diodo-3,5-dimethyl pyridine N-oxide (15.5 g, 41 mmol) at 0°C. The reaction mixture was heated to 70°C. After stirring for 12h, the reaction solution was cooled down to room temperature and cautiously poured into crushed ice. The precipitate was filtered off and dried on vacuum to afford the pure product, 72% yield. <sup>1</sup>H NMR (400 MHz, CDCl<sub>3</sub>) δ ppm 2.45 (s, 6H); <sup>13</sup>C NMR (100 MHz, CDCl<sub>3</sub>) δ ppm 132.5, 113.7, 23.5; ESI-HRMS (m/z) calculated for C<sub>7</sub>H<sub>6</sub>N<sub>2</sub>O<sub>3</sub>I<sub>2</sub> 419.8468, found 419.8464.

**42:** To a suspension of compound **41** in chloroform (300 mL) was added dropwise phosphorus trichloride (12.7 mL, 0.146 mol) at 0°C. The reaction mixture was refluxed for 24h. After the reaction was completed, the mixture was cautiously poured into ice-water and the solution was neutralized with ammonium hydroxide. The organic layers were collected, dried over anhydrous MgSO<sub>4</sub> and concentrated under reduced pressure. The crude product was purified with chromatography (hexane/chloroform: 2/1) to afford the pure light yellow solid (10.7g, 90% yield). <sup>1</sup>H NMR (400 MHz, CDCl<sub>3</sub>) δ ppm 2.26 (s, 6H); ESI-HRMS (m/z) calculated for C<sub>7</sub>H<sub>6</sub>N<sub>2</sub>O<sub>2</sub>I<sub>2</sub> 403.8519, found 403.8511.

**43:** 2-Tributyltinpyridine (21.5 g, 58.3 g), compound **42** (10.2 g, 26.5 mmol) and Pd(PPh<sub>3</sub>)<sub>4</sub> (5%mol, 1.53 g) in dry toluene (250 mL) were refluxed for 16h under nitrogen atmosphere. When cooled down to room temperature, the reaction solution was quenched with saturated ammonium chloride (50 mL) and filtered over celite. The precipitate was washed with toluene (40 mL) and the organic layer was separated. The solvent was removed under reduced pressure and the product was purified with chromatography (chloroform) to give pale yellow solid (6.97 g, 86% yield). <sup>1</sup>H NMR (400 MHz, CDCl<sub>3</sub>) δ

ppm 8.67 (m, 2H), 7.90 (m, 2H), 7.82 (m, 2H), 7.33 (m, 2H), 2.48 (s, 6H);  $^{13}\text{C}$  NMR (100 MHz,  $\text{CDCl}_3$ )  $\delta$  ppm 157.5, 155.0, 148.4, 136.8, 124.6, 123.2, 122.1, 14.1; ESI-HRMS (m/z) calculated for  $\text{C}_{17}\text{H}_{14}\text{N}_2\text{O}_2$  306.1117, found 306.1143.

**44:** Under nitrogen atmosphere, compound **43** (0.5 g, 1.63 mmol) was refluxed for 1h in ethanol (20 mL) in the presence of 10% (0.45 g) Pd/C. Hydrazine hydrate (15 ml) was cautiously added. The reaction solution was refluxed for another 30min. Once cooled down to room temperature, the reaction mixture was filtered through celite. Water (80 mL) was added into the filtrate and the solution was extracted with chloroform (2x50 mL). The combined organic phases were then dried over anhydrous  $\text{MgSO}_4$ , filtered and chloroform was removed to give pure product, 91% yield.  $^1\text{H}$  NMR (400 MHz,  $\text{CDCl}_3$ )  $\delta$  ppm 8.67 (m, 2H), 7.78 (m, 4H), 7.28 (m, 2H), 4.39 (s, 2H), 2.30 (s, 6H);  $^{13}\text{C}$  NMR (100 MHz,  $\text{CDCl}_3$ )  $\delta$  ppm 159.8, 153.6, 151.6, 148.2, 136.4, 124.7, 122.2, 114.4, 13.2; ESI-HRMS (m/z) calculated for  $\text{C}_{17}\text{H}_{16}\text{N}_2$  276.1375, found 276.1347.

### 3.5 References

1. Reynisson, J.; McDonald, E. *J. Comput. Aided Mol. Des.* **2004**, *18*, 421.
2. Cheng, M.; Pu, X.; Wong, N. -B.; Li, M.; Tian, A. *New J. Chem.* **2008**, *32*, 1060.
3. Chang, S. -Y.; Kim, H. S.; Chang, K. -J.; Jeong, K.-S. *Org. Lett.* **2004**, *6*, 181.
4. Xue, C.; Popelier, P. L. A. *J. Phys. Chem. B* **2008**, *112*, 5257.
5. Xue, C.; Popelier, P. L. A. *J. Phys. Chem. B* **2009**, *113*, 3245.
6. Gooch, A.; McGhee, A. M.; Pellizzaro, M. L.; Lindsay, C. I.; Wilson, A. J. *Org. Lett.* **2011**, *13*, 240.

7. Newman, S. G.; Taylor, A.; Boyd, R. J. *Chem. Phys. Lett.* **2008**, *450*, 210.
8. Sundermeier, M.; Zapf, A.; Beller, M. *Eur. J. Inorg. Chem.* **2003**, 3513.
9. Sessler, J.; Gross, D. E.; Cho, W.-S.; Lynch, V. M.; Schmidtchen, F. P.; Bates, G. W.; Light, M. E.; Gale, P. A. *J. Am. Chem. Soc.* **2006**, *128*, 12281.
10. Hansch, C.; Leo, A.; Taft, R. W. *Chem. Rev.* **1991**, *91*, 165.
11. Kaminski, T.; Gros, P.; Fort, Y. *Eur. J. Org. Chem.* **2003**, 3855.
12. Fallahpour, R. -A.; Neuburger, M.; Zehnder, M. *New J. Chem.* **1999**, 53.

## CHAPTER 4

### Supramolecular Copolymer Formed from Ditopic Monomers Containing AAA-DDD Hydrogen Bonds

#### 4.1 Supramolecular Polymers

In the last few years a strong interest in polymers that respond to environmental stimuli (such as pH, temperature and solvent) is expanding the potential field of applications for such materials that still retain the excellent properties of traditional polymers. Because there exists a dynamic equilibrium between polymers and monomers in the process of supramolecular polymerization, supramolecular polymers are naturally stimuli-responsive. Hence, supramolecular polymers based on noncovalent intermolecular interactions may be considered as reversible materials, thus opening a new window for them as advanced soft materials.<sup>1</sup>

Molecular recognition and self-organization are the mechanisms of supramolecular growth. The use of reversible, directional and selective hydrogen bonds is one of the best ways to construct stimuli-responsive polymer materials.<sup>2-4</sup> Controlled geometric placement of hydrogen bonded motifs leads to efficient molecular recognition, which is optimized through self-organization. Furthermore, the directionality of hydrogen bonds assists in the construction of supramolecular architectures.

In the field of polymer processing, thermoreversibility is an interesting feature because of the promise for lower melt viscosities of hydrogen-bond-containing polymers. Thus, a lower molecular weight hydrogen-bonded polymer could potentially afford

mechanical properties approaching those of a higher molecular weight nonfunctional polymer over a short time scale, and exhibit lower melt viscosity when heated above the dissociation temperature of the hydrogen bonded motifs.<sup>5</sup> Hydrogen bonded polymers would exhibit a higher apparent molecular weight at room temperature than they actually possessed. Another feature of hydrogen bonded systems is that they are dynamic, and this allows them to achieve the most thermodynamically favored state available. This dynamic property of hydrogen bonds allows the self-assembly to occur at ambient conditions, unlike many covalent polymerizations.<sup>6</sup> Hydrogen bonded supramolecular assembly in conjunction with covalent polymer synthesis often leads to a positive impact on the mechanical properties such as the stress at break and percentage of elongation<sup>7</sup>, as well as the elastic modulus<sup>8</sup>. In addition, other potential applications for hydrogen-bond-containing polymers exist, such as reversible attachment of guest molecules<sup>9</sup>, reversible cross-linking<sup>10</sup>, improved melt processing behavior<sup>11</sup>, self-healing materials<sup>12</sup>, shape-memory polymers<sup>13</sup>, induction of liquid crystallinity<sup>14</sup>, templated polymerization<sup>15</sup>, drug-selective chromatographic media<sup>16</sup>, hydrogen bonded layer by layer assemblies<sup>17</sup>, and reinforcement of the orientation of nonlinear optic materials<sup>18</sup>.

Here, we summarize main-chain supramolecular polymers based on *complementary* hydrogen bond arrays in the current literature.

#### **4.1.1 Supramolecular Polymerization Based on Three-Point Complementary Hydrogen Bonds**

Melamine and cyanuric acid can form a remarkably stable lattice and the stability possibly reflects that removing a molecule of melamine or cyanuric acid from the lattice requires 7 kcal/mol to break nine hydrogen bonds.<sup>19</sup> Therefore, melamine/cyanuric acid

and their derivatives have been used to make noncovalent polymeric nanostructures from these low-molecular-weight building blocks.

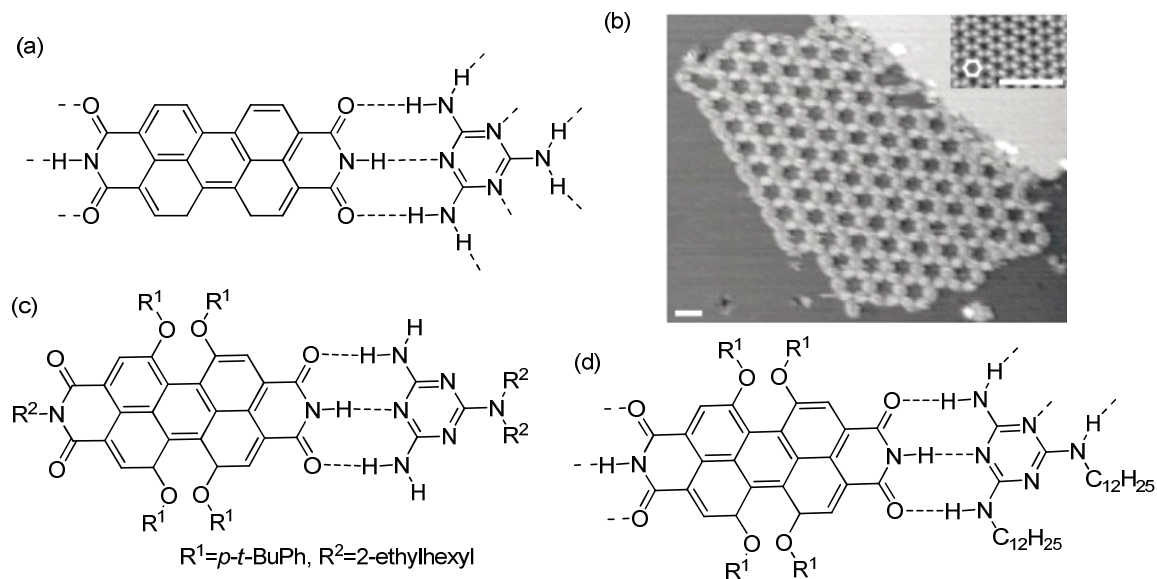
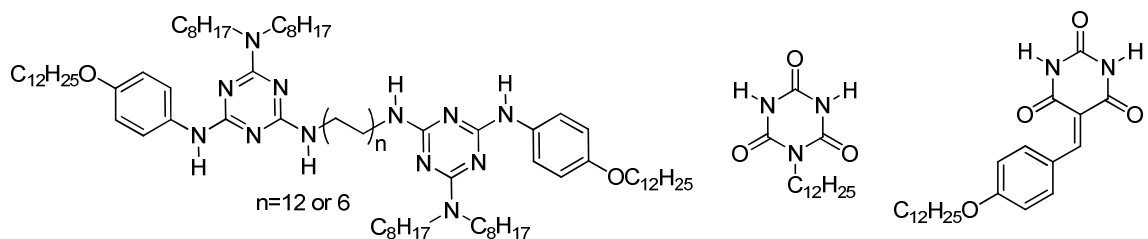


**Figure 4-1** (a) Chemical junction of perylene tetra-carboxylic di-imide and melamine; (b) STM image of the honeycomb network; (c) monotopic imide/melamine complex; (d) binding model of ditopic imide and melamine.

Theobald and coworkers investigated perylene tetra-carboxylic di-imide and melamine self-assembled into an open honeycomb network on a silver-terminated silicon surface (Figure 4-1).<sup>20</sup> The two-dimensional network, stabilized by the ADA-DAD hydrogen bonds between imide and melamine, can accommodate deposited fullerene molecules and serve as a template for the formation of a fullerene layer. Modified perylene imides and melamines formed supramolecular polymers on carbon-Formvar-coated nickel grids, even though the binding constant of monotopic melamine and imide is only  $240 \text{ M}^{-1}$  in chloroform.<sup>21</sup>

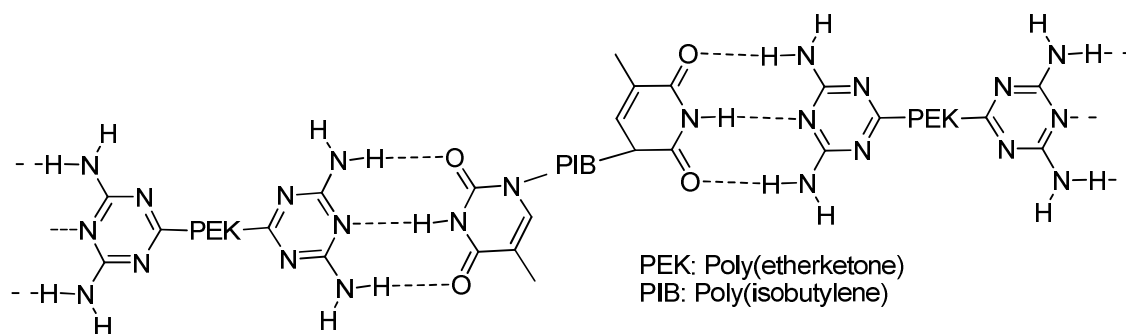
Yagai and coworkers reported supramolecular gels based on bismelamine that can noncovalently polymerize upon binding with cyanurates or barbiturates through complementary triple hydrogen bonds (Scheme 4-1).<sup>22</sup> Bismelamine (n=12) did successfully gelate in the presence of cyanurate or barbiturate in apolar solvents at a 5 mM concentration but gelation of only bismelamine was not observed. The length of the linker between two melamine moieties definitely affects the gelation. When a bismelamine including a shorter linker (n=6) was mixed with cyanurate or barbiturate, it did not gelate in any solvent even at high concentration (over 150 mM) while “macrocycles” similar to the binding of a Hamilton wedge and cyanuric acid were formed.<sup>22</sup>



**Scheme 4-1** Gels based on bismelamine/cyanurate or barbiturate hydrogen bonds.

The association constant between 2,6-diamino-1,3,5-triazine and thymine is about  $890 \text{ M}^{-1}$  in  $\text{CDCl}_3$ .<sup>23</sup> Binder and coworkers reported telechelic hydrogen bonded poly(isobutylene) and poly(etherketone) pseudo-block copolymers (Scheme 4-2). The end-group 2,6-diamino-1,3,5-triazine/thymines and 2,6-diamino-1,3,5-triazine/cytosine on the respective poly(isobutylene) and poly(etherketone) lead to a dramatic increase in the miscibility between the normally immiscible poly(isobutylene) and poly(etherketone) polymers.<sup>24</sup>





**Scheme 4-2** Pseudo-block copolymers consisting of poly(isobutylene) and poly(ether ketone) held together by three hydrogen bonds.

An oligo(*p*-phenylenevinylene) (OPV) dimer, in which the OPV units are capped on their end by monotopic melamine hydrogen bond units, self-assembles in methyl-cyclohexane to form flexible fibrous nanostructures. Those fibrous nanostructures are transformed into rigid nanostrips upon adding ditopic cyanurates and reconverted to nanaofibers upon adding a *m*-xylene-linked bismelamine because of the formation of a more stable complex (Figure 4-2).<sup>25</sup> When one equivalent *N*-monosubstituted cyanurate was added into the methyl-cyclohexane solution of OPV, a blue shift in the UV-vis spectrum was observed, suggesting that co-aggregation occurs through complementary triple hydrogen bonds and the OPV chromophores are tightly packed.

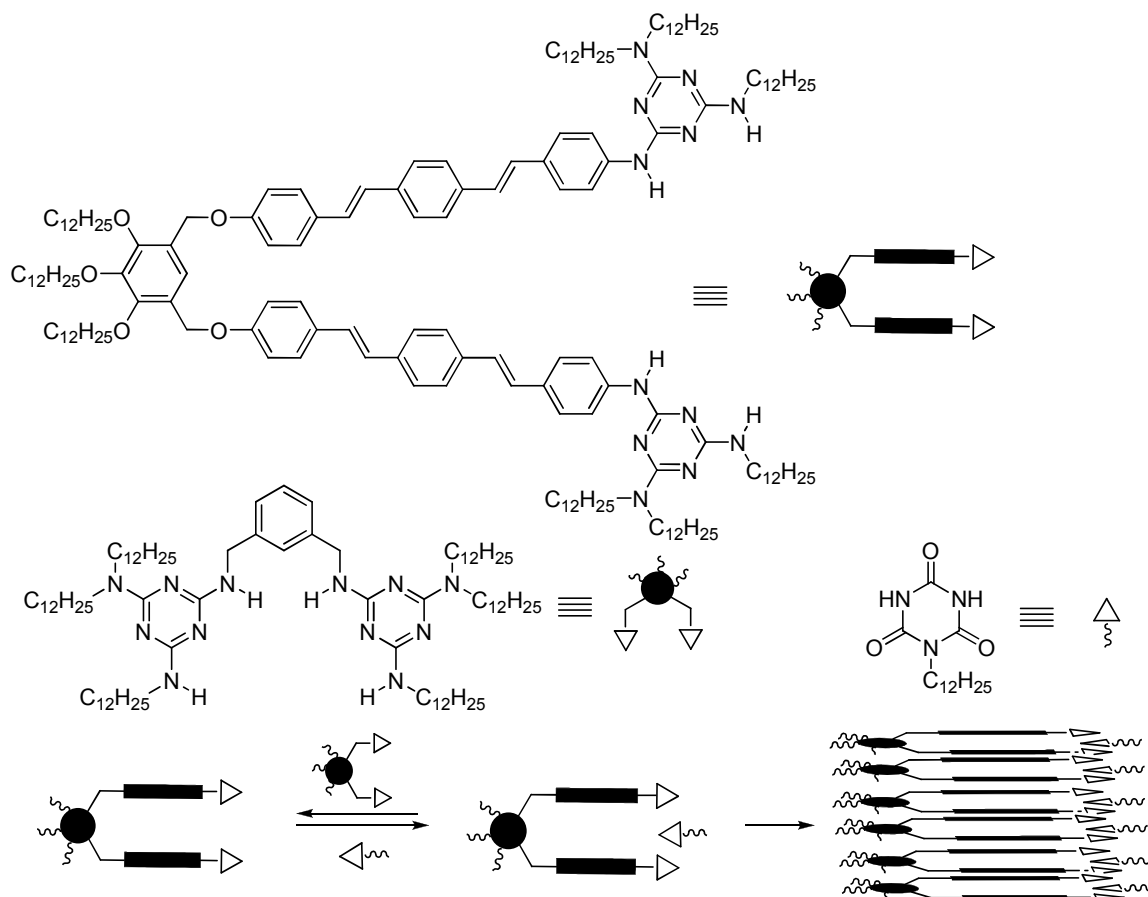
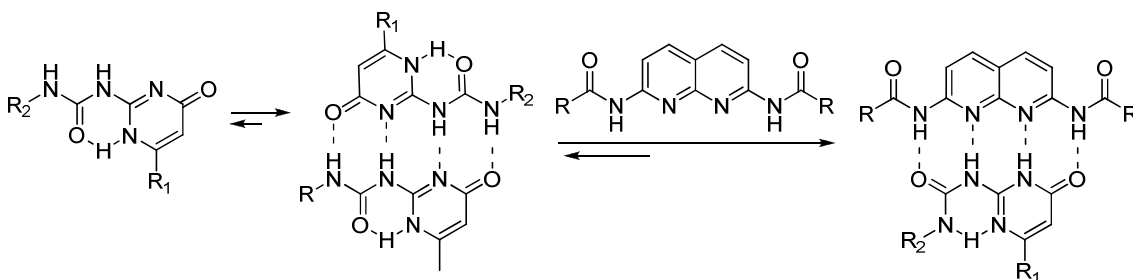


**Figure 4-2** Co-aggregations of OPVs and cyanurates.

#### 4.1.2 Supramolecular Polymerization Based on Four-Point Complementary Hydrogen Bonds

Meijer's famous self-complementary AADD sequence (2-ureido-4[1H]-pyrimidinone) shows an extremely high self-association strength. However, Li and coworkers reported the strong and selective complexation of the 6[1H] tautomeric form of 2-ureido-4[1H]-pyrimidinone with 2,7-diamino-1,8-naphthyridine via four hydrogen bonds between ADDA and DAAD sequences (Scheme 4-3).<sup>26</sup> One equivalent of 2,7-diamino-1,8-naphthyridine can disrupt the 2-ureido-4[1H]-pyrimidinone dimer effectively. The high selectivity and strength render the heterodimer attractive for building complementary complexes. Meijer and coworkers have demonstrated that the

selective heterocomplex formation of 2-ureido-4[1H]-pyrimidinone with 2,7-diamino-1,8-naphthyridine is dependent on concentration. For a 1:1 mixture of 2-ureido-4[1H]-pyrimidinone with 2,7-diamino-1,8-naphthyridine, dilution ( $5 \times 10^{-2}$  to  $2 \times 10^{-5}$  M) resulted in a decrease in selectivity from 93% to 56% heterocomplexation.<sup>27</sup>



**Scheme 4-3** Competitive association between self-complementary AADD and complementary ADDA-DAAD.

Meijer and coworkers also investigated the influence of selectivity on the supramolecular polymerization of AB-type polymers capable of both A/A and A/B-type interactions.<sup>28</sup> In order to increase the selectivity of complementary heterocomplex formation, one approach is to reduce the dimerization association ( $K_{\text{dim}}$ ) of 2-ureido-4[1H]-pyrimidinone. The  $K_{\text{dim}}$  of dibutylamino-substituted 2-ureido-4[1H]-pyrimidinone is approximately  $9 \times 10^5 \text{ M}^{-1}$ , which is lower than that of methyl-substituted 2-ureido-4[1H]-pyrimidinone ( $6 \times 10^7 \text{ M}^{-1}$ ). To ensure a fair comparison between the two AB monomers including different substituent group it was important to include the same linker between the hydrogen bonded motifs (Figure 4-3). Unexpectedly, the increased selectivity for complementary association not only influences the concentration-dependent degree of polymerization but also the ring-chain equilibrium by increasing the trend to cyclization.

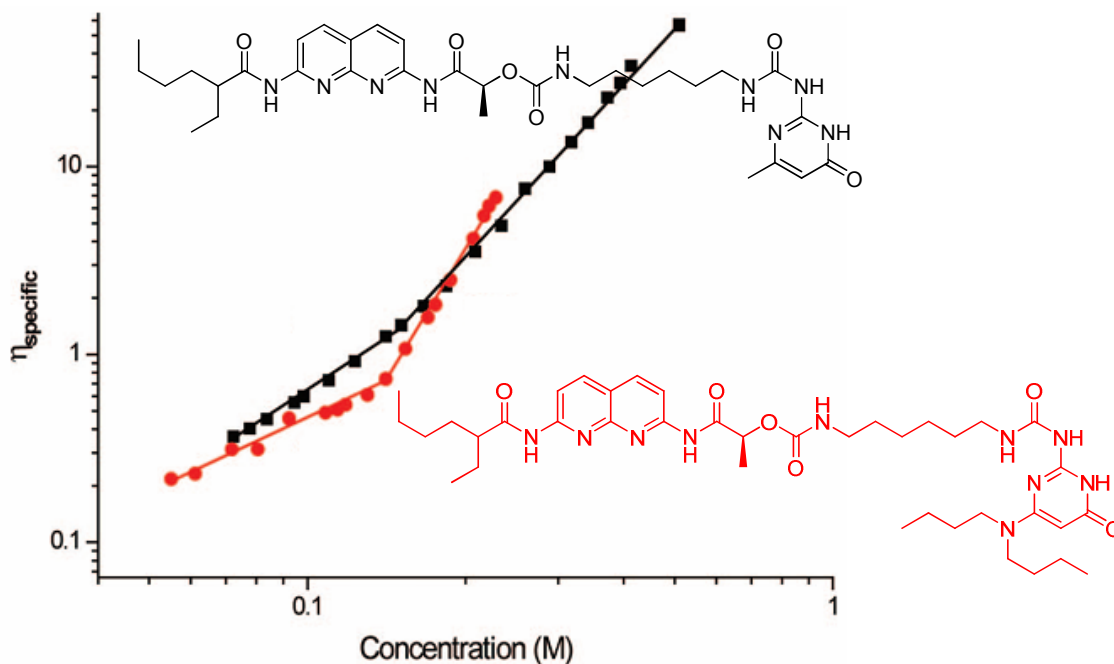
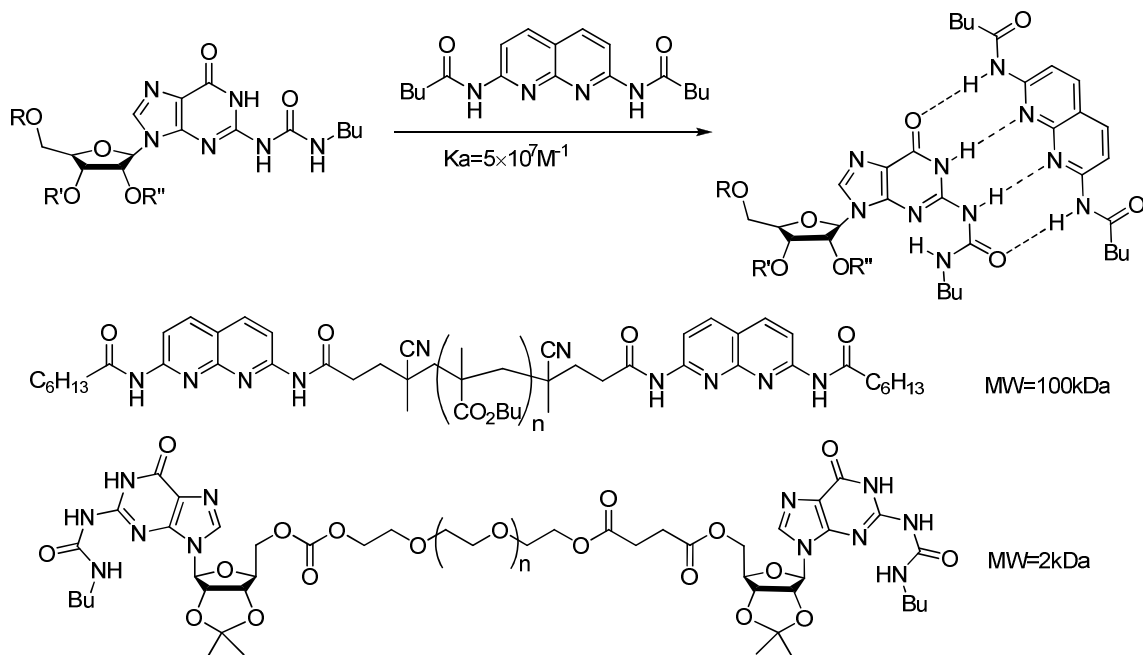


**Figure 4-3** Solution viscosities of 2,7-diamino-1,8-naphthyridine / 2-ureido-4[1H]-pyrimidinone monomers in chloroform at 25°C.

Zimmerman and coworkers have developed another ADDA-DAAD system and used a guanosine urea derivative which weakly self-associates ( $K_{\text{dim}} = 200 \text{ M}^{-1}$ ) but has a high association constant with 2,7-diamino-1,8-naphthyridine ( $K_{\text{a}} = 5 \times 10^7 \text{ M}^{-1}$ ).<sup>29</sup> Compared with Meijer's case, Zimmerman's system has an extremely low self-association. Oligomers or polymers with complementary recognition motifs at both pairs of chain ends may be mixed to form superstructures. Poly (butyl methacrylate) (PBMA) and poly (ethylene glycol) (PEG) were respectively linked by two complementary hydrogen bonded units (Scheme 4-4). Although PBMA and PEG are not normally miscible, inclusion of these hydrogen-bonded motifs results in their complete miscibility. The viscosity of the two polymer mixture exhibited a significantly larger increase than

did each polymer alone. The authors concluded a linear supramolecular multi-block copolymer was formed.

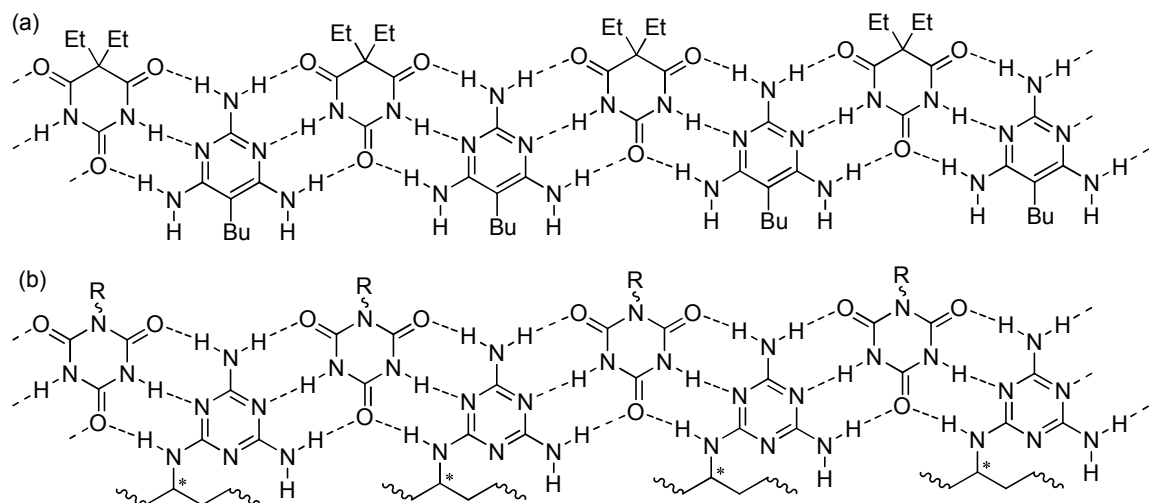


**Scheme 4-4** Zimmerman's ADDA-DAAD and bifunctional polymers.

#### 4.1.3 Supramolecular Polymerization Based on Six-Point Complementary Hydrogen Bonds

Lehn and coworkers investigated the self-assembly of complementary barbituric acid and 2,4,6-triaminopyrimidine derivatives as molecular components.<sup>30</sup> From the x-ray crystal structure, barbituric acid forms six hydrogen bonds with its two neighbouring 2,4,6-triaminopyrimidines and all like the residues ethyl and butyl are respectively located on the same side of the strand, as represented in Scheme 4-5. Similar hydrogen-bonded pairs of hydrophobic, chiral, long-chain derived melamine and cyanuric acid including hydrophilic ammonium salts drive the formation of supramolecular membranes

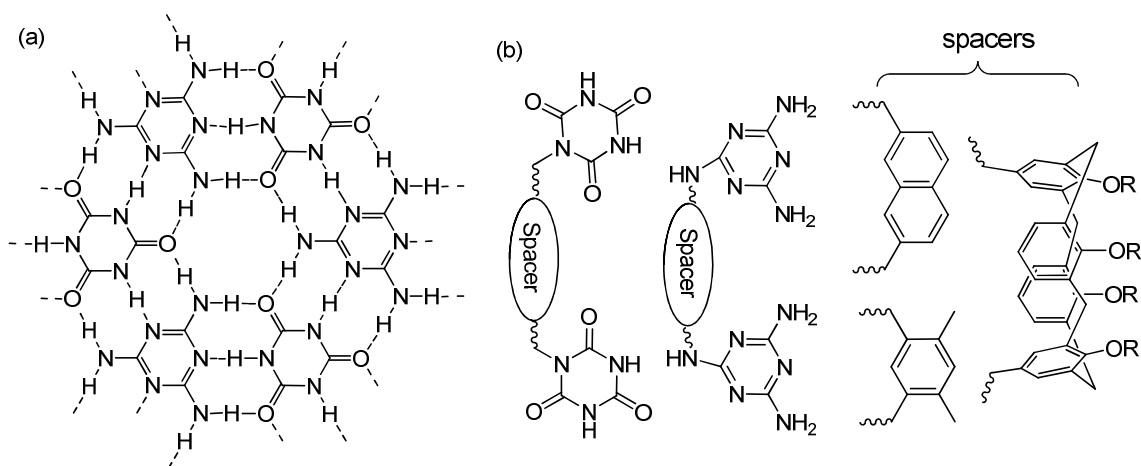
in water.<sup>31</sup> Spectral titration experiments demonstrated the stoichiometric integration of the complementary subunits with an association constant of  $1.13 \times 10^5 \text{ M}^{-1}$ .



**Scheme 4-5** (a) An ordered supramolecular strand by the molecular recognition of barbituric acid and 2,4,6-triaminopyrimidine derivatives; (b) Complementary hydrogen bonded networks from CA and M monomers.

Two melamines or cyanuric acids may be connected by a spacer to form bismelamine (bisM) or biscyanuric acid (bisCA). Whitesides and coworkers used aromatic rings (benzene and naphthalene) as spacers for bisCA and bisM (Scheme 4-6).<sup>32</sup> A 1:1 mixture of bis CA and bisM self-assembled into polymeric nanorods [(bisCA)<sub>n</sub>(bisM)<sub>n</sub>] composed of parallel rosettes. TEM (transmission electron microscopy) analysis suggested that those nanorods aggregated as bundles whose length ranged from 100 nm to 1500 nm and whose diameter ranged from 15 nm to 500 nm. Klok *et al* reported two melamines or cyanuric acids linked by a calix[4]arene.<sup>33</sup> Although similar rod-like nanostructures were formed, the solubility of hydrogen-bonded polymeric calix[4]arenes depended on the length of the alkoxy chains of the

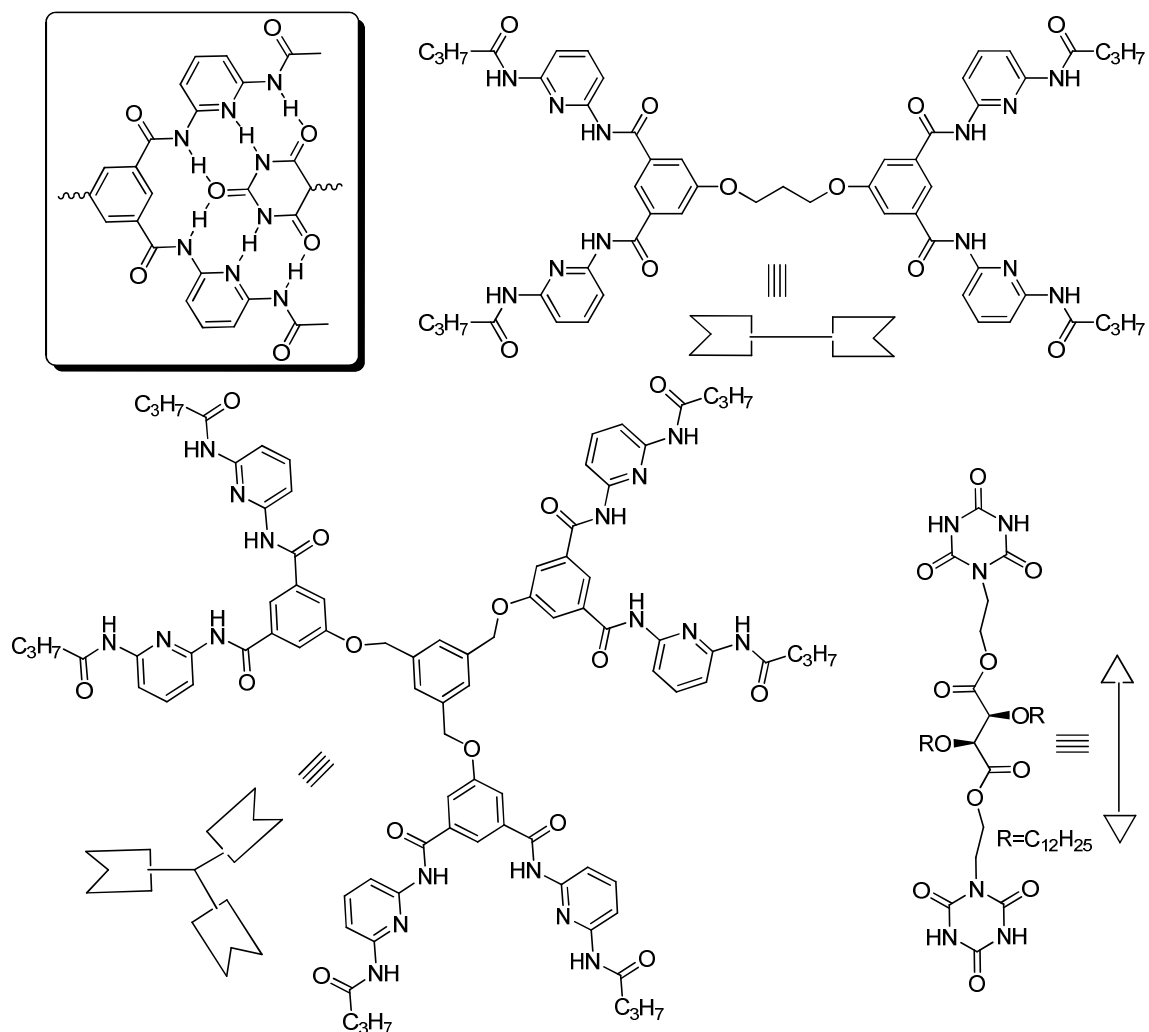
calix[4]arene. Shorter chains ( $C_3H_7$ ) resulted in insoluble polymer in any solvent except DMSO (after all, DMSO breaks the hydrogen bonding.); however, longer chain ( $C_{12}H_{25}$ ) in calix[4]arene provided soluble polymer in apolar solvents.



**Scheme 4-6** (a) A rosette formation in the melamine/cyanuric acid lattice; (b) Bismelamine, biscyanic acid and some spacers.

Strong association ( $K_a = 4 \times 10^4 M^{-1}$ ) is achieved through the use of the Hamilton wedge (ADA-ADA array) and a corresponding barbituric acid (or N-alkyl cyanurate) system.<sup>34</sup> As shown in Scheme 4-7, the building blocks including two or three complementary monomers can generate linear or cross-linked supramolecular polymer fibers, gels and networks through the Hamilton wedge and barbituric acid system.<sup>35</sup> These supramolecular polymer formations have been confirmed based on the determination of the association constants, variable-temperature NMR experiments and viscosity measurements. In addition, linear or zigzag supramolecular polymers including bifunctional hydrogen bonded motifs were observed by STM (scanning tunneling microscopy) on highly oriented pyrolytic graphite (HOPG) surfaces.<sup>36</sup> Control of the

geometry of 1D supramolecular architecture was obtained by using two different connecting molecules with different conformational rigidity, affording either linear or zigzag motifs.



**Scheme 4-7** Hamilton wedge type Building blocks for linear or cross-linked supramolecular polymers.

Combination of supramolecular chemistry and reversible covalent bonds leads to the concept of constitutional dynamic chemistry.<sup>37</sup> The formation of double dynamic supramolecular polymers, that are dynamic on both the molecular and supramolecular



levels, was achieved via high affinity six hydrogen bond formation and reversible acylhydrazone bond formation by condensation of hydrazides with aldehydes.<sup>38</sup> Because of both reversible covalent and noncovalent connections, the different component exchanges allow the generation of constitutional diversity on the molecular and supramolecular levels. Thus, selection processes may be driven by both hydrogen bond interactions and reversible covalent bond formation (Figure 4-4).

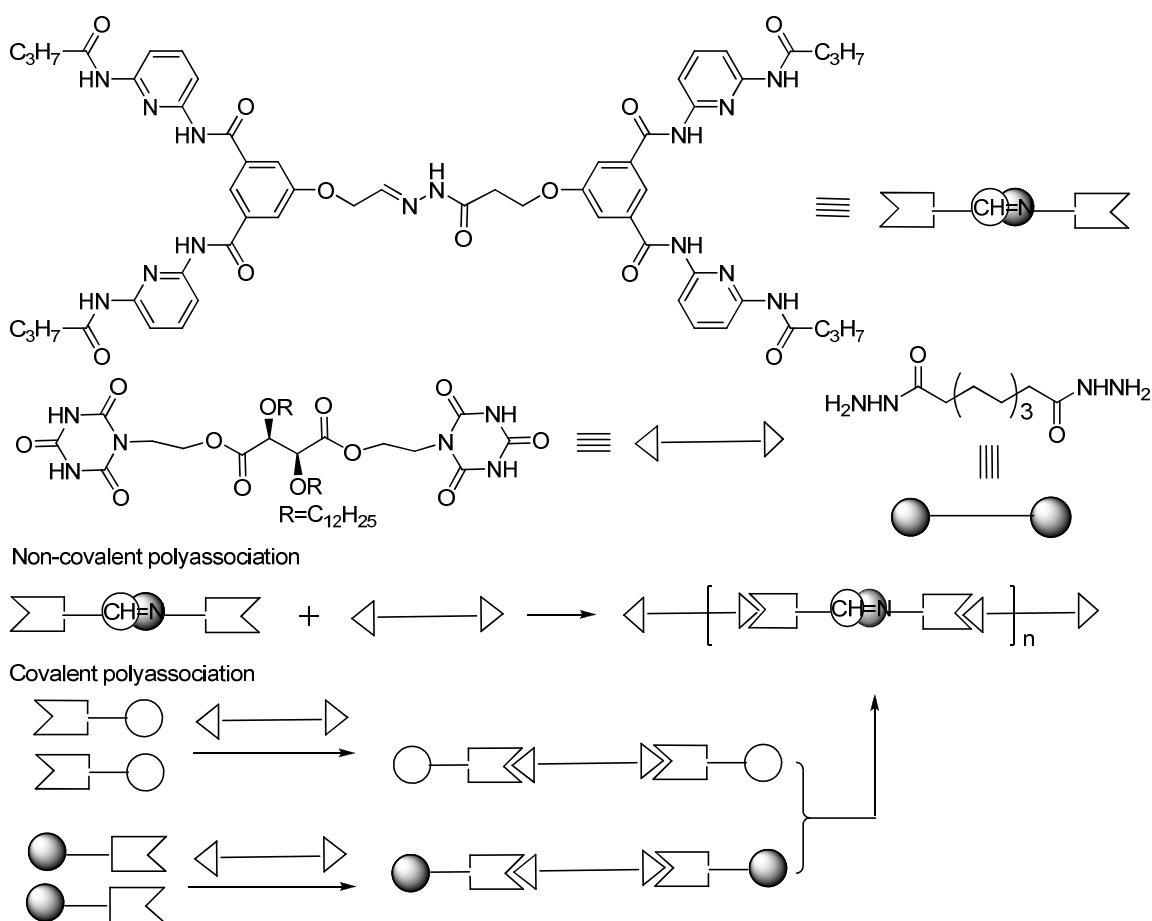
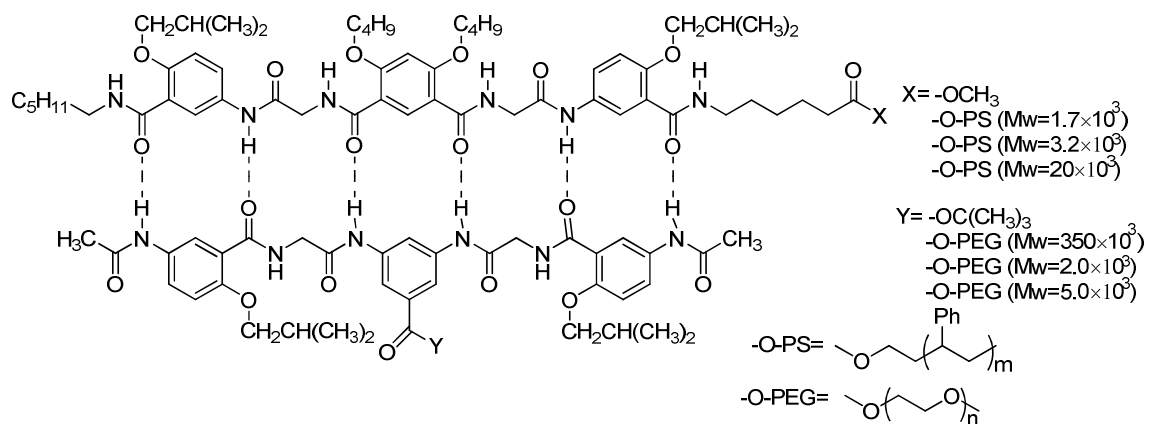


**Figure 4-4** Double dynamic supramolecular polymers generated by reversible covalent and noncovalent bonds.

Gong and coworkers have reported that two complementary oligoamide strands formed a six-hydrogen-bond heteroduplex with a high association constant ( $K_a > 10^9 \text{ M}^{-1}$  in  $\text{CHCl}_3$ ).<sup>39</sup> Hydroxyl-terminated polystyrene (PS) and poly (ethylene glycol) monomethyl ether (PEG) chains were coupled to two complementary oligoamide strands (Scheme 4-8). The mixture of equivalent molar ratio modified PS and PEG chains led to the formation of supramolecular diblock polymers.<sup>40</sup>



**Scheme 4-8** AB diblock copolymers linked by six hydrogen bonds.

## 4.2 Supramolecular Copolymers Based on Double Helical AAA-DDD Hydrogen Bonds

A number of sequences that have more than three (i. e. four, six or nine) hydrogen bonds have been applied for supramolecular polymers. Although for most of known complementary triply hydrogen bonded systems with weaker association constants, surface-aided supramolecular polymerization of them can be still achieved, the cornerstone for main-chain supramolecular polymers is strong hydrogen-bonded interactions between binding sites. The hydrogen-bond strength of the binding motifs

significantly affects the formation of supramolecular polymers and degrees of polymerization (Figure 4-5). The degree of noncovalent polymerization (DP) is also important to measure the formation of supramolecular polymers. DP directly depends on the association constant ( $K_a$ ) and the concentration of the molecules ( $C$ ) as shown:  $DP = (2K_aC)^{0.5}$ .<sup>41</sup> This equation assumes that the supramolecular polymerization is isodesmic and there are no cyclic species. Due to the limited solubility of many molecules in organic solvents, the concentration of the solution is limited and thus the association constant must be high enough to obtain supramolecular polymers with a high molecular weight at these concentrations.

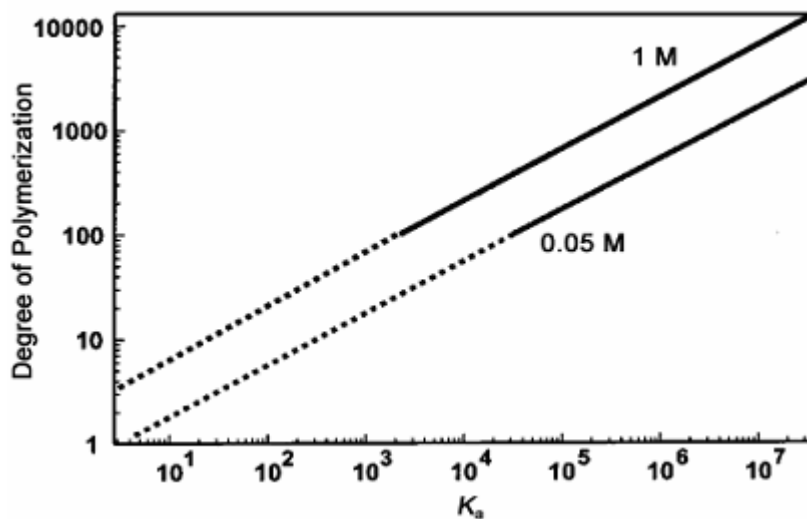
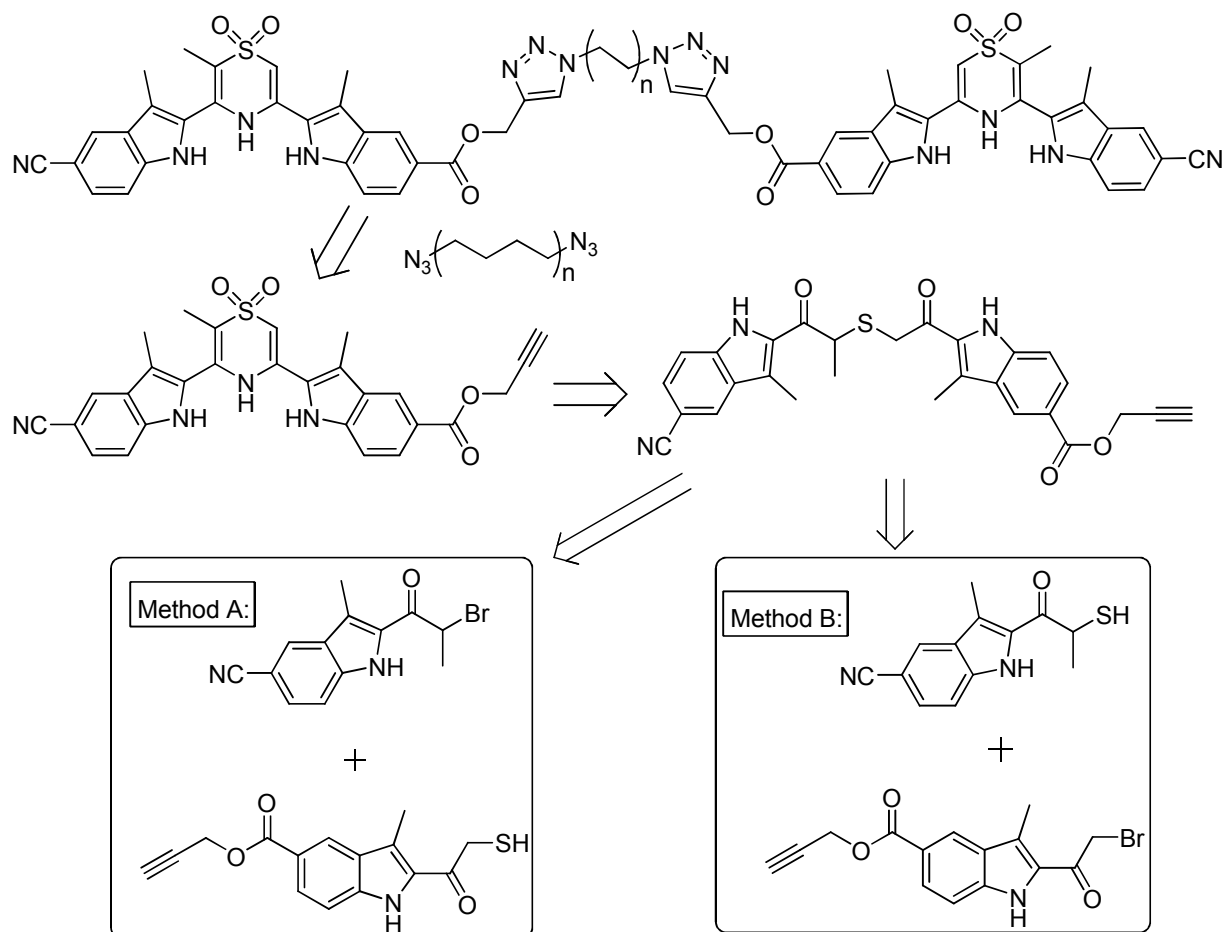


**Figure 4-5** The relationship between degree of polymerization and association constant.

In chapters 2 and 3, double helical AAA-DDD systems with high association constants were investigated. Their association constants could reach  $>10^5 \text{ M}^{-1}$ , which is high enough for the formation of main-chain supramolecular polymers.

### 4.2.1 Synthesis of Monomers Ready for BisDDD and BisAAA

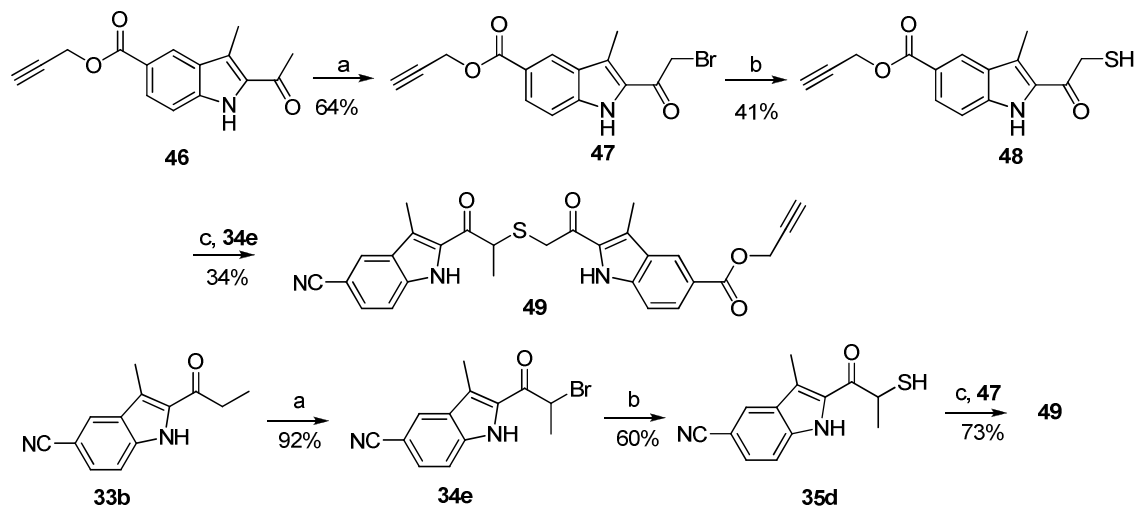
Retrosynthesis of bisDDD is shown in Scheme 4-9. Click chemistry has been used extensively in organic synthesis and polymerization.<sup>42</sup> BisDDD was prepared via the click chemistry of a diazide and a monomer including a propargyl group.



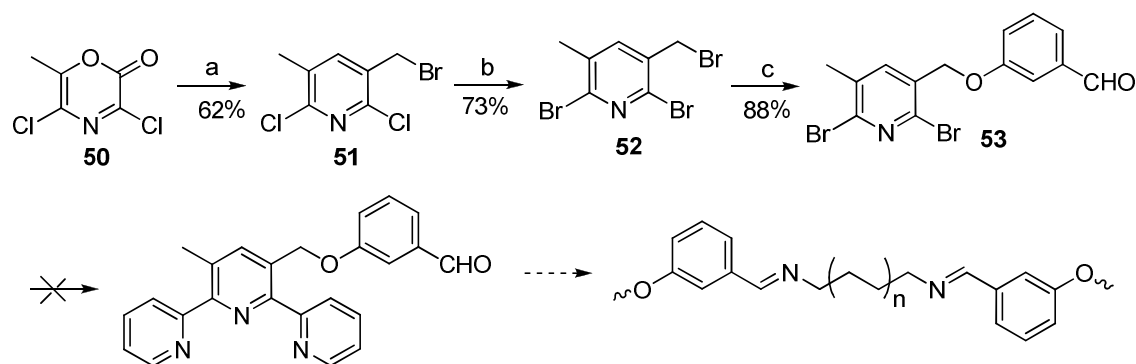
**Scheme 4-9** Retrosynthetic analysis for bisDDD.

There are two ways to obtain the intermediate thioether and wished to compare which method is much more effective to synthesize thioether (Scheme 4-10). Although the bromination step is always effective, the synthesis of thiol **48** is low yielding and the

further elaboration of thioether **49** proceeded in even lower yield. Method B for the synthesis of thioether **49** proved to be much better than Method A.

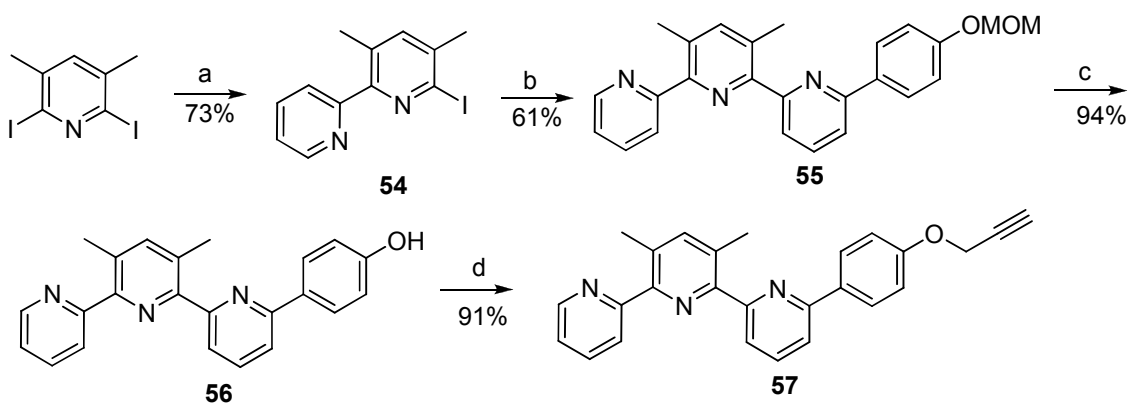


**Scheme 4-10** Synthesis of the intermediate thioether **49**. Reagents and conditions: a)  $\text{PhNMe}_3\text{Br}_3$ , THF, reflux, 1h; b) (i) KSAc, DMF, 12h; (ii) cysteamine hydrochloride,  $\text{NaHCO}_3$ ,  $\text{CH}_3\text{CN}$ , 18h; c)  $\text{Et}_3\text{N}$ ,  $\text{CH}_3\text{CN}$ , 18h



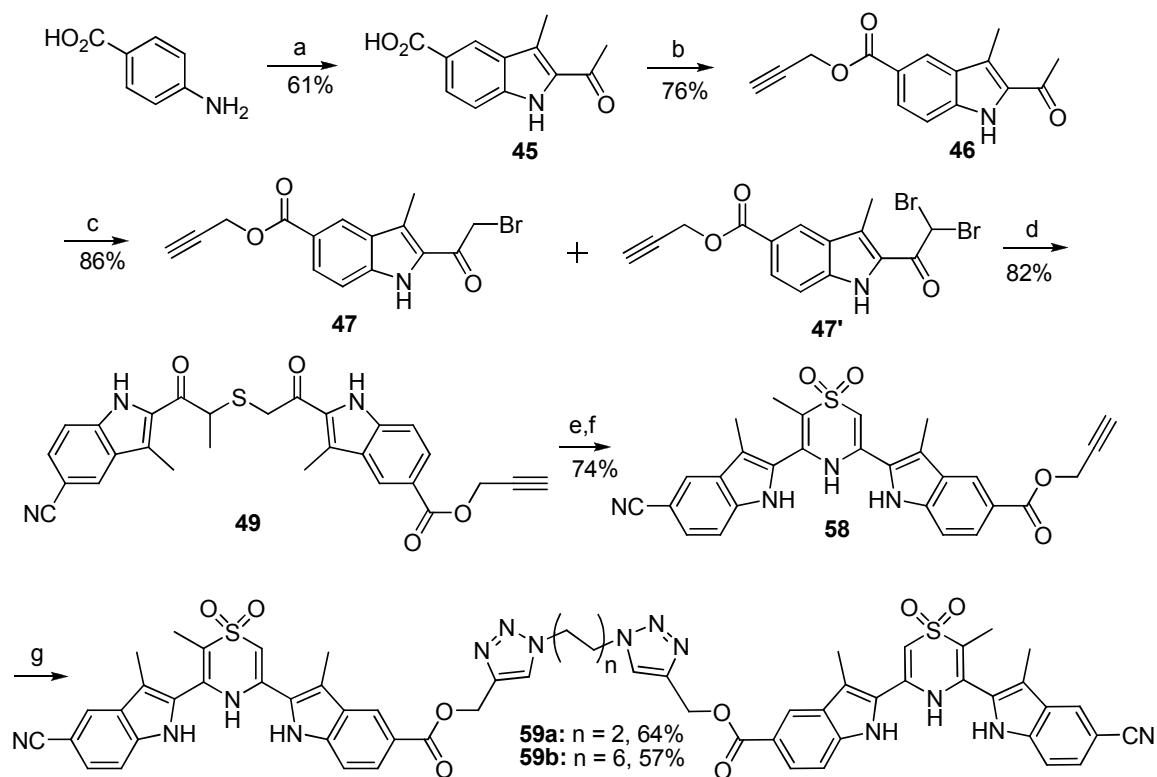
**Scheme 4-11** Synthesis of the possible monomer for bisAAA. Reagents and conditions: a) propargyl bromide, toluene,  $70^\circ\text{C}$ , 16h; b) HBr, AcOH, reflux; c)  $\text{K}_2\text{CO}_3$ , EtOH, 3-hydroxybenzaldehyde.

As discussed, imines have been used in the synthesis of dynamic covalent polymers. We also expected that two AAA arrays including an aldehyde group and a diamine would form the bisAAA monomer (Scheme 4-11). 3,5-Dichloro-2H-1,4-oxazin-2-one **50**, obtained from the cyclocondensation of lactonitrile and oxalyl chloride, was subjected to a Diels-Alder reaction with propargyl bromide and followed by the elimination of CO<sub>2</sub> to form 2,6-dichloro-3-(bromomethyl)pyridine **51**.<sup>43</sup> In order to make the Stille coupling more facile, the bromination of 2,6-dichloro-3-(bromomethyl)pyridine afforded the corresponding 2,6-dibromo-3-(bromomethyl)pyridine **52**. Unfortunately, in the case of compounds **52** and 2-tributyltinpyridine, the Stille coupling did not proceed. We also expected that click chemistry could be used in the synthesis of bisAAA. Therefore, we designed and synthesized end group **57** intended for click chemistry to a diazide (Scheme 4-12).



**Scheme 4-12** Synthesis of the possible bisAAA end group **57**. Reagents and conditions: a) 2-tributyltinpyridine, Pd(PPh<sub>3</sub>)<sub>4</sub>, toluene, reflux, 16h; b) 6-(4-methoxymethoxy phenyl)-2-tributyltinpyridine, Pd(PPh<sub>3</sub>)<sub>4</sub>, toluene, reflux, 48h; c) 2 M aqueous HCl, 3h; d) propargyl bromide (80% in toluene), K<sub>2</sub>CO<sub>3</sub>, DMF.

#### 4.2.2 Synthesis of BisDDD and BisAAA



**Scheme 4-13** Synthesis of bisDDD monomers linked with two different length chains.

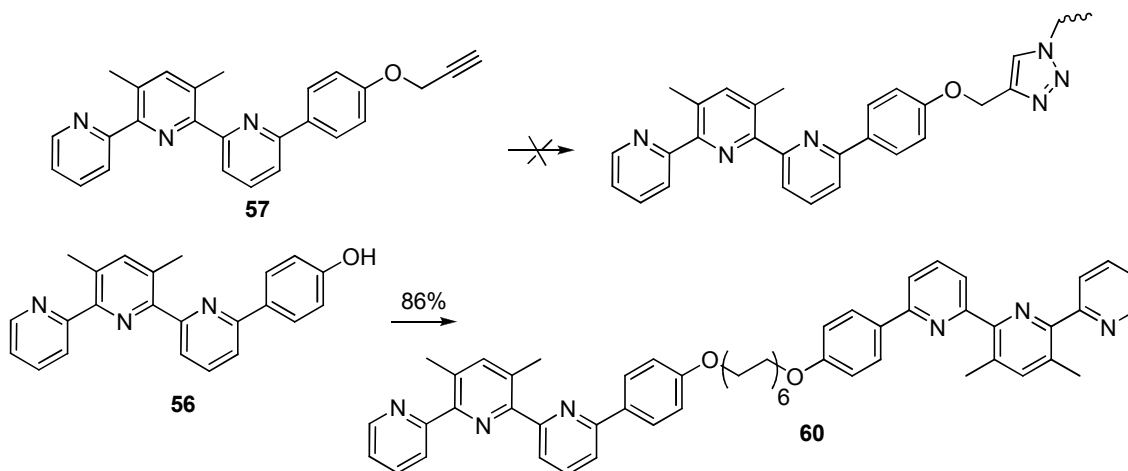
Reagents and conditions: a) (i) NaNO<sub>2</sub>, conc. HCl/H<sub>2</sub>O, (ii) NaOH, ethyl 2-ethylacetoacetate, EtOH/H<sub>2</sub>O, (iii) formic acid, reflux; b) propargyl alcohol, EDC, DMF/THF; c) PhNMe<sub>3</sub>Br<sub>3</sub>, THF, reflux; d) **35d**, Et<sub>3</sub>N, CH<sub>3</sub>CN; e) m-CPBA, DMF, -20°C to r. t.; f) NH<sub>4</sub>OAc, glacial acetic acid, reflux; g) 1,12-diazidodecane for **12a** or 1,4-diazidobutane for **12b**, CuSO<sub>4</sub>·5H<sub>2</sub>O, sodium ascorbate, THF/H<sub>2</sub>O (5/1), 55°C.

Because the chain linker (such as chain length<sup>44</sup>, chain conformation<sup>45</sup> and chain polarity<sup>46</sup>) between two hydrogen bonded motifs significantly affects the formation of supramolecular polymers, an aliphatic spacer (12 carbon chain) was chosen as a flexible linker for the self-assembly of hydrogen bonded polymers. In addition, Gibson and

coworkers have demonstrated that longer linkers result in more polymerization and less cyclization.<sup>47</sup>

The bromination of **46** produced a mixture of monobromo **47** and dibromo **47'**, but this mixture can still react with the intermediate **35d** to give only thioether product **49**. After the oxidation and cyclization reactions, the intermediate **58** was reacted with two different diazides to produce bisDDD **59 a**, **59b**. The synthesis is summarized in Scheme 4-13.

Although we also tried to use the same click chemistry as a straightforward method to obtain bisAAA, the coordination effect of AAA may affect the click reaction. BisAAA was effectively synthesized from 1,12-dibromododecane and compound **56** under the basic condition.



**Scheme 4-14** Synthesis of bisAAA **60**. Reagents and conditions:  $K_2CO_3$ , KI, DMF, dibromododecane,  $90^\circ C$ .



### 4.3 Results and Discussion

The association constants of hydrogen-bonded sequences useful for main-chain supramolecular polymers should be greater than  $10^5 \text{ M}^{-1}$ . The complexation of model end groups **55** and **58** (AAA+DDD) was investigated to conform their suitability (Figure 4-6). Isothermal titration calorimetry (ITC) confirmed that the association constant ( $K_a$ ) is as high as  $1.28(\pm 0.09) \times 10^5 \text{ M}^{-1}$ .

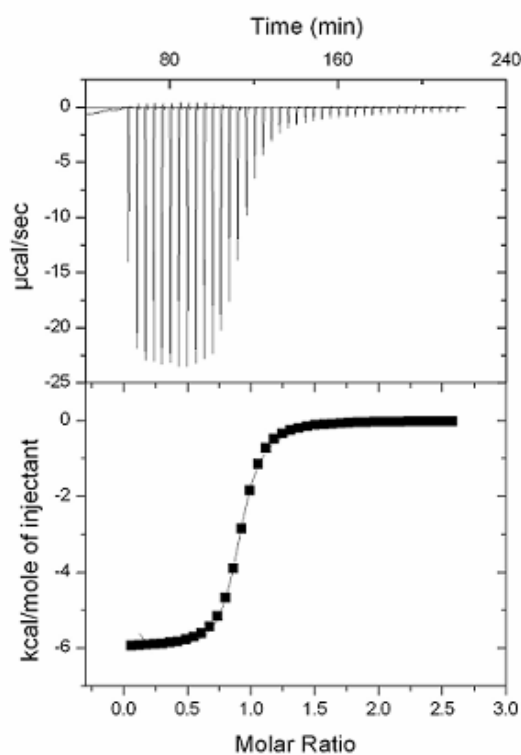


**Figure 4-6** ITC data for the binding of **55** and **58** in chloroform at 25°C. The top plot shows the power as a function of time and the bottom plot shows integrated enthalpy values as a function of the molar ratio of **55** titrated into **58** ( $\Delta G = -29.18 \pm 0.14 \text{ kJ/mol}$ ,  $\Delta H = -25.08 \pm 0.14 \text{ kJ/mol}$  and  $\Delta S = 13.8 \text{ J/mol}$ ).

Viscosity is a powerful physical technique for determining the formation of supramolecular polymers in solution. Viscosity measurements were carried out in chloroform with an Ubbelohde semi-micro viscometer. It is a simple method to calculate specific viscosity by comparing the flow time of the solution ( $t$ ) to the flow time of pure solvent ( $t_0$ ):

$$\eta_{sp} = \frac{\eta - \eta_0}{\eta_0} = \frac{t - t_0}{t_0}$$

Plots of specific viscosity vs concentration at different temperatures are displayed in Figure 4-7. It is demonstrated that the viscosity is dependent on concentration and temperature in a similar manner as other hydrogen-bonded supramolecular polymers. At some concentration (the so-called critical polymerization concentration), there is a sudden sharp increase in the viscosities, especially at low temperature (-15°C). This is evidence of the formation of supramolecular polymers at higher concentrations. In our case, the critical polymerization concentration is approximately 0.07 M at 25°C, 0.06 M at 5°C and 0.05 M at -15°C respectively. As the temperature decreases, the critical polymerization concentration also decreases and supramolecular polymers are formed at these lower concentrations likely as a result of the increase in the association constants.

The formation of supramolecular polymers exhibited viscosity transitions and was characterized by a change in slope in the double logarithmic plots of specific viscosity versus concentration. The double-logarithmic plots of specific viscosity versus concentration indicated there is a gradual transition from cyclic oligomers to linear oligomers and supramolecular polymers. At low concentrations, the slopes of all the

linear fits are approximately 1, which is expected for monomers or supramolecular cyclic oligomers with constant size.<sup>48</sup> At intermediate concentrations, there is an equilibrium of supramolecular cyclic and linear oligomers (slope = 1.75, 1.73) at 25°C and 5°C, which implies that the fraction of linear oligomers increases with the increase of concentration. However, there is no intermediate phase for the formation of supramolecular polymers at -15°C. At high concentrations, the logarithm of the specific viscosity against the logarithm of the concentration is still linear at three different temperatures. This slope is lower than that of the Meijer's hydrogen bonded supramolecular polymers (slope = 3.76), but when the temperature is decreasing, the slope increases and in particular is as high as 3.49 at -15°C, which is very close to the theoretical value (around 3.6) from Cates's model for reversible telechelic polymers. That means at low temperature there is extremely strong association between the monomers.<sup>48</sup>

The viscosity of the AA-BB type supramolecular polymers is also related to the ratio of AA and BB monomers. We investigated how the ratio of bisAAA **60** and bisDDD **59a** monomers affects the viscosity. As shown in Figure 4-9, the ratio  $x$  of approximately 1 of **60** and **59a** leads to the highest specific viscosity. As the proportion of **60** and **59a** increases, the specific viscosity decreases. The reason may be that during the chain growth, the equivalent mixture of bisAAA and bisDDD self-assembles like the traditional polymerization, but the excess of bisAAA or bisDDD (relative to the equivalent mixture) acts as a chain growth terminator and results in the limitation of chain growth. Therefore, an equivalent mixture of bisAAA and bisDDD monomers is key for the optimal formation of the supramolecular polymer.

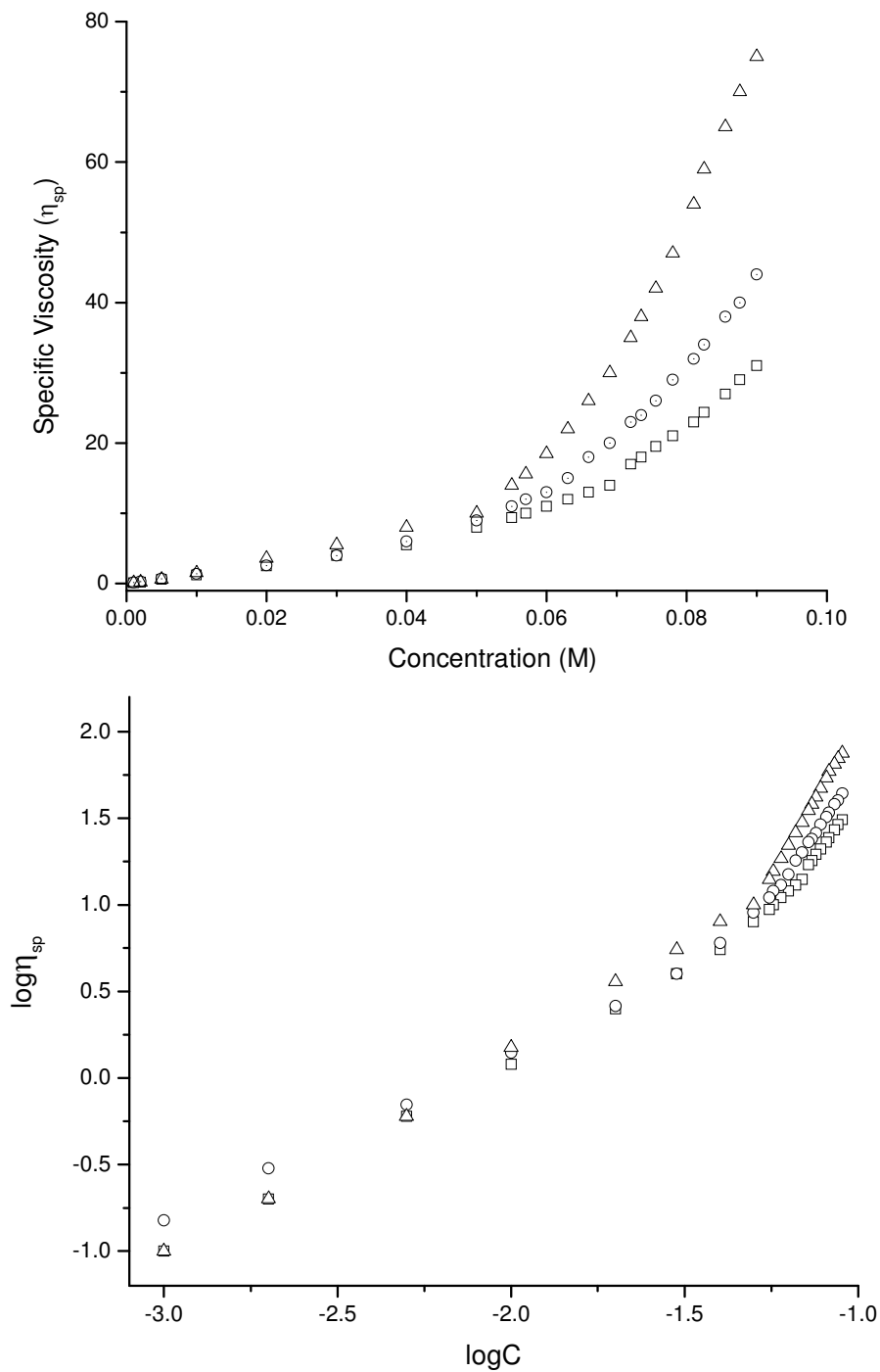


**Figure 4-7** Specific viscosity vs concentration plot for the 1:1 mixture of **59a** and **60** at different temperatures (top) and their double-logarithmic plot (bottom).  $\Delta$  corresponds to  $-15^\circ\text{C}$ , o to  $5^\circ\text{C}$  and  $\square$  to  $25^\circ\text{C}$ .

Further evidence for the formation of supramolecular polymers was observed by dynamic light scattering (DLS). There are no peaks observed in either a bisAAA **60** or bisDDD **59a** solution. However, the 1:1 mixture of **60** and **59a** result in the formation of approximately 86 nm particles on average (Figure 4-8).

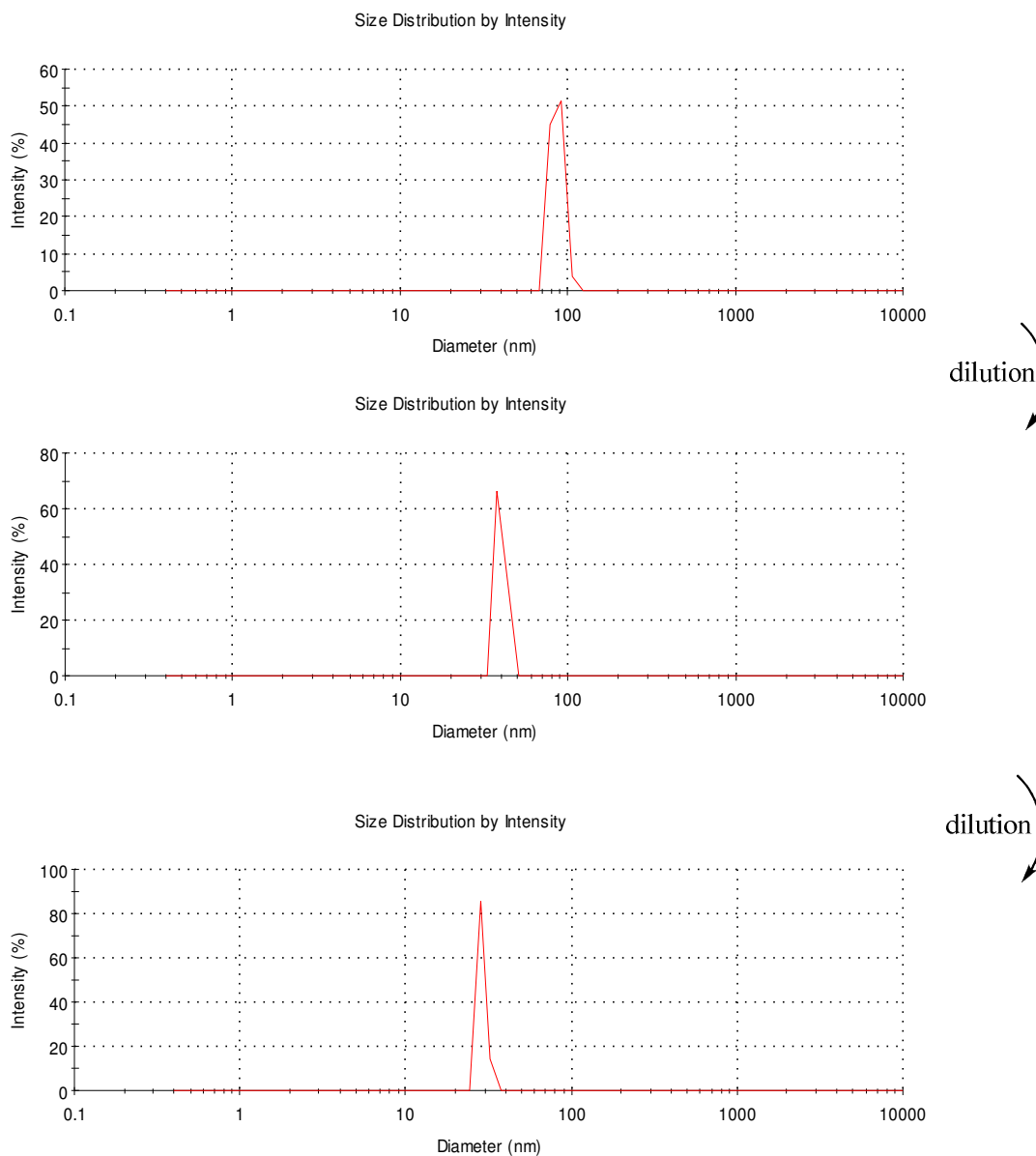


**Figure 4-8** Dynamic light scattering of an equimolar solution of **60** and **59a** (0.08 M) in chloroform at 25°C.

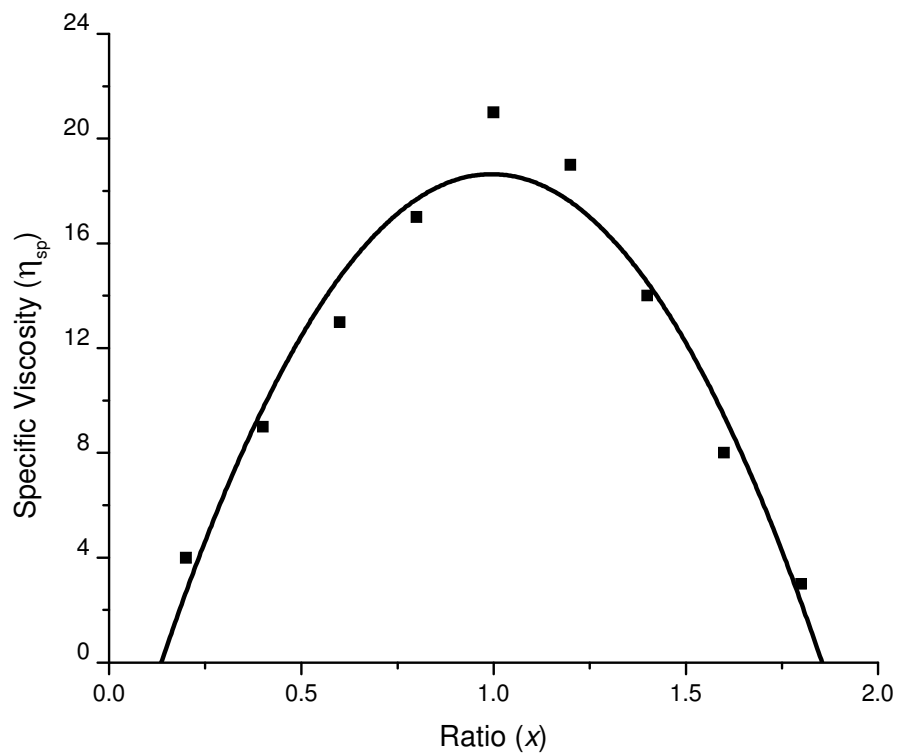


**Figure 4-9** Specific viscosity vs molar ratio of bisAAA **60** and bisDDD **59a**.

We also used compound **55** as a polymerization terminator to study how the monomer affects the polymerization of bisAAA and bisDDD monomers. Addition of a small fraction of compound **55** decreased the viscosity of the self-assembled polymer greatly (Figure 4-10) indicating that monomer **55** significantly terminated the supramolecular polymerization.

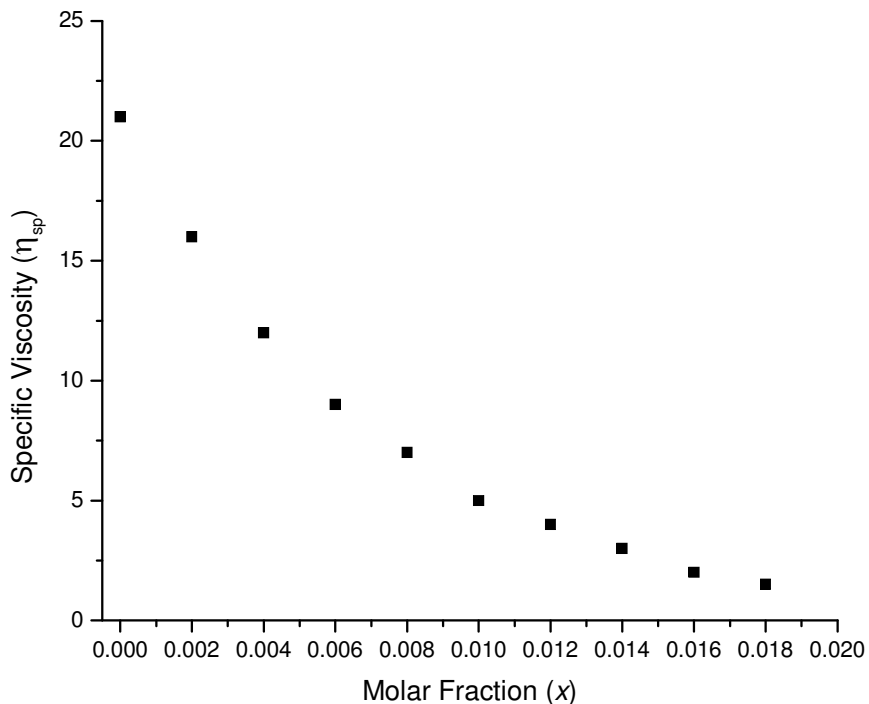


**Figure 4-10** Specific viscosity vs molar fraction of **55** in the 1:1 mixture of **60** and **59a**.

The lengths of two linkers for bisAAA **60** and bisDDD **59a** monomers are almost identical and for this kind of system, there are some general association processes: cyclization, linear oligomers (open ring) and polymerization growth. Viscosity experiments demonstrated that the self-assembly of bisAAA **60** and bisDDD **59a** follows this mechanism for supramolecular polymerization. We wondered whether asymmetric linkers in the two monomers would affect the supramolecular polymerization or not. Hence, we synthesized another bisDDD **59b** containing a shorter linker (only four carbons) and investigated the viscosities at different concentrations. There is no surprise that the viscosity increase with the increase of concentration. As is shown in Figure 4-11, there is an exponent growth relationship between concentration and specific viscosity. The critical polymerization concentration is around 0.045 M, which is slightly lower than that of **60** and **59a**. The self-assembly of **60** and **59b** still follows the ring-chain

supramolecular polymerization. Due to the asymmetric linkers of **60** and **59b**, they may not easily and totally transform into macrocycles at low concentrations. Therefore, this kind of asymmetrically linked bisAAA and bisDDD can form supramolecular polymers at lower concentrations relative to symmetrically linked bisAAA and bisDDD.

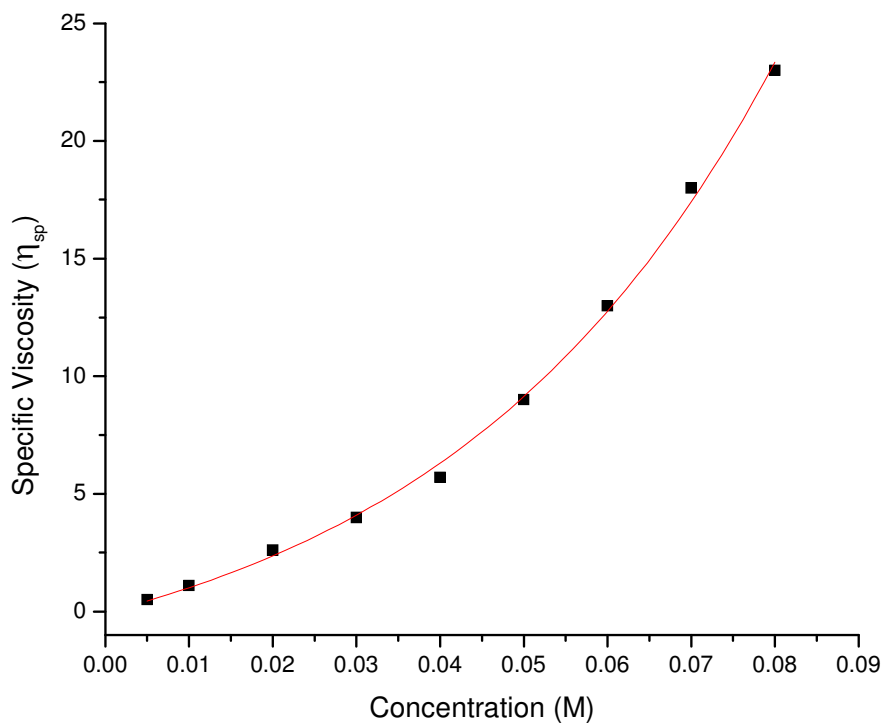


**Figure 4-11** Specific viscosity vs concentration for the 1:1 mixture of **60** and **59b** at room temperature.

#### 4.4 Summary

In summary, AA-BB ditopic supramolecular polymers based on double helical AAA-DDD hydrogen-bonded complexes have been prepared. Generally, there are three growth main mechanisms for supramolecular polymerization: isodesmic, cooperative and ring-chain supramolecular polymerizations. The self-assembly of ditopic AA-BB



monomers follows this mechanism of ring-chain supramolecular polymerization. The 1:1 ratio of bisAAA and bisDDD is a key for the formation of this kind of AA-BB supramolecular polymers. Specific viscosity experiments indicated that temperature and concentration of bisAAA and bisDDD have a large impact on the formation of the supramolecular polymer. When the bisAAA and bisDDD monomers contained the same length linkers, they easily formed macrocycles at low concentrations. A large linker-length difference resulted in the formation of supramolecular polymers at lower concentrations.

## 4.5 Experimental Section

Chemicals were purchased from Aldrich and used as received. All non-deuterated solvents were dried using an Innovative Technology solvent purification system SPS-400-5. Chromatography was performed on Merck 240-400 mesh silica gel-60.  $^1\text{H}$  and  $^{13}\text{C}$  NMR spectra were collected on a Varian Mercury 400 MHz spectrometer. Spectra are reported with residual solvent peak as reference from TMS. EI and CI ( $\text{CH}_4$ ) mass spectra were obtained on a Finnigan MAT 8200 mass spectrometer and ESI mass spectra were obtained using Micromass LCT instrumentation. Dynamic light scattering measurements were carried out with a Malvern Zeta Nano-S. A Cannon-Ubbelohde viscometer (size 50) was used to measure the viscosity.

Isothermal titration calorimetry experiments were carried out with a Microcal VP-ITC microcalorimeter. ITC experiment: 2 mM compound **57** in chloroform and 0.2 mM compound **60** in chloroform were prepared respectively. The solution of compound **57** was titrated into the solution of compound **60**. For the different ratio of bisAAA and

bisDDD in specific viscosity measurements, the initial concentrations for both bisAAA and bisDDD are 0.08 M.

Compounds **50** and **51** were synthesized according to the literature methods.<sup>43</sup>

General method for the synthesis of diazides: The mixture of sodium azide (25 mmol, 1.5 g) and dibromo alkane (10 mmol) in DMF (20 mL) was stirred at 70°C overnight. The reaction solution was added to water (200 mL) and extracted with diethyl ether (3× 50 mL). After the solvent was evaporated, pure diazide was obtained.

6-(4-methoxymethoxyphenyl)-2-tributyltinpyridine: The mixture of tributyl[4-(methoxymethoxy)phenyl]stannane<sup>48</sup> (2.06 g, 4.82 mmol), 2,6-dibromopyridine (1.11 g, 4.69 mmol) and Pd(PPh<sub>3</sub>)<sub>4</sub> (0.18g) in dry toluene was refluxed for 18h. The reaction solution was filtered through the celite and the filtrate was concentrated under reduced pressure. The crude product was recrystallized from ethanol to afford white solid (87% yield). <sup>1</sup>H NMR (400 MHz, CDCl<sub>3</sub>) δ ppm 7.94(d, *J*= 8.8 Hz, 2H), 7.63-7.54(m, 2H), 7.35(m, 1H), 7.12(d, *J*= 8.8 Hz, 2H), 5.23(s, 2H), 3.50(s, 3H); <sup>13</sup>C NMR (100 MHz, CDCl<sub>3</sub>) δ ppm 158.2, 142.0, 138.9, 134.7, 133.6, 128.3, 127.0, 125.6, 118.3, 116.3, 109.8, 94.3, 56.1; ESI-HRMS (*m/z*) calculated for C<sub>13</sub>H<sub>12</sub>BrNO<sub>2</sub> 293.0051, found 293.0049. To the solution of compound 12 (0.737 g, 2.5 mmol) in 10 mL dry THF at -78°C was added *n*-BuLi (2.5 M in hexane, 1.2 mL). After 2 h, tributyltin chloride (0.75 mL) was added dropwise. The reaction solution was stirred at -78°C for another 2 h and low-temperature bath was removed. The reaction was quenched with aqueous NH<sub>4</sub>Cl solution, and extracted with chloroform. The organic layer was dried over anhydrous

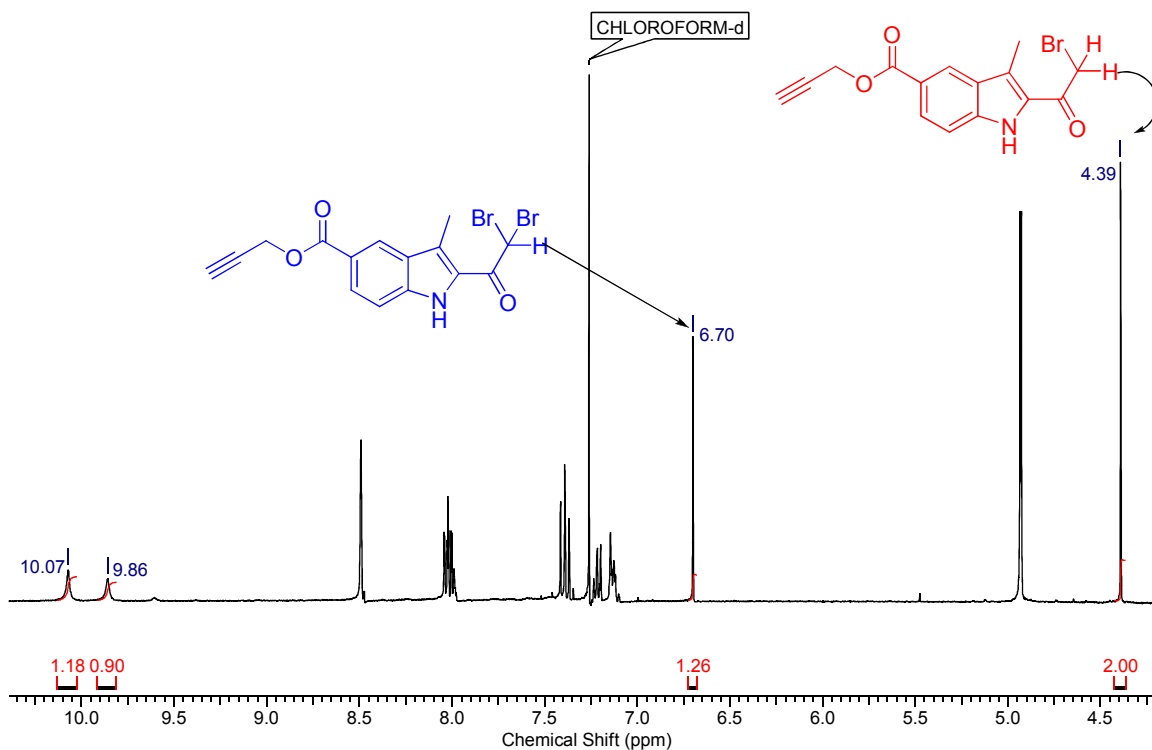
MgSO<sub>4</sub> and solvent was removed under reduced pressure. The crude product was not purified for further reactions.

**45:** Methyl 2-ethylacetoacetate (50 mmol, 7.2 g) and NaOH (4.0 g) were dissolved and stirred for 10 hours in a water/ethanol solution. The diazonium salt was prepared from 4-aminobenzoic acid (50 mmol, 6.85 g), concentrated HCl (60 mL) and aqueous solution of sodium nitrate (60 mmol, 4.3 g) in an ice bath according to the standard procedure. The diazonium salt was added to the pre-prepared sodium carboxylate solution at 0°C. The resulting solution was modified at pH 7-8 with sodium acetate and stirred at room temperature for 3 hours. The precipitate was collected, dried and refluxed in formic acid (100 mL) for 36 hours. Then the reaction solution was cooled down and diluted with water (500 mL). The precipitate was pure product (6.53 g, 61% yield). <sup>1</sup>H NMR (400 MHz, DMSO-d<sub>6</sub>) δ ppm 12.64(s, 1H), 11.76(s, 1H), 8.37(m, 1H), 7.86(m, 1H), 7.45 (m, 1H), 2.59(s, 3H), 2.58(s, 3H); <sup>13</sup>C NMR (100 MHz, DMSO-d<sub>6</sub>) δ ppm 190.7, 168.0, 138.4, 133.6, 127.6, 126.1, 123.8, 122.1, 119.1, 112.3, 29.1, 10.5; ESI-HRMS (m/z) calculated for C<sub>12</sub>H<sub>11</sub>NO<sub>3</sub> 217.0740, found 187.0743.

**46:** Compound 47 (3.56 g, 16 mmol) was dissolved in the mixture of DMF (20 mL) and THF (80 mL). To the reaction flask was 1-ethyl-3-(3-dimethylaminopropyl) carbodiimide (EDC, 1.64 g, 32 mmol). The reaction solution was stirred for 30 minutes, and then propargyl alcohol (1.8 g, 32 mmol) and DMAP (0.98 g, 8 mmol) was added. The reaction mixture was kept at this temperature overnight and poured into the ice/water solution. The collected precipitate was purified with chromatography to afford light yellow solid (3.2 g, 76% yield). <sup>1</sup>H NMR (400 MHz, DMSO-d<sub>6</sub>) δ ppm 11.85(s, 1H), 8.37(m, 1H),

7.86(m, 1H), 7.49 (m, 1H), 4.98(d,  $J=2.3$  Hz, 2H), 3.61(t,  $J=2.3$  Hz, 1H), 2.60(s, 3H), 2.58(s, 3H);  $^{13}\text{C}$  NMR (100 MHz, DMSO- $d_6$ )  $\delta$  ppm 190.7, 165.6, 138.7, 133.8, 127.6, 125.6, 124.0, 120.2, 119.1, 112.6, 78.8, 77.7, 52.1, 29.1, 10.4; ESI-HRMS ( $m/z$ ) calculated for  $\text{C}_{15}\text{H}_{13}\text{NO}_3$  255.0895, found 255.0894.

**47** and **47'**: Compound 48 (1.15 g, 4.5 mmol) was dissolved in dry THF (50 mL) and trimethylphenylammonium tribromide (1.6g, 4.5 mmol) was added. The reaction solution was refluxed for 1.5 hours and then cooled down to room temperature. The reaction solution was filtered through the celite and the filtrate was concentrated. The residue was extracted with dichloromethane and washed with water. The organic layer was dried over anhydrous  $\text{MgSO}_4$  and solvent was removed under reduced pressure. The product was the mixture of monobromo- and dibromo-indoles.



**48:** Since the bromination results in a mixed product, we started from compound 46 (7.0 g, 27.5 mmol). After the bromination and standard work-up, the solid dissolved in dry DMF (120 mL) and potassium thioacetate (3.14 g, 27.5 mmol) was added. The reaction solution was stirred overnight at a nitrogen atmosphere and then poured into the ice/water (600 mL). The precipitate was collected and dried.  $^1\text{H}$  NMR spectrum confirmed the only one thioacetate product.  $^1\text{H}$  NMR (400 MHz,  $\text{CDCl}_3$ )  $\delta$  ppm 9.30 (s, 1H), 8.53 (m, 1H), 8.06 (dd,  $J=9.0, 2.0$  Hz, 1H), 7.41 (d,  $J=9.0$  Hz, 1H), 4.97 (d,  $J=2.3$  Hz, 2H), 4.32 (s, 2H), 2.75 (s, 3H), 2.54 (t,  $J=2.3$  Hz, 1H), 2.45 (s, 3H). The solid in dry  $\text{CH}_3\text{CN}$  (250 mL) was degassed with nitrogen. Cysteamine hydrochloride (3.4 g, 30 mmol) and sodium bicarbonate (2.6 g, 31 mmol) were added. After 14 h, the reaction solution was acidified with dilute HCl at  $5^\circ\text{C}$ . When concentrated under reduced pressure, the residue was purified with flash chromatography, (two-step yield 47%).  $^1\text{H}$  NMR (400 MHz,  $\text{CDCl}_3$ )  $\delta$  ppm 9.15 (s, 1H), 8.53 (m, 1H), 8.06 (dd,  $J=8.6, 1.6$  Hz, 1H), 7.40 (d,  $J=8.2$  Hz, 1H), 4.96 (d,  $J=2.3$  Hz, 2H), 3.91 (d,  $J=7.4$  Hz, 2H), 2.70 (s, 3H), 2.53 (t,  $J=2.3$  Hz, 1H), 2.16 (t,  $J=7.4$  Hz, 1H). HRMS ( $m/z$ ) calculated for  $\text{C}_{15}\text{H}_{13}\text{NO}_3\text{S}$  287.0616, found 287.0611.

**49:** Compound 35d (2.8 g, 11.48 mmol) in dry  $\text{CH}_3\text{CN}$  (70 mL) and the mixture of 47 and 47' (10.3 mmol) in dry  $\text{CH}_3\text{CN}$  (90 mL) was degassed with nitrogen, respectively. The solution of 47 and 47' was dropwise added into the solution of compound 35d and then Triethylamine (1 mL) was added via syringe. The reaction mixture was stirred overnight and poured into the water (400 mL). The solution was acidified with citric acid and the precipitate was collected. The solid was crude product, which was purified with flash chromatography, 82% yield.  $^1\text{H}$  NMR (400 MHz,  $\text{DMSO}-d_6$ )  $\delta$  ppm 11.96 (s, 1H), 11.52 (s, 1H), 8.92 (s, 1H), 8.67 (1H), 8.42 (dd,  $J= 1.6, 8.6$  Hz, 1H), 8.11 (dd,  $J= 0.8, 8.6$

Hz, 1H), 8.01 (m, 2H), 5.45 (d,  $J= 2.3$  Hz, 2H), 5.06 (q,  $J= 6.6$  Hz, 1H), 4.72 (d,  $J= 16.0$  Hz, 1H), 4.62 (d,  $J= 16.0$  Hz, 1H), 3.57 (t,  $J= 2.3$  Hz, 1H), 3.17 (s, 3H), 3.14 (s, 3H), 2.07 (d,  $J= 6.6$  Hz, 3H);  $^{13}\text{C}$  NMR (100 MHz, DMSO- $d_6$ )  $\delta$  ppm 187.3, 165.7, 138.4, 136.4, 134.7, 132.5, 129.5, 128.4, 127.8, 125.3, 124.1, 121.5, 120.0, 113.4, 112.1, 111.5, 111.0, 100.0, 78.8, 77.6, 52.1, 40.1, 9.3, 9.1, 8.5; ESI-HRMS (m/z) calculated for  $\text{C}_{28}\text{H}_{23}\text{N}_3\text{O}_4\text{S}$  497.1409, found 497.1402.

**52:** Compound 51 (1.6 g) in glacial acetic acid (20 mL) was refluxed and 48% HBr in acetic acid (5 mL) was dropwise added. After 2 h, another 5 mL HBr was added. The reaction mixture was refluxed for 3 h. After cooled down to room temperature, the reaction mixture was poured into the ice/water and the solution was neutralized with 1 M NaOH solution. The precipitate is collected and purified with flash chromatography, 73% yield.  $^1\text{H}$  NMR (400 MHz,  $\text{CDCl}_3$ )  $\delta$  ppm 7.57 (s, 1H), 4.47 (s, 2H), 3.17 (s, 3H);  $^{13}\text{C}$  NMR (100 MHz,  $\text{CDCl}_3$ )  $\delta$  ppm 142.5, 141.8, 141.1, 135.3, 133.7, 30.4, 21.1. ESI-HRMS (m/z) calculated for  $\text{C}_7\text{H}_6\text{NBr}_3$  340.8050, found 340.8057.

**53:** To the solution of 3-hydroxybenzaldehyde (9 mmol, 1.1 g) in dry DMF (10 mL) was added NaH (0.36 g, 60% dispersion in mineral oil) and the mixture was stirred for 30 min at a nitrogen atmosphere. Then a solution of compound 52 (6 mmol, 2.06 g) in dry DMF (10 mL) was added dropwise. The reaction solution was stirred for 4 h and poured into the ice/water solution (150 mL). The precipitate is pure product and confirmed by the  $^1\text{H}$  NMR spectrum, 88% yield.  $^1\text{H}$  NMR (400 MHz,  $\text{CDCl}_3$ )  $\delta$  ppm 10.03(s, 1H), 7.99(s, 1H), 7.60 (m, 1H), 7.41(s, 1H), 5.22 (s, 2H), 2.39 (s, 3H). HRMS (m/z) calculated for  $\text{C}_{14}\text{H}_{11}\text{NBr}_2\text{O}_2$  382.9157, found 382.9163.

**54:** The mixture of 2-tributyltinpyridine (13.7 g, 37.3 mmol), 3,5-dimethyl-2,6-diiodopyridine (13.4 g, 37.3 mmol) and Pd(PPh<sub>3</sub>)<sub>4</sub> (1.39 g, 1.2 mmol) in toluene (300 mL) was refluxed under nitrogen atmosphere for 18 h. The reaction solution was filtered through the celite and the filtrate was concentrated under reduced pressure. The crude product was purified with flash chromatography (chloroform) to afford light yellow solid (8.4 g, 73% yield). <sup>1</sup>H NMR (400 MHz, CDCl<sub>3</sub>) δ ppm 8.64(d, *J* = 4.8 Hz, 1H), 7.86(d, *J* = 7.9 Hz, 1H), 7.79(dd, *J* = 7.9, 4.7 Hz, 1H), 7.35(s, 1H), 7.27(m, 1H), 2.46(s, 3H), 2.39(s, 3H); <sup>13</sup>C NMR (100 MHz, CDCl<sub>3</sub>) δ ppm 154.7, 148.2, 140.3, 138.3, 136.5, 135.9, 132.0, 124.3, 122.7, 120.7, 25.6, 19.3; HRMS (*m/z*) calculated for C<sub>12</sub>H<sub>11</sub>N<sub>2</sub>I 309.9967, found 309.9965.

**55:** The mixture of 6-(4-methoxymethoxyphenyl)-2-tributyltinpyridine (1.569 g, 3.1 mmol), compound 54 (0.965 g, 3.1 mmol) and Pd(PPh<sub>3</sub>)<sub>4</sub> (0.12 g, 0.1 mmol) in toluene (10 mL) was refluxed under nitrogen atmosphere for 24 h. The reaction solution was filtered through the celite and the filtrate was concentrated under reduced pressure. The crude product was purified with flash chromatography, 61% yield. <sup>1</sup>H NMR (400 MHz, CDCl<sub>3</sub>) δ ppm 8.66(m, 1H), 8.04(d, *J* = 9.0 Hz, 2H), 7.96-7.93(m, 2H), 7.81- 7.75(m, 2H), 7.66- 7.63(m, 1H), 7.53(s, 1H), 7.25-7.23(m, 2H), 7.14(d, *J* = 9.0 Hz, 2H), 5.21(s, 2H), 3.48(s, 3H), 2.72(s, 3H), 2.57(s, 3H); <sup>13</sup>C NMR (100 MHz, CDCl<sub>3</sub>) δ ppm 159.0, 158.6, 157.8, 154.9, 152.6, 148.0, 142.8, 137.1, 136.3, 133.2, 132.0, 131.7, 128.0, 124.2, 122.2, 122.0, 118.1, 116.1, 94.2, 55.9, 20.4, 19.6, 14.1; HRMS (*m/z*) calculated for C<sub>25</sub>H<sub>23</sub>N<sub>3</sub>O<sub>2</sub> 397.1790, found 397.1786.

**56:** Compound 55 (0.633 g, 1.6 mmol) in 1M HCl (4 ml) was stirred at room temperature for 24 h and the yield is 94%.  $^1\text{H}$  NMR (400 MHz,  $\text{CDCl}_3$ )  $\delta$  ppm 8.66(m, 1H), 8.04(d,  $J=9.0$  Hz, 2H), 7.96-7.93(m, 2H), 7.81- 7.75(m, 2H), 7.66- 7.63(m, 1H), 7.53(s, 1H), 7.25-7.23(m, 2H), 7.14(d,  $J=9.0$  Hz, 2H), 2.72(s, 3H), 2.57(s, 3H);  $^{13}\text{C}$  NMR (100 MHz,  $\text{CDCl}_3$ )  $\delta$  ppm 158.5, 158.0 157.5, 155.7, 153.4, 152.8, 148.1, 142.6, 137.1, 132.5, 131.7, 131.0, 128.1, 124.7, 122.8, 121.7, 118.2, 115.7, 20.2, 19.2; HRMS (m/z) calculated for  $\text{C}_{23}\text{H}_{19}\text{N}_3\text{O}$  353.1528, found 353.1534.

**57:** Compound 56 (5.66 mmol, 2.0 g) was dissolved in dry DMF (20 mL) and potassium carbonate (8.49 mmol, 1.17 g) was added. Propargyl bromide (80% in toluene, 6.08 mmol) was added via syringe. The reaction mixture was stirred for 6 h and then poured into the ice/water (200 mL). The precipitate was collected and washed with water to afford the pure product, yield 91%.  $^1\text{H}$  NMR (400 MHz,  $\text{CDCl}_3$ )  $\delta$  ppm 8.68 (m, 1H), 8.06 (d,  $J=8.8$  Hz, 2H), 7.96-7.93 (m, 2H), 7.84- 7.79(m, 2H), 7.68 (d,  $J=7.0$  Hz, 1H), 7.56 (s, 1H), 7.29-7.27 (m, 2H), 7.08 (d,  $J=8.8$  Hz, 2H), 4.76 (d,  $J=2.3$  Hz, 2H), 2.73 (s, 3H), 2.58 (s, 3H), 2.55 (t,  $J=2.3$  Hz, 1H);  $^{13}\text{C}$  NMR (100 MHz,  $\text{CDCl}_3$ )  $\delta$  ppm 158.5, 158.0, 157.5, 155.7, 153.4, 152.8, 148.1, 142.6, 137.1, 132.5, 131.7, 131.0, 128.1, 124.7, 122.8, 121.7, 118.2, 115.7, 20.2, 19.2; HRMS (m/z) calculated for  $\text{C}_{26}\text{H}_{21}\text{N}_3\text{O}$  391.1658, found 391.1681.

**58:** To the solution of compound 49 (1.2 g, 2.41 mmol) in dry DMF (15 mL) at  $-20^\circ\text{C}$  was added the solution of m-CPBA in dry DMF (10 mL). The reaction mixture was stirred overnight and reaction temperature slowly increased to room temperature. The reaction solution was poured into the ice/water (100 mL) and basified with aqueous



$\text{Na}_2\text{SO}_3$ . The precipitate was collected and dried. The solid and ammonium acetate (1.5g) in glacial acetic acid (20 mL) was refluxed for two days. The reaction solution was poured into the ice/water (100 mL) and the precipitate was collected. The crude product was purified with flash chromatography, 74% yield.  $^1\text{H}$  NMR (400 MHz,  $\text{DMSO-}d_6$ )  $\delta$  ppm 11.73 (s, 1H), 11.55 (s, 1H), 10.67 (s, 1H), 8.30 (s, 1H), 7.85-7.81 (m, 2H), 7.51 (d,  $J=8.6$  Hz, 1H), 7.39 (d,  $J=8.6$  Hz, 1H), 7.31 (dd,  $J=8.6, 2.0$  Hz, 1H), 6.28 (s, 1H), 4.97 (d,  $J=2.7$  Hz, 2H), 3.61 (t,  $J=2.7$  Hz, 1H), 2.48 (s, 3H), 2.26 (s, 3H), 1.95 (s, 3H);  $^{13}\text{C}$  NMR (100 MHz,  $\text{DMSO-}d_6$ )  $\delta$  ppm 170.1, 165.8, 138.5, 136.4, 134.7, 132.5, 129.5, 128.4, 127.8, 125.3, 124.1, 121.5, 120.0, 113.4, 112.1, 111.5, 111.0, 100.0, 78.8, 77.7, 52.1, 9.3, 9.1, 8.5; HRMS (m/z) calculated for  $\text{C}_{28}\text{H}_{22}\text{N}_4\text{SO}_4$  510.1362, found 510.1368.

**59:** Compound 58 (2.9 g, 5.69 mmol) and diazide (2.8 mmol) were dissolved in THF (40 mL), followed by addition of sodium ascorbate (0.22 g). An aqueous solution (8 ml) of  $\text{CuSO}_4 \cdot 5\text{H}_2\text{O}$  (0.3 g) was added dropwise into the reaction solution which was stirred overnight at  $50^\circ\text{C}$ . The reaction solution was poured into the ice/water (120 mL) and the precipitate was collected. The crude product was purified with flash chromatography.

**59a:** 61% yield.  $^1\text{H}$  NMR (400 MHz,  $\text{DMSO-}d_6$ )  $\delta$  ppm  $^1\text{H}$  NMR (400 MHz,  $\text{DMSO-}d_6$ )  $\delta$  ppm 11.77 (s, 1H), 11.54 (s, 1H), 10.66 (s, 1H), 8.29 (s, 1H), 8.01 (s, 1H) 7.85-7.81 (m, 2H), 7.51 (d,  $J=8.6$  Hz, 1H), 7.39 (d,  $J=8.6$  Hz, 1H), 7.31 (dd,  $J=8.6, 2.0$  Hz, 1H), 6.28 (s, 1H), 5.35 (s, 2H), 4.11 (t,  $J=6.8$  Hz, 2H), 2.48 (s, 3H), 2.26 (s, 3H), 1.95 (s, 3H), 1.85 (q,  $J=6.8$  Hz, 2H), 1.54 (m, 2H), 1.36 (m, 6H). TOF-MS calculated for  $\text{C}_{68}\text{H}_{68}\text{N}_{14}\text{O}_8\text{S}_2$  1272.5, found 1274.2.

**59b:** 57% yield.  $^1\text{H}$  NMR (400 MHz,  $\text{DMSO-}d_6$ )  $\delta$  ppm 11.73 (s, 1H), 11.55 (s, 1H), 10.67 (s, 1H), 8.30 (s, 1H), 8.11 (s, 1H), 7.82-7.84 (m, 2H), 7.41 (d,  $J=8.6\text{ Hz}$ , 1H), 7.36 (d,  $J=8.6\text{ Hz}$ , 1H), 7.34 (dd,  $J=8.6, 2.0\text{ Hz}$ , 1H), 6.29 (s, 1H), 5.17 (s, 2H), 4.14 (t,  $J=6.7\text{ Hz}$ , 2H), 2.48 (s, 3H), 2.26 (s, 3H), 1.95 (s, 3H), 1.41 (m, 2H). TOF-MS calculated for  $\text{C}_{60}\text{H}_{52}\text{N}_{14}\text{O}_8\text{S}_2$  1160.3, found 1161.4.

**60:** The mixture of compound 56 (0.6 g, 1.7 mmol), potassium carbonate (0.55 g, 4 mmol), potassium iodide (0.14 g, 0.84 mmol) and dibromododecane (0.28 g, 0.84 mmol) in dry DMF (10 mL) was stirred overnight at  $90^\circ\text{C}$  at a nitrogen atmosphere. The reaction solution was poured into the ice/water (80 mL). The precipitate was collected to afford the pure product, 86% yield.  $^1\text{H}$  NMR (400 MHz,  $\text{CDCl}_3$ )  $\delta$  ppm 8.68 (d,  $J=4.3\text{ Hz}$ , 2H), 8.03 (d,  $J=4.3\text{ Hz}$ , 4H), 7.92 (m, 4H), 7.81 (m, 4H), 7.66 (d,  $J=7.8\text{ Hz}$ , 2H), 7.55 (s, 2H), 7.28 (m, 2H), 6.99 (d,  $J=9.0\text{ Hz}$ , 4H), 4.01 (t,  $J=6.6\text{ Hz}$ , 4H), 2.72 (s, 6H), 2.57 (s, 6H), 1.81 (q,  $J=6.6\text{ Hz}$ , 4H), 1.47 (m, 4H), 1.30 (m, 12H);  $^{13}\text{C}$  NMR (100 MHz,  $\text{CDCl}_3$ )  $\delta$  ppm 158.5, 158.0, 157.5, 155.7, 153.4, 152.8, 148.1, 142.6, 137.1, 132.5, 131.7, 131.0, 128.1, 124.7, 122.8, 121.7, 118.2, 115.7, 74.3, 29.4, 26.7, 20.2, 19.2; MS ( $m/z$ ) calculated for  $\text{C}_{58}\text{H}_{60}\text{N}_6\text{O}_2$  872.5, found 873.6.

## 4.6 References

1. (a) Folmer, B. J. B.; Sijbesma, R. P.; Versteegen, R. M.; van der Rijt, J. A. J.; Meijer, E. W. *Adv. Mater.* **2000**, *12*, 874. (b) Lehn, J. -M. *Polym. Int.* **2002**, *51*, 825. (c) Bosman, A. W.; Brunsveld, L.; Folmer, B. J. B.; Sijbesma, R. P.; Meijer, E. W. *Macromol. Symp.* **2003**, *201*, 143. (d) Harada, A.; Takashima, Y.; Yamaguchi, H. *Chem. Soc. Rev.* **2009**, *38*, 875. (e) De Greef, T. F.; Smulders, M. M. J.; Wolffs, M.;

- Schenning, A. P. H. J.; Sijbesma, R. P.; Meijer, E. W. *Chem. Rev.* **2009**, *109*, 5687.
- (f) Fox, J. D.; Rowan, S. J. *Macromolecules* **2009**, *42*, 6823. (g) Bergman, S. D.; Wudl, F. *J. Mater. Chem.* **2008**, *18*, 41.
2. (a) Lehn, J. -M. *Supramolecular Chemistry: concepts and perspectives*; Wiley-VCH: Weinheim, **1995**. (b) Brunsveld, L.; Folmer, B. J. B.; Meijer, E. W.; Sijbesma, R. P. *Chem. Rev.* **2001**, *101*, 4071. (c) Ciferri, A. *Supramolecular Polymers*; Marcel Dekker: New York, **2000**.
3. (a) Glusker, J. P. *Top Curr. Chem.* **1998**, *198*, 1. (b) Tessa ten Cate, A.; Sijbesma, R. P. *Macromol. Rapid Commun.* **2002**, *23*, 1094. (c) Wilson, A. J. *Soft Matter* **2007**, *3*, 409.
4. de Greef, T. F. A.; Meijer, E. W. *Nature* **2008**, *453*, 171.
5. (a) Yamauchi, K. Lizotte, J. R.; Hercules, D. M.; Vergne, M. J.; Long, T. E. *J. Am. Soc. Chem.* **2002**, *124*, 8599. (b) Yamauchi, K.; Kanomata, A.; Inoue, T.; Long, T. E. *Macromolecules* **2004**, *37*, 3519.
6. Saadeh, H.; Wang, L.; Yu, L. *J. Am. Soc. Chem.* **2000**, *122*, 546.
7. Reith, R. L.; Eaton, F. R.; Coates, W. G. *Angew. Chem. Int. Ed.* **2001**, *40*, 2153.
8. Shandryuk, G. A.; Kuptsov, S. A.; Shatalova, A. M.; Plate, N. A.; Talroze, R. V. *Macromolecules* **2003**, *36*, 3417.
9. Ilhan, F.; Gray, M.; Rotello, V. M. *Macromolecules* **2001**, *34*, 2597.
10. Thibault, R. J.; Hotchkiss, P. J.; Gray, M.; Rotello, V. M. *J. Am. Soc. Chem.* **2003**, *125*, 11249.

11. Yamauchi, K.; Lizotte, J. R.; Hercules, D. M.; Vergne, M. J.; Long, T. E. *J. Am. Soc. Chem.* **2002**, *124*, 8599.
12. Lange, R. F. M.; van Gorp, M.; Meijer, E. W. *J. Polym. Sci. Part A. Polym. Chem.* **1999**, *37*, 3657.
13. Liu, G.; Guan, C.; Xia, H.; Guo, F.; Ding, X.; Peng, Y. *Macromol. Rapid Commun.* **2006**, *27*, 1100.
14. Gulik-Krzywicki, T.; Fouquey, C.; Lehn, J. -M. *Proc. Natl. Acad. Sci. USA* **1993**, *90*, 163.
15. Khan, A.; Haddleton, D. M.; Hannon, M. J.; Kukulj, D.; Marsh, A. *Macromolecules* **1999**, *32*, 6560.
16. Kugimiya, A.; Mukawa, T.; Takeuchi, T. *Analyst* **2001**, *126*, 772.
17. Wang, L.; Fu, Y.; Wang, Z.; Fan, Y.; Zhang, X. *Langmuir* **1999**, *15*, 1360.
18. Huggins, K. E.; Son, S.; Stupp, S. I. *Macromolecules* **1997**, *30*, 5305.
19. Whitesides, G. M.; Simanee, E. E.; Mathias, J. P.; Seto, C. T.; Chin, D. N.; Mammen, M.; Gordon, D. M. *Acc. Chem. Res.* **1995**, *28*, 37 and references therein.
20. Theobald, J. A.; Oxtoby, N. S.; Philips, M. A.; Champness, N. R.; Beton, P. H. *Nature* **2003**, *424*, 1029.
21. Würthner, F.; Thalacker, C.; Sautter, A. *Adv. Mater.* **1999**, *11*, 754.
22. Yagai, S.; Higashi, M.; Karatsu, T.; Kitamura, A. *Chem. Mater.* **2004**, *16*, 3582.
23. Beijer, F. H.; Sijbesma, R. P.; Vekemans, J. M.; Meijer, E. W.; Kooijman, H.; Spek, A. L. *J. Org. Chem.* **1996**, *61*, 6371.

24. (a) Binder, W. H.; Kunz, M. J.; Ingolic, E. *J. Polym. Sci. A Polym. Chem.* **2004**, *42*, 162. (b) Kunz, M. J.; Hayn, G.; Saf, R.; Binder, W. H. *J. Polym. Sci. A Polym. Chem.* **2004**, *42*, 661.
25. Tazawa, T.; Yagai, S.; Kikkawa, Y.; Karatsu, T.; Kitamura, A.; Ajayaghosh, A. *Chem. Commun.* **2010**, *46*, 1076.
26. (a) Wang, X. -Z.; Li, X. -Q.; Shao, X. -B.; Zhao, X.; Deng, P.; Jiang, X. -K.; Li, Z. -T.; Chen, Y. -Q. *Chem. Eur. J.* **2003**, *9*, 2904. (b) Zhao, X.; Wang, X. -Z.; Jiang, X. -K.; Chen, Y. -Q.; Li, Z. -T.; Chen, G. -J. *J. Am. Chem. Soc.* **2003**, *125*, 15128. (c) Li, X. -Q.; Jiang, X. -K.; Wang, X. -Z.; Li, Z. -T. *Tetrahedron* **2004**, *60*, 2063. (d) Li, X. -Q.; Feng, D. -J.; Jiang, X. -K.; Li, Z. -T. *Tetrahedron* **2004**, *60*, 8275.
27. Ligthart, G. B. W. L.; Ohkawa, H.; Sijbesma, R. P.; Meijer, E. W. *J. Am. Chem. Soc.* **2005**, *127*, 810.
28. De Greef, T. F. A.; Ercolani, G.; Ligthart, G. B. W. L.; Meijer, E. W.; Sijbesma, R. P. *J. Am. Chem. Soc.* **2008**, *130*, 13755.
29. (a) Park, T.; Zimmerman, S. C.; Nakashima, S. *J. Am. Chem. Soc.* **2005**, *127*, 6520. (b) Park, T.; Zimmerman, S. C. *J. Am. Chem. Soc.* **2006**, *128*, 11582. (c) Park, T.; Zimmerman, S. C. *J. Am. Chem. Soc.* **2006**, *128*, 13986. (d) Park, T.; Zimmerman, S. C. *J. Am. Chem. Soc.* **2006**, *128*, 14236.
30. Lehn, J. -M.; Mascal, M.; DeCian, A.; Fischer, J. *J. Chem. Soc., Chem. Commun.* **1990**, 479.
31. Kawasaki, T.; Tokuhira, M.; Kimizuka, N.; Kunitake, T. *J. Am. Chem. Soc.* **2001**, *123*, 6792.

32. Choi, I. S.; Li, X.; Simanek, E. E.; Akaba, R.; Whitesides, G. M. *Chem. Mater.* **1999**, *11*, 684.
33. Klok, H.-A.; Jolliffe, K. A.; Schauer, C. L.; Prins, L. J.; Spatz, J. P.; Moller, M.; Timmerman, P. Reinhoudt, D. N. *J. Am. Chem. Soc.* **1999**, *121*, 7154.
34. (a) Chang, S. K.; Hamilton, A. D. *J. Am. Chem. Soc.* **1988**, *110*, 1318. (b) Chang, S. K.; van Engen, D.; Hamilton, A. D. *J. Am. Chem. Soc.* **1991**, *113*, 7640.
35. Berl, V.; Schmutz, M.; Krische, M. J.; Khoury, R. G.; Lehn, J. -M. *Chem. Eur. J.* **2002**, *8*, 1227.
36. Ciesielski, A.; Schaeffer, G.; Petitjean, A.; Lehn, J. -M.; Samori, P. *Angew. Chem. Int. Ed.* **2009**, *48*, 2039.
37. Lehn, J. -M. *Chem. Soc. Rev.* **2007**, *36*, 151.
38. Kolomiets, E.; Lehn, J. -M. *Chem. Commun.* **2005**, 1519.
39. (a) Zeng, H. Q.; Miller, R. S.; Flowers, R. A.; Gong, B. *J. Am. Chem. Soc.* **2000**, *122*, 2635. (b) Zeng, H. Q.; Yang, X. W.; Flowers, R. A.; Gong, B. *J. Am. Chem. Soc.* **2002**, *124*, 2903. (c) Yang, X. W.; Martinovic, S.; Smith, R. D.; Gong, B. *J. Am. Chem. Soc.* **2003**, *125*, 9932.
40. Yang, X.; Hua, F.; Yamato, K.; Ruckenstein, E.; Gong, B.; Kim, W.; Ryu, C. Y. *Angew. Chem. Int. Ed.* **2004**, *43*, 6471.
41. Xu, J.; Fogleman, E. A.; Craig, S. L. *Macromolecules* **2004**, *37*, 1863.
42. There is a special issue for click chemistry and its application in *Chem. Soc. Rev.*, **2010**, *39*, 1231-1388.

43. (a) Vanlaer, S.; De Borggraeve, W. M.; Compennolle, F. *Eur. J. Org. Chem.* **2007**, 4995. (b) Meerpoel, L.; Hoornaert, G. J. *Synthesis* **1990**, 905.
43. (a) Scherman, O. A.; Ligthart, G. B. W. L.; Sijbesma, R. P.; Meijer, E. W. *Angew. Chem. Int. Ed.* **2006**, *45*, 2072. (b) Chen, C. -C.; Dormidontova, E. E. *Macromolecules* **2004**, *37*, 3905.
44. ten Cate, A T.; Kooijman, H.; Spek, A. L.; Sijbesma, R. P.; Meijer, E. W. *J. Am. Chem. Soc.* **2004**, *126*, 3801.
45. (a) Obert, E.; Bellot, M.; Bouteiller, L.; Andrioletti, F.; Lehen-Ferrenbach, C.; Boue, F. *J. Am. Chem. Soc.* **2007**, *129*, 15601. (b) Yoshikawa, I.; Sawayama, J.; Araki, K. *Angew. Chem. Int. Ed.* **2008**, *47*, 1038. (c) de Greef, T. F. A.; Nieuwenhuizen, M. M. L.; Stals, P. J. M.; Fitié, C. F. C.; Palmans, A. R. A.; Sijbesma, R. P.; Meijer, E. W. *Chem. Commun.* **2008**, 4306.
46. (a) Gibson, H. W.; Yamaguchi, N.; Jones, J. W. *J. Am. Chem. Soc.* **2003**, *125*, 3522. (b) Yamaguchi, N.; Gibson, H. W. *J. Chem. Soc., Chem. Commun.* **1999**, 789.
47. (a) Gates, M. E. *Macromolecules* **1987**, *20*, 2289. (b) Huang, F.; Nagvekar, D. S.; Gibson, H. W. *Macromolecules* **2007**, *40*, 3561.
48. Morita, Y.; Kashiwagi, A.; Nakasuji, K. *J. Org. Chem.* **1997**, *62*, 7464.

## CHAPTER 5

### Conclusion and Outlook

#### 5.1 Conclusion

Previous work has determined that the influence of secondary interactions in non-coplanar hydrogen-bonded structures renders the AAA/DDD array as the most stable among the three possible configurations (AAD-DDA, ADA/DAD and AAA/DDD). We have developed a new kind of non-coplanar AAA/DDD (**7/11**) [pyridine-lutidine-pyridine/tri(thiazine dioxide)] hydrogen-bonded system. Although the single crystal structure confirmed the formation of a complementary double helical complex, the DDD component was not soluble in chloroform. In the meanwhile, the crystal structure of analogous DDD **16** based on indole-thiazine dioxide-indole provided a reason that both **7** and **16** are not soluble in chloroform, namely, intermolecular hydrogen bonding. The modification of **16** (addition of a methyl group to the thiazine dioxide subunit) may block intermolecular hydrogen bonds and resulted in the soluble DDD **28**.  $^1\text{H}$  NMR titrations indicated that the association constant of **28/11** was only  $3700 \text{ M}^{-1}$ .

Secondly, how substituent groups affect the binding stability of hydrogen-bonded AAA/DDD complexes was investigated. It was demonstrated that electron withdrawing groups on the DDD component and/or electron donating groups on AAA component enhance the binding stability of non-coplanar AAA/DDD hydrogen-bonded complexes. The complex stabilities can be manipulated over more than three orders of magnitude ( $>20 \text{ kJ mol}^{-1}$ ) using both electron withdrawing groups on DDD component and/or



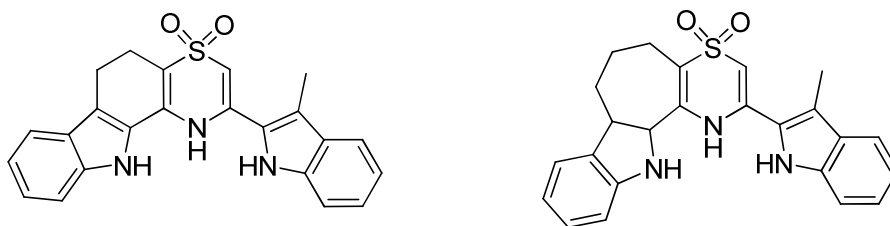
electron donating groups on AAA part. From the Hammett plots, the magnitude of the effect of electron withdrawing groups on DDD component is almost identical to that of electron donating groups on AAA part. However, there was no so-called “enthalpy-entropy compensation” in our AAA/DDD system. In addition, substituent groups appear to modify both the molecular electronic properties and conformations of AAA and DDD components.

Ultimately, a DDD component including electron withdrawing groups (cyano and ester) and an AAA array (the simple pyridine-lutidine-pyridine array) yielded a high enough association constant ( $K_a > 10^5 \text{ M}^{-1}$ ) to be used as the hydrogen bond motifs in a potential main-chain supramolecular polymer. Thus, one bisAAA and two bisDDD monomers were prepared. Specific viscosity and dynamic light scattering indicated the formation of main-chain supramolecular polymers based on mixtures of bisAAA and bisDDD monomers. An equivalent molar ratio of bisAAA and bisDDD is very important for the formation of supramolecular polymers. Although this supramolecular polymerization still follows a ring-chain polymerization, institution of different-length linkers in the bisAAA and bisDDD monomers affects the critical polymerization concentration.

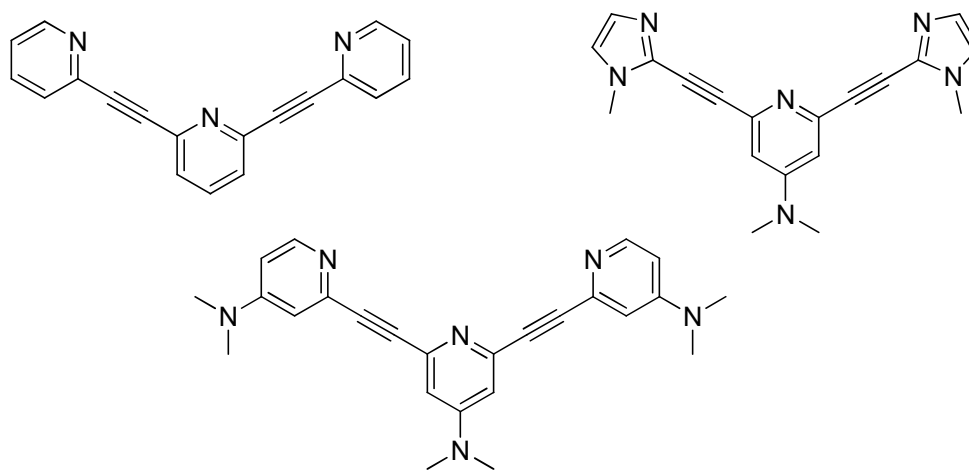
In conclusion, we have constructed complementary double helical architectures and applied these highly stable complexes ( $K_a > 10^5 \text{ M}^{-1}$ ) as hydrogen-bonded motifs for main-chain supramolecular polymers.

## 5.2 Outlook

The three heterocyclic subunits are not fixed in the DDD structure and thus it is not pre-organized. Because a pre-organized DDD would provide much more stable double helical complexes, the three subunits should be fixed to obtain a pre-organized structure. However, from the view of organic synthesis, it is impossible to fix all three subunits including two indole and one thiazine rings. Therefore, only two of three subunits may be fixed with a ring. Considering that ring size possibly affects the conformation, we designed two different rings: six-member ring and seven-member ring for pre-organized DDD molecules in Scheme 5-1.



**Scheme 5-1** Pre-organized DDD arrays.



**Scheme 5-2** Potential AAA arrays including spacers.

Following the induced-fit principle, AAA and DDD components form the double helical structures. We may be able to put a spacer between each pyridine ring to develop a new kind of AAA array (Scheme 5-2). The synthesis of this kind of oligomers is known and straightforward. AAA components including the excellent hydrogen bond acceptor 1-methylimidazole might even be synthesized.

Supramolecular polymers were formed from hydrogen-bonded AAA/DDD complexes and there are a lot of opportunities for further studies. For example, two polymers including DDD and AAA side functional groups respectively could be coated on two different surfaces, which might stick together because of strong complementary hydrogen bonds. Because the AAA-DDD complex is complementary, it is easy to make AB-type main-chain supramolecular polymers via dynamic covalent chemistry such as imines. However, if the supramolecular polymers are to be commercialized, simpler and more easily synthesized hydrogen-bonded systems should be developed.

## Appendices

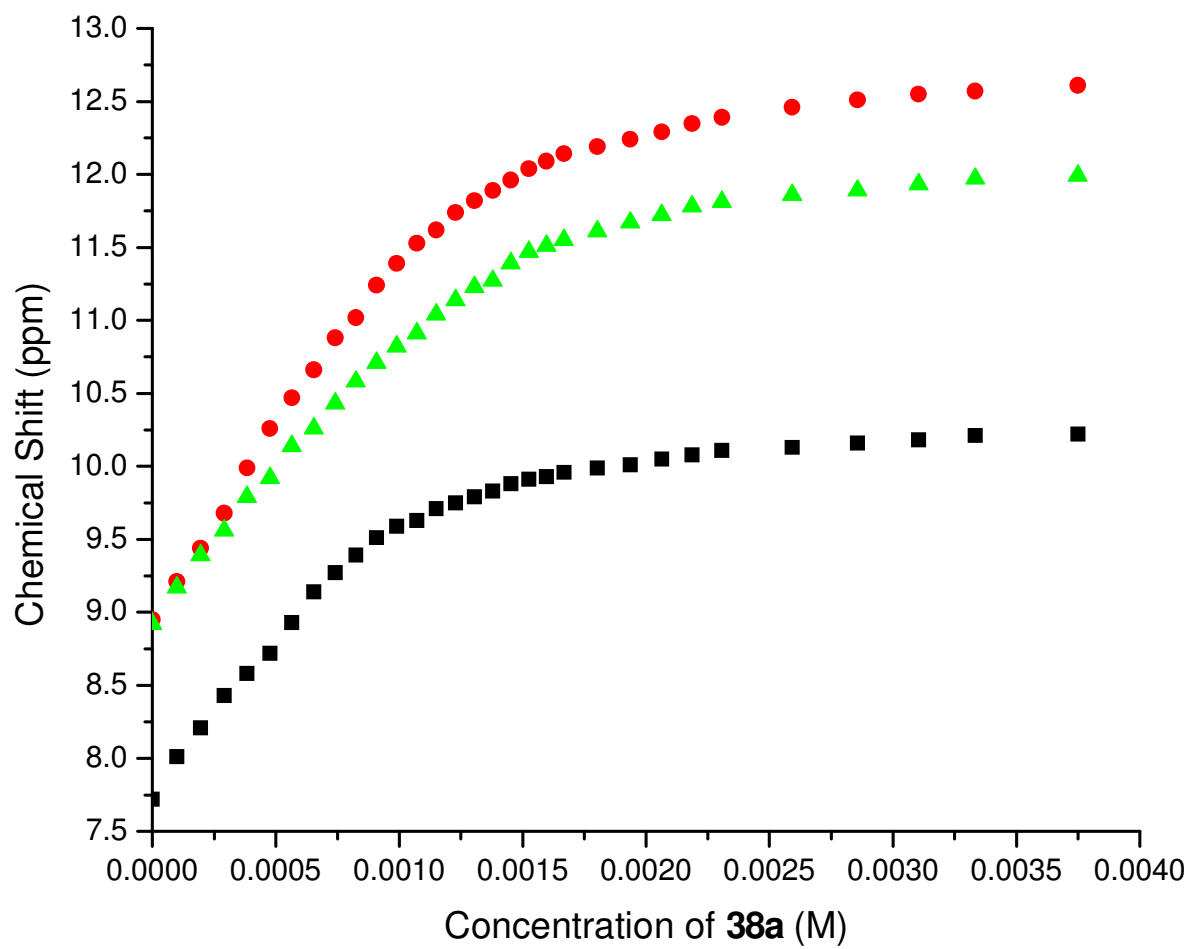


**Figure A-1**  $^1\text{H}$  NMR titration curve of **38a** and **11** in  $\text{CDCl}_3$  at 298K.

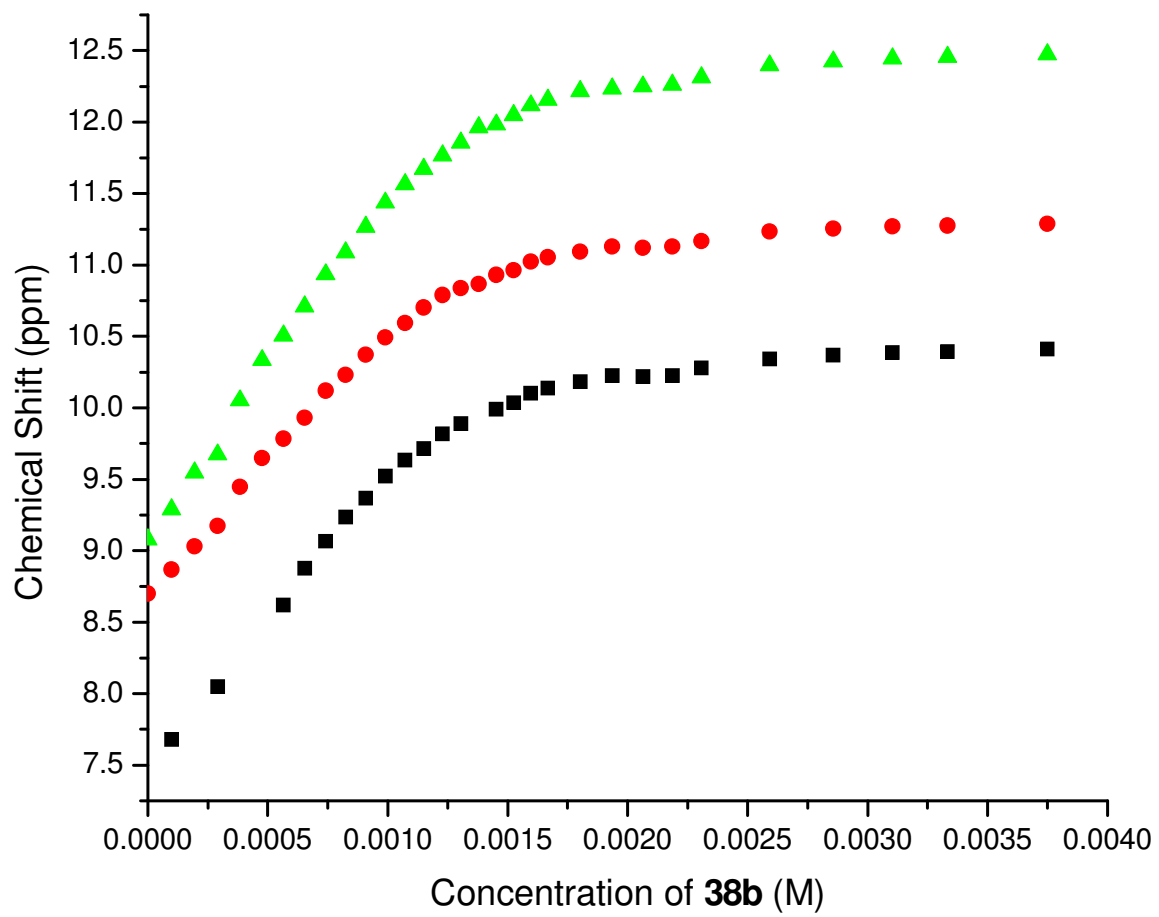


**Figure A-2**  $^1\text{H}$  NMR titration curve of **38b** and **11** in  $\text{CDCl}_3$  at 298K.

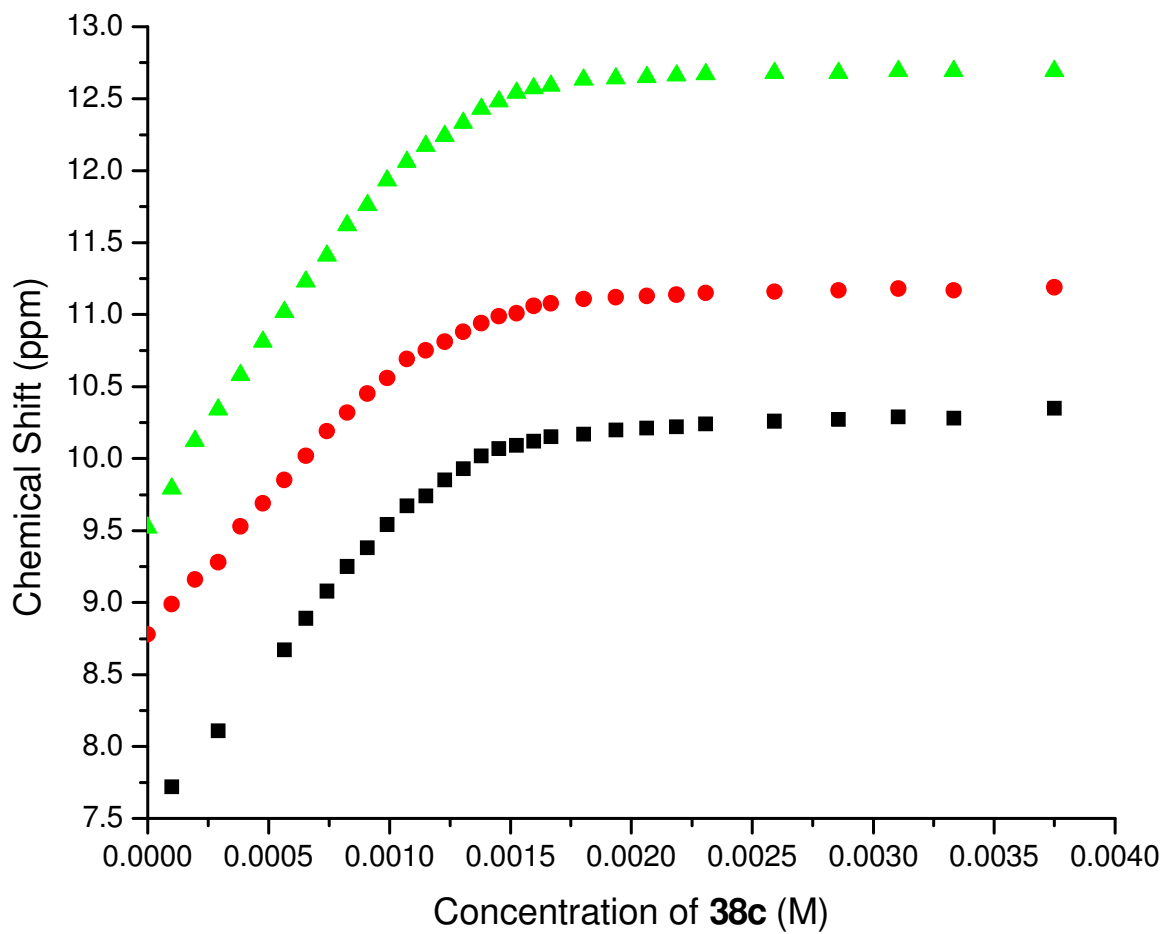


**Figure A-3**  $^1\text{H}$  NMR titration curve of **38c** and **11** in  $\text{CDCl}_3$  at 298K.

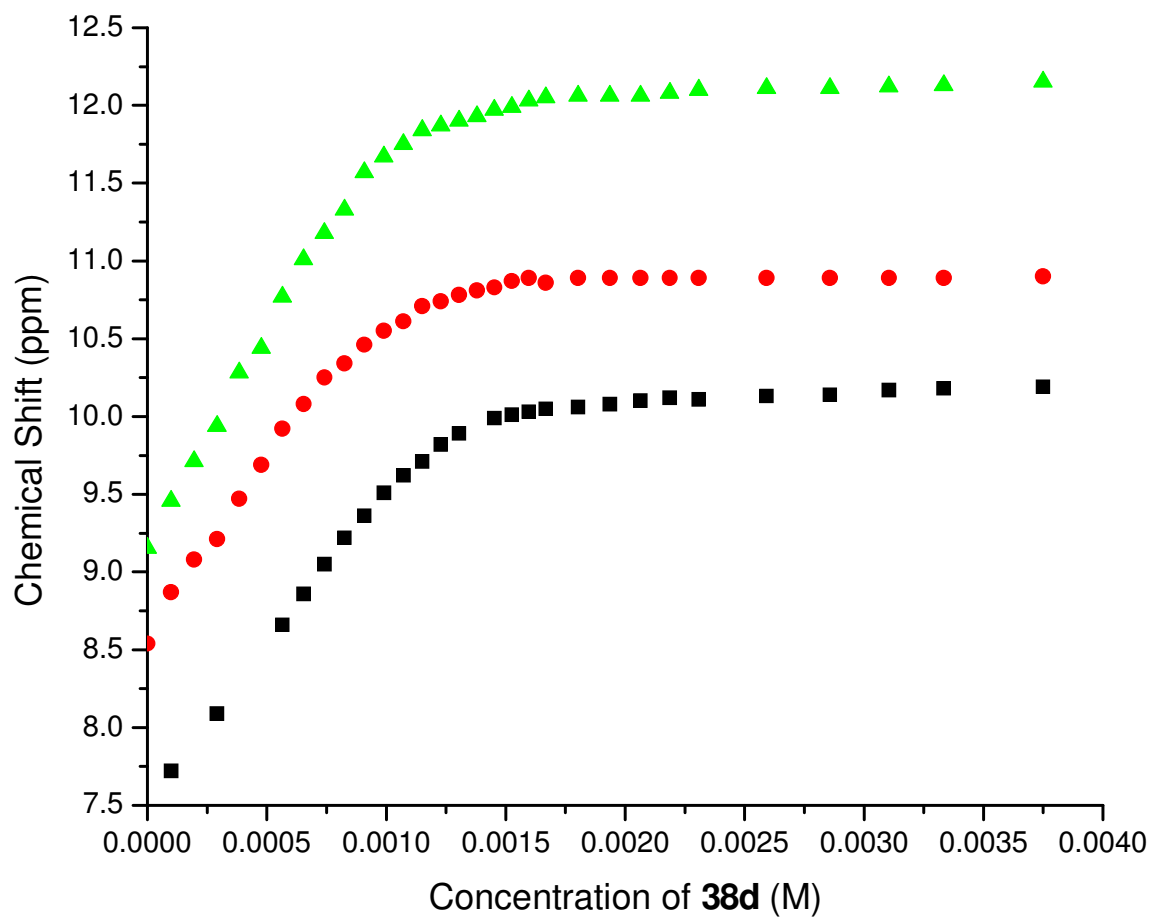


**Figure A-4**  $^1\text{H}$  NMR titration curve of **38d** and **11** in  $\text{CDCl}_3$  at 298K.

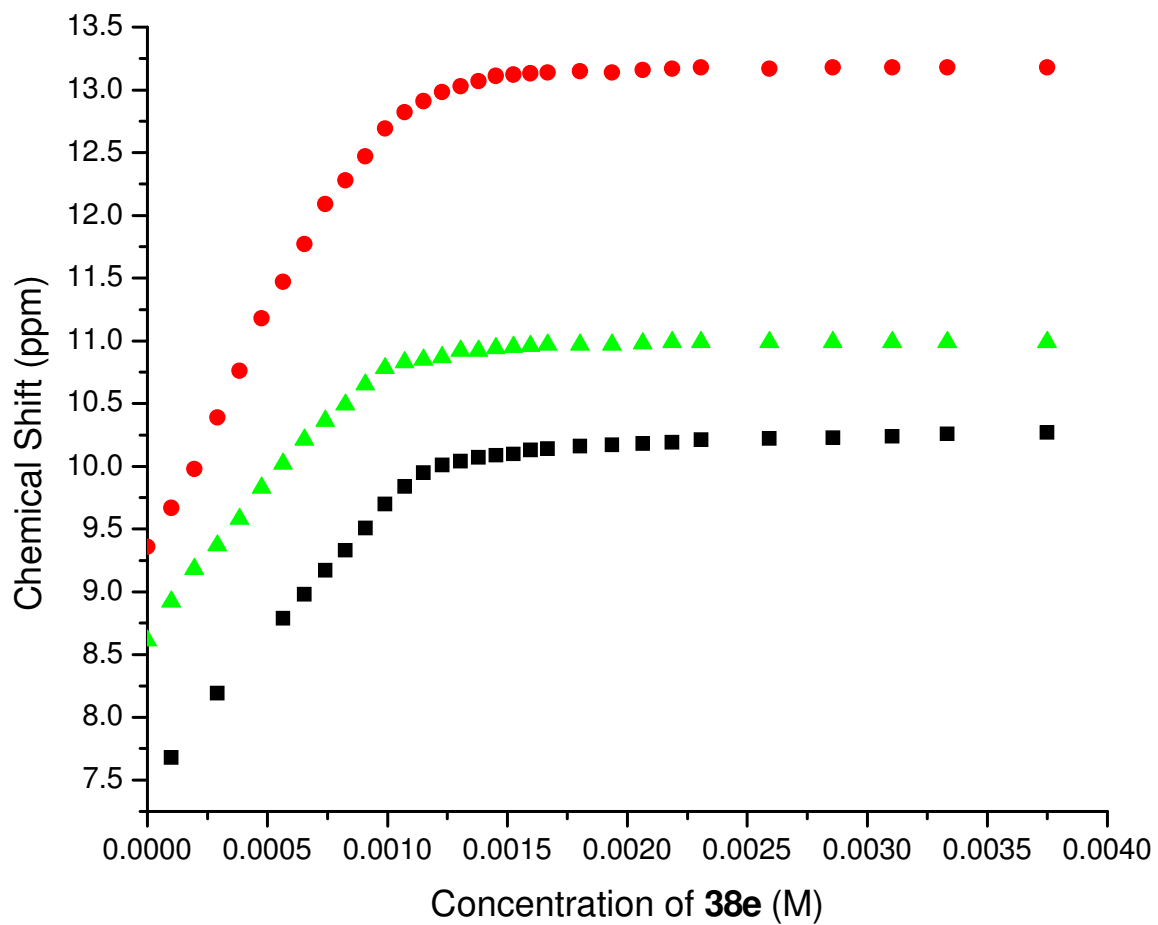


**Figure A-5**  $^1\text{H}$  NMR titration curve of **38e** and **11** in  $\text{CDCl}_3$  at 298K.



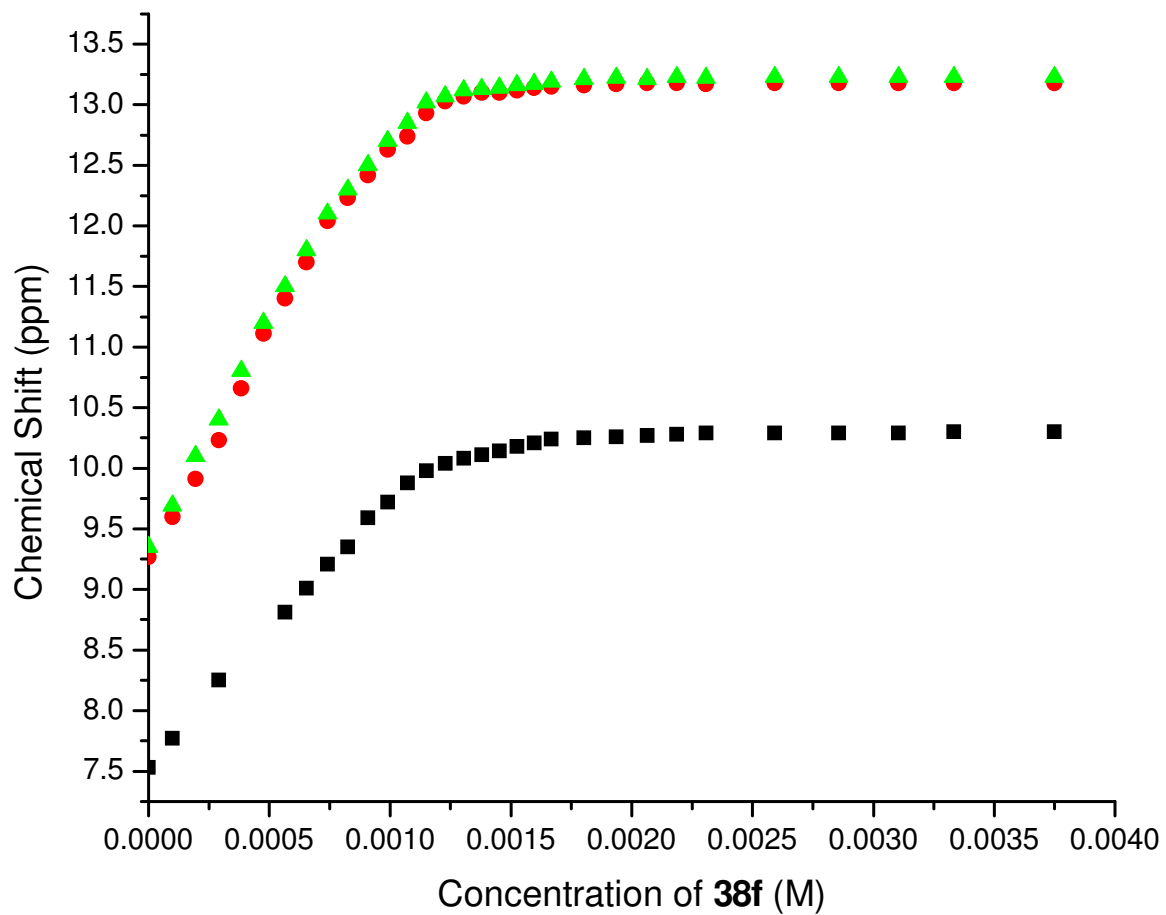


**Figure A-6**  $^1\text{H}$  NMR titration curve of **38f** and **11** in  $\text{CDCl}_3$  at 298K.

## Curriculum Vitae

<b>Name:</b>	Hong-Bo Wang
<b>Post-secondary Education and Degrees:</b>	<p>Huazhong Agricultural University Wuhan, Hubei, China 1999-2003 B.Sc.</p> <p>Central China Normal University Wuhan, Hubei, China 2003-2006 M.Sc.</p> <p>The University of Western Ontario London, Ontario, Canada 2006-2011 Ph.D.</p>
<b>Honours and Awards:</b>	<p>Graduate Thesis Research Award 2011 Dissertation Year Fellowship 2010 Western Graduate Research Scholarship 2008-2009 Western Graduate Scholarship 2006-2008 Hubei Provincial Outstanding Master Thesis 2007 HZAU Innovation Award 2003 HZAU Outstanding Undergraduate 2003 Hubei Provincial Outstanding Undergraduate Scientific Research (2<sup>nd</sup> class) 2002, 2003</p>
<b>Related Work Experience</b>	<p>Teaching Assistant The University of Western Ontario 2006-2011</p>

### Publications:

1. **Wang, H. -B.**; Mudraboyina, B. P.; Li, J.; Wisner, J. A.\* Minimal complementary hydrogen- bonded double helices. *Chemical Communications* **2010**, 46 (39), 7343-7345.
2. **Wang, H. -B.**; Wisner, J. A.\*; Jennings, M. C. Anion receptors containing thiazine-1,1- dioxide heterocycles as hydrogen bond donors. *Beilstein Journal of Organic Chemistry* **2010**, 6, No. 50. doi:10.3762/bjoc.6.50.
3. Liu, Z. M.; **Wang, H. -B.**; Zhu, X. -L.; Tu, H. -Y.; Yang, G. -F. Blue organic light-emitting supramolecular microfibers: the self-assembly of a 1,2,4-triazolo[1,5-a]pyrimidine derivative. *Molecules* **2008**, 13(4), 855-863.
4. Zhu, X. -L.<sup>§</sup>; **Wang, H. -B.**<sup>§</sup>; Chen, Q.; Yang, W. -C.; Yang, G. -F.\* Preparation and Characterization of inclusion complex of iprodione and  $\beta$ -cyclodextrin to improve fungicidal activity. *Journal of Agricultural and Food Chemistry* **2007**, 55(9), 3535-3539. (<sup>§</sup>These authors contributed equally to this work)

5. Yang, G. -F.\*; **Wang, H. -B.**; Yang, W. -C.; Gao, D.; Zhan, C. -G.\* Formation of supramolecular permethrin/ $\beta$ -cyclodextrin nanorods. *The Journal of Chemical Physics* **2006**, *125(11)*, 11110441-11110444.
6. Yang, G. -F.\*; **Wang, H. -B.**; Yang, W. -C.; Gao, D.; Zhan, C. -G.\* Bioactive permethrin/ $\beta$ -yclodextrin inclusion complex. *Journal of Physical Chemistry B* **2006**, *110(13)*, 7044-7048.
7. Ma, J.\*; **Wang, H. -B.**; Jiang, H. Synthesis and herbicidal activity of 1,4-dioxoquinoxaline-2 -carbaldehyde acylhydrazones. *Jingxi Huagong* **2004**, *21(4)*, 309-312. (in Chinese)
8. **Wang, H. -B.**; Ma, J.\*; Zhang, F. Y. Synthesis and fungicidal activity of some 1,4-di-N- oxoquinoxalineformaldehyde derivatives. *Hubei Huagong* **2003**, *20(2)*, 21-23. (in Chinese)
9. **Wang, H. -B.**; Ma, J.\*; Chen, D. L. Synthesis of cinnamic acid by using the catalyst KF/Al<sub>2</sub>O<sub>3</sub>. *Hubei Huagong* **2002**, *19 (6)*, 26-27. (in Chinese)

#### Conference Presentations:

1. **Wang, H. -B.**; Wisner, J. A.\* Double-helical hydrogen bonded AAA-DDD complexes and supramolecular polymers. 94<sup>th</sup> Canadian Chemistry Conference and Exhibition, Montréal, Québec, Canada, June 5-9, 2011. (Oral)
2. **Wang, H. -B.**; Wisner, J. A.\* Double Helical AAA-DDD Hydrogen Bond Complexes. 3<sup>rd</sup> French-Canadian Workshop in Supramolecular Chemistry, Université de Montréal, Montréal, Québec, Canada, June 21-23, 2010. (Oral)
3. **Wang, H. -B.**; Wisner, J. A.\* Sythesis and optimization of double helical AAA-DDD hydrogen bond complexes. 5<sup>th</sup> International Symposium On Macrocyclic & Supramolcular Chemistry, Nara, Japan, June 6-10, 2010. (Poster)
4. **Wang, H. -B.**; Wisner, J. A.\* Development of complementary AAA-DDD triply hydrogen- bonded complexes. 92<sup>nd</sup> Canadian Chemistry Conference and Exhibition, Hamilton, Ontario, Canada, May 30-June 3, 2009. (Poster)
5. **Wang, H. -B.**; Wisner, J. A.\*New anion receptors based on thiazine-1,1-dioxide subunits. 91<sup>st</sup> Canadian Chemistry Conference and Exhibition, Edmonton, Alberta, Canada, May 24-28, 2008. (Poster)
6. **Wang, H. -B.**; Yang, W. -C.; Yang, G. -F.\* Preparation and characterization of the permethrin/  $\beta$ -cyclodextrin inclusion complex. 3<sup>rd</sup> Asian Cyclodextrin Conference, Tianjin, China, May 8-12, 2005. (Poster)